



SCHOOL OF ELECTRICAL AND ELECTRONIC ENGINEERING

ELECTRIC POWER SYSTEMS GROUP

# **An Evaluation of Dynamic Thermal Ratings for Load Accommodation in Power Distribution Networks**

---

A THESIS SUBMITTED FOR THE DEGREE OF DOCTOR OF  
PHILOSOPHY

Peter James Davison

November 2017



# Declaration

I declare that this thesis is my own work and that I have correctly acknowledged the work of others. This submission is in accordance with University and School guidance on good academic conduct

I certify that no part of the material offered has been previously submitted by myself for a degree or other qualification in this or any other University.

# Abstract

This thesis presents an evaluation of the use of Dynamic Thermal Ratings (DTRs) to provide additional network headroom for load consumer connections in electrical power distribution networks. The requirement for additional headroom can come from a number of sources including, limitations in the current network configuration, the need to provide connections to new consumers at minimal cost and to provide additional capacity in the transition to the low carbon economy.

DTRs are a method by which the current carrying capacity of power system components such as transformers and overhead lines can be estimated in real-time through analysis of the surrounding meteorological conditions. The use of this technique has typically shown significant increases in available network capacity, however much of this work has considered such benefits in the context of increasing the capacity for wind generation connections. This research differs in its analysis of such benefits with regards to customer connection.

Analysis of the present overhead line rating standards in the UK has shown that the system potentially over estimates the level of risk at which the network is operated. A set of adjusted ratings which meet these criteria are presented in this thesis.

A generic, temperature sensitive load synthesis method is presented in order to estimate the benefits of DTRs within distribution networks. Through the use of such time-series load profiles the additional requirements of such an approach are exposed and analysed.

Implementation of such a system has been shown to deliver additional network capacity for customer connections in both fit and forget and active network management scenarios.

# Acknowledgements

First and foremost thanks must go to my supervisor Professor Phil Taylor. Without his help, support and guidance I would certainly not have reached this point.

I must also thank my colleagues, in particular Dr Pádraig Lyons and Dr David Greenwood, their advice and counsel has been incredibly useful. I would also like to acknowledge my industrial partners, in particular Dave Miller, Andrew Webster, Rosie Hetherington and Ian Lloyd at Northern Powergrid.

Finally my thanks must go to Sophie, for her patience, understanding and for always being there. I cannot thank her enough.



# Acronyms

<b>Acronym</b>	<b>Description</b>
ANM	Active Network Management
AC	Alternating Current
ADD	After Diversity Demand
ADMD	After Diversity Maximum Demand
ARIMA	Autoregressive Integrated Moving Average
ARX	Autoregressive with Exogenous Inputs
AvgSC	Average Silhouette Coefficient
BaU	Business as Usual
CDD	Cooling Degree Day
CDF	Cumulative Distribution Function
CIGRÉ	Conseil international des grands réseaux électriques
CSC	Correlation Sensitivity Coefficient
DC	Direct Current
DNO	Distribution Network Operator
DSR	Demand Side Response
DTR	Dynamic Thermal Rating
EENS	Expected Energy Not Supplied

EES	Electrical Energy Storage
ENA	Energy Networks Association
ER	Engineering Recommendation
FES	Future Energy Scenarios
HDD	Heating Degree Day
IEC	International Electro technical Commission
IEEE	Institute of Electrical and Electronic Engineers
KNN	K-Nearest Neighbour
LCNF	Low Carbon Networks Fund
LOLE	Loss of Load Expectation
LOOCV	Leave-One-Out-Cross-Validation
LV	Low Voltage
MAE	Mean Absolute Error
MIA	Mean Index Adequacy
MLR	Multiple Linear Regression
MV	Medium Voltage
OAC	Output Area Classification
OHL	Overhead Line
PDF	Probability Density Function
PFSF	Power Flow Sensitivity Factor
PTR	Power Transformer

RMSE	Root Mean Square Error
RRMSE	Relative Root Mean Square Error
RTTR	Real-Time Thermal Rating
SC	Silhouette Coefficient
SMI	Similarity Matrix Indicator
TSC	Temperature Sensitivity Coefficient
UGC	Underground Cable
WCBCR	Within Cluster Between Cluster Ratio

## Nomenclature

Symbol	Description	Unit
$A_{1,2}$	Constant	
$B_{1,2}$	Constant	
$c$	Cluster centroid	
$cov$	Covariance	
$C$	Pearson Correlation Coefficient	
$C$	Cluster members	
$C_p$	Specific heat	J/kg°C
$C_T$	Correlation Term	
$d$	Euclidean Distance	
$d$	Conductor inner strand diameter	m
$d$	Elexon daily period	
$D$	Conductor outer diameter	m
$E$	Expectation	
$E_k$	Elexon ADD Profile for consumer class $k$	kW

$E_{kNorm}$	Normalised Elexon ADD Profile for consumer class $k$	
$g$	Gravitational acceleration	m/s <sup>2</sup>
$G$	Grashof Number	
$G_t$	Difference between RTTR and Load at $t$	A
$i$	Load group index	
$I$	Conductor Current	A
$j$	OAC Supergroup index	
$k$	Elexon Consumer Class	
$k_f$	Thermal conductivity of the air film in contact with the conductor	W/m/°C
$k_j$	Skin Effect Factor	
$K_{Dom}$	Number of Elexon Domestic Consumer Classes	
$K_{I\&C}$	Number of Elexon Industrial and Commercial Consumer Classes	
$K_r$	Radial thermal conductivity of the conductor	W/m°C
$L_i$	Electrical Load of demand group $i$	kW / A
$m$	Mass of the conductor per metre	kg/m
$m_{1,2}$	Constants	
$n$	Number of dataset time periods	
$Nu$	Nusselt Number	
$N_k$	Number of consumers in Elexon Class $k$	
$P_F$	Heat loss due to forced convection	W/m
$P_k$	ADD Profile for consumer class $k$	kW
$P_{kNorm}$	Normalised ADD Profile for consumer class $k$	
$P_kOAC_j$	ADD Profile for OAC group $j$ and consumer class $k$	kW
$P_R$	Heat loss due to radiation	W/m
$Pr$	Prandtl Number	
$Q_{conv}$	Convective cooling	W/m
$Q_{joule}$	Joule heating (I <sup>2</sup> R loss)	W/m
$Q_{rad}$	Radiative cooling	W/m
$Q_{sol}$	Heating due to solar radiation	W/m

$R$	Ratio between domestic and non-domestic consumers	
$ROAC_j$	Ratio of consumers of OAC supergroup $j$ to the overall demand group composition	
$Re$	Reynolds number	
$R_T$	DC Electrical resistance at T	$\Omega/m$
$R_{T1}$	DC resistance at temperature T1	$\Omega/m$
$R_{T2}$	DC resistance at temperature T2	$\Omega/m$
$s$	Elexon seasonal period	
$S_r$	Solar radiation	$W/m^2$
$t$	Time	
$T$	Temperature	$^{\circ}C$
$T_a$	Ambient temperature	$^{\circ}C$
$T_e$	Exceedence	%
$T_s$	Conductor Surface Temperature	$^{\circ}C$
$T_f$	Average Conductor Temperature	$^{\circ}C$
$u, W_s$	Wind speed	m/s
$Y$	Yaw factor of incident wind speed	
$y$	Conductor height above sea level	m
$a$	Solar radiation absorption coefficient	
$a$	Temperature coefficient of electrical resistance at T1	
$\varepsilon$	Emissivity coefficient with respect to black body	
$\lambda_f$	Thermal conductivity of the air film in contact with the conductor	$W/m/K$
$\rho_r$	Relative air density at conductor height ( $y$ )	
$\mu$	Mean	
$\sigma_{S-B}$	Stefan-Boltzmann constant	$W/m^2/K^4$
		also
		$W/m^2$
$\nu$	kinematic viscosity of the air	$m^2/s$

$\nu_f$  kinematic viscosity of the air film at the conductor surface  $\text{m}^2/\text{s}$

## List of Publications

### Journal Papers

S. Blake, **P. Davison**, D. Greenwood, and N. Wade, "Climate change risks in electricity networks," *Infrastructure Asset Management*, vol. 2, pp. 42-51, 2015.

D. M. Greenwood, J. P. Gentle, K. S. Myers, **P. J. Davison**, I. J. West, J. W. Bush, et al., "A comparison of real-time thermal rating systems in the US and the UK," *IEEE Transactions on Power Delivery*, vol. 29, pp. 1849-1858, 2014.

P. Wang, D. H. Liang, J. Yi, P. F. Lyons, **P. J. Davison**, and P. C. Taylor, "Integrating Electrical Energy Storage Into Coordinated Voltage Control Schemes for Distribution Networks," *IEEE Transactions on Smart Grid*, vol. 5, pp. 1018-1032, 2014.

J. Yi, P. F. Lyons, **P. J. Davison**, P. Wang, and P. C. Taylor, "Robust Scheduling Scheme for Energy Storage to Facilitate High Penetration of Renewables," *IEEE Transactions on Sustainable Energy*, vol. 7, pp. 797-807, 2016.

**P. J. Davison**, P. C. Taylor, "Examining The Relationship Between Grouped Electrical Loads And Temperature For Distribution Network Customers" *Applied Energy* (IN PREPARATION) 2016.

**P. J. Davison**, P. F. Lyons, P. C. Taylor "An Evaluation of the Value of Dynamic Thermal Ratings for Load Accommodation in Medium-Voltage Sheltered Overhead Lines," *IEEE Transactions on Power Systems* (IN PREPARATION) 2016.

### Conference Papers

S. Blake, **P. Davison**, P. Taylor, D. Miller, and A. Webster, "Use of real time thermal ratings to Increase Network Reliability under Faulted Conditions,"

presented at the CIGRÉ Regional South-East European Conference (RSEEC 2012) Sibiu, Romania, 2012.

S. Blake, **P. Davison**, P. Taylor, D. Miller, and A. Webster, "Use of real time thermal ratings to support customers under faulted network conditions," in Electricity Distribution (CIRED 2013), 22nd International Conference and Exhibition on, 2013, pp. 1-4.

J. Yi, P. Wang, P. C. Taylor, **P. J. Davison**, P. F. Lyons, D. Liang, et al., "Distribution network voltage control using energy storage and demand side response," in Innovative Smart Grid Technologies (ISGT Europe), 2012 3rd IEEE PES International Conference and Exhibition on, 2012, pp. 1-8.

### **Project Output Reports**

P. Davison, CLNR Trial Analysis EHV and HV Real-Time Thermal Rating Trials 2014.

P. Davison, CLNR Trial Analysis Real-Time Thermal Rating for Power Transformers, 2014

P. Davison, CLNR Trial Analysis Real-Time Thermal Rating – Underground Cables, 2014

All CLNR Reports available at:

<http://www.networkrevolution.co.uk/resources/project-library/>

# Table of Contents

<b>1</b>	<b>Introduction .....</b>	<b>1</b>
1.1	Background.....	1
1.2	Dynamic and Real-Time Thermal Ratings .....	4
1.3	Distribution network feeder load synthesis.....	7
1.4	Network Ancillary Services.....	9
1.5	Research Objectives .....	10
1.6	Thesis Contributions .....	11
1.7	Thesis Outline .....	13
1.8	Note on the Customer-Led Network Revolution Project.....	15
<b>2</b>	<b>Dynamic and Real-Time Thermal Ratings .....</b>	<b>16</b>
2.1	Introduction.....	16
2.1.1	Chapter Outline Block Diagram .....	17
2.2	Dynamic or Real-Time Thermal Ratings? .....	17
2.3	Conductor Thermal Rating Equations.....	18
2.4	Heat Balance Equation .....	18
2.4.1	Heating elements .....	19
2.4.2	Cooling elements .....	20
2.4.3	Additional parameters .....	23
2.4.4	Iterative calculation of the conductor surface temperature.....	24
2.4.5	Conductor Sag .....	24
2.4.6	CIGRÉ Rating Model Sensitivity Analysis.....	25
2.5	Overhead Line Rating Literature .....	25
2.6	Categorisation of RTTR Technologies.....	26
2.6.1	Weather monitoring .....	26
2.6.2	Conductor Temperature and tension monitoring.....	27
2.6.3	Sag monitoring .....	28
2.6.4	Real-Time Thermal Ratings as part of an ANM scheme .....	28
2.6.5	Real-Time Thermal Ratings for increased system reliability .....	28
2.6.6	Load Modelling in Real-Time Thermal Rating analyses.....	29
2.7	Forecasting of DTRs and RTTRs .....	29
2.8	Real-Time Thermal Ratings as a response to Climate Change .....	29
2.9	Conclusions.....	30

<b>3</b>	<b>Overhead Line Monitoring Site Analysis .....</b>	<b>31</b>
3.1	Introduction.....	31
3.2	Chapter Goals / Objectives and Contributions .....	32
3.2.1	Goals / Objectives .....	32
3.2.2	Transition from existing literature and research / Contribution.....	32
3.2.3	Attainment of Goals .....	32
3.2.4	Chapter Outline Block Diagram.....	32
3.3	Site Description.....	33
3.3.1	Overhead Line Construction.....	34
3.3.2	Site Monitoring Equipment .....	34
3.3.3	Monitoring Instrumentation Accuracy .....	36
3.4	Monitoring Sites.....	37
3.5	Validation – Data Quality and Instrumentation.....	38
3.6	Data Quality Study Results – Missing Parameter Values.....	40
3.6.1	Ambient Monitoring Parameters.....	40
3.6.2	Line monitoring parameters .....	41
3.7	Data Quality Study Results – Site States .....	43
3.8	Data Quality Study Results – System States.....	44
3.8.1	Conclusions of Data Quality Analysis .....	47
3.9	Weather Parameter Distributions .....	47
3.9.1	HV OHL Monitoring Sites – Wind Speed.....	48
3.9.2	HV Monitoring Sites – Ambient Temperature .....	50
3.9.3	HV Monitoring Sites – Wind Direction.....	52
3.9.4	Solar Radiation Percentiles .....	57
3.10	Real-Time and Dynamic Thermal Rating Validation .....	58
3.10.1	Dynamic Conductor Response .....	59
3.10.2	Conductor Surface Temperature .....	60
3.11	RTTR Monitoring Site Results.....	62
3.11.1	Winter Results .....	62
3.11.2	Spring / Autumn Results.....	64
3.11.3	Summer Results .....	65
3.12	OHL monitoring site conclusions.....	66
3.13	Selection of the ‘Critical Span’ .....	66
3.14	Conclusions.....	68
<b>4</b>	<b>Examining the accuracy of the presently used UK overhead line rating standard .....</b>	<b>69</b>

4.1	Introduction.....	69
4.2	Chapter Goals / Objectives and Contributions .....	69
4.2.1	Goals / Objectives .....	69
4.2.2	Transition from existing literature and research / Contribution.....	70
4.2.3	Attainment of Goals .....	70
4.2.4	Chapter Outline Block Diagram .....	70
4.3	Price and Gibbon Heat Transfer Model.....	71
4.3.1	AC Resistance.....	71
4.3.2	Cooling elements .....	71
4.3.3	CERL Experimental Procedure .....	73
4.4	Recreation of the CERL experimental procedure.....	77
4.4.1	Correlation Term line of best fit .....	78
4.4.2	Use of the CIGRÉ rating method to generate conductor temperatures .....	82
4.4.3	Excursion Ambient Temperature .....	85
4.4.4	Excursion Wind Speeds.....	87
4.5	Conclusions.....	89
<b>5</b>	<b>HV Feeder Load Synthesis: After Diversity Demand.....</b>	<b>90</b>
5.1	Introduction.....	90
5.2	Chapter Goals / Objectives and Contributions .....	91
5.2.1	Goal / Objective .....	91
5.2.2	Transition from existing literature and research / Contribution.....	92
5.2.3	Attainment of Goals .....	92
5.2.4	Chapter Outline Block Diagram .....	92
5.3	Parameter Monitoring Data.....	93
5.3.1	Overall Primary Substation Descriptions .....	93
5.3.2	Network Monitoring.....	93
5.4	Load Group consumer data.....	95
5.4.1	Elexon Profiling.....	95
5.5	Electrical Diversity.....	97
5.5.1	Socio-Demographics and the Output Area Classification .....	98
5.6	Allowable Deviation from the Northern Powergrid Elexon Customer Compositions.....	107
5.6.1	Test Case .....	108
5.7	Final OAC ADD Model Parameters.....	111
5.7.1	Test Case Results .....	113
5.8	Conclusions.....	114

<b>6</b>	<b>HV Feeder Load Synthesis: Load-Temperature Relationship..</b>	<b>115</b>
6.1	Introduction.....	115
6.2	Chapter Goals / Objectives and Contributions .....	115
6.2.1	Goals / Objectives .....	115
6.2.2	Transition from existing literature and research / Contribution.....	115
6.2.3	Attainment of Goals .....	116
6.2.4	Chapter Outline Block Diagram.....	116
6.3	Background .....	117
6.4	Outline of the work in this chapter.....	120
6.5	DBSCAN Clustering Algorithm.....	121
6.5.1	Automated determination of the Eps .....	122
6.6	DBSCAN Results .....	124
6.7	Load-Temperature correlation.....	126
6.7.1	Group Correlation Profiles.....	127
6.7.2	Analysis of Correlation Error.....	128
6.8	Generalised Correlation Model.....	131
6.9	Conclusions.....	141
<b>7</b>	<b>HV Feeder Load Synthesis – Temperature Sensitive Load modelling</b>	<b>142</b>
7.1	Introduction.....	142
7.2	Chapter Goals / Objectives and Contributions .....	143
7.2.1	Goals and Objectives .....	143
7.2.2	Transition away from existing literature / Contributions.....	143
7.2.3	Attainment of Goals .....	143
7.2.4	Chapter Outline Block Diagram.....	144
7.3	Background .....	144
7.4	Load Synthesis Method.....	148
7.5	Conclusions.....	156
<b>8</b>	<b>Load Group Classification and combination with Dynamic Thermal Ratings.....</b>	<b>158</b>
8.1	Introduction.....	158
8.2	Chapter Goals / Objectives and Contributions .....	159
8.2.1	Goals / Objectives .....	159
8.2.2	Transition from existing literature and research / Contribution.....	159
8.2.3	Attainment of Goals .....	159
8.2.4	Chapter Outline Block Diagram.....	159

8.3	Chosen Clustering Approach .....	160
8.3.1	Hierarchical Clustering.....	162
8.3.2	K-means and K-means++.....	163
8.3.3	Accuracy criteria .....	163
8.3.4	Mean Index Accuracy (MIA) .....	163
8.3.5	Similarity Matrix Indicator (SMI) .....	163
8.3.6	Average Silhouette and Global Silhouette Coefficients (AvgSC and GSC) .....	164
8.3.7	Within Cluster between Cluster Ratio (WCBCR) .....	164
8.4	Representative Distribution Network Cluster Group Results .....	165
8.5	Derived Generic Customer Load Groups .....	167
8.6	Conclusions.....	168
<b>9</b>	<b>Analysis of the requirements for the use of Dynamic Thermal Ratings in Electrical Distribution Networks.....</b>	<b>169</b>
9.1	Introduction.....	169
9.2	Outline of the work in this chapter.....	171
9.3	Chapter Goals / Objectives and Contributions .....	172
9.3.1	Goals / Objectives .....	172
9.3.2	Transition from existing literature and research / Contribution.....	172
9.3.3	Attainment of Goals .....	173
9.3.4	Chapter Outline Block Diagram.....	173
9.4	Verification of Derived Conductor Temperatures using the DTR Method.....	174
9.5	Customer Numbers supported by the present UK OHL rating standard.....	176
9.5.1	Comparison against N-d scenarios .....	178
9.6	Zonal Analysis .....	178
9.6.1	Zone A.....	179
9.6.2	Zone B.....	179
9.6.3	Zone C.....	181
9.7	Examining the capabilities of a Dynamic Thermal Rating Solution for Load Accommodation.....	182
9.7.1	Loss of Load Expectation (LOLE).....	182
9.7.2	Expected Energy Not Supplied (EENS).....	183
9.8	Zonal Analysis of Dynamic Thermal Ratings .....	186
9.8.1	Comparison of Loss of Load Expectation values .....	187
9.8.2	Comparison of EENS values .....	188
9.9	Cumulative Distribution Functions of the Required DSR Services.....	189
9.9.1	Cumulative Distribution Function of Required DSR Service Magnitudes .....	189

9.9.2	Cumulative Distribution Function of Required DSR Energy Values .....	190
9.9.3	Cumulative Distribution Functions of DSR Service Durations and Times between Services .....	191
9.9.4	Percentage of Conductor Thermal Excursions per Zone .....	196
9.9.5	Example Profiles of Required DSR.....	196
9.10	Conclusions.....	198
<b>10</b>	<b>Discussion.....</b>	<b>200</b>
10.1	Introduction.....	200
10.2	Current UK network rating practice .....	200
10.3	Socio Demographics and Residential demand side response .....	201
10.4	Investigating the relationship between load and temperature for grouped electrical loads .....	202
10.5	Temperature Sensitive Load Synthesis.....	203
10.6	Consumer Load Group Classifications .....	204
10.7	Identification of the potential network service requirements.....	204
10.7.1	Network Risk.....	205
10.8	Issues with Demand Side Response as a Control Technique.....	206
10.9	Forecasting.....	206
<b>11</b>	<b>Conclusions .....</b>	<b>208</b>
11.1	RTTRs for Sheltered OHL sites .....	208
11.2	Presently Implemented UK Line Rating Standard.....	208
11.3	Socio-Demographic ADD Modelling.....	209
11.4	Load-Temperature Relationship for Distribution Network Load groups	209
11.5	Time-Series Feeder Load Modelling.....	209
11.6	Evaluation of the benefits of DTRs for Load Accommodation .....	210
<b>12</b>	<b>References .....</b>	<b>211</b>
<b>Appendix 1 – OAC Annual Consumption Values .....</b>		<b>221</b>
OAC Group Energy Consumption Statistics.....		221
Subgroup OAC Energy Consumption Statistics .....		222
<b>Appendix 2 - Correlation Sensitivity Coefficients .....</b>		<b>225</b>
<b>Appendix 3 - Temperature Sensitivity Coefficients .....</b>		<b>227</b>

# Table of Figures

Figure 1-1 – National Grid Future Energy Scenarios [10] .....	1
Figure 1-2 - UK Future Energy Scenario Energy consumption values [10] .....	2
Figure 1-3 – Example of Overhead Line RTTR and the currently used seasonal line ratings .....	6
Figure 1-4 – Thesis Structure Block Diagram.....	13
Figure 2-1 – Chapter 2 Block Diagram.....	17
Figure 2-2 – CIGRÉ model input parameter sensitivity analysis .....	25
Figure 3-1 – Chapter 3 Block Diagram.....	33
Figure 3-2 – OHL MV monitoring site locations .....	33
Figure 3-3 – An example of an HV Thermal rating monitoring site. Note the clamps attached to the OHL itself recording phase current and conductor core and surface temperatures .....	36
Figure 3-4 – HV RTTR Monitoring Locations .....	37
Figure 3-5 – Histogram of percentage missing ambient monitoring points .....	41
Figure 3-6 – Histogram of percentage missing line monitoring poin ...	42
Figure 3-7 – Total number of missing ambient parameters at all sites at the same points in time .....	44
Figure 3-8 – Total number of missing line parameters across all monitoring sites .....	46
Figure 3-9 – Winter Wind Speed Probability Distribution – All HV Sites	48
Figure 3-10 – Spring / Autumn Wind Speed Probability Distribution – All HV Sites .....	49
Figure 3-11 - Summer Wind Speed Probability Distribution – All HV Sites .....	49
Figure 3-12 - Winter Ambient Temperature Probability Distribution – All HV Sites .....	50
Figure 3-13 – Spring / Autumn Ambient Temperature Probability Distribution – All HV Sites.....	51

Figure 3-14 – Summer Ambient Temperature Probability Distribution – All HV Sites .....	51
Figure 3-15 – Wind Rose for Broxfield HV Site .....	52
Figure 3-16 –Orientation of Broxfield HV Wind Direction Monitoring	53
Figure 3-17 - Wind Rose for Whitehouse HV Site.....	53
Figure 3-18 – Whitehouse Wind Rose with site satellite image.....	54
Figure 3-19 - Wind Rose for Eglingham HV Site .....	54
Figure 3-20 - Eglingham Wind Rose with site satellite image.....	55
Figure 3-21 - Wind Rose for Scar Brae HV Site.....	55
Figure 3-22 – Scar Brae Wind Rose with site satellite image.....	56
Figure 3-23 - Wind Rose for Earle Mill HV Site .....	56
Figure 3-24 – Earle Mill Wind Rose with site satellite image .....	57
Figure 3-25 – Example Solar Radiation Percentile Plot at the Eglingham HV Monitoring Site – Summer .....	58
Figure 3-26 – Dynamic response of Conductor to step change in current	60
Figure 3-27 - MV Conductor surface temperature.....	61
Figure 3-28 – Winter RTTR CDF for all Sites.....	63
Figure 3-29 – Spring/Autumn RTTR CDF for all Sites .....	64
Figure 3-30 - Summer RTTR CDF for all HV Sites .....	65
Figure 3-31 – Empirical CDF of Ambient Temperatures at low wind speeds .....	67
Figure 4-1 – Chapter 4 Block Diagram .....	70
Figure 4-2 – Correlation of Zebra temperature excursion data for the seasons and for various design temperatures, recreated from [62].....	75
Figure 4-3 – Interpolated Linear Relationship between $C_T$ and $T_e$ from [109] .....	79
Figure 4-4 – $C_T$ values as quoted in [22] with theoretical linear fits ...	79
Figure 4-5 – Conductor Temperatures due to constant loading at the P27 seasonal rating values .....	83
Figure 4-6 – Newly derived Temperature exceedance plots in line with those found in [62] .....	84
Figure 4-7 – CDFs of ambient temperature values during conductor temperature excursions – Non-Sheltered Site.....	85

Figure 4-8 - Ambient temperature values during conductor temperature excursions – Sheltered Site.....	86
Figure 4-9 - Wind Speed values during conductor temperature excursions – Non-Sheltered Site .....	87
Figure 4-10 – Wind Speed values during conductor temperature excursions – Sheltered Site .....	88
Figure 5-1 – Chapter 5 Block Diagram.....	93
Figure 5-2 – Domestic Elexon ADD Profiles.....	96
Figure 5-3 – Non-Domestic Elexon ADD Profiles.....	97
Figure 5-4 – Map of the Rise Carr Primary Substation with the OAs and their respective OACs .....	99
Figure 5-5 – A close up of the area surrounding the Rise Carr Primary Substation.....	99
Figure 5-6 – Frequency count of number of customers per Elexon class in DECC postcode dataset.....	102
Figure 5-7 – Empirical CDF for all data.....	102
Figure 5-8 – Elexon Class 1 consumer Maximum ADD values for different customer number bins.....	104
Figure 5-9 - Elexon Class 2 consumer Maximum ADD values for different customer number bins.....	104
Figure 5-10 – Maximum ADD customer number relationship for Class 1 customers.....	110
Figure 5-11 – Maximum ADD customer number relationship for Class 2 customers.....	111
Figure 5-12 – Elexon and OAC ADD profiles for Class 1 consumers ..	112
Figure 5-13 - Elexon and OAC ADD profiles for Class 2 consumers ..	112
Figure 5-14 – RMSE Error using the OAC ADD and Elexon only methods .....	113
Figure 6-1 – Chapter 6 Block Diagram.....	117
Figure 6-2 - Examples of half hourly load and temperature values and the resultant DBSCAN derived clusters .....	121
Figure 6-3 – Example of the Sorted KNN distances from the DBSCAN clustering algorithm inputs .....	123

Figure 6-4 – Original half hourly input data .....	125
Figure 6-5 – DBSCAN derived clusters within the input dataset .....	125
Figure 6-6 - Examples of Group Correlation Profiles .....	127
Figure 6-7 – Load Temperature correlation profile after smoothing .	128
Figure 6-8 – Examples of half hourly correlation values.....	129
Figure 6-9 – Percentage Load Error due to ambient temperature error as a function of correlation.....	130
Figure 6-10 – Upper and Lower bounds of demand group load based on ‘forecast error’ .....	131
Figure 6-11 - Correlation sensitivity Coefficients for Elexon Class 1 consumers.....	138
Figure 6-12 – Actual and Synthesised Correlation using the finally selected method.....	139
Figure 6-13 – Upper and Lower correlation estimation bounds and the resultant effect on overall percentage error .....	140
Figure 7-1 – Chapter 7 Block Diagram .....	144
Figure 7-2 – Example of Conditional PDF for example load group at 00:00 .....	146
Figure 7-3 – PDFs evaluated at specific ambient temperatures for example load group at 17:00 .....	146
Figure 7-4 – Additionally Temperature Sensitive element and linear fit	150
Figure 7-5 – Temperature Sensitivity Coefficients for the Weekday period .....	154
Figure 7-6 – Original and final synthesised group load profile.....	156
Figure 8-1 – Chapter 8 Block Diagram .....	160
Figure 8-2 - Dendrogram of all data – Average linkage method .....	162
Figure 9-1 – Chapter 9 Block Diagram .....	174
Figure 9-2 – Example of a Zone B service requirement.....	180
Figure 9-3 – Example of conductor temperatures before and after provision of network services. Original conductor temperature for actual network loads shown for comparison.....	181
Figure 9-4 – Example of a Zone C service requirement which exceeds the duration threshold .....	182

Figure 9-5 – LOLE Values for the RTTR, DTR and P27 rating cases	183
Figure 9-6 – EENS Values for the RTTR, DTR and P27 cases.....	184
Figure 9-7 – Ratio between resultant EENS values for the RTTR and DTR cases, for Load group 3.....	185
Figure 9-8 – Examples of Group Load Profiles.....	187
Figure 9-9 – Empirical CDF of the required DSR service magnitudes	189
Figure 9-10 - Empirical CDF of the required DSR Energy service values	191
Figure 9-11– Empirical CDF of the required DSR service durations.	192
Figure 9-12– Empirical CDF of the time between required DSR services	193
Figure 9-13 – Examples of joint CDFs between service duration and time between services .....	195
Figure 9-14 – Zonal Results for Load Group 3 .....	196
Figure 9-15 – Average and 99 <sup>th</sup> percentile profiles of required services for Group 3 – Winter Weekday.....	197
Figure 9-16 - Average and 99 <sup>th</sup> percentile profiles of required services for Group 4 – Winter Weekday.....	197

## Table of Tables

Table 2-1 – Table of $B_1$ and $n$ constants as a function of the Reynolds number and Conductor roughness values ( $R_f$ ).....	22
Table 2-2 – Selection of $A_1$ $B_2$ and $m_1$ constants based on the incident wind direction.....	22
Table 2-3 – Selection of $A_2$ and $m_2$ constants based on the value of $Gr \cdot Pr$ .....	23
Table 3-1 – OHL Conductor Parameters .....	34
Table 3-2 – HV Conductor Heights .....	37
Table 3-3 – HV overhead line P27 static ratings.....	38
Table 3-4 – Data Quality Study Results – Ambient Monitoring Parameters .....	40
Table 3-5 - Data Quality Study Results – Line Monitoring Parameters	41
Table 3-6 - Seasonal Data Quality at all HV RTTR Monitoring points	43
Table 3-7 - Percentage of total period for which combinations of ambient parameters are missing at each sample point .....	45

Table 3-8 – Percentage of total period for which combinations of line parameters are missing at each sample point.....	46
Table 3-9 – Winter RTTR Statistics – All HV Sites.....	63
Table 3-10 – Spring / Autumn RTTR Statistics – All Sites .....	64
Table 3-11 - Summer RTTR Statistics – All Sites.....	66
Table 3-12 – Average, 99 <sup>th</sup> percentile and Maximum Ambient Temperature values at low wind speeds .....	68
Table 4-1 – Correlation Terms ( $C_T$ ) as quoted in [62] and results from the line of best fit.....	76
Table 4-2 – Circuit rating values, their equivalent design currents and the results of the MATLAB implementation .....	78
Table 4-3 – Performance of Line of Best Fit equations.....	80
Table 4-4 – Parameters for Fit A choice for $C_T$ line of best fit.....	81
Table 4-5 – Newly derived seasonal ratings in comparison to the presently implemented ratings and their associated ‘design’ currents .....	81
Table 4-6 – Verification of the CIGRÉ dynamic model surface temperature calculation .....	82
Table 4-7 Number of five minute periods and percentage per period for which conductor temperature exceeds circuit rated temperature.....	83
Table 4-8 – Newly derived P27 seasonal line ratings for Sheltered and Non-Sheltered example sites.....	84
Table 4-9 – Ambient temperature values during conductor temperature excursions.....	86
Table 4-10 – Wind speed values during conductor temperature excursions .....	88
Table 5-1 – Elexon Annual Consumption Vs. OAC Supergroup consumption .....	100
Table 5-2 – 99 <sup>th</sup> percentile of customers per OAC Supergroup and per Elexon consumer class .....	103
Table 5-3 – Original Consumer Breakdowns per load group from Northern Powergrid .....	107
Table 5-4 – Maximum percentage customer deviations from the original quoted values .....	108

Table 5-5 – Percentage of OAC groups per network area .....	109
Table 5-6 Average profile RMSE per customer using both original Elexon and OAC ADD values .....	110
Table 5-7 – Final A and B parameters for derivation of maximum ADD values for each of the OAC Supergroups .....	111
Table 5-8 – Final Elexon consumer class breakdown for load groups	114
Table 6-1 - Number of Load-Temperature relationships per half hourly period .....	126
Table 6-2 – Percentage of OAC groups per network area .....	132
Table 6-3 – Load group normalisation candidate methods .....	133
Table 6-4 – Proposed Correlation Model Structures .....	135
Table 6-5 – Total correlation estimation error for all input models ...	137
Table 6-6 – Percentage differences bewteen ‘temperature forecast’ error bounds and those added as a result of the chosen correlation model .....	140
Table 7-1 – Load group normalisation candidate methods .....	151
Table 7-2 – Proposed Correlation Model Structures .....	151
Table 7-3 – Total correlation estimation error for all input models ...	153
Table 7-3 – Temperature sensitive load synthesis results shown in comparison to the group ADD profiles developed in Chapter 5 .....	155
Table 8-1 - Clustering Algorithm Sample Sizes .....	161
Table 8-2 – Clustering Algorithm Results for all data aggregation levels	166
Table 8-3 – Adequacy criteria for chosen clustering algorithm in each of the test cases.....	167
Table 8-4 – Clustering Results – Percentage Elexon Class per representative load group .....	167
Table 9-1 – Conductor Temperature estimation accuracy of synthesised load group .....	176
Table 9-2 – Number of customers per generic load group supported by revised P276 seasonal ratings .....	178
Table 9-3 – Total customer numbers per load group in each of the support cases .....	186
Table 9-4 – LOLE in hours/year at the Zone A and B total number of customers supported per group .....	188

Table 9-5 - EENS in MWh/year at the Zone A and B total number of customers supported per group.....	188
Table 9-6 – Maximum and percentiles of required DSR services .....	190
Table 9-7 – HV overhead line P27 static ratings (MVA) .....	190
Table 9-8 – Maximum and percentiles of required DSR Energy services	191
Table 9-9 – Percentiles of DSR service durations .....	192
Table 9-10 – Percentiles of time between DSR services .....	193



# 1 Introduction

## 1.1 Background

The transition to the ‘low carbon economy’ [1] will have substantial impacts on the transmission and distribution of electrical power [2, 3]. The requirement to balance supply and demand for electricity in a system with an increasing penetration of variable output generation sources such as wind [4, 5] and solar [6, 7] and other low carbon technologies (LCTs) whilst decommissioning existing fossil fuel generation plant present significant challenges to network owners and operators [8, 9]. In addition to the challenges presented by the low carbon transition with regards to technologies, there is also considerable variability as to the estimated speed of the transition itself. In an attempt to categorise this, National Grid, the Transmission System Operator in the UK has outlined a series of Future Energy scenarios (FESs) [10]. Figure 1-1 shows a diagrammatic representation of these scenarios.



Figure 1-1 – National Grid Future Energy Scenarios [10]

In addition to these scenario descriptions, National Grid has also estimated the total UK energy usage from the present day to 2035 and beyond, dependent upon the particular ‘transition path’ followed by the UK as a whole.

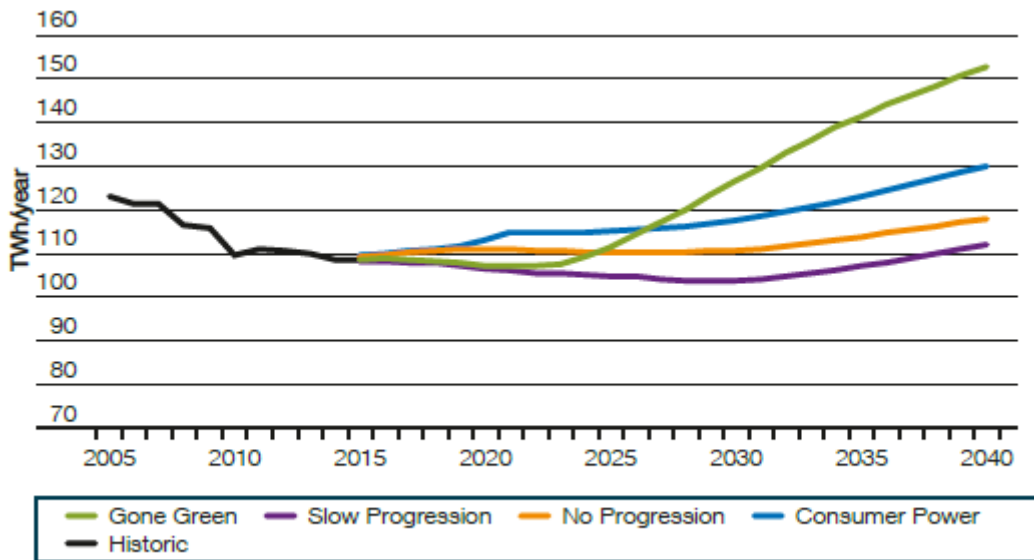


Figure 1-2 - UK Future Energy Scenario Energy consumption values [10]

As can be seen in Figure 1-2 each of the scenarios with the exception of the ‘slow progression’ model shows increasing energy requirements with reference to 2015 values towards 2030, with all scenarios forecast to result in increased consumption by 2040.

Whilst these ‘low carbon’ transitions will place additional demands on the existing network infrastructure, the need to provide increased network capacity for additional consumer connections in the present day should not be overlooked. The requirements of current planning standards [11] must still be met and there are various scenarios in which the present system cannot supply all of the required electrical demand. In [12, 13] RTTRs are presented as an option to provide network support coincident with an N-2 circuit outage scenario in rural Northern England. In such a scenario, the present OHL circuit is unable to supply all of the required demand with the present OHL circuit ratings in place. These papers examine the potential of RTTRs to deliver the required increase in circuit capacity to maintain supply to the affected customers. The business as usual (BaU) approach to ensure that grid infrastructure has the required capacity for these

transition scenarios would be to upgrade or reinforce the existing network assets however this approach faces considerable challenges in the future.

Firstly, whilst previous network price control periods for Distribution Network Operators (DNOs) [14] have given considerable weight to their asset base, the introduction of RII0-ED1 (Revenue = Incentives + Innovation + Outputs) [15] by the industry regulator Ofgem (Office of Gas and Electricity Markets), shifts the focus for revenue collection away from traditional asset ownership, towards achieving the same network security of supply level, at a lower cost, through the use of innovative techniques and technologies. This model has been in place as of the 31<sup>st</sup> of April 2015. It is also important to consider the potential difficulties that network reinforcement may encounter, for example, planning restrictions, customer interruptions and the inflation of raw material prices, all of which represent barriers to implementation [16].

Furthermore, as shown in Figure 1-2, there is clear variability in the energy requirements of each of the respective 'transition pathways' [17]. New infrastructure is currently sized such that it can support required demand over a particular asset lifetime, and such that peak network capacity can be accommodated. Depending upon the nature of the transition pathway followed by the UK, it is therefore particularly difficult for the asset to be optimally sized. Additionally, the asset must be sized such that is capable of supporting network peak loading conditions, however the occurrences of peak loading typically constitute a small fraction of the year-round load cycle. The question must therefore be raised as to whether networks sized for such a loading pattern are an efficient and cost-effective use of capital. Once new physical assets such as overhead lines (OHLs) have been installed, there is also a limited potential for re-deployment.

An alternative approach would be to utilise network ancillary services in combination with techniques such as voltage control or power flow management [18]. In these cases the capacity requirements of assets such as OHLs, power transformer (PTRs) and underground cables (UGCs) would be reduced. The consideration of such services and their potential contributions to network security of supply is being currently undertaken in the UK [19].

In addition to the use of network ancillary services, another solution to provide additional system capacity is to examine if the capacity of currently installed assets can be increased above their present ratings. In the context of the assets previously discussed these are referred to as Dynamic and Real-Time Thermal Ratings (DTRs and RTTRs). Within this work is the consideration that dynamic thermal ratings can be used to alleviate network problems. Much of the literature to date has considered an integrated RTTR system as a way of deferring or negating the need for network reinforcement and thus providing additional capacity for variable output, embedded generation sources. There are a number of reasons as to why this approach has often been taken:

- An increase in renewable or less carbon intensive generation sources is necessary, to meet both national and international commitments to climate change.
- Such new generation sources are often located at both geographically distant and electrically weak sections of the country.
- The electrically weak nature of the network would traditionally lead to a network reinforcement solution in order to give the requisite capacity increase, however the geographic consideration brings with it significant planning, economic and potential timescale problems, as seen in the case of the Beaulieu-Denny transmission line upgrade in Scotland [16, 20].
- Since RTTR requires no upgrades to existing infrastructure, merely the installation of small-scale monitoring equipment and sensors a significant proportion of the problems detailed above can be bypassed.

In a scenario where increased levels of variable generation sources are connected to the UK network, RTTRs have been shown to allow significant increases in connection capability due to their gains over traditional static asset ratings.

## **1.2 Dynamic and Real-Time Thermal Ratings**

The capacity ratings of network assets in the UK and beyond presently use a series of worst case scenario conditions intended to result in minimal risk of a

thermal overload [21, 22]. High ambient temperatures and low wind speeds tend to give low ratings in the case of OHLs, with the converse of both parameters yielding higher ratings.

In the case of OHLs, high conductor temperatures can lead to increased sag and violation of ground clearance limits. For PTRs and UGCs greater than stipulated internal temperatures can violate winding temperature limits leading to increased thermal stress and can reduce the strength of various dielectric materials. Derivation of an assets' capacity is carried out through use of the relevant heat balance equation. Equation (1) shows the overall heat balance equation for OHLs.

$$Q_{joule} + Q_{sol} = Q_{conv} + Q_{rad} \quad (1)$$

Where:

$Q_{joule}$	is the Joule heating ( $I^2R$ loss)
$Q_{sol}$	is the heating due to solar radiation
$Q_{conv}$	is the convective cooling
$Q_{rad}$	is the radiative cooling

Each term of the heat balance equation with the exception of the Joule heating contains an input from a meteorological variable. It is these conditions which are currently used in their 'worst case' in order to derive asset ratings. The techniques of DTRs and RTTRs have been investigated previously as methods to increase the load transfer capacity of assets such as OHLs [23], PTRs [24, 25] and UGCs [26] by exploiting available differences between the real-time and relevant worst case scenario conditions. In the context of OHLs which will be focussed upon in this thesis, RTTR values represent the maximum possible conductor loading based on a set of observed conditions, such that a particular thermal limit is not violated. This is typically the present circuit rated temperature [27]. The DTR calculates the resultant conductor temperature over time based on a particular value of loading, which acts as an input as opposed to an output of the model.

Figure 1-3 shows an example of RTTR values in addition to the presently used conductor seasonal ratings. As can be seen, there are clearly significant periods of time for which the conductor's potential capacity is far greater than its current

rating. There are also periods during which the RTTR values are lower than the seasonal ratings, based on ‘worst case’ scenario conditions.

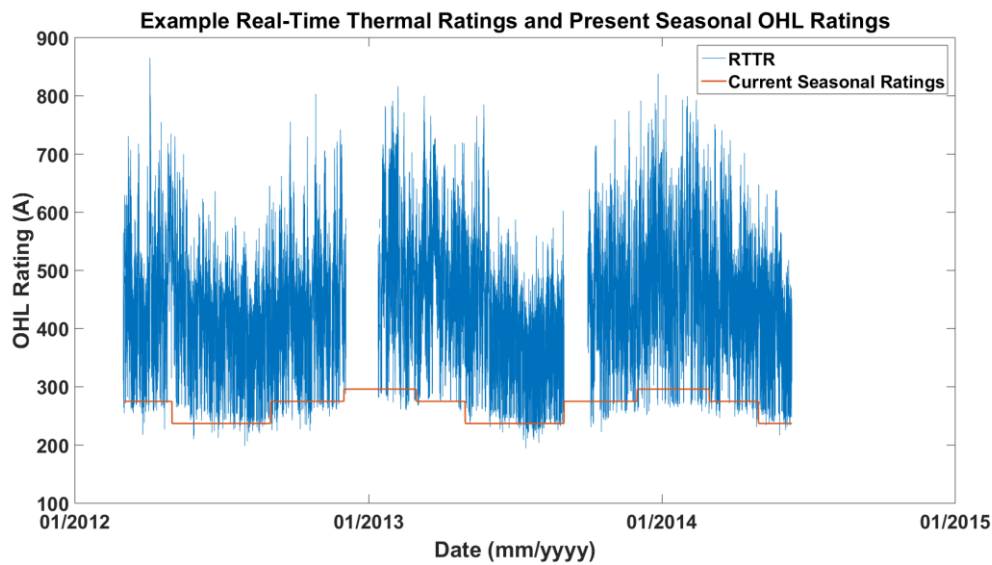


Figure 1-3 – Example of Overhead Line RTTR and the currently used seasonal line ratings

It is important however to consider the loading of the conductor during these periods, since the present line ratings are not simply a function of ambient meteorological conditions. The currently implemented standard will be discussed in greater detail in Chapter 4 of this thesis. As an additional contribution this research will also consider the validity of these present ratings as suitable reference values.

Considering real-time operation of the network, the RTTR provides visibility as to the current state of the available capacity. With an increasing need to provide additional network capacity, it is this visibility which will support the efficient and economic utilisation of existing asset capacities. Whilst there is the potential for periods of reduced capacity over the present method, this visibility also indicates significant periods at which capacity is shown to be far greater.

The majority of previous work on the use of RTTRs and DTRs have focussed upon increasing network capacity for embedded or distributed generation (EG / DG) sources and in particular, upon increasing the ratings of overhead lines. RTTR and DTR systems have often been investigated as a method to improve capacity for wind generation connections [28-30], since as an additional benefit wind provides the dominant cooling factor for overhead lines [31]. This technique

has also been considered as part of wider active network management (ANM) schemes [32-34] .

Whilst some research has considered the potential for RTTRs to provide a network benefit towards load accommodation [35, 36] such analyses have assumed that load is independent from the resultant RTTRs and also have used typical load duration curves in order to probabilistically examine the resultant Expected Energy Not Supplied (EENS) figures.

Whilst the mutual benefit between Aeolian cooling of the OHLs in conjunction with high wind turbine outputs has been discussed [31], in a similar way, usage of DTRs allows for exploration of the correlation between electrical network demand and the variability of the derived DTR values. An understanding of how the same ambient conditions affect both the power system components and the demand served by the component allows us to ascertain a clearer estimation of the assets' true latent capacity and to assist with the making of network planning and operation decisions [37]. Similar analysis concerning the rating of PTRs and the coincidence of loading conditions with transformers was carried out in [38]. Here, loading conditions are related to hot spot temperatures within low voltage distribution networks.

Therefore, the research in this thesis will use DTRs in conjunction with feeder load profiles in order to evaluate the potential to increase the number of load consumer connections and also to examine the potential for network ancillary services. In order to comprehensively evaluate this potential, the impact of ambient temperature on feeder load profiles needs to be accurately modelled which requires development of an appropriate method for synthesising network feeder loads.

### **1.3 Distribution network feeder load synthesis**

Within distribution networks typical load flow calculations are typically carried out using maximum demand or fixed load estimations [39, 40]. In addition to new techniques which will enhance the visibility and capacity of existing techniques, there is also a requirement to model demand within distribution networks with increased accuracy in order to complement such developments. As

a means of contributing to this domain this thesis will outline a new method for deriving accurate temperature sensitive distribution network feeder load profiles.

Whilst typical load flow calculations and other such studies often use point load estimates, time-series load profiles have also been examined, often in the domain of load forecasting. In [41] electrical load is broken down into three components, the expected demand, temperature sensitive demand and a stochastic element. As such, many load forecasting approaches have included weather variables, typically ambient temperature. A review of such schemes can be found in [42] which clearly shows ambient temperature as the second most considered model input after values of the load itself.

The relationship between electricity demand and ambient meteorological parameters such as air temperature have been well documented [43-46]. The main aspect of this research however is its consideration of the relationship for national demand, or for the modelling of individual consumers. In this research the relationship between load and temperature is considered at the intermediary levels of grouped electrical loads, within the distribution network of the UK. These relationships will be used as part of the new temperature-sensitive feeder load synthesis method proposed in this thesis.

In order to credibly evaluate the capabilities of DTRs for load accommodation, this thesis will model loading scenarios based on recently observed actual network loads, and evaluate the capability of DTRs for OHLs to safely accommodate additional customers, which would normally trigger the requirement for network reinforcement based on the current planning standard. A factor in the decision to model additional present network consumers as opposed to those with LCTs is the speed at which DTR technologies can be deployed on active networks. In almost any location where network reinforcement is being considered to provide thermal headroom, DTR equipment can be installed and operational long before planning or investment plans have been finalized, and at a considerable reduction in capital cost. If the decision is taken to reinforce at a later date, the original instrumentation can be re-deployed and put to use again.

As opposed to generation growth, demand increases can also be considered as uncontrolled with limited visibility from the point of view of the network operator. Visibility of the actual network capacity is therefore a crucial factor in ensuring

that the network can cope with these increased demand levels, whether due to LCT growth or other factors. Limiting the number of customer connections due to a perceived lack of network capacity should be avoided.

Since both the DTR of the OHL and the load profile have a temporal function, there are likely to be periods for which the DTR may be unable to support a particular set of connected customers. These events may be limited at present but are likely to increase in frequency in the future due to load growth.

By comparison of the resultant DTR and feeder load profiles, both the total probability of inability to supply customers and the times of day at which this is most likely to occur can be derived. This method will be compared against previous methods of assessment as shown in [35, 36, 47, 48] which have typically used real-time as opposed to dynamic thermal ratings. In addition to exposing these probabilities, the required power and energy of network ancillary services from sources such as Demand Side Response (DSR) or Electrical Energy Storage (EES) can also be estimated such that conductor temperatures are maintained within the present network limits.

#### **1.4 Network Ancillary Services**

Network ancillary services such as demand side response will be a key component of the smart grid [49-51]. The term demand side response in this research relates to services provided by consumers such as automated [52, 53] or participatory [54] load control techniques and to services procured from devices such as Electrical Energy Storage (EES) [18]. These services are important in the context of DTRs for load accommodation due to the nature of the network control actions which will be required. In the scenario where RTTRs are used to increase network capacity for variable generation sources such as wind power, respective of the contract between the generation owner and the DNO, a control scheme can be put in place to potentially curtail the generation output as and when required with no effect on end consumers. When considering the potential for load connections, the same requirement for control exists only such that now in the potential absence of generation, control must be resourced either from consumers themselves or as previously noted from a source such as EES. DNOs have commented upon the scenarios in which they would consider the use of DSR in [55]. Scenarios such as

post-fault load reduction and the creation of network headroom are commented upon as potential uses, both of which could be thought of as a form of network control to mitigate an event where conductor temperatures are likely to exceed their rated limits.

## **1.5 Research Objectives**

The most significant contribution of this research is in its evaluation of the capabilities of DTRs to increase the number of potential customer connections in distribution networks. As a means to deliver this overall contribution the research work in this thesis required successful completion of the following key research activities.

1. Analysis of the available real world data to determine the ‘worst case’ scenario for DTR and therefore provide generalised findings. In this context, ‘worst-case’ represents the OHL data monitoring location which results in the smallest potential uplift from the use of real-time or dynamic thermal ratings. Since the overall findings from this research will be delivered as a function of the selected monitoring site, the assumption has therefore been made that this provides an adequate representation of an OHL section which provides a reduced increase in network capacity from the introduction of DTRs and RTTRs.
2. Examine the present OHL rating standards in the UK and determine if they are fit for purpose in order to establish a correct baseline for assessment.
3. Investigate the influence of meteorological variables on aggregated distribution network load groups.
4. Develop suitable models of aggregate load profiles to act as inputs to the DTR model.
5. Examine the requirement for additional network ancillary services to mitigate conductor thermal overloads.

## 1.6 Thesis Contributions

- This thesis contributes analysis of a novel ambient parameter dataset at sheltered and non-sheltered rural 20kV OHL monitoring sites. RTTR values for these sections of OHL have been derived in addition to the meteorological analysis. Analysis at this voltage level represents a novel piece of analysis.
- Re-examination of the presently implemented method for the derivation of seasonal OHL ratings. New seasonal ratings have been derived using this method and new real-world monitoring site data to allow for direct comparison.
- Development of a method to deliver new socio-demographically grouped After Diversity Demand profiles, such as those presented by Elexon, with the ability to scale to a user defined as opposed to fixed number of consumers. This work builds upon previous work from the community which considered annual energy demands, but not time series demand profiles as a function of the same socio-demographic classification scheme.
- Much of the existing literature discussing the relationship between electrical demand and temperature considers the relationship at either the individual, or large area (country) level. The research presented here represents a novel contribution due to its analysis of the load-temperature relationship for grouped electrical consumers at distribution network aggregation levels. Linear correlation values have been implemented previously to describe this relationship, however this research provides contribution in its development of a generalised model to derive these correlation values as a function of the consumers within the electrical demand group. The use of the DBSCAN clustering algorithm with this dataset in order to analyse the variability of the relationship within a half hourly period also represents the first introduction of this algorithm to this type of analysis.
- This relationship has been extended beyond derivation of correlation values to develop a demand group load-synthesis method which takes

into account the relative sensitivities to temperature from the constituent components of the demand group.

- In order to test the ability of Dynamic Thermal Ratings to provide increased accommodation for demand beyond the present seasonal ratings, a series of generic distribution network load groups have been derived. These groups represent a contribution since they are based on group composition only. This deviates from previous work in this field, which has considered only LV networks and also included network parameters within its analysis.
- A contribution has been made through the use of DTRs and synthesised load profiles to demonstrate the potential benefits of this network technique. Much of the literature in this domain considers the use of RTTRs as opposed to DTRs and as an enabler of network headroom for generation connections as opposed to demand. Where DTRs have been considered, they have not been considered in the same manner regarding time series profiles as within this research. A key contribution is in the use of dynamic as opposed to real-time thermal ratings in combination with time series load profiles. This approach takes into account the time-coincident correlation between ambient parameters, electrical demand and the ratings of overhead lines. This approach also allows for critical evaluation of the required network ancillary services required to mitigate against conductor thermal overloads.

## 1.7 Thesis Outline

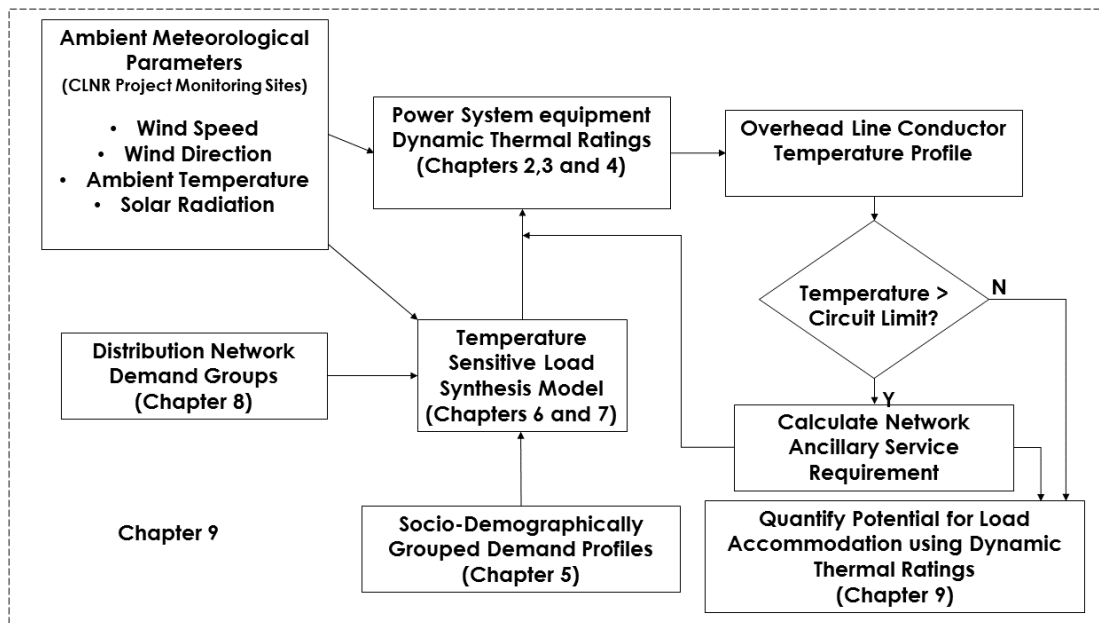


Figure 1-4 – Thesis Structure Block Diagram

Figure 1-4 shows a block diagram of the connections between the main thesis components. Within each chapter an additional block diagram is presented which provides greater details as to the inputs and outputs of each chapter. Concerning the research objectives and given the available data there are some limitations to the findings within the research presented in this thesis. Monitoring data used for testing and model selection procedures within this research are from real-world sites but represent a selection in themselves from a wider set of potential OHL monitoring points, or distribution network substations. Where possible, wider, publically available datasets have been integrated into the research, such as in the case of deriving the socio-demographically grouped demand profiles in Chapter 5, to provide a greater contribution to knowledge.

Chapter 2 discusses the use of RTTR and DTR technologies in the literature followed by a description of the modelling differences between the real-time and dynamic approaches.

Chapter 3 outlines a description of the available data from the test monitoring sites, including assessments of data quality and analysis of the ambient meteorological conditions. These are used to inform selection of the ‘worst case’ site to be used in further analysis steps. A verification study was also carried out to

ensure that the chosen DTR model provides sufficiently accurate results against data gathered at the sites.

Chapter 4 provides a discussion on the currently used OHL rating standard used in the UK. A recreation of the experimental method used to derive the ratings is carried out using the measured data gathered in the field. A set of new rating values are derived which meet the same level of network risk as is currently required.

Chapter 5 outlines a series of After Diversity Demand (ADD) models in order to derive expected demand values for any given number of consumers. These are informed by a series of socio-demographic indicators.

Chapter 6 discusses the relationship between ambient temperature and load for groups of distribution network consumers. In particular the correlation between these two variables is examined and is noted to be both time variable and also a significant function of the type of consumers within the group. The impact of a lack of correlation knowledge is also discussed. A generalised model is proposed for derivation of correlation coefficients for user-defined load group compositions. The accuracy of this model is discussed and its potential impact on the overall system error is also considered.

Chapter 7 builds on the temperature relationship work of Chapters 5 and 6 and presents a generalised temperature-sensitive MV feeder load synthesis method. These synthesised models are then used in conjunction with the DTR model discussed in Chapter 2 to determine the potential number of consumer connections, in comparison to the presently employed network rating standard. Based on these analyses the required energy and capacity budgets for network ancillary services are derived based on the season and time of day. A zonal method is proposed to categorise the resultant services.

Chapter 8 presents a clustering study of load group classifications carried out to determine a generic set of consumer load groups in order to test the capabilities of DTRs across a range of loading scenarios.

Chapter 9 presents an evaluation of the use of DTRs for load accommodation at the OHL monitoring site selected in Chapter 3. This Chapter utilises the temperature-sensitive load modelling procedure discussed in the previous Chapters.

Chapter 10 provides a discussion of the findings in the research and outlines the broader context into which they can contribute. Further work is also detailed and outlines some potential ways to extend and enhance the work presented in this thesis.

Chapter 11 gives the overall conclusions from the research presented in this thesis

## **1.8 Note on the Customer-Led Network Revolution Project**

The network monitoring and additional data presented in this thesis was gathered as part of the Customer-Led Network Revolution Project. This project was funded by Ofgem through the Low Carbon Networks Fund and represented a consortium between Northern Powergrid (UK DNO), British Gas (UK Energy Supplier) and the universities of Newcastle and Durham.

## 2 Dynamic and Real-Time Thermal Ratings

### 2.1 Introduction

As discussed in the previous Chapter, the techniques of RTTRs and DTRs have been shown to deliver increased network capacities. This Chapter provides additional information as to the available methods used to derive these ratings and the monitoring equipment which is required to do so. The concept of calculating the thermal behaviour of overhead lines is nothing new. Each OHL rating system currently employed throughout the world is fundamentally based on the same set of heat balance equations albeit with some variations. The key area in which present approaches differ from historic works is in the use of real-time monitoring equipment to subsequently deliver ratings in real time.

A series of British and International standards provide calculation methodologies for the thermal behaviour of various power system network components. In this thesis ratings of OHLs only will be considered, although similar methods for UGCs [56] and PTRs [57] are also available.

Whilst such methods outline the particular methods by which the thermal behaviour of components can be calculated, they do not constitute electrical standards for use by distribution or transmission network operators on their own. For this, in the UK, a series of Engineering Recommendations published by the Energy Networks Association (ENA) have been produced. These are ER P17 [58-60] and ER P27 [21], for UGCs and OHLs respectively. As of 2016 the standard for PTRs, ENA ER P15 [61] has been withdrawn. These documents provide the various ‘nameplate’ ratings which can be applied to the relevant components within distribution networks. Since asset longevity and security are seen as priority considerations the rating methodologies deliver highly conservative capacity ratings.

A set of seasonal ‘worst case’ meteorological conditions are used to derive the ratings for overhead lines, with a series of thermal insulation limits defining the rating ceilings for transformers and cables. For OHLs these conditions are intended to provide a statistically low level of risk, and to minimise the number of ‘conductor temperature excursions’. An excursion is defined as the percentage of

time for which a continuously loaded conductor may exceed its design temperature. The research of Price and Gibbon [22, 62] forms the basis of the ratings shown in ER P27 and attempts to statistically model various weather parameters and their influence upon the excursion of overhead conductors. A further discussion of the methods used in ER P27 can be found in Chapter 4.

### 2.1.1 Chapter Outline Block Diagram

Figure 2-1 a block diagram of the inputs, methods and outputs for this chapter. Since this chapter is concerned with background literature and definitions of the rating methods, the block diagram shows the differences between the dynamic and real-time thermal rating methods. Ambient meteorological parameters serve as inputs to the OHL thermal model delivering a maximum theoretical conductor loading at a particular point in time. In the dynamic implementation, synthesised or real values of electrical demand serve as inputs alongside the meteorological parameters in order to model the thermal response of the OHL to these inputs.

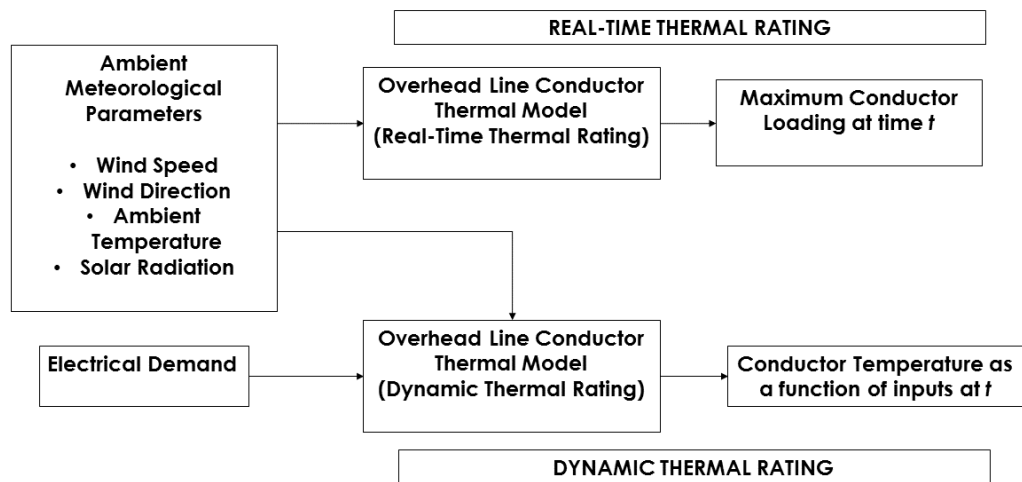


Figure 2-1 – Chapter 2 Block Diagram

## 2.2 Dynamic or Real-Time Thermal Ratings?

The terms Dynamic Thermal and Real-Time Thermal Ratings are often used interchangeably in the literature. The term ‘concurrent cooling’ has also been used

[63]. In this research, the following definitions have been used. The DTR can be represented as a differential equation modelling the components' reaction to step changes in variables with time. RTTRs provide a snapshot of the conductor's maximum possible current carrying capacity at that moment in time. The thermal time constant of the component is an important characteristic to consider when employing either methodology. The time constant of overhead lines is in the order of minutes, whereas the time constant of underground cables is in the order of many hours, if not days [64].

### 2.3 Conductor Thermal Rating Equations

The following sections outline the calculation methods used to determine both dynamic and real-time ratings of overhead lines. A series of potential methods have been developed for the derivation of such ratings, the most popular of which are the IEEE [65], IEC [66] and CIGRÉ [67] methods. In the IEC method no considerations are made with regard to wind direction incident upon the conductor; similarly natural convection is not taken into account. Work at Durham University modified the IEC method to take these factors into account [68]. As in multiple previous studies the CIGRÉ rating method will be used in this thesis. An evaluation of the differences between each methodology can be found in [69].

### 2.4 Heat Balance Equation

Solution of equation (3) gives the maximum steady state rating of the conductor for a specific set of meteorological conditions, termed the RTTR. Rearrangement of equation (4) gives the dynamic implementation of the heat balance equation and gives the temperature response of the conductor as a function of step changes in the input values and therefore the DTR.

$$Q_{joule} + Q_{sol} = Q_{conv} + Q_{rad} \quad (2)$$

$$I_{max} = \left[ \frac{(Q_{rad} + Q_{conv} - Q_{sol})}{R_T} \right]^{1/2} \quad (3)$$

$$I^2R = Q_{conv} + Q_{rad} - Q_{sol} + mC_p \frac{dT}{dt} \quad (4)$$

Where:

$Q_{joule}$  is the heat generated by the Joule effect (W/m)

$Q_{sol}$  is the solar heat gain by the conductor surface (W/m)

$Q_{rad}$  is the heat loss by radiation of the conductor (W/m)

$Q_{conv}$  is the convective heat loss (W/m)

$m$  is the mass of the conductor per metre (kg/m)

$C_p$  is the specific heat (J/kg°C)

$R_T$  is the electrical resistance of the conductor at a temperature  $T$  ( $\Omega/m$ )

$I$  is the conductor current (A)

$T$  is the conductor temperature (°C)

## 2.4.1 Heating elements

The heating elements within the heat balance equation are derived from the Joule effect, and the heat gain from incident solar irradiance upon the surface of the conductor.

### 2.4.1.1 Joule effect

The joule heating of the conductor is the product of the conductor's resistance and the square of the current supplied by the conductor.

$$Q_{joule} = R_T \cdot I^2 \quad (5)$$

### 2.4.1.2 Solar Heat Gain

The solar heat gain at the conductor surface is the product of solar intensity at the conductor, the rate of absorption of the incident solar irradiance and the outer diameter of the conductor.

$$Q_{sol} = \alpha \cdot S_r \cdot D \quad (6)$$

Where:

$\alpha$  is the solar radiation absorption coefficient

$S_r$  is the intensity of solar radiation (W/m<sup>2</sup>)

$D$  is the conductor outer diameter (m)

## 2.4.2 Cooling elements

The cooling elements of the heat balance equation are composed of both radiative and cooling elements. The radiated heat loss is a function of the emissivity of heat from the surface of the conductor, and the convective cooling of the conductor. This convection is either natural, at null or low wind speeds, or is modelled as forced convection for wind speeds above 0.5m/s.

### 2.4.2.1 Radiated Heat Loss

$$Q_{rad} = \varepsilon \cdot \sigma_{S-B} [(T_s + 273)^4 - (T_a + 273)^4] \cdot \pi \cdot D \quad (7)$$

Where:

$\sigma_{S-B}$  is the Stefan-Boltzmann constant (5.67 x 10<sup>-8</sup> W/m<sup>2</sup>/K<sup>4</sup>)

$\varepsilon$  is the emissivity coefficient with respect to a black body

$T_a$  is the ambient temperature (°C)

$T_s$  is the Conductor Surface Temperature (°C)

### 2.4.2.2 Convection Heat Loss

Equation (8) shows the overall calculation of the convective heat loss from the conductor. This requires the parameter of the dimensionless Nusselt number. The Nusselt number is calculated based upon the incident wind speed to the conductor. If the wind speed is equal to 0m/s then natural convection occurs at the conductor surface. If the wind speed is greater than 0m/s then forced convection occurs. For wind speeds < 0.5m/s an iterative procedure is carried out which will be detailed.

$$Q_{conv} = \pi \cdot Nu \cdot \lambda_f (T_c - T_a) \quad (8)$$

$$\lambda_f = 2.42 \cdot 10^{-2} + 7.2 \cdot 10^{-5} \cdot T_f \quad (9)$$

$$T_f = 0.5(T_s + T_a) \quad (10)$$

Where:

$Nu$  is the Nusselt Number

$\lambda_f$  is the thermal conductivity of the air film in contact with the conductor (W/mK)

$T_f$  is the average conductor temperature ( $^{\circ}\text{C}$ )

#### 2.4.2.2.1 Forced Convection

$$Nu = B_1(Re)^n \quad (11)$$

$$Re = \frac{\rho_r \cdot W_s \cdot D}{\nu} \quad (12)$$

$$\rho_r = \exp(-1.16 \cdot 10^4 \cdot y) \quad (13)$$

Where:

$B_1$  is a constant

$n$  is a constant

$\rho_r$  is the relative air density at conductor height ( $y$ )

$y$  is the conductor height above sea level (m)

$Re$  is the Reynolds number

$W_s$  is the wind speed (m/s)

$\nu$  is the kinematic viscosity of the air ( $\text{m}^2/\text{s}$ )

The values of  $B_1$  and  $n$  are determined by the conductor surface roughness  $R_f$ .

$$R_f = d/[2(D - 2d)] \quad (14)$$

Where:

$R_f$  is the conductor surface roughness

$d$  is the diameter of the conductor strands (m)

Surface	Re		B <sub>1</sub>	n
	From	To		
Stranded all surfaces	10 <sup>2</sup>	2.65 · 10 <sup>3</sup>	0.641	0.471
Stranded R <sub>f</sub> ≤ 0.05	>2.65 · 10 <sup>3</sup>	5 · 10 <sup>3</sup>	0.178	0.633
Stranded R <sub>f</sub> > 0.05	>2.65 · 10 <sup>3</sup>	5 · 10 <sup>3</sup>	0.048	0.800

Table 2-1 – Table of B<sub>1</sub> and n constants as a function of the Reynolds number and Conductor roughness values (R<sub>f</sub>)

#### 2.4.2.2.2 Correction of the Nusselt number for wind direction

The calculated Nusselt number must be corrected to take into account the incident wind direction. This is carried out as follows:

$$Nu_{\delta} = Nu_{\delta=90} [A_1 + B_2 (\sin \delta)^{m_1}] \quad (15)$$

Where:

$\delta$  is the incident angle of wind speed upon the conductor (°)

$\delta$		A <sub>1</sub>	B <sub>2</sub>	m <sub>1</sub>
From	To			
0	24	0.42	0.68	1.08
24	90	0.68	0.58	0.90

Table 2-2 – Selection of A<sub>1</sub> B<sub>2</sub> and m<sub>1</sub> constants based on the incident wind direction

#### 2.4.2.2.3 Natural Convection

$$Nu = A_2 (Gr \cdot Pr)^{m_2} \quad (16)$$

$$Gr = \frac{D^3 (T_s - T_a) g}{(T_f + 273) \nu^2} \quad (17)$$

$$Pr = 0.715 - 2.5 \cdot 10^{-4} \cdot T_f \quad (18)$$

Where:

A<sub>2</sub> is a constant

- $m_2$  is a constant
- $Gr$  is the Grashof Number
- $Pr$  is the Prandtl Number
- $g$  is the gravitational acceleration (m/s<sup>2</sup>)

$Gr \cdot Pr$		$A_2$	$m_2$
From	To		
10 <sup>2</sup>	10 <sup>4</sup>	0.850	0.188
10 <sup>4</sup>	10 <sup>6</sup>	0.480	0.250

Table 2-3 – Selection of  $A_2$  and  $m_2$  constants based on the value of  $Gr \cdot Pr$

#### 2.4.2.2.4 Selection of the Nusselt Number

Where the wind speed lies between 0 and 0.5 m/s an iterative procedure is carried out to determine the correct Nusselt number. Three values of the parameter are calculated with the largest then chosen from the derived values [67].

No incident wind direction is considered beyond that of 45° in this case and the first value is calculated at this wind direction using (15). In the second case a corrected value is calculated of  $0.55 \cdot Nu$ , calculated in (11). Finally the natural convection is calculated (16).

### 2.4.3 Additional parameters

#### 2.4.3.1 AC Resistance

The effective AC resistance is calculated from knowledge of the DC resistance at 20°C and compensating through equation (19).

$$R_{T_2} = R_{T_1} [1 + \alpha(T_{average} - 20)] \quad (19)$$

Where:

- $R_{T_1}$  is the DC resistance at temperature  $T_1$  (20°C)
- $R_{T_2}$  is the DC resistance at temperature  $T_2$
- $\alpha$  is the temperature coefficient of electrical resistance at  $T_1$

for A1 Aluminium:	$\alpha=0.00403 \text{ K}^{-1}$
for A2/A3 Aluminium:	$\alpha=0.00360 \text{ K}^{-1}$
for Copper:	$\alpha=0.00381 \text{ K}^{-1}$

The DC resistance is converted to the AC resistance by taking into account the skin effect. For non-ferrous conductors such as those at the OHL monitoring sites, the recommended value of  $k_j$ , the skin effect factor is 1.0123.

$$R_{AC} = k_j \cdot R_{DC} \quad (20)$$

#### **2.4.4 Iterative calculation of the conductor surface temperature**

Due to the radial temperature distribution of the conductor, an iterative procedure is used within the CIGRÉ heat balance model in order to correctly determine the conductor surface temperature. An initial guess is made as to the conductor surface temperature as a result of the line loading and ambient conditions. The radial temperature distribution is then calculated and alterations made to the final result.

#### **2.4.5 Conductor Sag**

Since the limiting factor of OHLs is maintaining the minimum required ground clearance, methods have been developed in order to determine the line sag and therefore the available ground clearance [70] [71]. Since in this research the conductor temperature limits which are currently in place have not been exceeded the sag of the conductor was not calculated. The equations to derive this parameter are detailed in [68].

## 2.4.6 CIGRÉ Rating Model Sensitivity Analysis

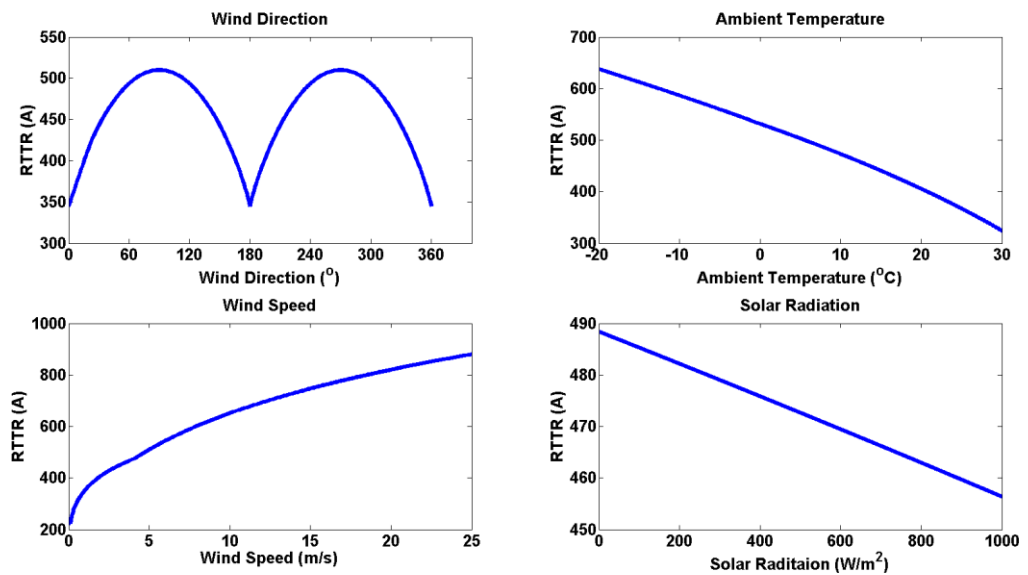


Figure 2-2 – CIGRÉ model input parameter sensitivity analysis

Figure 2-2 shows the results of a sensitivity analysis study on the CIGRÉ heat balance model. Previously, similar analyses have been presented in a tabular form [68], however it was felt that a graphical representation aids understanding of the influence of each meteorological input parameter on the CIGRÉ model. When considering the effect of each input parameter independently, all other parameters are fixed at a chosen representative value:

- *Wind Speed – 4 m/s*
- *Wind Direction – 45°*
- *Solar Radiation – 500 W/m<sup>2</sup>*
- *Ambient Temperature – 10°C*

As can be seen in Figure 2-2 wind speed has the greatest overall influence on the resultant values of RTTR, with solar radiation exhibiting the least overall effect.

## 2.5 Overhead Line Rating Literature

Some of the earliest work on the calculation of real-time thermal ratings of overhead lines can be found in [72, 73]. These papers provide highly detailed information on components of the conductor heat balance equation in addition to theoretical diagrams for wide-area system implementation. Davis outlines his justification for adoption of the RTTR methodology in [14], defines the heat balance

equation in [15] and provides a complete methodology for calculating the effects of solar radiation on thermal rating in [16]. Similar presentations of heat balance equations in both the real-time and dynamic forms can be found in [74]. The work of Morgan [75-77] also provides detailed information on convective and conductive heat transfer at the conductor surface. This work heavily influenced that of Price and Gibbon [62].

## **2.6 Categorisation of RTTR Technologies**

Within the field of DTRs and RTTRs there a number of potential technologies and method which have been used for their derivation. Jupe [78] and Fernandez [23] have provided state of the art reviews of the various techniques to calculate a real-time thermal rating in the case of overhead lines.

### **2.6.1 Weather monitoring**

As shown in equations (2) to (18) the convective and radiative cooling and solar heating elements of the OHL rating are functions of the ambient temperature, wind speed, wind direction and incident solar radiation surrounding the conductor. By placing monitoring instruments at OHL spans, determination of the rating can be made through the use of equations (2)-(20). Such methods are categorised as weather derived ratings.

The majority of research concerning RTTRs and DTRs has used this method, although it is not the only available method as will be shown. Work carried out at Durham University analysed such an approach on a section of 132kV OHL in North Wales. This study analysed the potential benefits that an RTTR system could bring to increasing the network's capacity for wind generation connections as has been a typical implementation of this technology [28, 79, 80]. Due to the variability of weather conditions over a typical area of distribution network, a number of potential methods have been proposed. The simplest, however also representing the highest capital cost would be to implement monitoring equipment at each span of the desired OHL section.

Alternatively, inverse distance interpolation methods have been used in [32, 68] to make estimations of ratings across a wide area are made. In [81] assumptions are made that over wide areas, a particular span will be oriented

parallel to incident wind speeds at any one point, resulting in minimum ratings. The ratings for a set of spans along a line can therefore be reduced to one single estimate using appropriate weather distributions.

Foss and Maraio [82] outline two differing deterministic approaches to calculating the real-time rating of an overhead conductor; weather derived and conductor temperature derived. The advantages and disadvantages of each methodology are commented upon in [21]. Weather derived ratings are stated to rely heavily on wind speed data where errors in measurement at low wind speeds have significant effects upon the rating. However, the weather derived method delivers a greater accuracy of rating at higher wind speeds. Conductor temperature ratings are inaccurate under low loading and/or if the difference between conductor and ambient temperature is small. The implications of conductor temperature monitoring may be more applicable to the calculation of the critical span of a particular section of overhead line. This information would undoubtedly be useful to network planners/operators.

McElvain and Mulnix have attempted to refine the traditionally implemented seasonal static ratings through generation of probability and cumulative density functions of conductor ratings for a singular site-trial network [83]. In particular they draw attention to the fact that statistical approaches as such those developed by Price and Gibbon were carried out in a period of reduced computational ability, therefore with the more advanced techniques now available, increased levels of analysis are possible.

### **2.6.2 Conductor Temperature and tension monitoring**

A number of systems exist which can be attached to the OHL itself to deliver values of conductor temperature directly. An early implementation of such technologies can be found in [84]. As noted in [23] only one commercial system exists which uses tension directly as a measure of available capacity [85]. Devices are located at both ends of the conductor span which is to be rated. The mechanical tension in the conductor is measured from which a conductor temperature and therefore sag, can be calculated. This system has potential benefits over alternatives since it is insensitive to ambient measurement or modelling errors.

### **2.6.3 Sag monitoring**

Since the limiting factor of OHLs is in maintaining spans which do not sag below the minimum required ground clearance, a number of methods have been proposed which determine this component directly. Perhaps the most commonly implemented version of this solution is that of the Ampacimon system [86-88]. This system uses vibrational harmonics to determine the conductor span directly, with this information being directly related to a network operator as part of an automated system. Sag has also been determined through the use of GPS techniques as in [89].

### **2.6.4 Real-Time Thermal Ratings as part of an ANM scheme**

Whilst RTTRs have been shown to deliver improvements over the presently implemented static thermal rating assumptions such improvements cannot exist in isolation. The purpose of the presently implemented standards is such that they are essentially fit and forget. The level of expected risk in exceeding a conductor thermal limit is such as to be considered negligible. If RTTRs and DTRs are to be utilised fully in the modern power system, additional methods of network control will be required. RTTRs have been studied as part of a wider Active Network Management (ANM) scheme in [33, 34] and in [90, 91].

### **2.6.5 Real-Time Thermal Ratings for increased system reliability**

The potential for the use of RTTRs as a method to increase system reliability has been considered in [35, 36, 47, 48, 92]. Two common methodologies have been presented for the assessment of RTTRs in their ability to supply load. These are the Loss of Load Expectation (LOLE) [35] and Expected Energy not Supplied (EENS) [36, 47, 48]. The use of these methods have shown considerable improvements over the presently implemented seasonal circuit ratings. These will be discussed in greater detail in Chapter 9.

As discussed in the Introduction section of this thesis, whilst Real-Time and Dynamic ratings have been shown to deliver increased network headroom, there is also the potential that due to their real-time nature, combined with the

assumptions of the presently implemented planning standard, that ratings have been observed which are lower than the presently implemented ratings. In the case of EENS, some OHL sections have shown  $\approx 25\%$  decreases in performance against the current OHL rating standard [47].

### **2.6.6 Load Modelling in Real-Time Thermal Rating analyses**

In [35, 36] a Monte Carlo type simulation has been carried out to predict network load values and determine the EENS and LOLE figures in these cases. These simulations have been noted as not taking into account the true correlation between load and the resultant thermal ratings. [47] tests the impact of loads significantly increased over those which are expected in order to test the potential capacity increases of RTTRs in various simulated network failure states.

In [93] an Autoregressive model with exogenous inputs (ARX) is used to forecast feeder loads as part of an assessment of RTTR capabilities, though the core aspect of this research is in its analysis of the potential network benefits for DG.

The research in this thesis will contribute towards a greater understanding of the benefits of Dynamic and Real-Time Thermal Ratings where time-series models as opposed to pure forecasts of feeder loads are used as inputs.

## **2.7 Forecasting of DTRs and RTTRs**

As discussed previously, RTTRs and DTRs cannot exist in isolation. Whilst studies such as those in [35, 36] outline the potential benefits of such a system in the planning domain, real-time operation of the power system must also be considered. In real-time operation as conditions vary, forecasting of the RTTRs, will assist economic scheduling and operation of the power system. Examples of forecasting RTTRs have typically made use of publically available forecasts [94-96] [97, 98], as opposed to development of a stand-alone forecasting method.

## **2.8 Real-Time Thermal Ratings as a response to Climate Change**

As climate scenarios such as those in the UKCP09 predictions [99] predict increases in both ambient temperature and wind speeds RTTRs have also been

considered as a method to remove the potential risks of the continued implementation of historical standards [100, 101].

## **2.9 Conclusions**

This Chapter has provided an outline of the meaning behind the terms of Real-Time and Dynamic thermal ratings for OHLs. The fundamental processes used to derive these ratings have also been shown.

Details have been provided as to the current state of the art in this field of research to which this thesis will contribute. Predominantly these techniques have been used to enable additional network capacity for wind generation connections. This research differs in both its examination of the use of dynamic thermal ratings to deliver additional capacity for load, and also in the approach taken with regards to the modelling of network loads.

### **3 Overhead Line Monitoring Site Analysis**

#### **3.1 Introduction**

In this research, meteorological and line data parameters have been gathered from five OHL monitoring sites installed as part of the CLNR project. These sites were installed on a radial 20kV distribution line of wood pole construction. A preliminary assessment of the meteorological and conductor parameters of the available OHL monitoring sites was made in order to:

- Determine the worst case scenario monitoring point from those available
- Validate the chosen dynamic thermal ratings approach

Before the commencement of this research a study was carried out to determine the locations for installation of the OHL monitoring equipment on the test network. This analysis was carried out prior to the commencing of this research by a consultancy, EA Technology. Locational decisions were made based on the relative degree of shading of the OHL but also in relation to the issue of site access. In order to install and maintain the equipment, OHL spans close to roads or access tracks were necessary.

In order to critically evaluate the potential of RTTRs and DTRs in the distribution network it is important to ensure that the data used as inputs to any models or simulations are of a worst-case scenario as is possible. In this context, the worst-case scenario refers to a geographic location along the length of the OHL which is likely to be unfavourable to capacity increases from either RTTRs or DTRs. This is likely to be a location with a high degree of shading, thus resulting in minimal cooling from incident wind speeds and potentially high ambient temperatures as a result of the reduced air flow.

Within the domain of RTTRs and DTRs for OHLs there is often a reference to the critical span of a network section. This can refer to the OHL span which has typically experiences the lowest rating, or can refer simply to the span with the lowest rating at a singular point in time. Clearly within the second definition of this parameter, there is the potential that the critical span can change as a

function of time. Since this research does not intend to contribute to the particular field of determining the critical span of a network section, the site which shows the worst-case potential from those available has been estimated and then used in the subsequent analyses.

Some of the content of this chapter is publically available as an output report from the Customer Led Network revolution project in [102].

## **3.2 Chapter Goals / Objectives and Contributions**

### **3.2.1 Goals / Objectives**

- Analyse data from the 20kV Overhead Line monitoring sites from the CLNR project
- Determine the site which presents the smallest uplift from the utilisation of RTTRs in order to provide inputs to a critical evaluation of the technique for load introduction.

### **3.2.2 Transition from existing literature and research / Contribution**

Previous academic literature has not examined the potential uplifts from the introduction of RTTRs at the 20kV rural distribution level. This Chapter provides this analysis and contributes additional research in its data analysis of the available ambient monitoring parameters.

### **3.2.3 Attainment of Goals**

Data analysis showed interesting results given the potential increases over the existing OHL ratings. The most sheltered site was identified from the data analysis carried out to provide suitable inputs to the further analysis within this research.

### **3.2.4 Chapter Outline Block Diagram**

Figure 3-1 a block diagram of the inputs, methods and outputs for this chapter. The red-dashed box represents the use of existing methods but utilising new monitored data. The use of this new dataset (analysis of OHL RTTRs for a set of 20kV rural monitoring sites) introduces a piece of novel analysis representing a

contribution to the wider community. As seen in the diagram key, boxes with a solid red outer line represent the contributions to knowledge made within the Chapter. This approach of identification has been continued within the block diagrams for each of the following chapters.

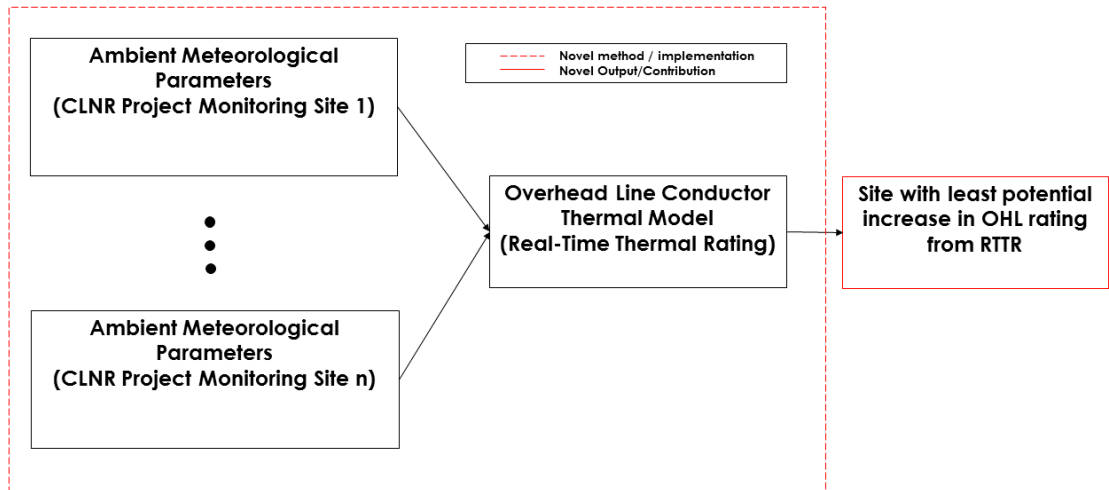


Figure 3-1 – Chapter 3 Block Diagram

### 3.3 Site Description



Figure 3-2 – OHL MV monitoring site locations

Figure 3-2 shows the location of the OHL monitoring sites on the MV system overlaid on an Ordnance Survey map of the wider area. The monitoring sites are shown as red dots. The area is predominantly rural with the significant load groups being found in Alnwick, shown just below centre in Figure 3-2 and Wooler towards the NW of the map.

### 3.3.1 Overhead Line Construction

At all of the 20kV monitoring sites the overhead lines construction is of the same type, a 0.1in<sup>2</sup> Copper conductor. This conductor is made up of 7 strands and is homogenous throughout, i.e. there are no dissimilar core materials. Table 3-1 shows the relevant conductor parameters used in (20) in order to calculate the conductor thermal ratings. The emissivity and absorptivity values were not known for the conductor exactly. The worst case conditions have therefore been implemented for both parameters.

Conductor Parameters	Values
Outer Diameter (mm)	10.4
Wire Diameter (mm)	3.45
Number of Strands	7
m	0.7552
C <sub>p</sub>	383
DC Resistance (Ω) (@20°C)	0.000273
Emissivity (ε)	0.9
Absorptivity (α)	0.9

Table 3-1 – OHL Conductor Parameters

### 3.3.2 Site Monitoring Equipment

At each of the RTTR monitoring sites a series of sensors to gather both conductor and ambient meteorological parameters have been installed. The ambient conditions monitored are:

- Air Temperature (°C)
- Wind Speed (m/s)

- Solar Radiation (W/m<sup>2</sup>)
- Wind Direction (°)

Three measurements are made using equipment installed on the span itself:

- Conductor core temperature (°C)
- L1,2,3 Phase currents (A)
- Conductor surface temperature (°C)

The ambient sensors at the 20kV locations are installed on the circuit's wooden pole at a height of roughly 10m. The conductor parameters are measured using clamp located on the OHL span itself. The conductor core measurements are taken by drilling into the conductor and securing a probe as close as possible to the core. The surface temperature measurements are taken using a probe bonded to the surface with an exposed section to ensure an accurate reading

The ambient monitoring equipment is powered from a solar panel mounted to the top of the sensor cabinet. The conductor sensor is powered from the line itself. Figure 3-3 shows an example of one of the monitoring sites. Information from the sensors was relayed to a central server via GPRS which collated all of the monitoring data from the CLNR project.



**Figure 3-3 – An example of an HV Thermal rating monitoring site. Note the clamps attached to the OHL itself recording phase current and conductor core and surface temperatures**

### **3.3.3 Monitoring Instrumentation Accuracy**

Each of the ambient monitoring sensors has associated with it a particular measurement error value. These are as follows:

- Ambient Temperature  $\pm 0.1^{\circ}\text{C}$
- Wind Speed  $\pm 1\text{m/s}$
- Wind Direction  $\pm 4^{\circ}$
- Solar Radiation  $\pm 5\%$

These impact of these tolerances will be commented upon when the DTR implementation of the OHL model is used in the Chapter 9 of this thesis. For all

other analyses the measured data has been used as inputs to the models with no upper and lower bounds regarding the measurements.

### 3.4 Monitoring Sites

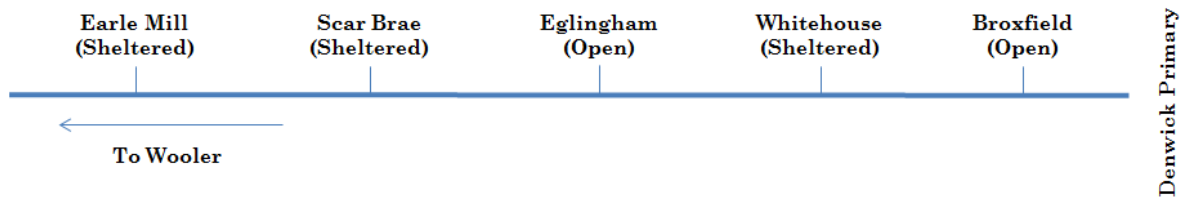


Figure 3-4 – HV RTTR Monitoring Locations

The RTTR monitoring devices installed on the HV system are located at 5 separate spans along the length of the overhead line. Only four of the devices record data at any point in time. As detailed in the introduction, the device at the ‘Eglingham’ span was relocated to ‘Earle Mill’ roughly 14 months into the trial period. Within the context of this thesis the term ‘open’ refers to the site being ‘non-sheltered’.

	Broxfield	Whitehouse	Eglingham	Scar Brae	Earle Mill
Conductor Height above Sea Level (m)	100	85	130	65	75

Table 3-2 – HV Conductor Heights

Table 3-2 shows the relative heights of the conductor monitoring sites above sea level. These values are used in equation (13) in order to correctly model the relative air density at each site. Data from the HV RTTR trials covers the period March 2012 - end June 2014 with observations recorded at 5 minute intervals. The relocation of the ‘Eglingham site took place in April 2013.

	Winter	Spring / Autumn	Summer
HV Overhead Line P27 Static Rating (A)	296	275	237

**Table 3-3 – HV overhead line P27 static ratings**

Table 3-3 shows the presently used P27 static overhead line thermal ratings and the seasonal periods for which they are valid. The months in each of these seasonal periods are as follows:

- Winter - December, January, February
- Spring Autumn –March, April, September, October, November
- Summer – May, June, July, August

These ratings are derived from work at CERL in the late 1970's [103]. This method generates ratings based on a probabilistic method related to the risk of conductor's exceeding their circuit rated temperature as a result of increased loads. This method will be discussed in greater detail in Chapter 4.

### **3.5 Validation – Data Quality and Instrumentation**

Data quality is an important aspect of RTTR or DTR system implementation. Ratings will be used to inform both operational and planning decisions; errors in these decisions due to poor data quality are likely to incur significant, avoidable costs and could lead to under or over estimation of the capabilities of the system.

Three states of operation have been defined for the monitoring sites during each sampling period, these so-called '*site states*' are:

1. All possible measurements are recorded
2. Some but not all measurements are recorded
3. No data is recorded

These states can be further broken down into the number of measurements made for both the ambient and line parameters separately. Since the two systems are not physically connected there is the potential for one of the sensors to malfunction whilst the other remains operational. For the purposes of this analysis sites are analysed both independently and also as a complete set. I.e. in the best case scenario for data quality (as far as measurements recorded is concerned) all 4 sites record all of their possible measurements at each sampling period. The

purpose of presenting such analysis is to infer the availability of real-time or dynamic thermal ratings. Since such ratings are derived as a function of available measurements, if there are significant periods in time where instrumentation has failed to record data, then additional research may be required as to methods to compensate for these periods, in order to deliver a reliable, available increase in network headroom. This analysis could also impact the requirements for redundancy when considering implementing such a system as part of business as usual network operation.

There is a wider point to be made in that if one site along the line can generate a rating, this could potentially be used with some interpolation to ‘fill the gaps’ at the remaining sites such as in [68], or if the single site recording data was considered to be the ‘critical span’ of the overhead line, then this rating should simply be the limiting factor for the circuit. These issues will not be considered within this work as they have been declared as out of scope. Since there are 4 monitoring sites for each of the systems and there are 3 possible states of operation, there are potentially 81 possible combinations of all the sites together i.e.

- *All sites record all measurements*
- *3 sites record all measurements; one site records some data*
- *3 sites record all measurements; one site records no data etc...*

The combinations of ‘*site states*’ can be further grouped to infer various ‘*system states*’ as a whole.

- All data is recorded at all of the sites.
- Some or all data is recorded for at least one site (i.e. the only combination not included is a total lack of data at all sites)
- Where no data is recorded at all of the sites, a total mobile network failure (i.e. GPRS) has occurred, all sites are out for maintenance, or a problem exists with the server which is to receive the measurements.
- Where some data is recorded, either at all sites or some of the sites, a local equipment failure is most likely, leading to a lack of particular measurement(s).
- Where no data is recorded at one or more (but not all) sites, a local mobile network failure is most likely. A total failure of all measurement devices was thought to be unlikely, though this may be an erroneous conclusion.

Clearly there is likely to be some overlap when considering the breakdown of sites into categories. Where a local equipment failure occurs at one site, the

remaining sites could record all, some or no measurements, and will therefore be included when considering those permutations. However the overall percentages remain accurate and are intended to provide a guide as to the quality of the data recorded.

### 3.6 Data Quality Study Results – Missing Parameter Values

#### 3.6.1 Ambient Monitoring Parameters

Table 3-4 shows the results of the ambient parameters data quality study. There are 5 ambient parameter measurements, Ambient Temperature, Wind Speed, Average Wind Speed, Solar Radiation and Wind Direction. As can be seen, the number of data points at which all 5 measurements are not recorded is significantly higher than the times where only 1 or two measurements are not recorded.

Parameters Missing	1 (%)	2 (%)	3 (%)	4 (%)	5 (%)
Broxfield (Site 1)	0.010	0	0	0	8.927
Whitehouse (Site 2)	0.026	0	0	0	25.614
Eglingham (Site 3)	0.005	0	0	0	17.005
Scar Brae (Site 4)	0.003	0	0	0	19.912
Earle Mill (Site 5)	0.004	0.001	0	0	68.413

**Table 3-4 – Data Quality Study Results – Ambient Monitoring Parameters**

In order to allow for a more visual representation of these findings, this data is also shown as a histogram in Figure 3-5. This histogram clearly highlights the significant result that the most typical system failure state regarding the ambient monitoring parameters, is where all measurements have failed to be recorded.

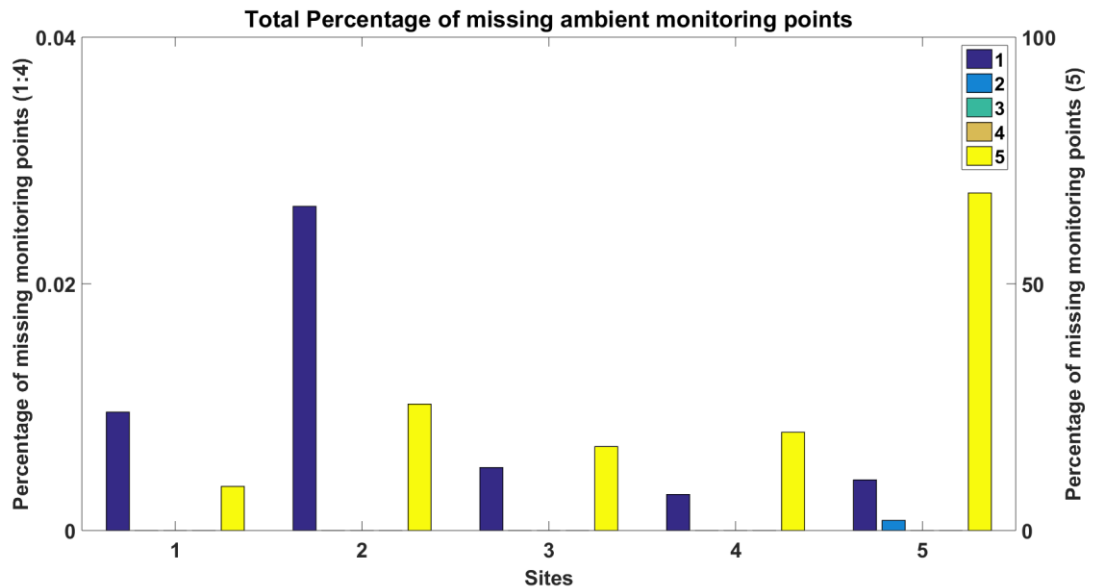


Figure 3-5 – Histogram of percentage missing ambient monitoring points

### 3.6.2 Line monitoring parameters

Table 3-5 shows the same analysis carried out as previously but for the line monitoring parameters, these are the average line phase current, and the surface and core temperature measurements of the conductor. In the case of the line parameters it is shown that is more likely for one or all of the measurements to not be recorded with the instances of two measurements being made being far lower.

Parameters Missing	1 (%)	2 (%)	3 (%)
Broxfield (Site 1)	40.227	1.280	8.813
Whitehouse (Site 2)	24.322	1.444	25.437
Eglingham (Site 3)	17.752	2.237	15.711
Scar Brae (Site 4)	33.975	2.031	19.782
Earle Mill (Site 5)	26.544	0.147	48.561

Table 3-5 - Data Quality Study Results – Line Monitoring Parameters

Again as per the ambient monitoring failure states, this information is shown as a histogram in Figure 3-6. For data concerning line parameter measurement

failures, the most common states are clearly shown as where either one or three parameters have failed to be recorded.

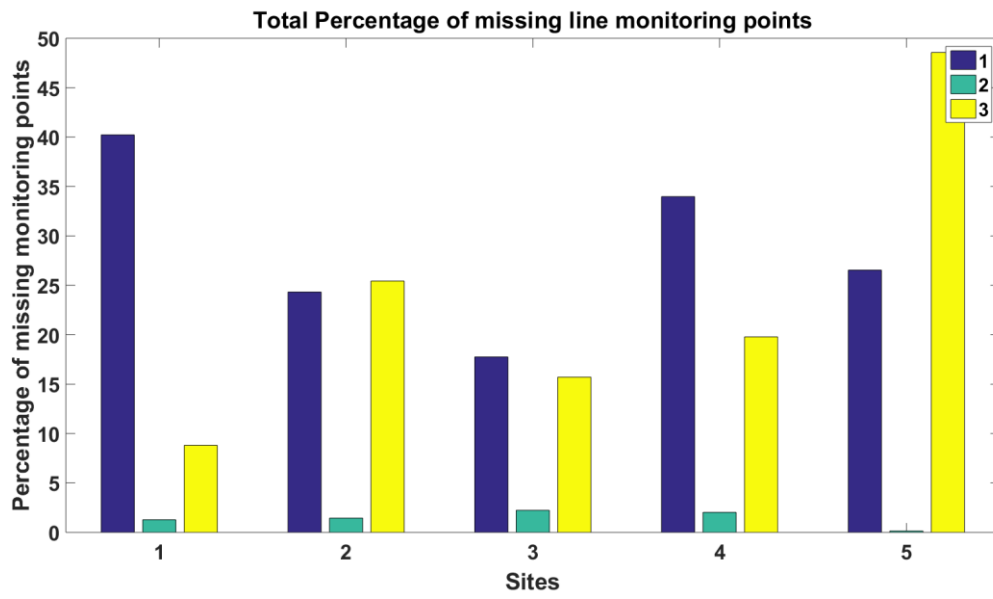


Figure 3-6 – Histogram of percentage missing line monitoring poin

### 3.7 Data Quality Study Results – Site States

	Scar Brae			Earle Mill		
	All Data	Some Data	No Data	All Data	Some Data	No Data
Winter	86.9	86.9	13.1	0.1	0.1	99.9
Spring/Autumn	74.8	74.8	25.2	20.5	20.5	79.5
Summer	82.5	82.5	17.5	60.2	60.2	39.8

Table 3-6 shows the three system states analysed per P27 seasonal rating period. As can be seen, significant quantities of data are not monitored at the Earle Mill site. It was known that after relocation from Eglingham that the site malfunctioned and large quantities of measurements were lost or not recorded. For the purposes of the final stage of the data quality analysis this site was therefore excluded from further analysis regarding the total number of measured parameters across each site.

	Broxfield			Whitehouse			Eglingham		
	All Data	Some Data	No Data	All Data	Some Data	No Data	All Data	Some Data	No Data
Winter	76.9	76.9	23.1	86.1	86.2	13.8	86.7	86.7	13.3
Spring/Autumn	91.2	91.2	8.8	66.8	66.8	33.2	75.8	75.8	24.2
Summer	99.8	99.8	0.2	76.6	76.6	23.4	91.8	91.8	8.2

	Scar Brae			Earle Mill		
	All Data	Some Data	No Data	All Data	Some Data	No Data
Winter	86.9	86.9	13.1	0.1	0.1	99.9
Spring/Autumn	74.8	74.8	25.2	20.5	20.5	79.5
Summer	82.5	82.5	17.5	60.2	60.2	39.8

**Table 3-6 - Seasonal Data Quality at all HV RTTR Monitoring points**

### 3.8 Data Quality Study Results – System States

Figure 3-7 shows the percentages of total missing parameters when considering the system as a whole. Zero parameters missing refers to all sites monitoring data at a particular point in time. These results differ from those previously presented in as such that now all sites are now considered in combination, with the maximum possible number of missing monitoring parameters being twenty at any point in time. The probability of all sites monitoring all data at the same point in time is shown as being lower, and in some cases significantly lower than the percentage of a particular seasonal period for which each individual site measures and records all possible data.

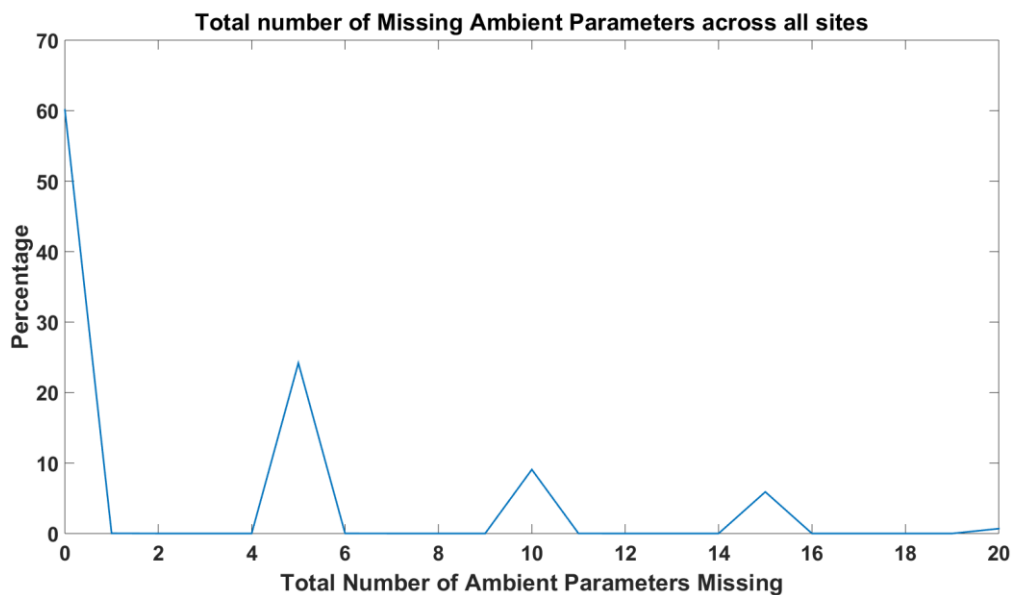


Figure 3-7 – Total number of missing ambient parameters at all sites at the same points in time

The peaks in Table 3-7 are directly influenced by the information shown in Figure 3-5 which shows that the most likely states for missing parameters is to either have one parameter or all parameters missing. As was also shown in Figure 3-5 the percentage of times where one parameter is missing relative to all missing is exposed by the significant peaks at multiples of 5 in Figure 3-7 with almost no data in between.

Total number of Ambient Parameters Missing	Percentage of total data monitoring period (%)
0	60.1075
1	0.0234
2	0.0000
3	0.0000
4	0.0000
5	24.1924
6	0.0129
7	0.0004
8	0.0000
9	0.0000
10	9.0744
11	0.0038
12	0.0000
13	0.0000
14	0.0000
15	5.9005
16	0.0004
17	0.0000
18	0.0000
19	0.0000
20	0.6843

**Table 3-7 - Percentage of total period for which combinations of ambient parameters are missing at each sample point**

Figure 3-8 shows the same analysis as carried out previously but for the line parameters. As can be seen, the percentage of data points for which one or three parameters are missing was typically between 15 and 40% of the monitored period (excluding the site at Earle Mill). Since these percentages are relatively high, their coincidence results in greater percentage combinations of missing parameters. Again as per the ambient parameter measurements, the largest data spike occurs when all data points are measured at all sites.

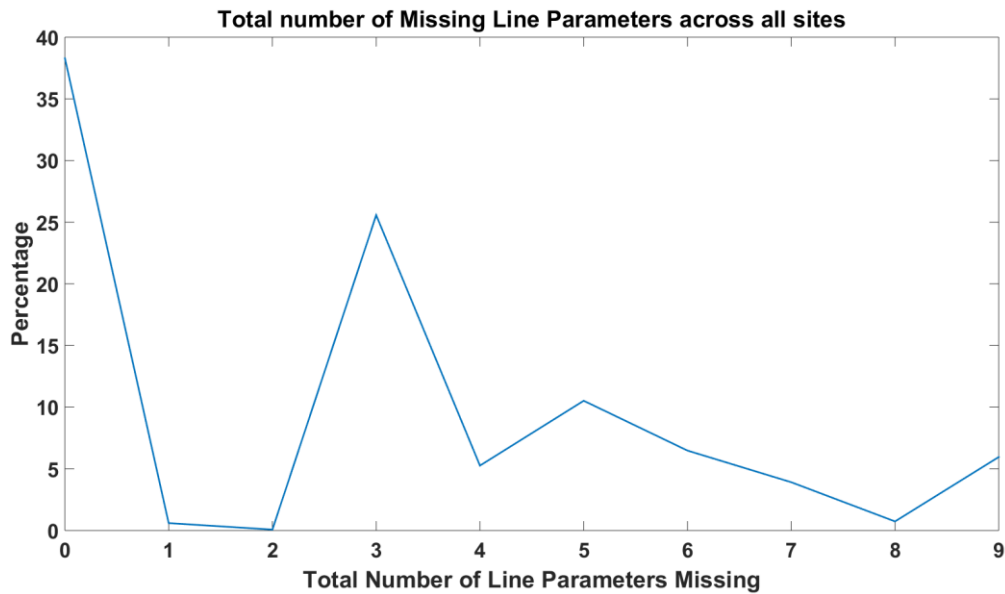


Figure 3-8 – Total number of missing line parameters across all monitoring sites

As opposed to the ambient measured parameters, combinations of one, or all line parameters not being recorded have almost equal likelihood. Since Figure 3-8 represents a combination of missing parameters across all sites, the trends observed in Figure 3-8 are somewhat different. The dominant failure states regarding ambient parameters results in obvious peaks at multiples of all ambient parameters not being present. Where line parameters are concerned, the trend is less clear, although there are peaks where combinations of one or all line parameters were not recorded.

Total number of Line Parameters Missing	Percentage of total data monitoring period (%)
0	38.29
1	0.60
2	0.07
3	25.57
4	5.26
5	10.52
6	6.48
7	3.91
8	0.734
9	5.96

Table 3-8 – Percentage of total period for which combinations of line parameters are missing at each sample point

### **3.8.1 Conclusions of Data Quality Analysis**

This data analysis study has shown that the most commonly occurring failures to measure data points concerning ambient and line parameters using the FMC Tech system affect either one or all of the parameters. Failure to monitor all measurements is likely to be a function of the local network system as opposed to intermittent failures of each independent monitoring device.

Provision of reliable communications infrastructure is key to delivery of the smart grid transition. As shown in Figure 3-5 the highest numbers of times for which all monitoring points are missing are at the sheltered sites. Since these are likely the results of GPRS network 'drop outs' as opposed to common mode sensor failures, careful consideration must be made as to the available GPRS network strengths at each location for which a DTR solution is considered, or as to whether such a data transfer solution is suitable to ensure overall reliability of the system.

### **3.9 Weather Parameter Distributions**

In this section, the distribution of the observed weather parameters used to derive the RTTR values will be discussed. In the case of the ambient temperature and wind speed values these are shown as probability distributions. For wind direction a series of wind roses have been produced. Since the wind roses also provide distributions of wind speed values, the results shown in Sections 3.9.1.1 to 3.9.1.3 are simply to represent the distributions according to the line rating periods.

It is important to note that since the wind directions used by the RTTR calculations are concerned only with the direction of the wind incident on the conductor, the angles shown in the wind roses are relative to the individual spans where the monitoring devices are located as opposed to relative to 0°.

For solar radiation, the 5<sup>th</sup>, 50<sup>th</sup> and 95<sup>th</sup> percentiles of the observed solar radiations at each measurement sampling period have been generated; again for each of the P27 rating periods. Due to the number of combinations of monitoring sites, percentiles and rating periods, a sample of the derived results for solar radiation are presented in this section. The remaining results can be found in the accompanying appendices.

### 3.9.1 HV OHL Monitoring Sites – Wind Speed

In each of the wind speed probability distributions the bin width was set to 0.5m/s.

#### 3.9.1.1 Winter

Figure 3-9 shows the wind speed distribution for each of the OHL monitoring sites. The highest observed wind speeds across the dataset were observed during the Winter period, with the lowest wind speed values being observed at the sheltered sites as expected.

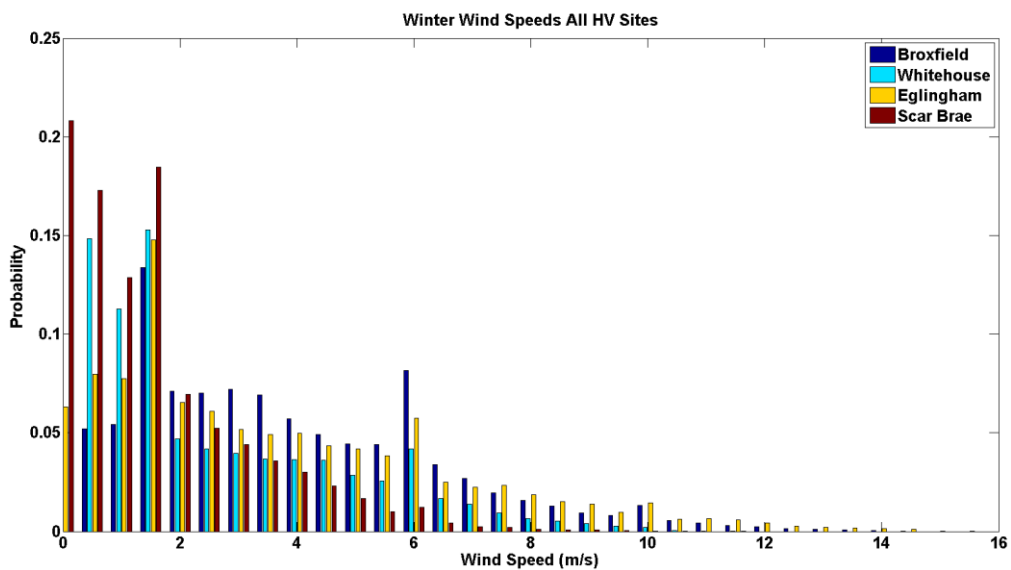


Figure 3-9 – Winter Wind Speed Probability Distribution – All HV Sites

#### 3.9.1.2 Spring / Autumn

As per the Winter analysis, wind speeds are observed as smallest during the Spring / Autumn period at the most sheltered sites. This seasonal period also shows the introduction of data from the monitoring site at Earle Mill. The probability of observing a wind speed of 0m/s is roughly 0.3 at the site of Scar Brae, resulting in a high probability of reduced potential uplift from RTTR at this site.

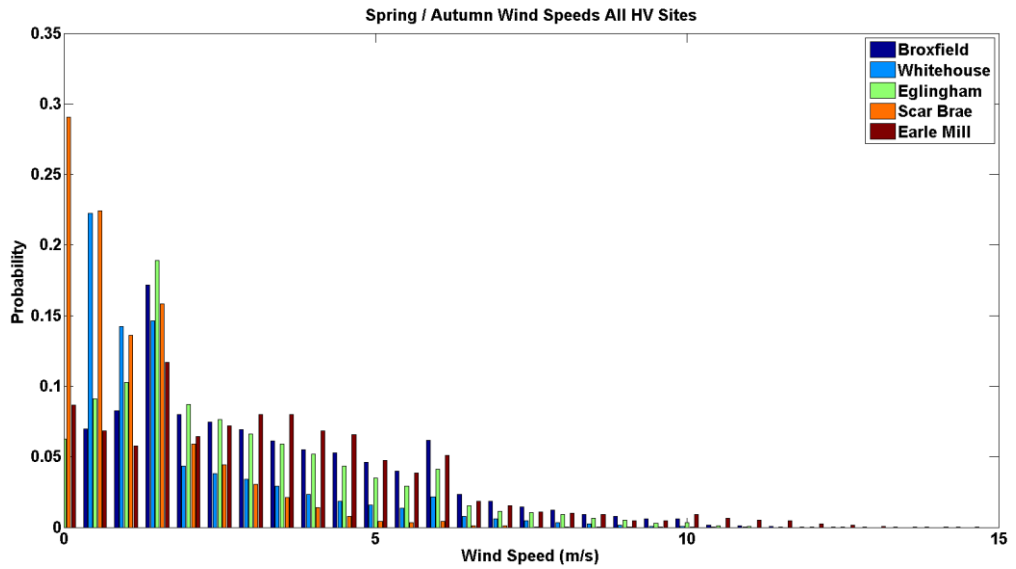


Figure 3-10 – Spring / Autumn Wind Speed Probability Distribution – All HV Sites

### 3.9.1.3 Summer

The smallest range of wind speeds is observed during the Summer period across all monitoring sites. The probability of 0m/s wind speeds exceeds 0.3 at both the Scar Brae and Earle Mill monitoring sites.

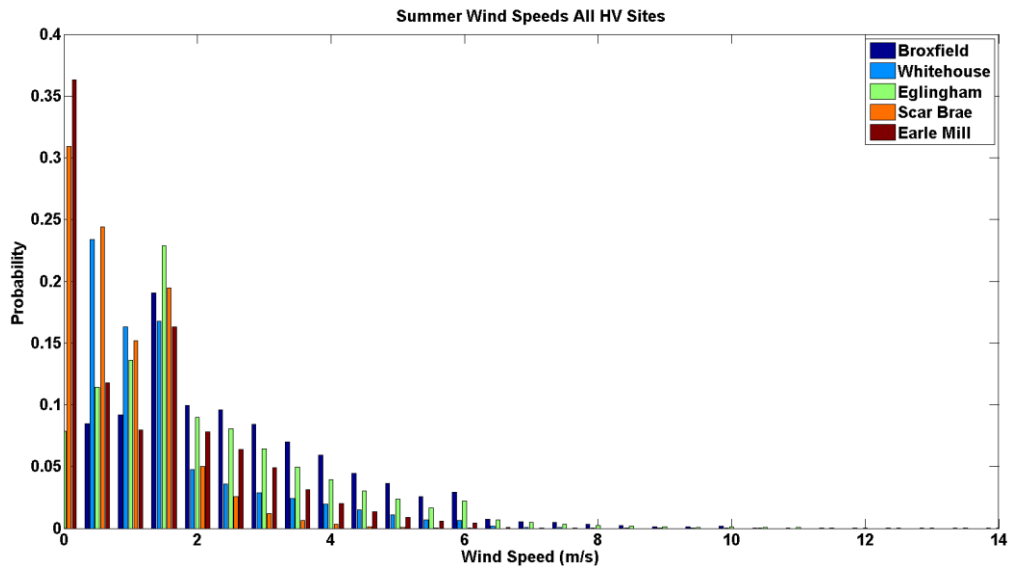


Figure 3-11 - Summer Wind Speed Probability Distribution – All HV Sites

### 3.9.2 HV Monitoring Sites – Ambient Temperature

#### 3.9.2.1 Winter

As expected, within the Winter period, the maximum recorded ambient temperature values are at a minimum across the set of rating periods. The sheltered monitoring sites show ambient temperature values which are typically increased over those open sites, reinforcing their candidacy for the most reduced uplift from RTTRs. These high temperatures are likely as the result of the coincident low wind speeds leading to stagnation.

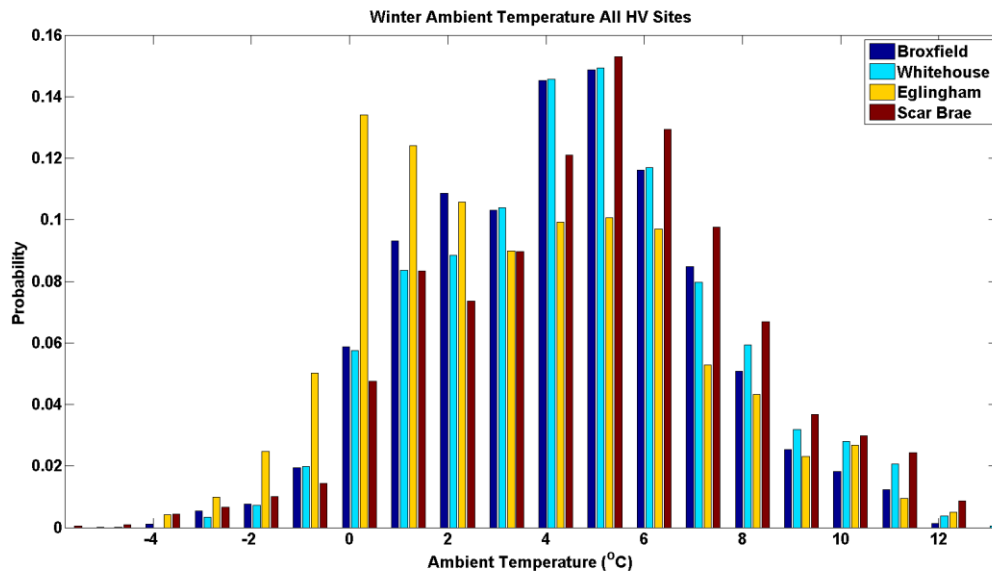


Figure 3-12 - Winter Ambient Temperature Probability Distribution – All HV Sites

#### 3.9.2.2 Spring / Autumn

As in the case of the Winter period, ambient temperature values are typically observed to be higher at the sheltered sites in the Spring / Autumn period. The Eglingham monitoring site in particular has significant probability of low temperatures during this period.

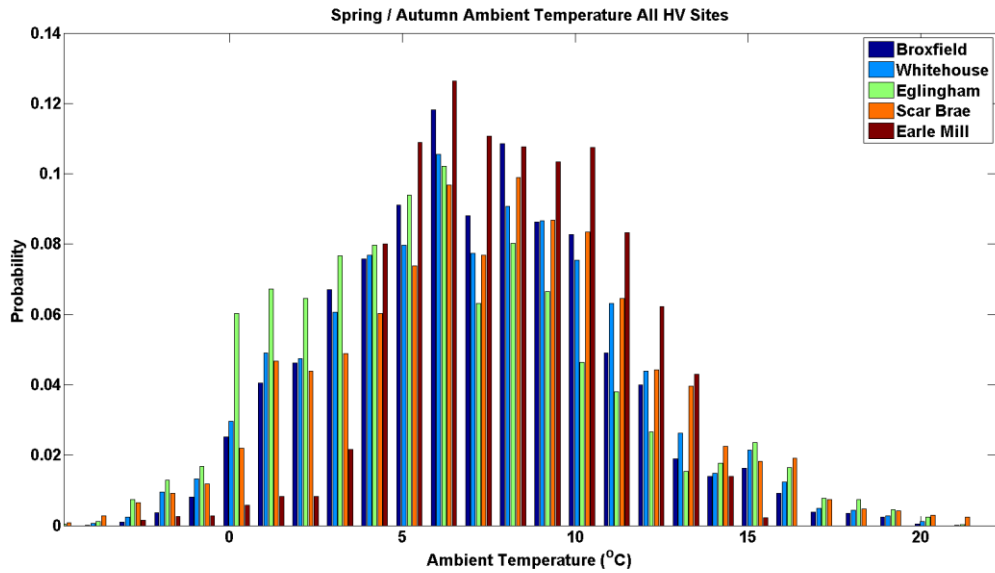


Figure 3-13 – Spring / Autumn Ambient Temperature Probability Distribution – All HV Sites

### 3.9.2.3 Summer

The largest ambient temperatures are, as expected, observed during the Summer seasonal period. As in each of the remaining seasonal periods, the sheltered sites display a typically increased temperature when measured against the non-sheltered sites.

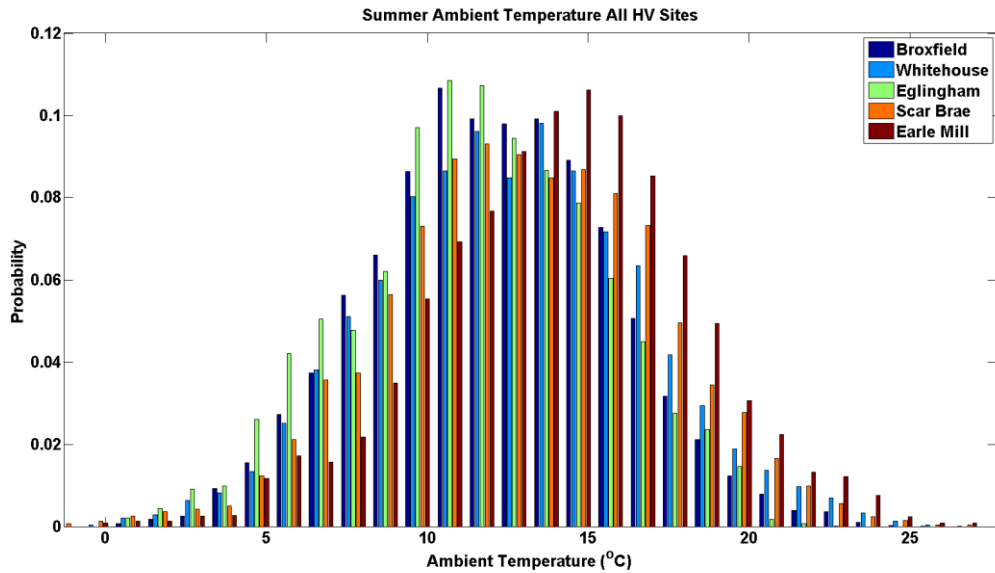


Figure 3-14 – Summer Ambient Temperature Probability Distribution – All HV Sites

### 3.9.3 HV Monitoring Sites – Wind Direction

This section shows the wind speeds and wind directions observed at each of the sites, represented as wind roses. For this analysis, the datum of 0° incident angle is relative to the span of the conductor, not to the cardinal point of North. I.e. an angle of 0° or 180° refers to wind travelling along the length of the conductor.

#### 3.9.3.1 Broxfield

At the Broxfield HV site, it is clear that the majority of incident wind speeds are from the 0-180° range. In this range the dominant angles are at around 50° and 150°. Figure 3-16 shows the orientation of the wind rose relative to the conductor span. As can be seen, there is shading present from the collection of trees close to the OHL monitoring site. However, the distance of the OHL site from the trees, in combination with the relatively high wind speeds results in relatively good performance in terms of network uplift at this site.

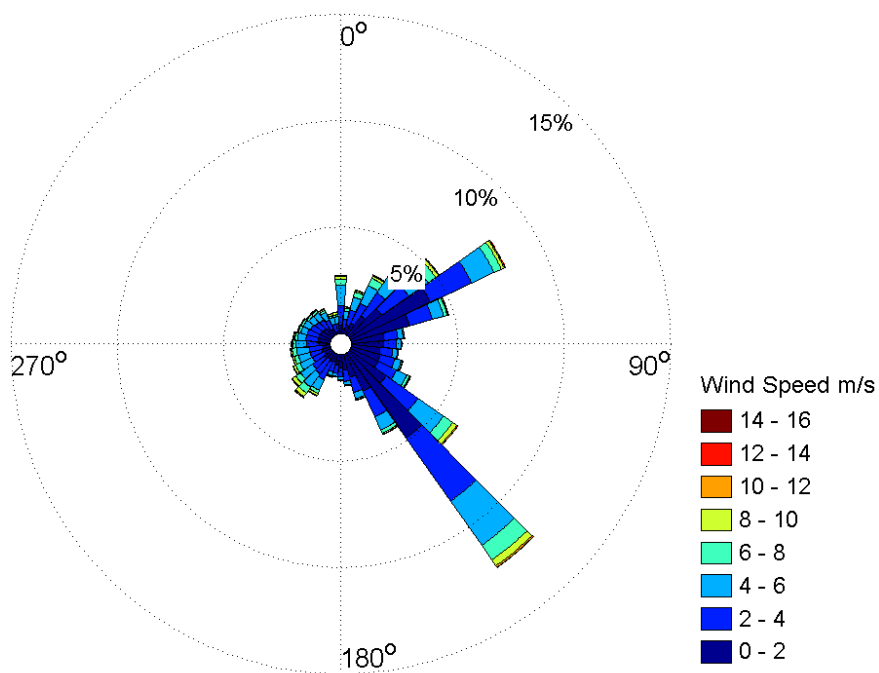


Figure 3-15 – Wind Rose for Broxfield HV Site

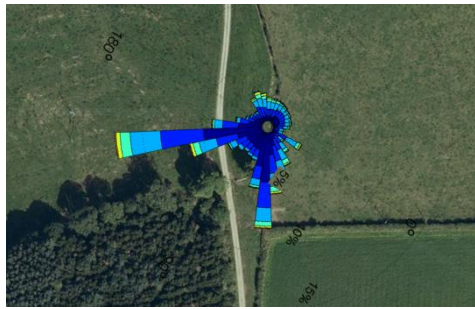


Figure 3-16 –Orientation of Broxfield HV Wind Direction Monitoring

### 3.9.3.2 Whitehouse

At the Whitehouse site, very few wind speeds are observed between  $\approx 150$ - $270^\circ$ . As the orientation of the measurement devices is in line with the span this is most likely to be caused by the heavily wooded area behind the monitoring site. This is shown in Figure 3-18.

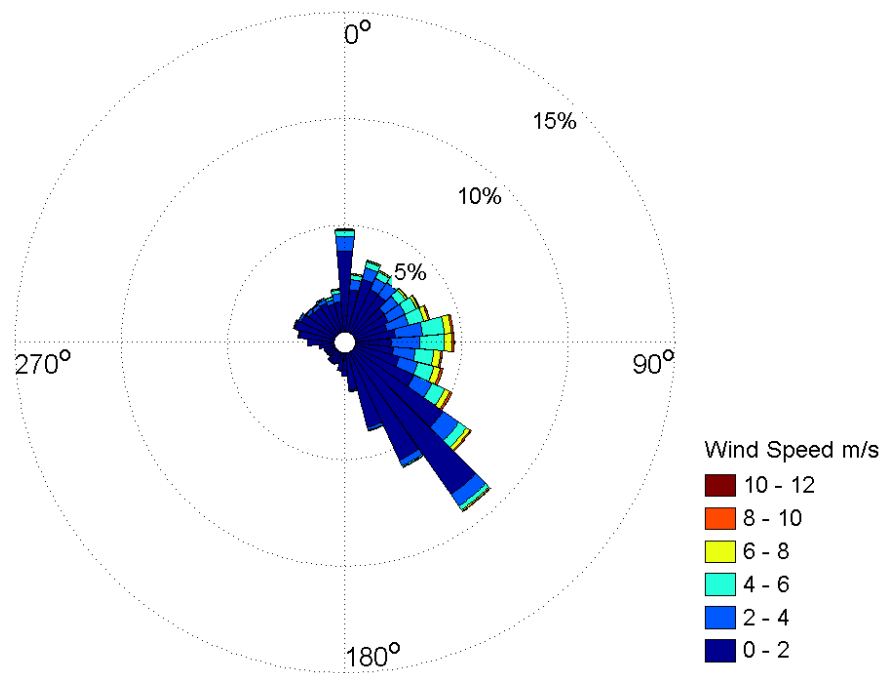


Figure 3-17 - Wind Rose for Whitehouse HV Site

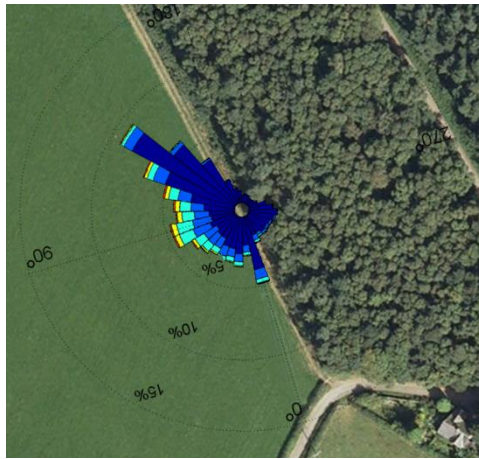


Figure 3-18 – Whitehouse Wind Rose with site satellite image

### 3.9.3.3 Eglingham

Observed wind speeds at the Eglingham site appear to be in a singular corridor across the conductor. Very few wind speeds are recorded outside of these incident angles. The overlay of the wind rose on a satellite image of the site is shown in Figure 3-20.

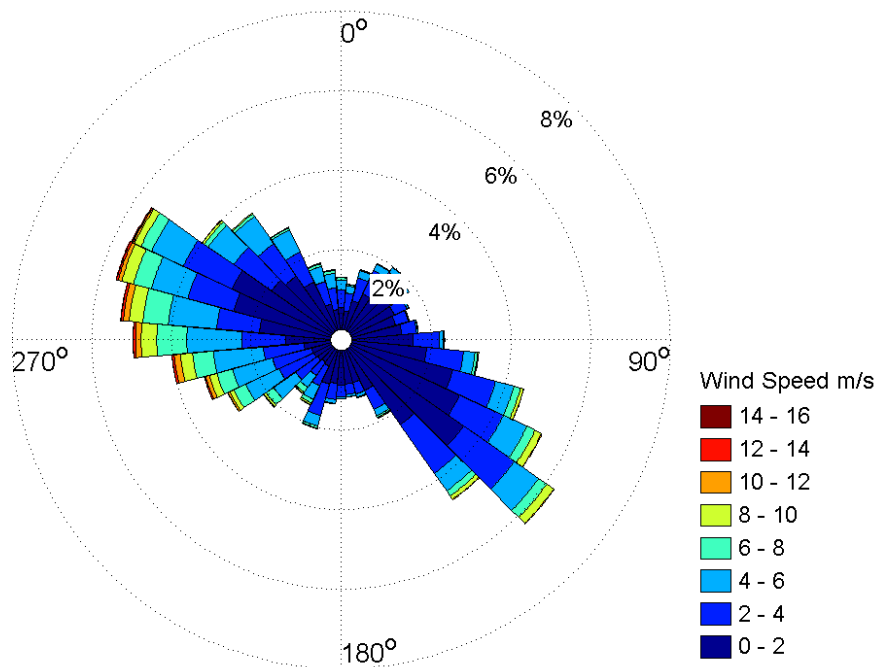


Figure 3-19 - Wind Rose for Eglingham HV Site

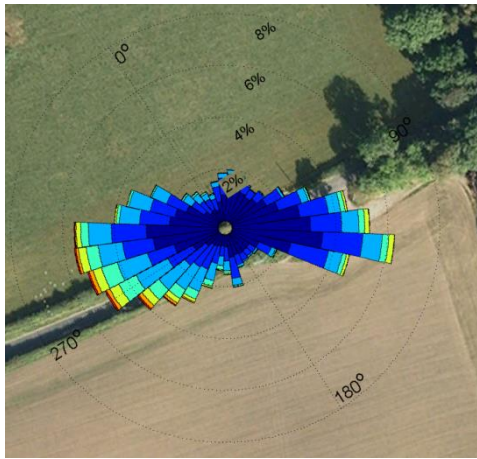


Figure 3-20 - Eglingham Wind Rose with site satellite image

### 3.9.3.4 Scar Brae

The Scar Brae HV monitoring site is highly sheltered as can be seen in the very low observed wind speeds. Figure 3-22 shows the wind rose overlaid on the site satellite image. As per the Whitehouse and Broxfield monitoring sites the surrounding trees shelter the OHL site, however the sheltering here as opposed to the Broxfield site is such that the incident wind speeds are relatively low at this site.

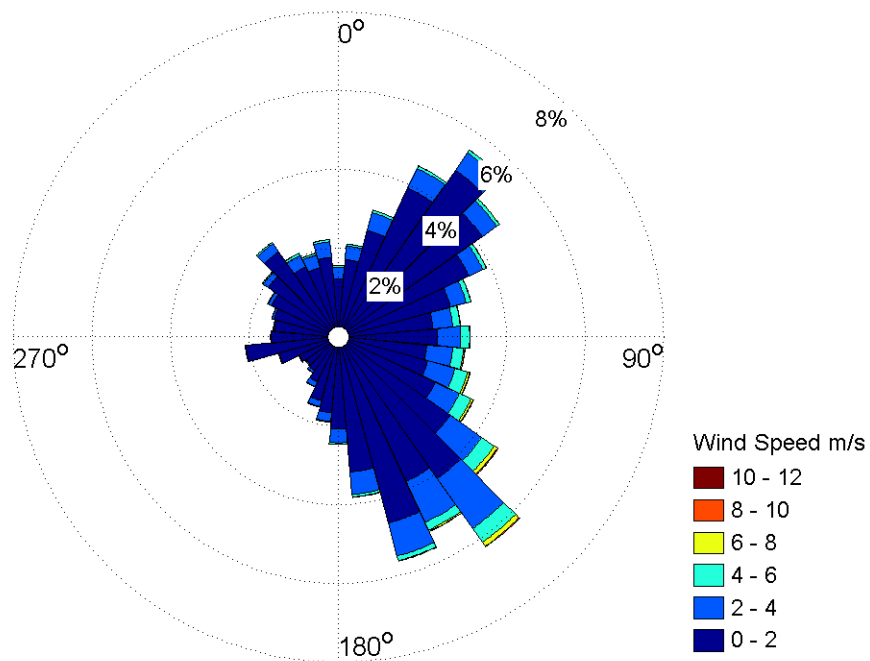


Figure 3-21 - Wind Rose for Scar Brae HV Site

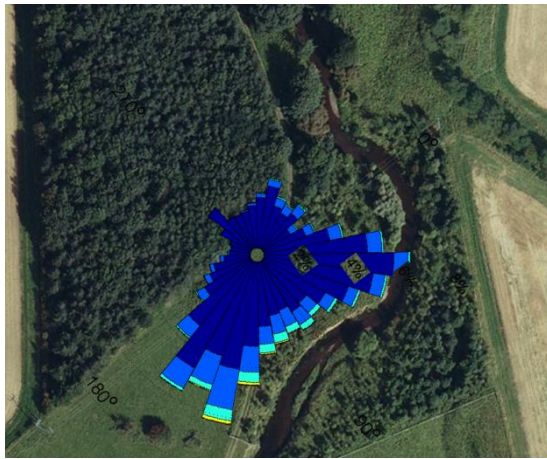


Figure 3-22 – Scar Brae Wind Rose with site satellite image

### 3.9.3.5 Earle Mill

Earle Mill has significant shading on one side of the monitoring location, and almost no shading on the alternate side. Again, as per Scar Brae, the sheltering of the site is shown in the relatively low observed wind speeds. The reduced sheltering on one side is the likely reason for the occasionally observed high wind speeds.

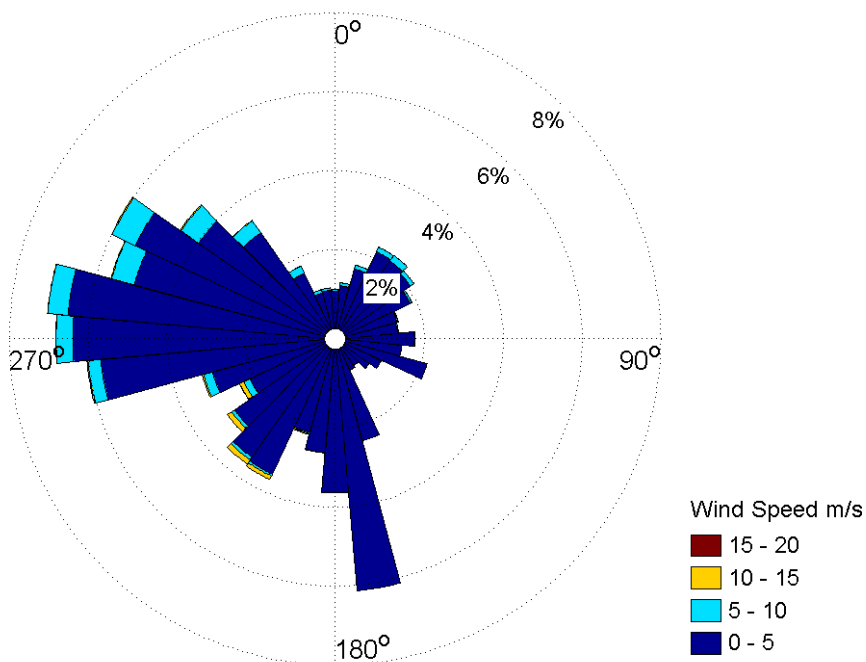


Figure 3-23 - Wind Rose for Earle Mill HV Site

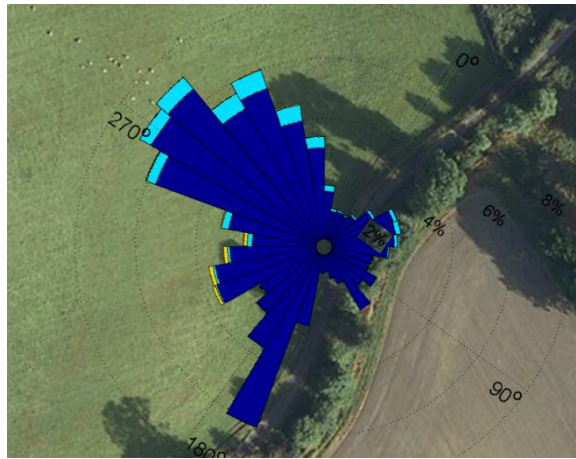


Figure 3-24 – Earle Mill Wind Rose with site satellite image

### 3.9.4 Solar Radiation Percentiles

Figure 3-25 shows a time series profile sample of the available solar radiation percentiles. The 5<sup>th</sup>, 50<sup>th</sup> (median) and 95<sup>th</sup> percentile values of solar radiation seen at each sampling point during the day (288 possible measurement points of 5 minute intervals), have been generated.

Figure 3-25 shows results for the Eglington HV monitoring site in Summer. The typical sinusoidal curvature of the solar radiation curve is clearly present within each of the percentile curves. 95<sup>th</sup> percentile solar radiation values at this site typically peak at around 1000 W/m<sup>2</sup>.

As shown in Section 2.4.6 the influence of solar radiation is the smallest of the influential weather parameters. Similar solar radiation results have been observed at all sites. On a limited number of occasions there are examples of site specific shading which result in lower solar radiations at certain times of day.

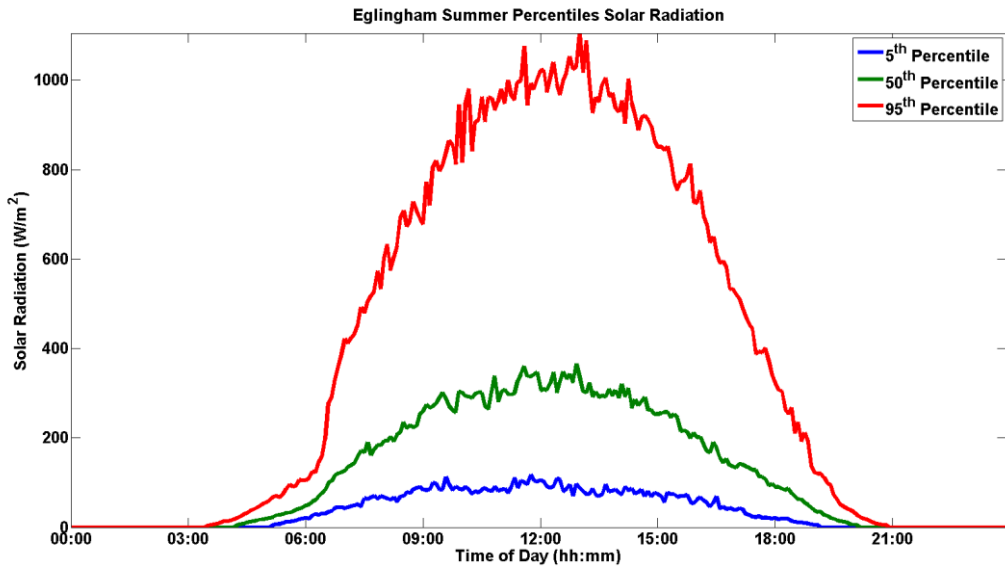


Figure 3-25 – Example Solar Radiation Percentile Plot at the Eglingham HV Monitoring Site – Summer

It is therefore felt that in future systems, a typical 95<sup>th</sup> percentile curve for each season could be used in an attempt to reduce parameter measurement numbers. In cases where shading is present, the use of a standard curve does not affect the rating significantly, when compared to the effect of the remaining ambient parameters.

### 3.10 Real-Time and Dynamic Thermal Rating Validation

To calculate all ratings in this study an offline conductor thermal model has been developed based on the CIGRÉ standard [67]. The model is capable of calculating three separate values of thermal rating, based on different combinations of available inputs.

- The real-time thermal rating (RTTR) (maximum current carrying capacity) using the conductor maximum temperature and the measured meteorological conditions,
- The conductor surface temperature using the measured current and weather variables
- The dynamic response of the conductor over time to a step change in the input parameters

Each of these three model outputs will be discussed in further detail in this section.

### 3.10.1 Dynamic Conductor Response

The dynamic implementation of the CIGRÉ model as shown in (4) can be used to calculate the conductor thermal response with respect to time. Since the conductor's thermal response is non-instantaneous we can calculate the length of time which is required for the conductor to reach the steady-state equilibrium and also the time constant of the conductor (the time taken to reach 63% of the final steady-state value), which is often discussed.

The implementation of the CIGRÉ equation involves utilising the dynamic format of the IEEE standard [65] whilst maintaining the CIGRÉ heat balance calculation methods. This represents a small contribution since it combines the iterative procedure for calculation of the effective conductor temperature distribution as detailed previously and removes the need for the magnetic heating term found within the standard dynamic implementation of the CIGRÉ rating method.

The dynamic behaviour of the conductor temperature, in response to step increase in current of both 2.5 and 10A respectively is shown in Figure 3-26. The figure of 2.5A represents the average difference in conductor loading over a five minute period from the monitoring site. 10A represents a value taken at the 99<sup>th</sup> percentile of loading differences. This percentile has been chosen to remove the effect of data capture errors resulting in atypical loading differences. If all of the remaining parameters (ambient) are held at a constant value, Figure 3-26 shows the conductor increasing in temperature as a function of time as expected, due to the increased joule heating. Since the ambient meteorological parameters remain constant over this period, the time constant is shown to be the same in both scenarios. This is in line with the result shown from the dynamic conductor response shown in [65]. The time constant for the conductor in this case is 5.995 minutes. The time constant is itself not a constant value, since the prevailing conditions will alter the rate of heat transfer away from the surface, and therefore affect the time taken to reach the equilibrium point. This has also been shown in Figure 3-26, where a 2.5A step change in current has been modelled at an

increased value of incident wind speed. Since the rate of heat transfer at the surface is greater, the incident cooling results in a lower value of conductor temperature which occurs at a faster rate.

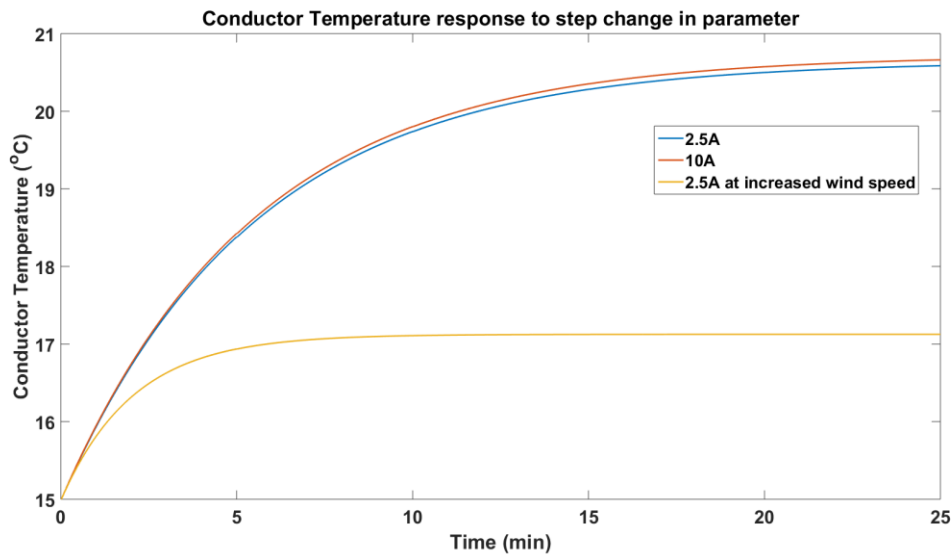


Figure 3-26 – Dynamic response of Conductor to step change in current

### 3.10.2 Conductor Surface Temperature

Equation (4) can also be rearranged to make the conductor surface temperature the subject. The additionally required parameter for this will be the measured line current. It should be noted that the RTTR monitoring devices average the three individual phase currents to determine the ‘average’ line current. If no data is measured from one of the three phases the average is calculated from the remaining phases. Whilst this is acceptable where the phases are similarly loaded, there can be large discrepancies between the actual average values, and the calculated values if a particular phase was heavily loaded and then suffered a loss of data.

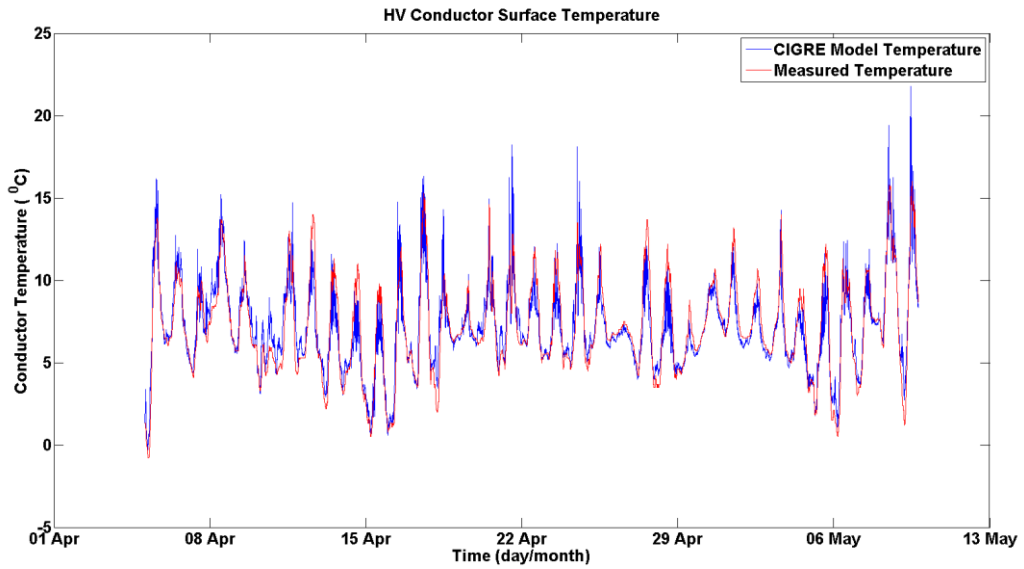


Figure 3-27 - MV Conductor surface temperature

The same iterative procedure as referred to in Section 2.4.4 is used to derive the conductor surface temperature. Figure 3-27 shows the calculated surface temperature values against those measured by the RTTR monitoring devices.

In [104] a conservative use of the CIGRÉ rating methodology resulted in conductor temperature model errors of between 3.4°C and 11.1°C, while the accuracy of the actual CIGRÉ method is within  $\pm 2^\circ\text{C}$  of a tested reference value for 99.4% of the monitoring period. In an earlier work, Bush [105] notes the performance of a regime which predicted conductor temperatures as being within  $\pm 10^\circ\text{C}$  of the measured values.

A study was carried out to determine the accuracy of the CIGRÉ surface temperature model using the parameters shown in Table 3-1 over a randomly selected data sample. Conductor surface temperature values were calculated for the complete data monitoring period and a random sample of 10000 data points were selected. The Mean Absolute Error (MAE) between the two datasets was calculated as follows:

$$MAE = \frac{1}{n} \sum_{i=1}^n | \text{Measured Conductor Surface Temperature}_i - \text{CIGRE Modelled Temperature}_i | \quad n = 10000$$

The MAE was found to be 1.346°C and therefore this value will be applied where future conductor temperature values are derived.

This value is also within the bounds of the quoted accuracy of the measured conductor line temperatures. This figure is quoted as being  $\pm 2^{\circ}\text{C}$  [106].

### **3.11 RTTR Monitoring Site Results**

When implementing an RTTR system, it is seldom used as a stand-alone tool. More often than not, the RTTR is proposed as an additional input into a wider ANM control scheme. As a comparison to the present seasonal circuit ratings, the percentage of time for which a particular RTTR can be implemented, without risk of over-stating the span's current carrying capacity has been determined. The following statistics have been derived for each of the OHL monitoring sites

- Percentage of observed RTTRs above the static P27 Rating
- Percentage of observed RTTRs below the static P27 Rating
- Percentage of possible RTTRs calculated within each period

The last of these statistics is related to the previous data quality study. In this section, no interpolation of the raw ambient data has been carried out and therefore, where ambient monitoring parameters are missing, no RTTR value has been calculated.

#### **3.11.1 Winter Results**

Figure 3-28 shows the cumulative distribution functions of the observed RTTRs during the Winter rating period. No data is shown for the Earle Mill monitoring site as this site was not installed in Winter 2012 and for Winter 2013 failed to record any meaningful data. In addition to the RTTRs from each site, and for each of the following seasonal RTTR CDF plots, the relevant P27 seasonal line rating has also been shown.

The observed RTTRs are in general greater at the open sites as expected. The open and sheltered sites also show similar characteristics within their categories. The lowest ratings on average are observed at the Scar Brae site. The maximum calculated RTTR value in this period is observed at the Eglingham site.

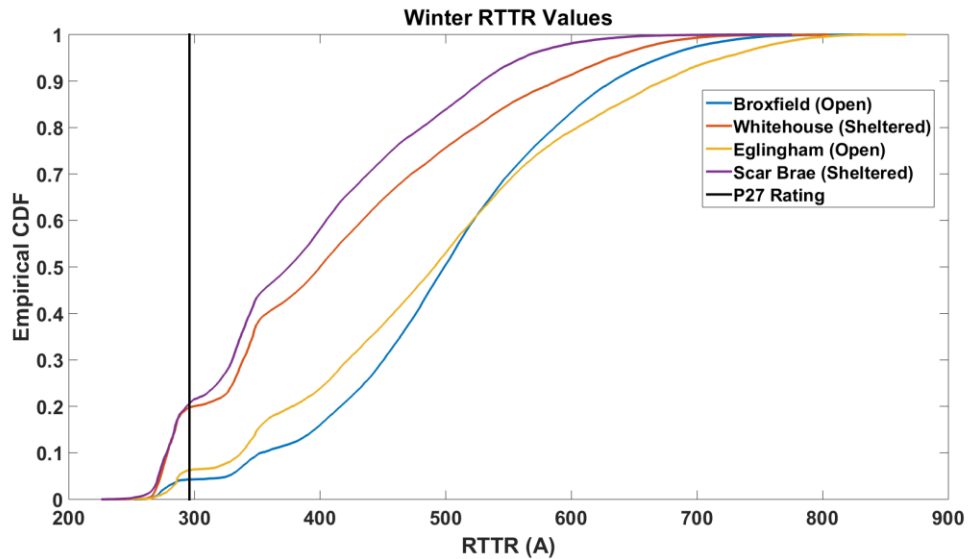


Figure 3-28 – Winter RTTR CDF for all Sites

Around 20% of ratings observed at the sheltered sites are lower than the presently implemented P27 static ratings. Since the present distribution network planning standard calls for N-1 circuit security at this level [11], these periods of low ratings would also have had to be combined with appropriate network outage conditions to have any significant effect on the conductor temperatures. Additionally the cumulative distribution functions shown here make no reference towards the duration of the observed RTTRs. RTTRs lower than the static rating may have been observed for only a single 5 minute period at a time. The importance of this fact will be discussed in the sections of this thesis concerning the use of Dynamic as opposed to Real-Time thermal ratings.

	Broxfield	Whitehouse	Eglingham	Scar Brae	Earle Mill
Percentage of RTTR > P27 Static Rating	95.8	80.9	94.0	80.4	N/A
Percentage of RTTR < P27 Static Rating	4.2	19.1	6.0	19.6	N/A
Percentage of possible RTTRs calculated	76.9	86.1	86.7	86.9	N/A

Table 3-9 – Winter RTTR Statistics – All HV Sites

### 3.11.2 Spring / Autumn Results

In the Spring/Autumn period the Earle Mill site displays a high correlation with the RTTRs observed at the non-sheltered sites. The observed ratings appear to be somewhat similar to the Winter ratings at first examination, however the slope of the CDF shows that the ratings are generally smaller than those observed in the Winter period. A rating of 300A is valid for around 75% of the Spring period at the Whitehouse site, whereas this rating is valid for around 80% of the Winter period at the same site.

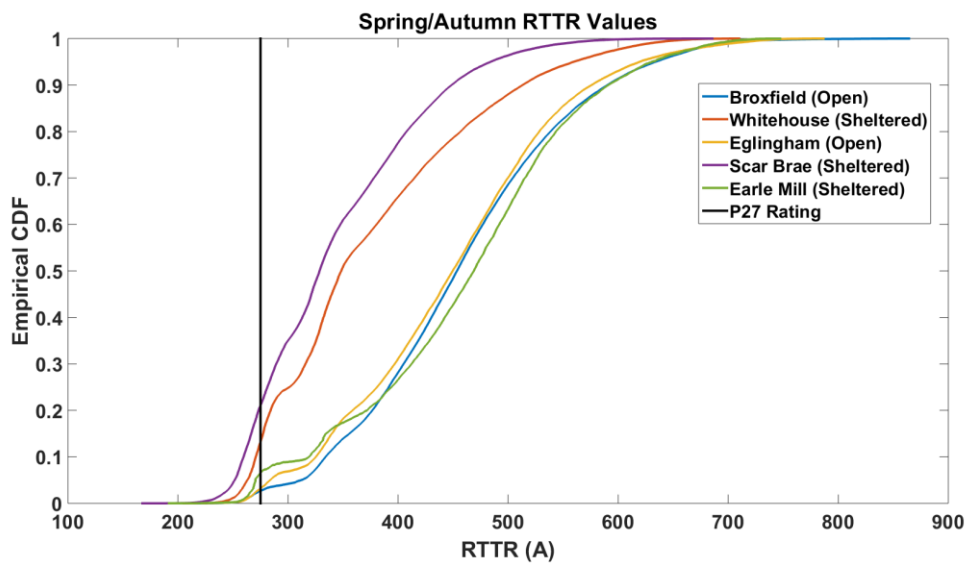


Figure 3-29 – Spring/Autumn RTTR CDF for all Sites

The percentage of ratings greater than the static rating also increases in comparison to the Winter period. Roughly 20% of the ratings at the Scar Brae site still remain below the P27 rating.

	Broxfield	Whitehouse	Eglingham	Scar Brae	Earle Mill
Percentage of RTTR > P27 Static Rating	97.7	89.2	97.3	81.1	94.4
Percentage of RTTR < P27 Static Rating	2.3	10.8	2.7	18.9	5.6
Percentage of possible RTTRs calculated	91.2	66.8	75.8	74.8	20.5

Table 3-10 – Spring / Autumn RTTR Statistics – All Sites

### 3.11.3 Summer Results

As expected, the observed RTTRs are at their minimum in the Summer period. Increased ambient temperatures and reduced wind speeds result in lower RTTRs due to the degree of atmospheric heating and the reduction in convective cooling.

The Earle Mill site here displays greater similarity to the sheltered sites, as opposed to during the Spring / Autumn period. It also shows the greatest percentage of ratings below the static rating. The percentage of ratings greater than the P27 rating is also at a maximum in this period. Suggesting that the ratings are perhaps somewhat overly pessimistic in the Summer period, and are generous in the Winter period.

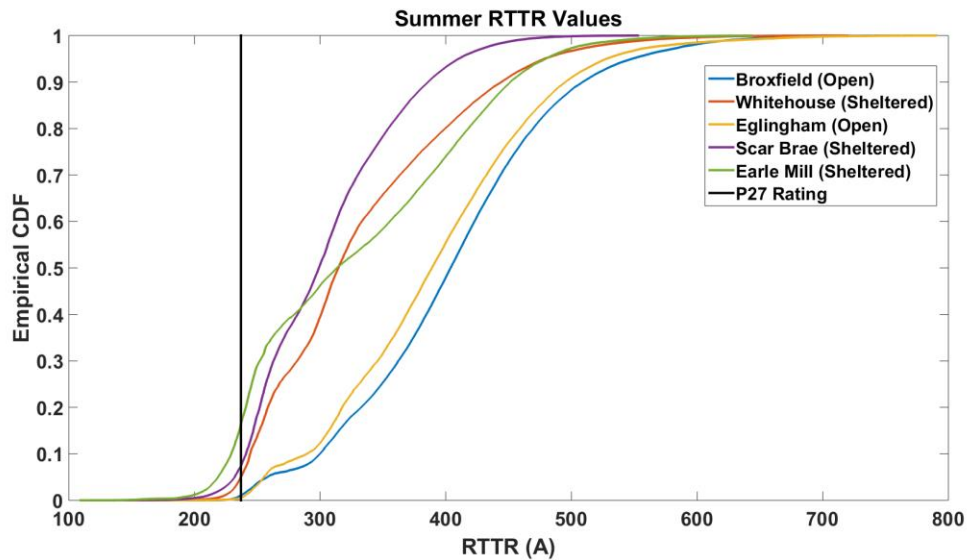


Figure 3-30 - Summer RTTR CDF for all HV Sites

In the Spring / Autumn period the difference between the observed ratings at the sites is more pronounced than in the Winter period. Again a very high percentage of ratings are greater than the static rating. Also the percentage of ratings which were able to be calculated is high.

	Broxfield	Whitehouse	Eglingham	Scar Brae	Earle Mill
Percentage of RTTR > P27 Static Rating	99.3	96.4	99.7	94.0	86.3
Percentage of RTTR < P27 Static Rating	0.7	3.6	0.3	6.0	13.7
Percentage of possible RTTRs calculated	99.8	76.6	91.8	82.5	60.2

Table 3-11 - Summer RTTR Statistics – All Sites

### 3.12 OHL monitoring site conclusions

As discussed previously the findings of these data quality results are useful in as such that DTRs and RTTRs need to be reliable for implementation within power networks. As has been shown, for certain sites good data quality is present, e.g. 99.8% of possible data measurements are made, and also that the coincidence of ‘wide area’ problems, such as server malfunction are relatively limited. The more critical factor however is in the percentage of missing parameters when considering the sites as a whole. If the system is to be implemented across a large area, potentially using interpolation to deliver network ratings unserved by monitoring equipment, a drop out in measurements could have a serious effect on the reliability of the resultant ratings.

### 3.13 Selection of the ‘Critical Span’

The final section of this Chapter is a determination of the ‘critical span’ of the available monitoring points. A method for selection of the critical span has been commented upon in [107]. Here, a wide area meteorological method is used. Since a direct contribution to the field of critical span selection was beyond the scope of this research, the following method has been used in order to determine the ‘critical span’ from the available monitoring sites.

As the results of Section 2.4.6 show, wind speed is the predominant variable which affects the overall thermal performance of overhead lines and is therefore a dominant characteristic when choosing the overall critical span. The thermal performance of the OHL is governed by the balance between heating and cooling elements. Wind speed is the dominant variable when concerning cooling, and

ambient air temperature is dominant when considering heating. Combination of these two elements results in a worst case scenario where cooling is at a minimum and air temperature heating is at a maximum.

Therefore when selecting the site which is deemed to be the overall ‘critical span’ of those available, the decision was made to consider the distribution of air temperature values when wind speeds tend towards 0m/s. For the purposes of this analysis, low wind speeds are those defined as below 1m/s. Within this analysis, due to the relocation of the Eglingham OHL site to Earle Mill, both these sites were removed from the analysis this was for two reasons:

- In order to give the highest number of data points for analysis
- Eglingham was considered as a non-sheltered site and was therefore unlikely to be the critical span
- After replacement, the site at Earle Mill was significantly more unreliable with regards to gathering data than the other sites.

Figure 3-31 and Table 3-12 and show the results of this analysis.

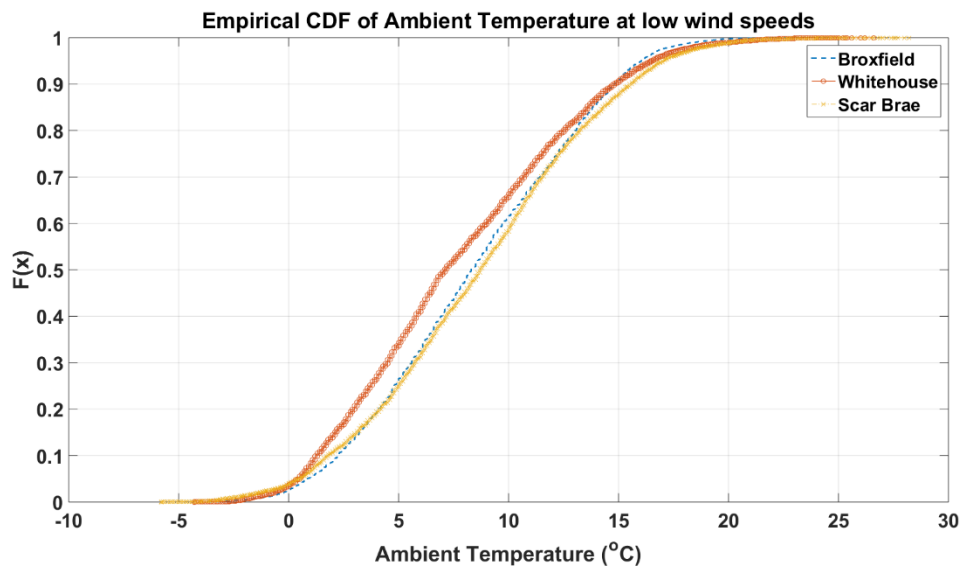


Figure 3-31 – Empirical CDF of Ambient Temperatures at low wind speeds

Site	Broxfield	Whitehouse	Scar Brae
Average Temperature (°C)	8.5	7.8	8.7
99 <sup>th</sup> percentile Temperature (°C)	18.4	20.1	20.2
Maximum Temperature (°C)	23.5	26.6	28.2

**Table 3-12 – Average, 99<sup>th</sup> percentile and Maximum Ambient Temperature values at low wind speeds**

As can be seen in Table 3-12 the Scar Brae site exhibits the highest ambient temperature in each of the test cases at low wind speeds. This site was therefore selected as the 'worst-case' scenario of the available monitoring sites and used in all further analysis.

### **3.14 Conclusions**

This section has provided information as to the RTTRs at the available monitoring sites. Significant increases in network capacity over the existing P27 rating standard have been shown even at the most sheltered available site. Ratings have conversely been shown to also be lower than expected at all sites. Though this is potentially a function of missing data, even at the non-sheltered sites where data monitoring was on the whole of higher quality, periods of RTTR values lower than the seasonal static ratings have been observed.

Since the network is presently operated with N-1 security i.e. a level of redundancy whereby the network must be capable of supporting demand when a particular asset is not in service, in this case 1 asset, the levels of line utilisation are low in comparison to the seasonal rating and the observed conductor temperatures do not exceed the circuit rated temperature.

At the sheltered site there is however the potential that in a scenario whereby the feeder on which the monitoring devices are located is carrying increased load due to a network outage and the meteorological conditions are unfavourable, this could potentially result in the line loading exceeding the RTTR.

## **4 Examining the accuracy of the presently used UK overhead line rating standard**

### **4.1 Introduction**

In order to accurately evaluate the potential benefits that DTRs and RTTRs can bring to distribution networks, an understanding of the current method used to rate OHLs in the UK is required. This Chapter gives details of a series of analyses intended to evaluate the present OHL rating method and draw conclusions as to its effectiveness.

The foundation of the existing P27 method lies in an experiment carried out at the Central Electricity Research Laboratory (CERL) in Leatherhead, Surrey during the years 1975-77. The aim of this experiment was to quantify acceptable ratings for all overhead lines in the UK regardless of construction type or location. In this context, construction type refers to the type of pole or support mechanism used to carry the OHL and the material composition of the line itself. This work built on previous studies of overhead lines in wind tunnels, and definition of the conductor's heat balance equation based on its conductor type.

The results of this experiment are detailed in CERL Report RD/L/N 129/79 [22]. Further information on the experiment, in particular the experimental method is detailed in a later paper by Price and Gibbon [62]. There are a number of points within these reports which are crucial to the understanding of overhead line ratings in the UK and to allow comparison with the results which will be discussed in Chapter 9, therefore a description will be detailed here.

### **4.2 Chapter Goals / Objectives and Contributions**

#### **4.2.1 Goals / Objectives**

Given the newly available datasets provided by the CLNR projects, to examine the suitability of P27 to describe line ratings for such monitoring sites. Based upon this information, evaluate if P27 represents a credible baseline against which to evaluate the potential uplifts from techniques such as RTTR and DTR.

## 4.2.2 Transition from existing literature and research / Contribution

Most of the existing literature in this field is related directly to the derivation of the present seasonal line ratings. The main contribution from this section is in its derivation of updated OHL rating values using the P27 method based upon the real-world monitoring site data.

## 4.2.3 Attainment of Goals

The introduction of new monitoring site data to the existing P27 conductor rating method allowed for evaluation of the present P27 ratings. This evaluation was determined the ability of the existing ratings to match the required levels of network risk, and delivered updated ratings where required.

## 4.2.4 Chapter Outline Block Diagram

Figure 4-1 a block diagram of the inputs, methods and outputs for this chapter. The introduction of monitoring data from the CLNR project into a recreation of the CERL experimental method represents a contribution from this chapter. The use of this method delivers a new dataset in the form of a set of newly calculated seasonal ratings. These allow for direct comparison against the existing seasonal ratings.

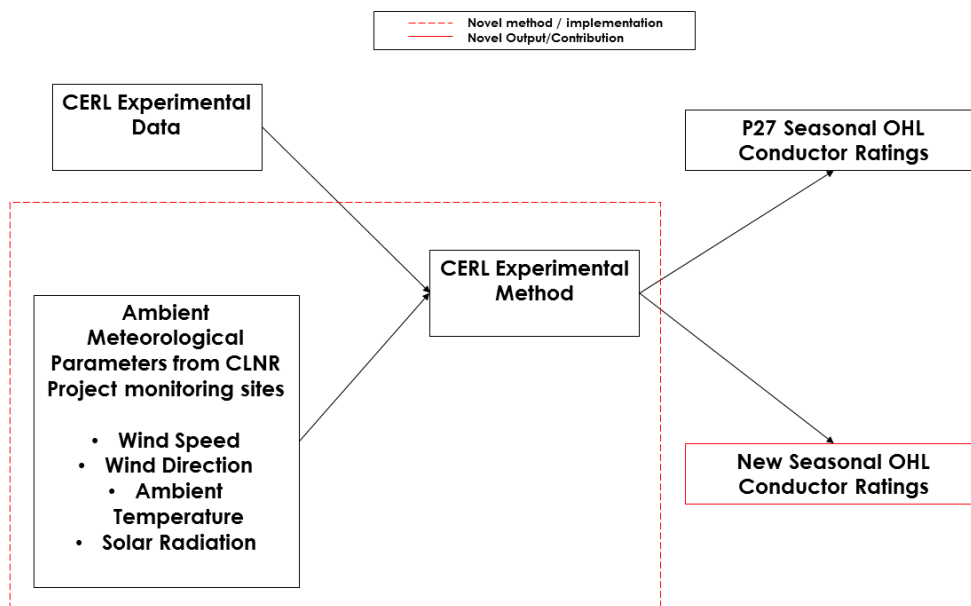


Figure 4-1 – Chapter 4 Block Diagram

### 4.3 Price and Gibbon Heat Transfer Model

The Price and Gibbon model is similar in a number of ways to the CIGRÉ method chosen for calculation of the real-time and dynamic thermal ratings. There are however small differences between the methods used to derive the various coefficients and an outline of the model is detailed below.

#### 4.3.1 AC Resistance

The effective AC resistance is calculated from knowledge of the DC resistance at 20°C and compensating through equation (21)

$$R_{T_2} = R_{T_1} [1 + 0.5 \cdot \alpha (T_c + T_s - 40)] \quad (21)$$

Where:

$R_{T_1}$  is the DC resistance at temperature  $T_1$  (20°C)

$R_{T_2}$  is the DC resistance at temperature  $T_2$  (This value is used to replace  $R_T$  in equation (4))

$T_c$  is the core temperature of the conductor (K)

$T_s$  is the surface temperature of the conductor (K)

$\alpha$  is the temperature coefficient of electrical resistance at  $T_1$   
for Copper:  $\alpha = 0.00381 \text{ K}^{-1}$

#### 4.3.2 Cooling elements

##### 4.3.2.1 Radiated Heat Loss

$$P_R = \varepsilon \cdot \sigma_{S-B} (T_s^4 - T_a^4) \cdot \pi \cdot D \quad (22)$$

$$T_s = T_c \frac{I^2 R \left[ 1 + \alpha \left( \frac{T_c + T_s - 40}{2} \right) \right]}{4\pi K_r} \quad (23)$$

Where:

$P_R$  is the radiated heat loss (W/m)

$\sigma_{S-B}$  is the Stefan-Boltzmann constant ( $5.67 \times 10^{-8} \text{ W/m}^2/\text{K}^4$ )

$\varepsilon$  is the emissivity coefficient with respect to black body

$T_a$  is the ambient temperature (K)

$D$  is the outer diameter of the conductor (mm)

- $d$  is the core diameter of the conductor (mm)  
 $I$  is the initial guess of the final design current (A)  
 $K_r$  is the radial thermal conductivity of the conductor (W/m°C)

The surface temperature of the conductor is calculated through an iterative process. Initially a guess is made that the surface temperature is equal to the core or design temperature. A guess is also made that the final design current is 1000A. After all additional calculations have been made such as those for joule heating and convective heat loss, a single iteration of (8) is carried out.

The updated  $I_{design}$  allows a new value of the surface temperature to be generated. The new values of  $I_{design}$  and  $T_s$  are then input to the equations as necessary and another iteration is carried out. This process is repeated until the estimate for  $I_{design}$  and the calculated value has a difference of less than 0.01. Typical differences between the surface and core temperatures range from 0.5 to 7°C [3]. The emissivity of the conductor is pre-determined and has a value of 0.9. The radial thermal conductivity of the conductor is assumed to be 4 W/m°C.

#### 4.3.2.1.1 Convection Heat Loss

$$P_F = \pi \cdot Nu \cdot k_f (T_s - T_a) \quad (24)$$

$$k_f = \left[ 2.42 + 0.007 \left( \frac{T_s + T_a}{2} \right) \right] \times 10^{-2} \quad (25)$$

$$Re = \frac{u \cdot D}{1000 \cdot \nu_f} \quad (26)$$

$$\nu_f = [132 + 0.48(T_s + T_a)] \times 10^{-7} \quad (27)$$

$$If \begin{cases} Re < 3200 & Nu = Y \cdot (0.034 + 0.034Re^{0.487}) \\ Re > 3200 & Nu = Y \cdot (0.071 + 0.901Re^{0.715}) \end{cases} \quad (28)$$

Where:

- $P_F$  is the loss due to Forced Convection (W/m)  
 $Re$  is the Reynolds number and is calculated from equation (25).  
 $Nu$  is the Nusselt Number and is calculated from equation (28).

- $k_f$  is the thermal conductivity of the air film in contact with the conductor W/m/ deg C
- $u$  is the wind speed in m/s
- $Y$  is the yaw factor of the wind
- $\nu_f$  is the kinematic viscosity of the air film at the conductor surface (m<sup>2</sup>/s)

The yaw factor of the wind, is a function of the angle of attack of the incident wind speed on the conductor. In [62] the yaw factor is stated as 0.55 however no explanation of how this figure was arrived at is given. A study was carried out in order to determine the conditions in which the value of 0.55 can be obtained. The final conclusions of this study were that the incident angle of wind speed against the conductor should be around 12.5°. It appears that this value is taken from the earlier work of Morgan [76] in which he discusses the effect of wind being channelled across the surface of a conductor when it's angle of attack approaches the lay angle of the conductor. The lay angle of the conductor refers to the angle made to the vertical plane of the helical stranding of the wires used to make up the bundled conductor.

The heat transfer effect of the wind in cooling the OHL is reduced as the wind passes through the channel resulting in a reduced cross sectional area over which the wind is acting. This effect was found to result in a minimum cooling effect where the angle of attack is around 12.5°. It is presumed that this angle has been used in order to result in a worst case cooling scenario for the OHL.

### 4.3.3 CERL Experimental Procedure

Prior to the work of Price and Gibbon in the CERL experiment, a number of studies had previously been carried out with regards to the rating of OHLs. These studies fall into two categories. The first relates to investigating the thermal properties of OHLs in largely static scenarios with constant wind speeds and angles of attack relative to the conductor. Meteorological studies were also carried out, with the main conclusion from these experiments being that values of maximum ambient air temperature rarely coincide with low values of wind speed. The work of Price and Gibbon aimed to combine these two strands of research by performing similar constant conductor loading tests as those found in the first set

of experiments but in open, exposed conditions. In order to do this a section of 400mm<sup>2</sup> Aluminium Conductor Steel Reinforced (ACSR) conductor (commonly referred to as a 'Zebra' conductor) was loaded with various constant current values throughout the experiment and ambient meteorological conditions were recorded throughout at a 6 minute time interval on a series of punch tape recordings. The meteorological monitoring equipment was installed on a 10m high wood pole close to the OHL to measure, wind direction, wind speed, ambient temperature and solar radiation.

Prior work, from a CEGB report of 1974 details constant current values intended to result in a particular conductor temperature based on the prevailing conditions. It is these constant current values which Price and Gibbon now proceeded to load their conductor with. There are three values covering the annual period, divided into seasonal categories. The seasons are denoted as Winter, Normal and Summer. In most literature, including the P27 technical report itself, the Normal period is referred to as the 'Spring/Autumn' period, so this will be used for future reference.

As stated previously the experiment ran for a total of three years in the period of 1975-77. In the first year of the experiment the conductor was loaded for each of the three seasonal rating periods with a constant current value which was designed to be representative of a 50°C conductor temperature. In the second year, the constant current value was altered to now be representative of a 75°C conductor temperature. The final year of the experiment saw the conductor loaded with a constant value of 1020A for all of the seasonal rating periods.

Analysis was then carried out to determine the number of 6 minute periods in which the conductor temperature was observed within a particular range. These varied from 45-90°C in 5°C bands. Within the original CERL experiment, temperature values below 45°C were not analysed. This is likely to be as a result of 45°C representing a minimum circuit rated temperature value for OHLs in the UK. Within each of these bins, the lower temperature i.e. 45°C is used as the reference circuit temperature. A circuit rated temperature is set for a particular circuit such that the magnitude of the conductor's sag will not exceed the minimum required ground clearance at a particular point determined along the length of the circuit. This is important to refer to in future calculations. Temperatures above the

circuit temperature are referred to as excursions, and it is this concept which is central to the analysis carried out by Price and Gibbon and forms the foundation of the current P27 rating methodology.

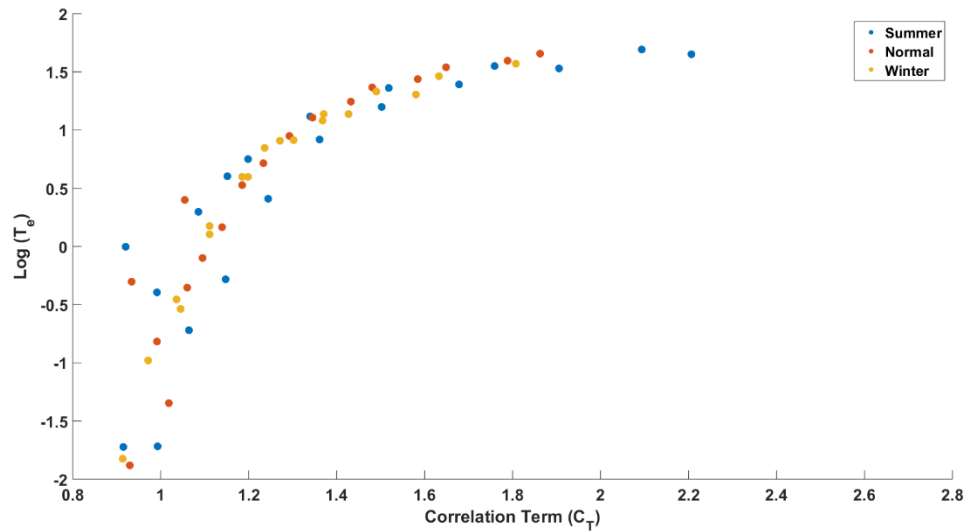


**Figure 4-2 – Correlation of Zebra temperature excursion data for the seasons and for various design temperatures, recreated from [62]**

The temperature frequency bins are converted into the scatter plot shown in Figure 4-2 using the following method. Firstly the frequency counts are converted into values of percentage ‘excursion time’ per seasonal period above the conductor rated temperature ( $T_e$ ). The log of these values is then taken and it is these values which are used to derive the line of best fit and extrapolate the results.

For each temperature bin, the value of the Correlation Term or  $C_T$  is calculated using (29).

$$C_T = \frac{I^2 R (\text{operating conditions})}{(P_F + P_R) (\text{design conditions})} \quad (29)$$

$$I = \sqrt{\frac{C_T (P_F + P_R)}{R}} \quad (30)$$

$$I_{\text{design}} = \frac{I_{NPG}}{\sqrt{0.912}} \quad (31)$$

For the original experiment the  $C_T$  values are:

Excursion Time % ( $T_e$ )	Correlation Term ( $C_T$ )	Selected Best Fit Correlation Term ( $C_T$ )
0.001	0.912	0.788
0.01	0.930	0.883
0.1	0.980	0.988
0.2	1	1.022
0.3	1.018	1.043
0.4	1.030	1.058
0.7	1.063	1.088
1.0	1.085	1.108
2.0	1.135	1.148
3.0	1.170	1.175
6.0	1.245	1.233
10.0	1.315	1.300
14.0	1.382	1.362
20.0	1.475	1.468
30.0	1.640	1.674
40.0	1.860	1.920

**Table 4-1 – Correlation Terms ( $C_T$ ) as quoted in [62] and results from the line of best fit**

The values shown as being from the selected best fit method will be commented upon further in Section 4.4.1. Values are shown in Table 4-1 to allow for direct comparison upon review of the method and to remove the need for further replication of the table.

For a pre-determined circuit rated temperature, and through rearrangement of (29) in the form of (30) the constant current value for the circuit rating can be derived. The final parameter required for calculation of these current values is a specific value of  $C_T$  and thus by definition and allowable conductor percentage excursion. At present in UK distribution networks the allowable risk is set at 0.001% for single circuit supply and at 3% for double circuits. For reference, the figure for National Grid circuit ratings is set to 12%. These percentages refer to the total time per seasonal rating period, and for reference a value of 0.001% of a seasonal period relates roughly to one, 6 minute period.

The values of  $P_F$  and  $P_R$  are calculated at the circuit temperature values discussed previously, whilst the value of  $R$  is calculated at the constant current value  $I$  which is already known. A line of best fit is generated in [62] for the scatter plot shown in Figure 4-2, and is used to generate the series of  $C_T$  values for the set of design conditions. Through rearrangement of (31) the value of  $I_{design}$  can be modified according to the chosen risk factor ( $C_T$ ).

These design conditions will be discussed in more detail in sections 4.4.3 and 4.4.4 but fundamentally the conditions refer to a set of seasonal weather conditions intended to be coincident with times of conductor temperature excursions. Analysis of the meteorological data from the Price and Gibbon found that where the conductor temperature was measured as exceeding 45°C, this commonly coincided with the following weather conditions:

- Wind Speed – 0.5 m/s
- Ambient Temperature
  - Winter – 2°C
  - Spring / Autumn – 9°C
  - Summer – 20°C
- Solar Radiation – 0 W/m<sup>2</sup>

These conditions are used when calculating the values of  $P_F$  and  $P_R$ . In order to ensure that the baseline comparison of the benefits of DTR over existing network practice was suitably accurate, an evaluation of the presently implemented OHL rating method was carried out at the ‘critical span’ selected in 3.13 and at a relatively non-sheltered site for comparison.

#### **4.4 Recreation of the CERL experimental procedure**

The experimental procedure has been recreated through use of the 50°C circuit rated temperature values as detailed in the Northern Powergrid tables for OHL loading. As a precursor to this step, the Price and Gibbon conductor heat balance model as detailed in [62] was recreated in MATLAB in order to determine the correct 50°C values of  $P_F$  and  $P_R$ . This model was verified through use of the original  $C_T$  values found in [62] and the constant current ratings for the OHL at

the case study site  $I_{NPG}$ , in the single circuit primary supply case from [108] were used.

	DNO Circuit Rating @ 0.001 % Excursion ( $I_{NPG}$ )	Design Current @ 50°C ( $I_{design}$ )	MATLAB Implementation
Winter	296	309.95	308.79
Spring / Autumn	275	287.96	286.67
Summer	236	247.12	247.02

**Table 4-2 – Circuit rating values, their equivalent design currents and the results of the MATLAB implementation**

Good agreement was found between the MATLAB model and the circuit rated values as shown in Table 4-2, therefore we can have confidence in the calculated values of  $P_F$  and  $P_R$ .

#### 4.4.1 Correlation Term line of best fit

In addition to the values of  $C_T$  quoted in [22, 62] Table 4-1 refers to newly derived values from the same data. In order to evaluate the results generated by the CERL experiment recreation, knowledge of the method behind the derivation of these best fit values was required. No details in [62] give the equation used to generate the line of best fit and therefore an approximation has been made using a series of proposed equations to describe the curve. The lack of a known method is also commented upon indirectly in [109]. Here a linear approximation is made between the  $C_T$  and  $T_e$  values as quoted in [22]. A series of limits are also noted which bound these results (32).

$$T_e = \begin{cases} 0.00001 & \text{if } C_T \leq 0.9 \\ 40 & \text{if } C_T \geq 1.860 \end{cases} \quad (32)$$

Figure 4-3 shows the nature of this relationship as shown in [109]

F5. INTERPOLATION OF AGGREGATE EXCURSION TIME PERCENTAGE,  $T_e$  ABOVE DESIGN TEMPERATURE FROM CALCULATED VALUES OF CORRELATION TERM  $C_T$

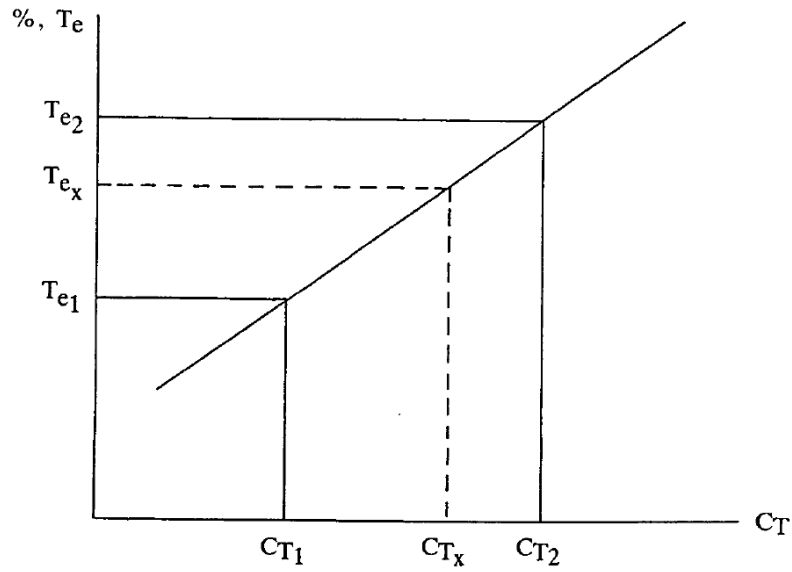


Figure 4-3 – Interpolated Linear Relationship between  $C_T$  and  $T_e$  from [109]

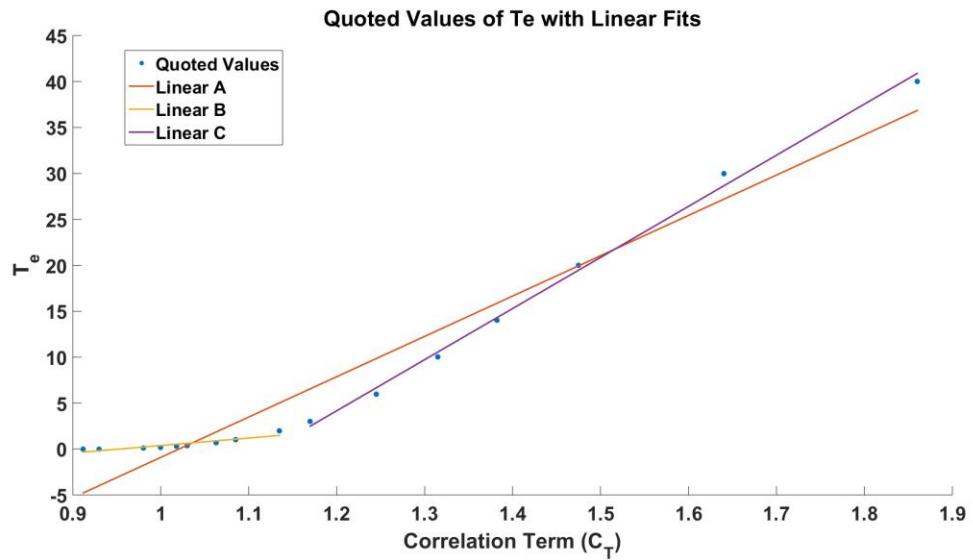


Figure 4-4 –  $C_T$  values as quoted in [22] with theoretical linear fits

Based on the approach taken in [109], Figure 4-4 shows an example of two potential linear approximations to the original quoted  $C_T$  values. As can be seen an overall fit of ‘Linear A’ is poor and the lower bounded value of  $T_e = 0.00001\%$  for  $C_T \leq 0.9$  is not adequately accounted for by the fit. Whilst an upper bound of  $T_e = 40\%$  is quoted in [109] and no reference is made to a linear fit which is not made

for all available data, the maximum value of  $T_e$  permitted within distribution systems (for Multi-Circuit Primary Supply distribution) is 3% and therefore it is potentially more likely to make a linear approximation at this level. Linear fits 'B and C' have therefore been made in a two section piecewise linear fit to the data.

These approximate the data with far greater accuracy than a single linear fit and the relationships could be approximated as being linear over these individual regions. These relationships are also far closer to that as shown in Figure 4-3. However, no comments are made as to a 'two stage' piecewise fit and therefore it must be assumed that the fit as according to 'Linear A' has been used. As a refinement to all three of these linear fits, a piecewise linear fit between all of the values quoted in [22] has been made and evaluated against a series of alternate potential fits as shown in (33) and (34)

Four potential forms of equation were considered which gave the best overall performance. These will be referred to as Fits A, B, C and D. In Fits A, B and C the equation has been rearranged so as to make  $C_T$  the subject. In Fit D due to the power relationship this was not possible and therefore a relationship was fitted in the format as presented in Figure 4-2.

Fit A: 
$$C_T = ae^{b(\log T_e)} + ce^{d(\log T_e)} \quad (33)$$

Fit B: 
$$C_T = ae^{b(\log T_e)} \quad (34)$$

Fit C: 
$$C_T = A \log T_e^2 + B \log T_e + C \quad (35)$$

Fit D: 
$$\log T_e = aC_T^b + c \quad (36)$$

	Piecewise Linear	Fit A	Fit B	Fit C	Fit D
Coefficient of determination (R-Square)	0.948	0.9560	0.7258	0.8403	0.8734

**Table 4-3 – Performance of Line of Best Fit equations**

As can be seen in Table 4-3 the performance of Fit A exceeds that of Fits B, C, D and the piecewise linear approximation from the original data points. This equation was therefore used to derive a series of  $C_T$  values for comparison with

those quoted in [62]. In addition to their improved accuracy over the piecewise approximation these fits also by definition have a known equational format and can therefore be used for generalisation by the wider community. From Fit A the parameters  $a$ ,  $b$ ,  $c$  and  $d$  are shown in Table 4-4.

Fit A Parameters	a	b	c	d
Value	1.106	0.113	0.001238	3.853

**Table 4-4 – Parameters for Fit A choice for  $C_T$  line of best fit**

As can be seen in Table 4-1 the best fit results do not match those as quoted in [22, 62]. As commented upon in [83] experimental methods such as those carried out at CERL were in an age of reduced computational ability. When analysing the accuracy of the originally quoted  $C_T$  values against the originally measured data, the R-Square value was found to be 0.9563. This value is very close to that of the derived values using the Fit A model presented here (0.9560). Whilst the accuracy of these individual data fits is almost identical, there are some notable discrepancies between the values derived from each fit. This is particularly noticeable in the derived value at 0.001%  $T_e$ , where a difference of 0.124 exists between the quoted value of 0.912 and the value derived from the line of best fit (0.788). If the newly derived values of  $C_T$  were to be used as opposed to those shown in [62] this would clearly have an effect on the values used by DNOs today. Table 4-5 shows the influence of these new  $C_T$  values on the current single circuit supply values as used at the OHL monitoring locations.

	Rating @ new 0.001 % Excursion (Table 4-1 values)	$I_{NPG}$	Design Current @ 50°C ( $I_{design}$ )
Winter	275.14	296	309.95
Spring / Autumn	255.62	275	287.96
Summer	219.37	236	247.12

**Table 4-5 – Newly derived seasonal ratings in comparison to the presently implemented ratings and their associated ‘design’ currents**

The results shown in Table 4-5 note that reductions of around 20A are necessary to conform to the newly derived  $C_T$  values. As a result of these findings,

analysis was carried out to investigate other aspects of the P27 rating method. These aspects entail the number of actual conductor temperature excursions observed at the OHL monitoring locations and also as to the distribution of ambient conditions at times of conductor excursions. Whilst in [22, 62] it is stated that during conductor excursions there are a set of typical weather conditions, the distribution of these variables is not given. The next section of this Chapter will determine these distributions and will investigate the accuracy of P27 at both sheltered and non-sheltered monitoring sites for comparison.

#### 4.4.2 Use of the CIGRÉ rating method to generate conductor temperatures

Since the Price and Gibbon model has been formulated to derive a current value which will result in a specific conductor core temperature, a significant reworking of the model would be required in order to derive new values of joule heating at deviations away from the design conditions, i.e. where the core temperature of the conductor is not equal to the circuit rated temperature. Therefore the decision was taken to use the validated CIGRÉ conductor temperature model to derive the new Joule heating values. To ensure that the calculations were consistent with those from the Price and Gibbon model, the CIGRÉ model was used with the design currents from Table 4-5 and ‘worst case’ ambient conditions as described previously in order to determine the surface temperature of the conductor at the design conditions.

	CIGRÉ model Surface Temperature (°C)
Winter	49.0300
Spring / Autumn	49.1700
Summer	49.3800

Table 4-6 – Verification of the CIGRÉ dynamic model surface temperature calculation

In [67] it is stated that the difference between the surface and core temperature of a conductor is typically between 0.5 and 7°C, therefore the results in Table 4-6 show that the CIGRÉ modelled surface temperatures are within the range that would result in a conductor core temperature of 50°C. As a means of determining the accuracy of P27 at the chosen sites a two stage method was carried

out. Firstly the present seasonal rating values are used as inputs to the CIGRÉ DTR model in order to derive conductor temperature values. The number of excursions per rating period was then derived. Figure 4-5 and Table 4-7 show the results of this analysis at the sheltered site.

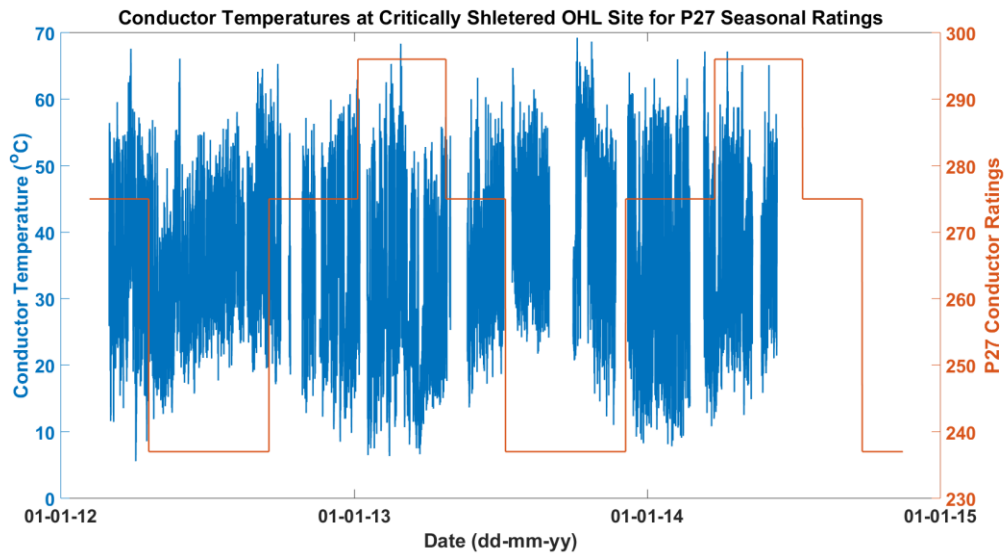


**Figure 4-5 – Conductor Temperatures due to constant loading at the P27 seasonal rating values**

As can be seen when using the current seasonal rating values a significant number of conductor temperature values exceed the circuit rated temperature value of 50°C. The most likely causes of this result being that the coincidence between low wind speed and high ambient temperatures appear with greater frequency than previously considered, and also that the average temperature values in each of the seasonal periods do not accurately represent those which are observed. In particular during the Spring / Autumn period the recorded ambient temperature values often exceed the value of 9°C. The number of excursions per seasonal rating period are shown in Table 4-7.

Seasonal Period	Number of Excursions	% of Period
Winter	7090	13.68
Spring / Autumn	11096	10.57
Summer	2209	2.67

**Table 4-7 Number of five minute periods and percentage per period for which conductor temperature exceeds circuit rated temperature**

As can be seen the percentage excursions per period are significantly greater than those stipulated by the P27 regulations (0.001%). This prompted the second part of this investigation, to examine the potential reductions required to deliver the same level of risk as is currently stipulated in P27. In order to evaluate this, reductions were made to the present seasonal P27 circuit rating values in single ampere steps in order to derive similar results to those found in [62] and to derive a new set of temperature excursion correlation curve as shown in Figure 4-2. The results of this analysis are shown in Figure 4-6.

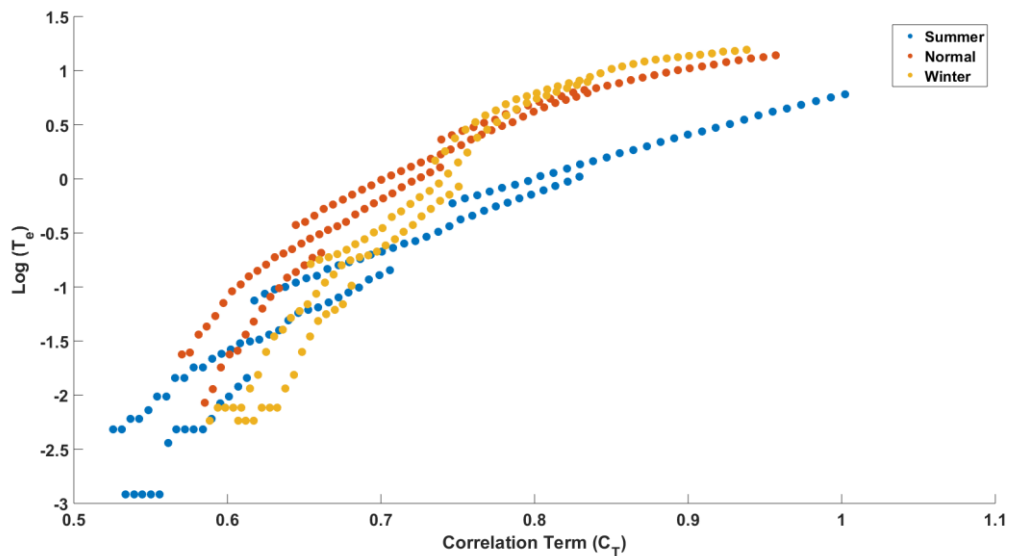


Figure 4-6 – Newly derived Temperature exceedance plots in line with those found in [62]

From the data shown in Figure 4-6 new constant circuit rated currents can be derived from a line of best fit, fitted to the data using the format of equation (33) albeit with newly derived parameters. This gives a new set of  $C_T$  values and as a result, a new set of seasonal circuit ratings.

	New P27 Seasonal Ratings (Non-Sheltered Site)	New P27 Seasonal Ratings (Sheltered Site)
Winter	278.64	230.37
Spring / Autumn	258.63	213.83
Summer	222.81	184.21

Table 4-8 – Newly derived P27 seasonal line ratings for Sheltered and Non-Sheltered example sites

At the non-sheltered site the newly derived seasonal ratings, whilst being lower than the presently used ratings have been shown to be in line with those derived from the new line of best fit as detailed in Section 4.4.1. At the sheltered site, the new circuit ratings have been shown to be significantly lower than these values. In order to examine the reasons as to why the new circuit ratings are lower than expected an analysis similar to that of Price and Gibbon has been carried out to determine the typical ambient meteorological parameters which coincide with conductor excursion events.

#### 4.4.3 Excursion Ambient Temperature

Figure 4-7 and Figure 4-8 show empirical CDFs of ambient temperature values at times where the conductor temperature was observed as exceeding the circuit rated temperature.

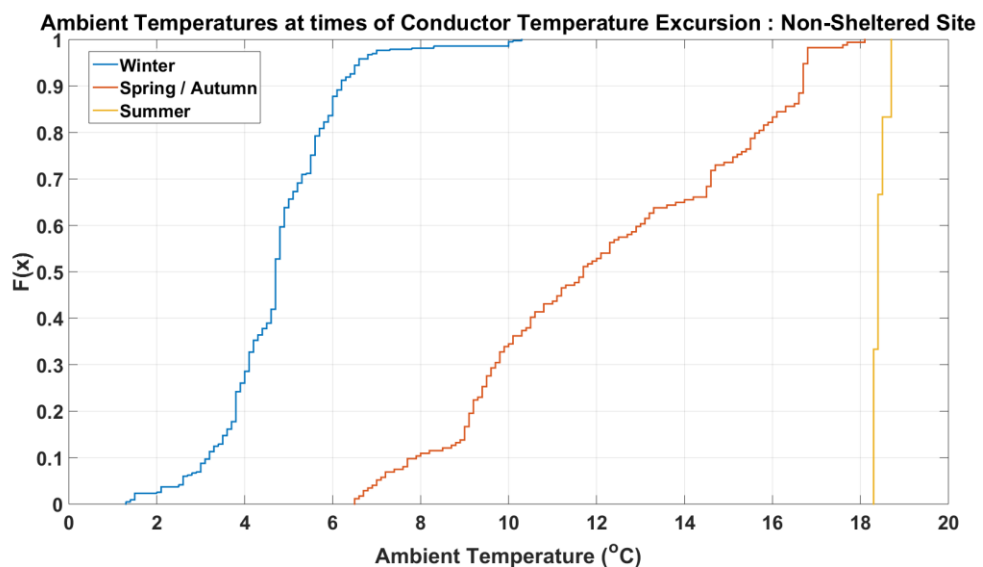


Figure 4-7 – CDFs of ambient temperature values during conductor temperature excursions – Non-Sheltered Site

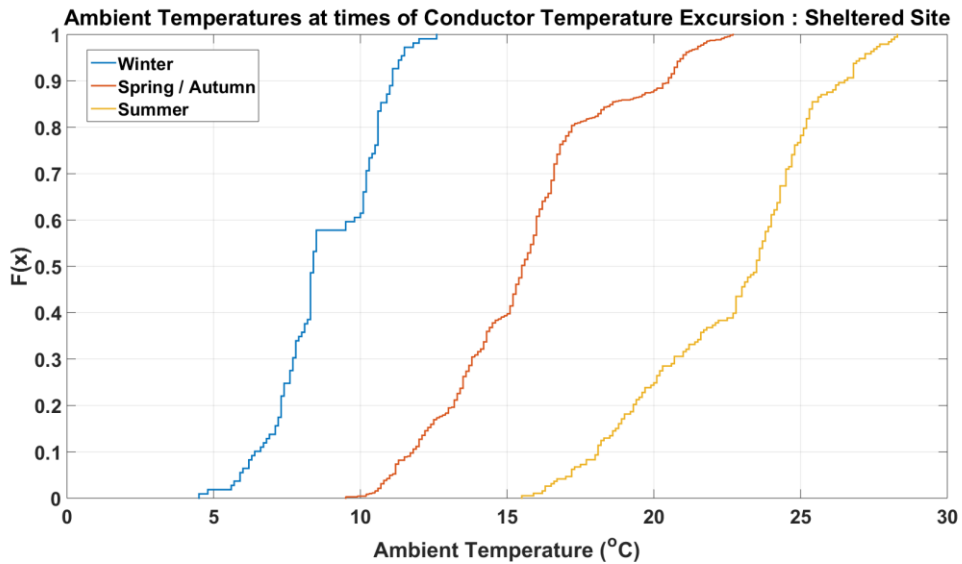


Figure 4-8 - Ambient temperature values during conductor temperature excursions – Sheltered Site

Table 4-9 details the mean, 99<sup>th</sup> percentile and maximum excursion ambient temperature values observed along with the stipulated P27 ambient values used to derive the ratings during each seasonal period.

Rating Period		P27 (°C)	Non-Sheltered Site (°C)	Sheltered Site (°C)
Winter	Mean	2	4.7	8.8
	99 <sup>th</sup> percentile		10.0	12.2
	Max		10.3	12.6
Spring / Autumn	Mean	9	12.1	15.6
	99 <sup>th</sup> percentile		17.7	22.3
	Max		18.1	22.7
Summer	Mean	20	18.4	22.6
	99 <sup>th</sup> percentile		18.7	28.2
	Max		18.7	28.3

Table 4-9 – Ambient temperature values during conductor temperature excursions

As can be seen, at all sites, the mean ambient temperature value at times of conductor temperature excursion with the exception of the Summer period at the non-sheltered site are greater than the values quoted in P27. For the rest of the potential combinations of season and monitoring site there are demonstrated increases in temperature from the quoted P27 values.

At the sheltered site the mean ambient temperature in the Spring / Autumn and Winter periods is roughly 7°C greater than the value outlined in P27. At the non-sheltered site for the same periods this increase is roughly 3°C.

These differences will play a significant role in overestimating the cooling capacity of the OHL in these periods and leads to the need for a reduction of static seasonal rating during these periods. One caveat is that as shown in the data quality study, the percentage of readings taken during these periods is not 100%. This may account for some discrepancies in the mean temperature due to the limited dataset. Though, as shown around 82.5% of the dataset was still monitored at the sheltered site.

#### 4.4.4 Excursion Wind Speeds

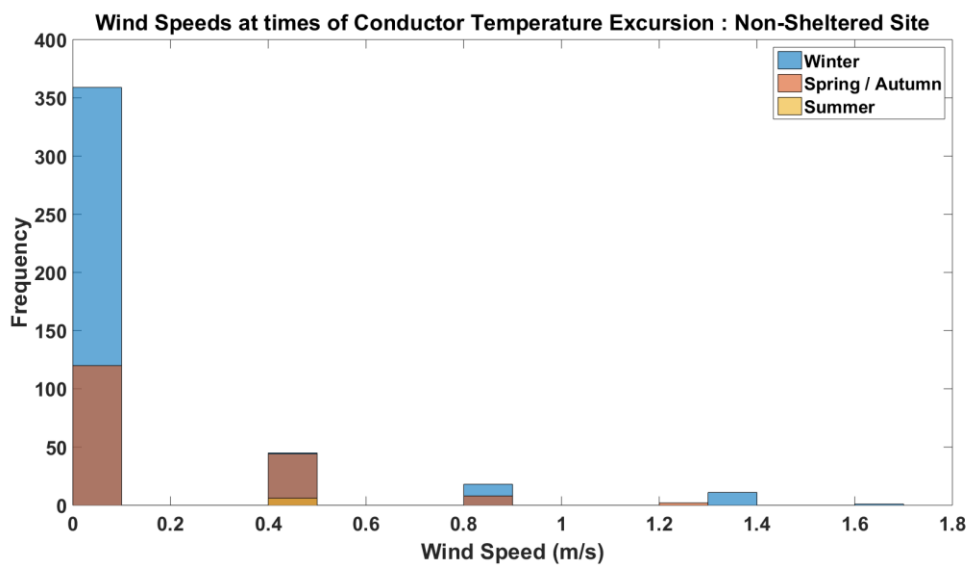
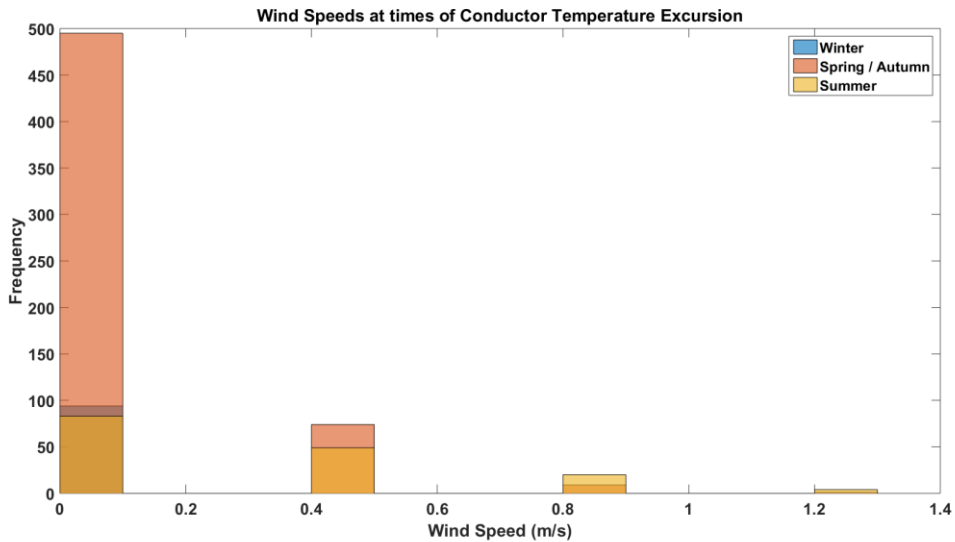


Figure 4-9 - Wind Speed values during conductor temperature excursions – Non-Sheltered Site



**Figure 4-10 – Wind Speed values during conductor temperature excursions – Sheltered Site**

Figure 4-10 show histograms of the observed wind speeds during times of conductor temperature excursions. As can be observed, a significant number of wind speeds have a value of 0m/s. Whilst this does not on the surface seem to be a significant deviation from the P27 figure of 0.5 m/s, the difference is such that the conductor surface moves from free to forced convection at this boundary. Forced convection offers increased cooling over free convection and therefore the lower wind speeds will result in lower than expected line ratings.

Rating Period		P27 (m/s)	Non-Sheltered Site (m/s)	Sheltered Site (m/s)
Winter	Mean	0.5	0.112	0.000
	99 <sup>th</sup> percentile		1.300	0.000
	Max		1.700	0.000
Spring / Autumn	Mean	0.5	0.153	0.065
	99 <sup>th</sup> percentile		1.180	0.800
	Max		1.300	1.300
Summer	Mean	0.5	0.400	0.258
	99 <sup>th</sup> percentile		0.400	1.300
	Max		0.400	1.300

**Table 4-10 – Wind speed values during conductor temperature excursions**

Table 4-10 shows the overall seasonal results for both the sheltered and non-sheltered sites. At both sites, whilst the maximum observed wind speed at times

of excursions was in some cases greater than the quoted figure of 0.5 m/s the mean value is smaller in all seasonal periods.

#### **4.5 Conclusions**

In this section, an analysis of the present P27 method for the rating of OHLs in the UK has shown that for specific sites there is the potential requirement for a de-rating factor to be applied. In particular at the sheltered Scar Brae site, significant reductions were necessary to the present seasonal ratings in order to deliver the required level of network risk. Since no equations are provided as to determination of the line of best fit of  $C_T$  values as shown in Figure 4-2 a series of potential equations have been proposed in order to replicate these results. When selecting the line of best fit which minimises the total error significant deviations have been found from those values quoted in the relevant sources.

Analysis from the 'critical span' has shown that for the majority of times where the conductor had a temperature greater than the circuit rated temperature the wind speed was at 0m/s. Due to the threshold in the heat transfer equations at 0.5 m/s this result has a significant impact on the overall heat balance of the conductor. Ambient temperatures in the Winter and Spring / Autumn (Normal) seasonal rating periods have also been demonstrated as being significant higher than those as quoted in [62]. These factors when coupled together have shown that in particular for the case of highly sheltered locations de-rating from the present circuit ratings is required, if the same level of network risk is required.

## **5 HV Feeder Load Synthesis: After Diversity Demand**

### **5.1 Introduction**

The following three Chapters outline the procedures required for development of feeder load profiles at the MV level of the distribution network to act as inputs to the DTR model.

When modelling the resultant loads there are a number of factors which need to be taken into account:

- The number and type of consumers within the group
- How does electrical diversity affect each consumer group?
- What is the response of those consumers to external influences such as ambient temperature?

The aggregation level at which the total profile is required can greatly affect the type of modelling required. When considering the modelling of load at the national level, often a multiple linear regression model or similar is used whereby the expected load is modelled as a function of parameters such as days of the week, ambient air temperature, humidity and economic factors such as GDP.

At the lowest level of aggregation, models for individual domestic consumption such as the model outlined in [110] use a combination of expected appliance usage, income, number of occupants and daylight hours in order to construct a highly accurate expected demand output.

The aim of the load synthesis method developed in this work is to deliver suitable profiles at the MV feeder level, in order to evaluate the capabilities of DTRs for load accommodation at this level. At this level, the decision was taken to ignore high level economic factors such as GDP to focus on more specific aspects of consumer's reaction to ambient meteorological conditions (more specifically ambient temperature) and on electrical diversity. This represents an assumption regarding suitable modelling inputs. At the aggregation level which this research considers, it has been assumed that the load group customer composition and ambient temperature values are of greater significance than parameters such as national GDP. GDP has often been included as a parameter within national

demand modelling, which represents an altogether different modelling problem. Whilst GDP has not been taken into account as a direct parameter, relative income has been taken into account through the use of national socio-demographic classifiers which have been used as a method to classify different domestic consumer attributes. This Chapter will firstly outline the rationale for deviation away from the presently used Elexon After Diversity Demand (ADD) consumer profiles, particularly when modelling consumer load groups of various sizes. The ADD has been used in this research as opposed to the After Diversity Maximum Demand (ADMD) since the requirement of the final feeder load profiles is to model the typically expected demands for load groups, as opposed to their maximum value. This is in line with the approach taken in [111].

A series of socio-demographically informed ADD profiles and a method for their derivation are then provided as a contribution from this thesis. These profiles will then be utilised in the following chapters as part of the overall load synthesis method to provide inputs to the DTR OHL model

In order to train and test the approaches outlined in this chapter, data from multiple monitoring points within the CLNR project was used. These monitoring sites were located at different points within the Northern Powergrid DNO area.

## **5.2 Chapter Goals / Objectives and Contributions**

### **5.2.1 Goal / Objective**

Since dynamic, as opposed to real-time thermal ratings will be used in this research, a suitable representation of demand group loads expressed as a time series is required to provide inputs to the thermal conductor model. The goal of this chapter is to develop a method of delivering such profiles, with the additional capability that the profiles must be capable of representing a demand group of any given size and combination of consumers. The effect of temperature on these demand groups must also be taken into account. This chapter will attempt to derive after diversity demand profiles which do not explicitly take into account temperature, but do so on a seasonal basis as per the presently used Elexon consumer demand profiles. The following chapters present a method to derive temperature sensitivities for these consumer groups and a method to combine each of these factors into an overall temperature sensitive demand group profile.

## **5.2.2 Transition from existing literature and research / Contribution**

Existing research in this field typically delivers demand profiles for large areas, or countries. After Diversity Demand profiles, such as those presented by Elexon, present demand profiles for individuals, however these represent a profile for a specific number of consumers. The ability to scale to any number of consumers, represents a key contribution of this chapter. An update to the existing profiles using a newly available public dataset also represents a contribution of this chapter, in addition to the ability to differentiate the expected demand profiles for consumers based on a set of socio-demographics, again a contribution of this chapter, building on previous work which considered annual energy demands as a function of the same socio-demographic classification scheme.

## **5.2.3 Attainment of Goals**

A socio-demographically grouped method for determining a more accurate representation of demand is presented in this chapter. This method has been tested against real-world measured data to determine its overall accuracy.

## **5.2.4 Chapter Outline Block Diagram**

Figure 5-1 a block diagram of the inputs, methods and outputs for this chapter. The combination of socio-demographics, publically available datasets regarding energy and the existing Elexon After diversity profiles represents a contribution in its selected sampling method from the newly presented DECC dataset. The derivation of new socio-demographically grouped ADD profiles represents the key contribution from this chapter, in addition to their testing against the available real-world monitoring data.

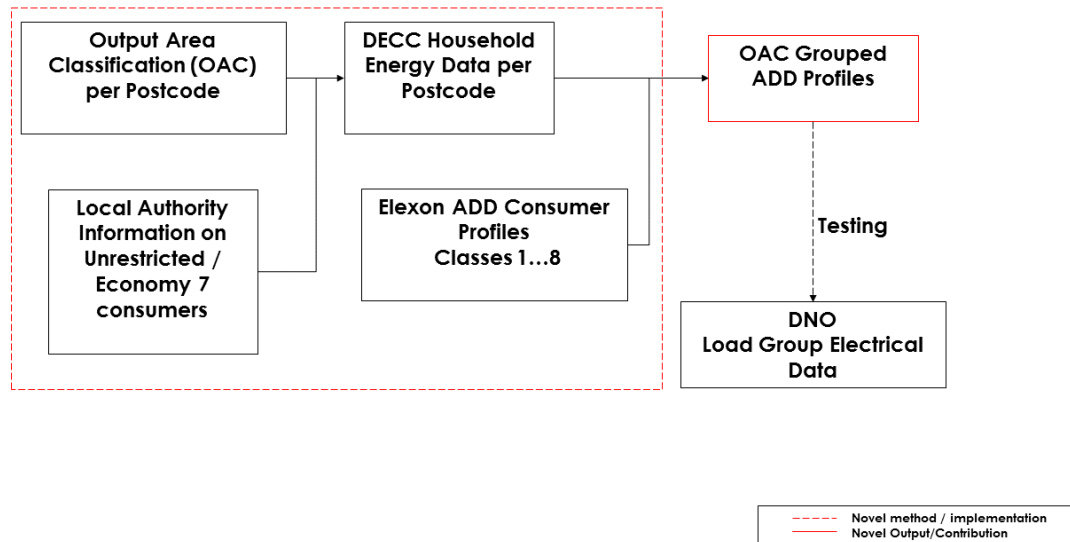


Figure 5-1 – Chapter 5 Block Diagram

## 5.3 Parameter Monitoring Data

### 5.3.1 Overall Primary Substation Descriptions

#### Denwick Primary Substation

- 66/20kV Primary substation
- Rural / Semi Rural
- HV feeders mostly of OHL construction
- Local Authority Area: Northumberland

#### Rise Carr Primary Substation

- 33/6kV Primary Substation
- Urban
- HV feeders mostly of UGC construction
- Local Authority Area: Darlington

### 5.3.2 Network Monitoring

These data range from monitoring at the LV Substation to HV feeder level. Data from each of the substation monitoring points comprised of:

- Three phase Real and Reactive power measurements
- Three phase voltages
- For some sites, ambient temperature.

At the primary substation level:

- ‘Real and Reactive’ current values
- Line voltage
- Ambient temperature

The values of real and reactive current at the primary substation levels are proxy measurements for real and reactive power and have therefore been converted using the measured voltage values in order to be directly comparable to the data from the LV substations. Ambient temperature monitoring was installed at each of the primary and secondary substations in the project. Again as per the electrical data, values were recorded at one minute intervals. The purpose of these sensors was for investigation of the ambient thermal conditions for distribution transformers and therefore some were located inside buildings. Due to the thermal effect of the transformer loading on the ambient temperature within the building, these sensors could not be used as they are not representative of the external air temperature. In these cases the closest ambient temperature sensor geographically was used as an indicative temperature value.

The monitored data was recorded at one minute intervals at all sites other than some ambient temperature values which were recorded at five minute intervals. Data in this research covers the period from 1/10/2013 to 30/09/2015.

A selection of 8 customer groups have been taken from the available data sources. These 8 were selected as a subset due to a number of factors. The most common was in relation to the number of missing data points within the datasets. Another significant factor was the presence of clear measurement errors as a function of the monitoring equipment used at the sites. These constitute profiles from customers located at Secondary substations (LV/MV) and from direct MV feeder monitoring at Primary substations. These monitoring points also represent a wide variety of customer compositions, with high concentrations of Industrial and Commercial customers, Economy 7 customers and typical residential customers.

Since the RTTR monitoring equipment is located on the 20kV network and some of the load data comes from the LV network, firstly a step must be taken to ensure all data is comparable. Information provided by Northern Powergrid concerning the transformer tap ratio and an estimation of the transformer losses on load allow us to make all data appear as if it were connected directly to the 20kV MV network.

## 5.4 Load Group consumer data

In addition to electrical and meteorological information gathered from the monitoring points, information on the type and number of consumers supplied at each of the monitoring points was made available by Northern Powergrid. The type of consumer refers to the Elexon profiling class to which they belong. An explanation of these profiling classes is provided below.

### 5.4.1 Elexon Profiling

Elexon governs the balancing of supply and demand within the UK electrical power system. Within their role, they have defined eight classes ( $k$ ) of electrical consumer for the purposes of profiling and billing. They are as follows:

- Class 1: Domestic Unrestricted
- Class 2: Domestic Economy 7
- Class 3: Non-Domestic Unrestricted
- Class 4: Non-Domestic Economy 7
- Class 5: Non-Domestic Maximum Demand with Peak Demand Load Factor < 20%
- Class 6: Non-Domestic Maximum Demand with Peak Demand Load Factor > 20% < 30%
- Class 7: Non-Domestic Maximum Demand with Peak Demand Load Factor > 30% < 40%
- Class 8: Non-Domestic Maximum Demand with Peak Demand Load Factor > 40%

For each of these classes an average demand profile also exists in the public domain [112]. These profiles are sub-divided into five seasonal categories, Winter, Autumn, Spring, Summer, High Summer and three daily periods, Weekday, Saturday and Sunday. When combined they give the 'After Diversity Demand' (ADD) values for each class throughout the year. These will be referred to as  $E_k$

and the number of customers in each Elexon class for each load group will be referred to as  $N_k$ . The seasonal and daily periods will be referred to as:

$$Seasonal = s = \begin{cases} 1 = Autumn \\ 2 = High Summer \\ 3 = Summer \\ 4 = Spring \\ 5 = Winter \end{cases} \quad Daily = d = \begin{cases} 1 = Weekday \\ 2 = Saturday \\ 3 = Sunday \end{cases}$$

Elexon currently states that on average for their demand profiling work their aim is for 2500 customers in each class [113], the number of customers used to compile the publically available dataset is unknown, however the assumption has been made in this research to consider the profile as a representative of a number of customers beyond which a significant change in the observed profile is not expected. This assumption has an impact upon the overall accuracy of the final method testing, however the profiles derived within this chapter are still able to provide an alternate method to those of the singularly available Elexon profiles in the public domain. Figure 5-2 and Figure 5-3 show the Elexon profiles for domestic and non-domestic consumers in the Winter weekday period.

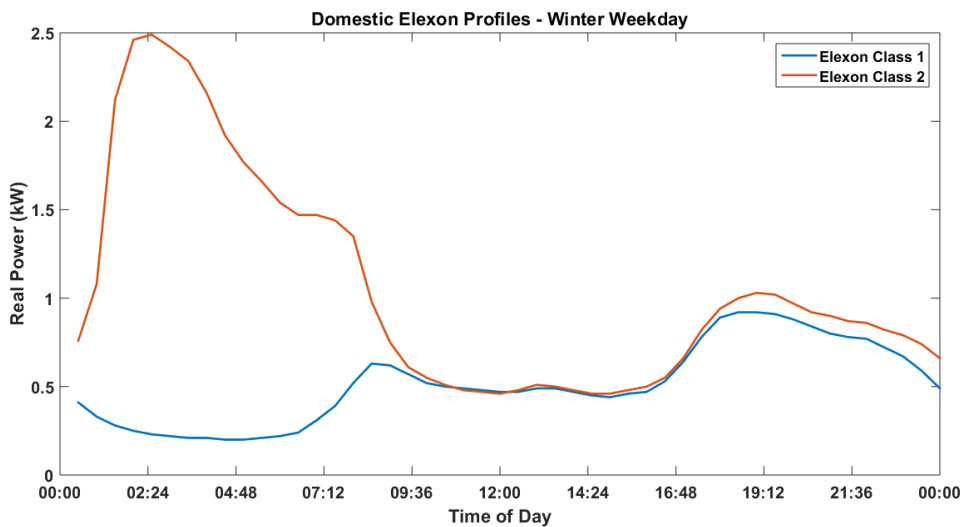


Figure 5-2 – Domestic Elexon ADD Profiles

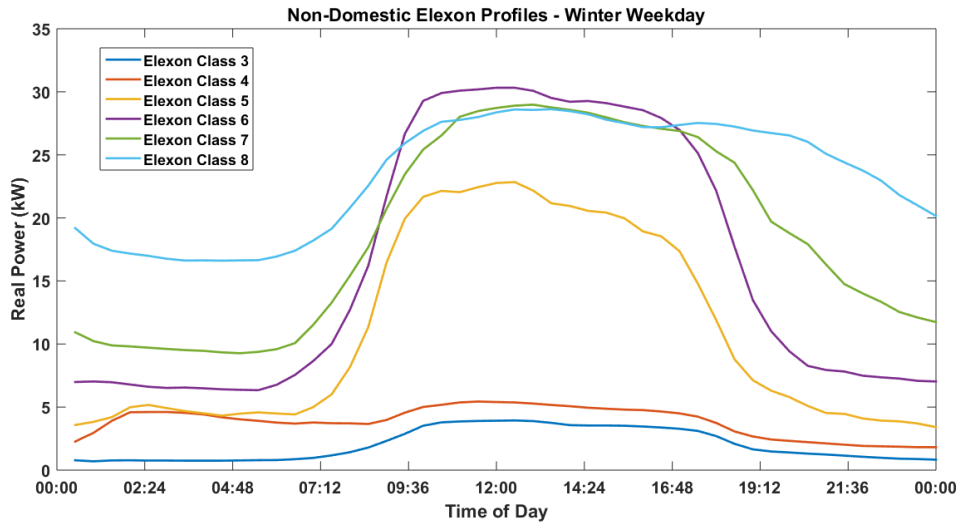


Figure 5-3 – Non-Domestic Elexon ADD Profiles

## 5.5 Electrical Diversity

Whilst the Elexon ADD profiles are useful for understanding the contribution of a particular load class to the overall load, the profiles used are representative of the ADD for group of roughly 2500 customers. As the number of customers tends towards one, the maximum demand or MD figure of the consumer is derived. For the purposes of deriving a load synthesis method which is applicable for any number of customers a method has been derived to deliver maximum ADD values as a function of the number of customers.

In 2015, the Department for Energy and Climate Change (DECC) released experimental figures which quantified the total electrical energy usage per full postcode in the UK (for example (NE1 7RU, as opposed to an ‘outer’ postcode such as NE1) [114]. The number of electrical energy consumers is also tabulated allowing calculation of the average energy usage per household, per postcode. Additional data was also released which quantified the percentage breakdown of Class 1 and Class 2 Elexon customers, although this dataset gives information at the local authority (LA) level [115]. An assumption has been made that the merging of these datasets in this way does not adversely affect the overall impact of the findings. Additional data regarding the breakdown at a lower level of aggregation was not possible, and represents a candidate for further work to extend the findings shown in this research. In line with this assumption, data at the LA level has also been used in the generic correlation and load synthesis

models proposed in this thesis to allow for recreation by members of the community, removing the requirement for non-publically available datasets as inputs.

Since data is available for the entirety of the UK it would be possible to derive more accurate UK profiles for both Class 1 and 2 customers beyond those found in the publically available Elexon profiles (which were gathered in 1997). This work however, aims to advance this potential work by deriving both socio-demographically categorised load profiles, and also for a range of final customer numbers when grouped together.

### **5.5.1 Socio-Demographics and the Output Area Classification**

Since electrical energy data is available per postcode, we can also categorise the data based on socio-demographic identifiers. The chosen categories in this work are based on those of the Output Area Classification (OAC) [116] derived from the UK national census of 2011. The rationale for the choice of the OAC is as follows, prior literature [117, 118] has utilised the OAC in analysis of energy consumption whilst examining degrees of social deprivation, and also the OAC is publically available and widely used within the social science community. Additionally the use of socio-demographically informed demand side response capabilities have also been explored in a pure power systems context in [119]. This work considered the potential DSR resource from consumers as a function of socio-demographics and its ability to provide ancillary network services to the distribution network. The research in this thesis examines the modelling of domestic consumer loads as a function of socio-demographics as opposed to assessing their flexible demand characteristics. Although the OAC classifiers have been used previously to model differences in energy consumption, there is an assumption within this work that this method is also valid for the classification of time series demand profiles.

The OAC categorises based on deviation away from the national average for a number of markers such as number of children per household, percentage of owner-occupiers and income level. A series of K-means clustering algorithms are used to divide the available census data and to derive the overall socio-demographic groupings.



was sub-divided at the highest possible level, that of the ‘Supergroup’. There are 8 high level supergroups within the OAC categorisation, which are as follows:

1. Rural
2. Cosmopolitans
3. Ethnicity Central
4. Multicultural Metropolitans
5. Urbanites
6. Suburbanites
7. Constrained city dwellers
8. Hard-pressed living

These categories will be referred to as  $OAC_j$   $j=[1...8]$ . The first stage of deriving updated Elexon profiles was therefore to group the electrical energy values per postcode according to their OAC supergroup. The second stage of the analysis involves use of the current Elexon Class profiles. Since the Elexon profiles are provided in kW, the sum of each class profile over the course of a year gives a figure for the total energy consumption in kWh. After grouping energy values per OAC Supergroup, average annual consumption figures per customer for each Supergroup can be derived and compared with those of the average Elexon profiles themselves. Table 5-1 shows the results of this analysis.

	Class 1 Energy Consumption (kWh)	Class 2 Energy Consumption (kWh)
Elexon Profile	3915	6929
OAC <sub>1</sub>	4667	8260
OAC <sub>2</sub>	3504	6202
OAC <sub>3</sub>	3049	5396
OAC <sub>4</sub>	3341	5913
OAC <sub>5</sub>	3544	6273
OAC <sub>6</sub>	3842	6799
OAC <sub>7</sub>	2924	5175
OAC <sub>8</sub>	3303	5845

**Table 5-1 – Elexon Annual Consumption Vs. OAC Supergroup consumption**

Table 5-1 shows that rural consumers found in OAC<sub>1</sub> areas are typically the highest consumers in both the Class 1 and 2 categories. Constrained city dwellers

on average consume the minimum electrical energy across both domestic categories, which is perhaps as to be expected due to the increased number of flats, and therefore reduced living space combined with the constraints relating to income. This analysis was also carried out at the Group and Subgroup levels and the derived energy consumption statistics can be found in Appendix 1.

If the original Elexon profiles ( $E_k$ ) are then normalised ( $E_{k_{Norm}}$ ) to their peak power i.e.:

$$E_{k_{Norm}} = \frac{E_k}{E_{k_{max}}} \quad (37)$$

A trapezoidal method such as that detailed in [111] can be used whereby the area under the curve (i.e. the annual energy consumption) is no longer that of the original Elexon profile, but is the energy value per postcode within each OAC Supergroup.

Before carrying out the area filling step, the final data pre-processing lies in proportionally assigning the energy values per postcode to Class 1 and 2 depending on the relative numbers in each class per postcode. Figures for this breakdown were unknown for each postcode therefore the percentage at the Local Authority was used.

After dividing the total number of consumers per postcode according to the Class1 to Class 2 ratio, the average energy per consumer is calculated based on the ratio between the original Elexon annual consumption values i.e.  $6929 / 3915 = 1.77$ . Therefore on average Class 2 consumers consume 1.77 times those in Class 1.

Whilst the original numbers of consumers per postcode range from 6 (since DECC were required to remove postcodes with fewer than 6 customers in total to preserve a relative level of anonymity) up to 434, with a mean of 234, after subdividing each postcode per the ratio between Class 1 and 2 consumers, clearly there will be numbers per postcode lower than the original value of 6 per postcode.

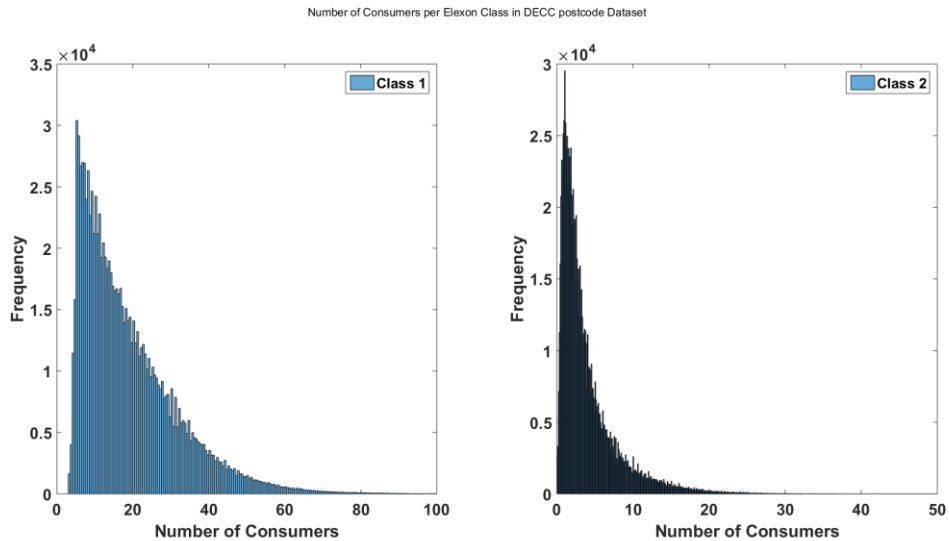


**Figure 5-6 – Frequency count of number of customers per Elexon class in DECC postcode dataset**

Figure 5-6 shows frequency counts of the numbers of consumers per class after the processing step detailed previously is carried out. As can be seen, whilst the maximum number of consumers per postcode was 434 prior to processing, the distribution of data shows that these numbers approach a minima after around 80 customers for Class 1 and around 30 for Class 2. This can be seen more clearly in the empirical CDF of the data shown in Figure 5-7.

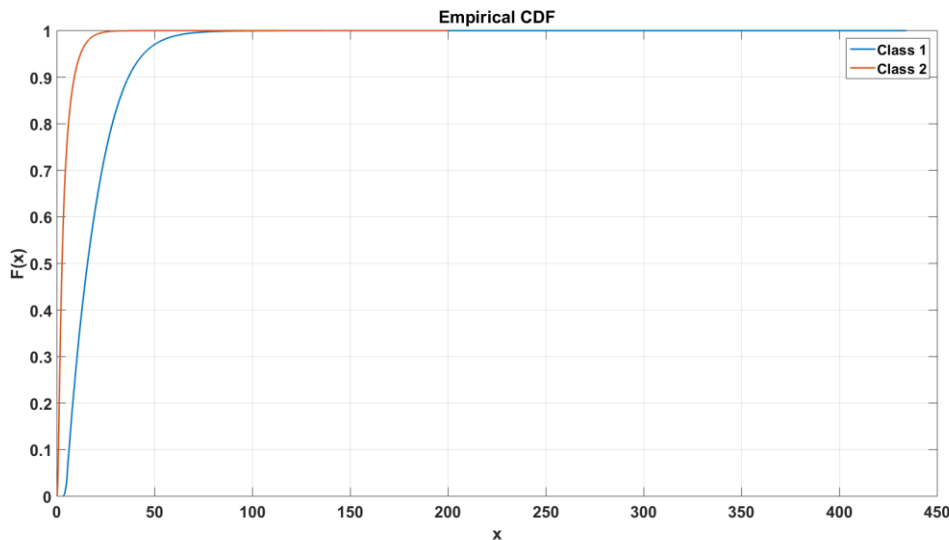


**Figure 5-7 – Empirical CDF for all data**

The customer numbers were evaluated at the 99<sup>th</sup> percentile level for each of the OAC super groups in order to minimise the amount of erroneous data located

in the tails of the distribution. At this level the total number of customers used for sampling are shown in Table 5-2. Numbers of consumers for Class 2 are lower than those for Class 1 due to the number of consumers with an Economy 7 tariff being typically lower than those with a standard unrestricted tariff.

99 <sup>th</sup> percentile (Customers)	Class 1	Class 2
OAC <sub>1</sub>	46.0	19.4
OAC <sub>2</sub>	85.0	22.2
OAC <sub>3</sub>	78.3	19.0
OAC <sub>4</sub>	58.2	18.8
OAC <sub>5</sub>	59.0	19.1
OAC <sub>6</sub>	55.2	18.8
OAC <sub>7</sub>	69.0	19.9
OAC <sub>8</sub>	58.1	19.1

**Table 5-2 – 99<sup>th</sup> percentile of customers per OAC Supergroup and per Elexon consumer class**

The values found in Table 5-2 were used as the maximum customer numbers in the subsequent calculation steps. Using the trapezoidal area filling procedure, the new maximum ADD values per consumer class can be derived for each postcode. Customers were grouped into bins ranging from one customer to the maximum number values in steps of two customers.

Figure 5-8 and Figure 5-9 show the distribution of maximum ADD values for a small subset of customer number bins. Data is shown for both Class 1 and 2 consumers. Both sets of histograms are shown here for the Rural (OAC<sub>1</sub>) Supergroup.

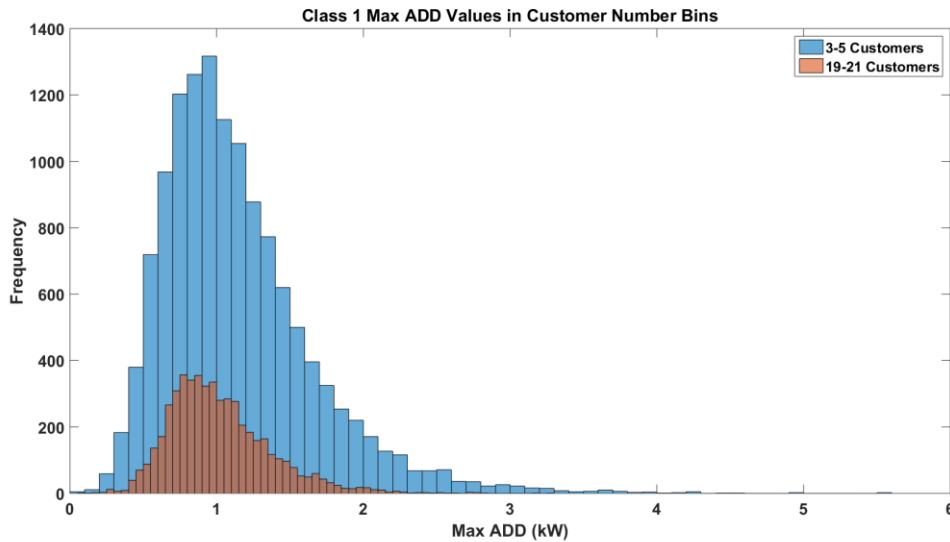


Figure 5-8 – Elexon Class 1 consumer Maximum ADD values for different customer number bins

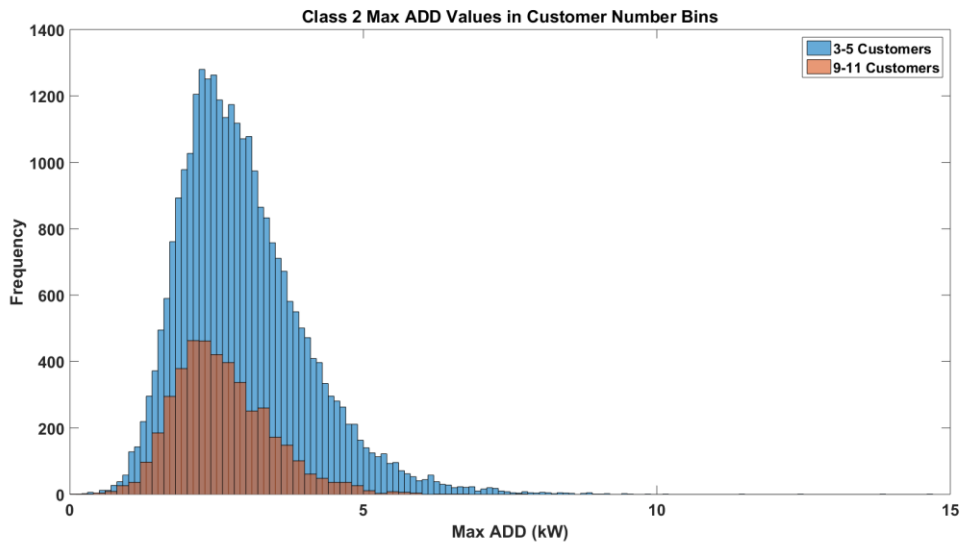


Figure 5-9 - Elexon Class 2 consumer Maximum ADD values for different customer number bins

In line with typical After Diversity Maximum Demand (ADMD) curves, as shown in [120], the mean value of the maximum ADD values is shown to decrease for an increase in customer numbers. In order to generalise the findings of this research, a series of ADD curve parameters were generated using this information. Due to the similarity in the trends between ADMD and ADD, the same power modelling approach as found in [120] was used, in the form of (38):

$$\text{Maximum ADD} = A \cdot N_k^B \quad (38)$$

This approach was modified in order to take into account the socio-demographics of the data and therefore the calculation becomes as follows:

$$\text{Maximum } ADD_{OAC_k} = A_{OAC_j} \cdot N_k^{B_{OAC_j}} \quad (39)$$

Based on these distributions, a representative value was taken from each of the binned frequency distributions. This was in order to derive an overall relationship for maximum ADD value as a function of the number of customers.

A series of tests was carried out to determine the correct value to take from each of the customer bins for combination overall. Percentiles were taken from each of the customer bin ADD distributions and a series of A and B coefficients derived for each OAC Supergroup. Percentile values were chosen at the 50<sup>th</sup>, 80<sup>th</sup>, 90<sup>th</sup>, 95<sup>th</sup>, 99<sup>th</sup> and 99.9<sup>th</sup> level. In this analysis step the procedure is as follows:

1. Values are sampled from the Maximum ADD customer distributions as shown in Figure 5-8 and Figure 5-9 according to the percentile value being tested.
2. A curve of Maximum ADD values per customer and per OAC Supergroup is then derived.
3. These curves are then used to scale the normalised Elexon ADD profiles per domestic consumer class relative to the total number of consumers within that class per load group.
4. Overall group load profiles are then synthesised using a model which will be outlined below
5. The accuracy of the finally derived group profiles are assessed and the sampling percentile which results in the minimum total error is selected.

For comparison, load profiles were also synthesised using the original Elexon profile values, scaled according to the number of customers ( $N_k$ ). As a first phase of the process, half hourly seasonal and daily average profiles were derived for each of the monitored load groups; in line with the half hourly average seasonal and daily individual profiles as detailed previously and was in order to provide an

adequate test of the accuracy of the OAC derived ADD ( $P_k$ ) values in comparison to the original Elexon ADD values.

The socio-demographic makeup of the local area where the load group data was observed is used in generating the new OAC ADD domestic component. This is carried out by calculating the relative maximum ADD values for the OAC supergroups  $P_k(OAC)_{j_{max}}$  and then calculating a weighted mean based on the actual OAC composition in the area under examination. The percentage representation of each OAC supergroup ( $j$ ) within the demand group ( $i$ ) is represented as:

$$ROAC_{ji} = \frac{N_{OACj}}{\sum_{j=1}^N N_{OACj}} \quad (40)$$

Where  $N_{OACj}$  represents the number of consumers having each OAC supergroup  $j$  within demand group  $i$ .

The final effective maximum ADD value for each domestic customer group is therefore calculated by:

$$ADD_{k_{max}} = \sum [P_k(OAC)_{1_{max}} \cdot ROAC_{ji} \cdots P_k(OAC)_{8_{max}} \cdot ROAC_{8i}] \quad (41)$$

$$Effective P_k = \begin{cases} P_{k_{Norm}} \cdot ADD_{k_{max}} \cdot N_k & k = 1,2 \\ E_k \cdot N_k & k = 3 \dots 8 \end{cases} \quad (42)$$

For non-domestic loads the original Elexon profile values have been used, scaled by the number of customers. The rationale behind this modelling approach is due to the reduced effect of diversity from non-domestic loads. This represents an assumption that the Elexon profiles adequately represent these loads and that diversity has a minimal effect on the ability to scale consumer profiles. This assumption has a potentially lower impact on the results of this research, since the relative percentage of industrial and commercial loads is low within the data from the available monitoring sites. This load synthesis method may therefore require suitable modifications if additional datasets with higher penetrations of industrial and commercial consumers become available.

## 5.6 Allowable Deviation from the Northern Powergrid Elexon Customer Compositions

During the course of this work, differences became apparent in the Elexon customer number composition values supplied by Northern Powergrid. Since the accuracy of the ADD values derived from the DECC postcode dataset will be tested against the monitoring data gathered during the CLNR project it is important that the classification breakdown per load group is as accurate as possible. Table 5-3 shows the variation in customer numbers according to various sources made available during the course of the research. As can be seen, the greatest potential for variation of the various class numbers occurs in Elexon classes 1-3. Additional variations are shown for some of the industrial customers though are typically limited to differences of 1 total customer per class. These variations and the ratio of variations between larger and smaller consumers is perhaps as to be expected since the time at which the information, and the period at which the information is updated would allow for non-observed switching between Economy 7 and unrestricted tariffs, or vice versa and the opening or closing of unrestricted small industrial consumers.

Substation	No. per Elexon Class							
	1	2	3	4	5	6	7	8
Elexon Class	1	2	3	4	5	6	7	8
Wooler St Mary	163	38	23	2	0	0	2	0
Wooler St Mary	173	36	18	2	0	0	1	0
Wooler St Mary	161	36	17	2	0	0	1	0
Alnwick St James	106	0	20	2	1	0	0	0
Alnwick St James	92	0	17	3	1	0	0	0
Darlington Melrose	279	15	0	0	0	0	0	0
Darlington Melrose	254	13	0	0	0	0	0	0

Table 5-3 – Original Consumer Breakdowns per load group from Northern Powergrid

The deviations of potential customer numbers per class were therefore converted to a percentage allowable difference from the quoted figures for each of the CLNR monitored load groups. This was carried out by calculating the maximum percentage differences between the customer number values per class

shown in Table 5-3. These were used as upper and lower bounds for potential customer number variations when selecting the most accurate percentiles from the ADD distributions as detailed previously. This was carried out for only Elexon classes 1-3 and in all future simulations and experiments the number of consumers in categories 4-8 remain as quoted by Northern Powergrid. The reason for the upper and lower values not having the same absolute value is that percentages are modelled as a difference for each of the possible class number combinations, i.e. 173 customers as a percentage increase over 161 represents an increase of 7.45% whereas a decrease from 173 would represent a decrease of 6.93%. Whilst the values for the subset of monitoring locations presented here have shown variations in customer numbers, an assumption has been made in this research that similar differences are possible across all of the available monitoring sites. Since the selected ADD modelling procedure will be tested against real-world data from these sites, these percentage deviations represent a wider tolerance for the successful fitting of the final model, which could have unwanted effects when deriving the A and B parameters in (39)

Elexon Class	1	2	3
Max Customer % Increase	13.21	13.33	26.09
Max Customer % Decrease	-15.22	-15.38	-27.78

Table 5-4 – Maximum percentage customer deviations from the original quoted values

### 5.6.1 Test Case

Since detailed information as to the exact OAC composition for the load group is unlikely to be available to those without access to a DNO, the decision was taken to additionally model the accuracy of the procedure outlined above through use of publically available socio-demographic information. Since exact information as to the OAC breakdown was not available for all load groups, and also due to this being the more likely scenario for general users of this method, it is the results from this level which will be used for the overall load synthesis method.

For the purposes of this analysis, each UK postcode was assigned to its appropriate OAC Supergroup. Each postcode is then tied to a particular Local

Authority and therefore the percentage breakdown per OAC Supergroup can be determined for this level.

For this work, the Local Authorities (LAs) of Northumberland and Darlington were used as these are the locations of the primary substation networks upon which the monitoring points were located. These LAs have the following OAC group composition:

OAC Supergroup	Northumberland %	Darlington %
1	7	27
2	1	0
3	0	0
4	1	0
5	22	14
6	32	20
7	15	9
8	22	30

**Table 5-5 – Percentage of OAC groups per network area**

The total error was then calculated using the Root Mean Square (RMSE) method and is calculated as the total error between the two profiles normalised to the total number of domestic customers, since the method for calculating the profile of non-domestic customer is the same for both approaches. As can be seen the OAC ADD values show improvement over the original Elexon profiles.

Percentile	Total RMSE Error per Domestic Consumer		Total Elexon RMSE Error per Domestic Consumer	
	Average	Minimum	Average	Minimum
50	1.8879	1.7551	1.8700	1.7354
80	1.8113	1.6836	1.8741	1.7311
90	1.7898	1.6751	1.8668	1.7350
95	1.7939	1.6903	1.8702	1.7389
99	2.0178	1.9178	1.8734	1.7355
99.9	2.7819	2.6877	1.8668	1.7348
100	3.0436	2.9377	1.8719	1.7303

**Table 5-6 Average profile RMSE per customer using both original Elexon and OAC ADD values**

Results show that the 90<sup>th</sup> percentile of the distribution resulted in the lowest total error, as shown in Table 5-6. Therefore this percentile has been taken from each of the binned distributions when calculating the overall A and B coefficients. An example of the resultant data used to derive the coefficients and the resultant lines of best fit are shown in Figure 5-10 and Figure 5-11.

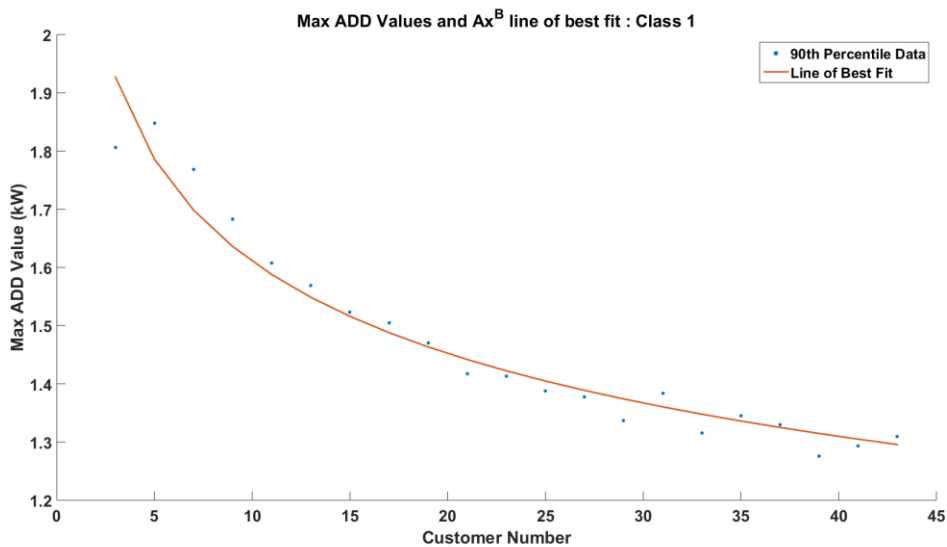


**Figure 5-10 – Maximum ADD customer number relationship for Class 1 customers**

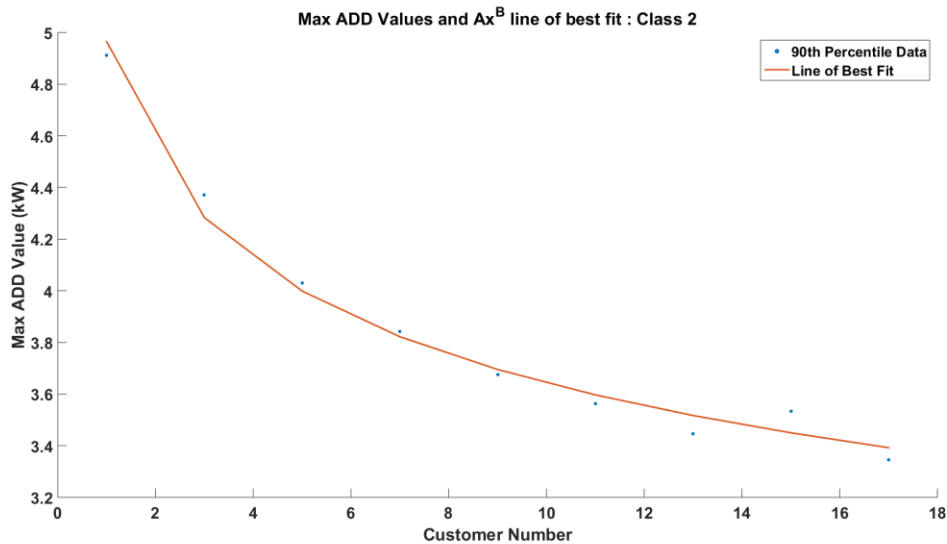


Figure 5-11 – Maximum ADD customer number relationship for Class 2 customers

### 5.7 Final OAC ADD Model Parameters

The finally derived values of A and B for each OAC Supergroup generated at the 90<sup>th</sup> percentile level can be found in Table 5-7. The value of parameter B for OAC 2 appears to represent an outlier relative to the parameters for the remaining OAC supergroups. This is potentially as a function of reduced data for this OAC supergroup when deriving the overall parameters.

Model Parameter	Class 1		Class 2	
	A	B	A	B
OAC 1	2.270	-0.149	4.965	-0.134
OAC 2	1.310	-2.9 <sup>^</sup> 10-10	3.902	-0.099
OAC 3	1.186	-0.031	3.038	-0.031
OAC 4	1.380	-0.095	3.179	-0.095
OAC 5	1.579	-0.112	3.557	-0.114
OAC 6	1.691	-0.127	3.664	-0.116
OAC 7	1.133	-0.047	2.841	-0.042
OAC 8	1.287	-0.083	2.963	-0.054

Table 5-7 – Final A and B parameters for derivation of maximum ADD values for each of the OAC Supergroups

Similar values to those shown in Table 5-7 could also be derived at each of the grouping levels within the OAC classification. As discussed in [113] a value of

2500 customers is typically used when calculating a representative profile for a consumer group. In line with these numbers, Figure 5-12 and Figure 5-13 show the profile for 2500 customers of the OAC<sub>7</sub> Supergroup shown relative to the original Elexon profile for the same period. Here data is shown for the Winter Weekday period.

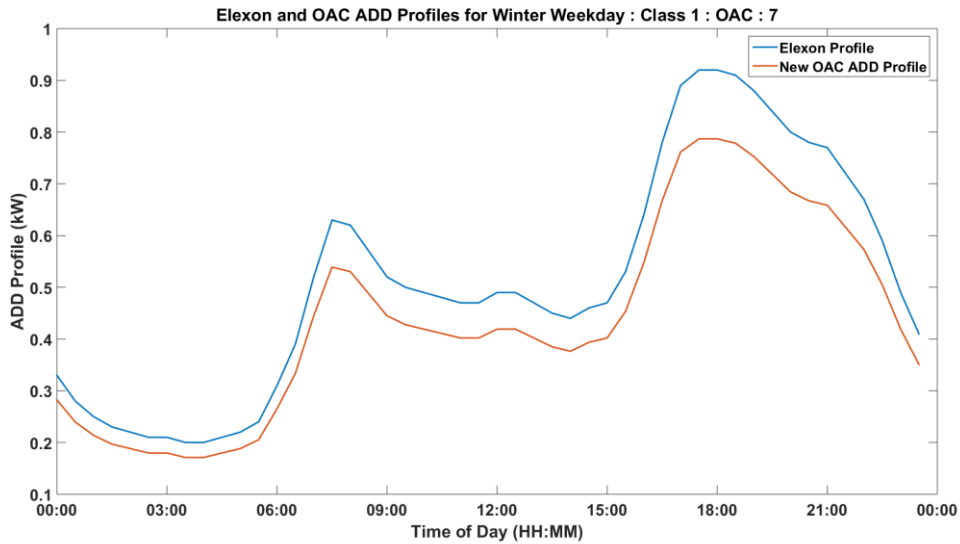


**Figure 5-12 – Elexon and OAC ADD profiles for Class 1 consumers**

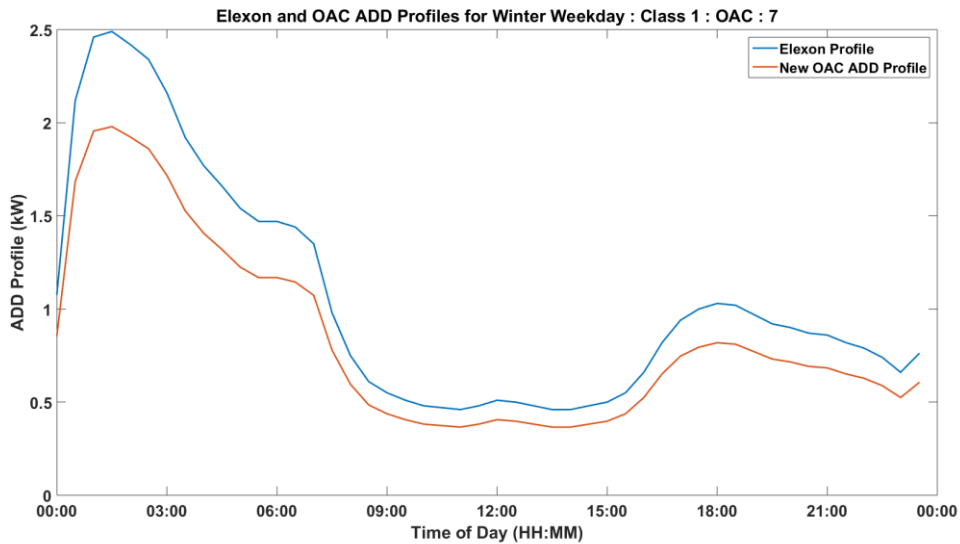


**Figure 5-13 - Elexon and OAC ADD profiles for Class 2 consumers**

Results for both Class 1 and 2 consumers have shown a decrease in their expected profiles for the OAC<sub>7</sub> supergroup. This is for a number of potential reasons. The Elexon profiles can be considered somewhat historic for profiling purposes, whilst the energy information used in the derivation of the new profiles

has been gathered relatively recently. Another potential reason for this reduction is that OAC group 7 represents a socio-demographic of relatively constrained circumstances against the remaining classifications. These constraints have been shown to result in typically reduced energy demands as in [118].

### 5.7.1 Test Case Results

Figure 5-14 shows a bar plot of the RMSE error when estimating the group ADD profile using both the OAC and Elexon only methods. As can be seen, as in the first test case, improvements over the Elexon method are made for each of the load groups. Significant improvements over the Elexon method are shown for load groups 4, 6 and 8. As in the first test case, additional refinements have been made to the original group consumer breakdown information supplied by Northern Powergrid.

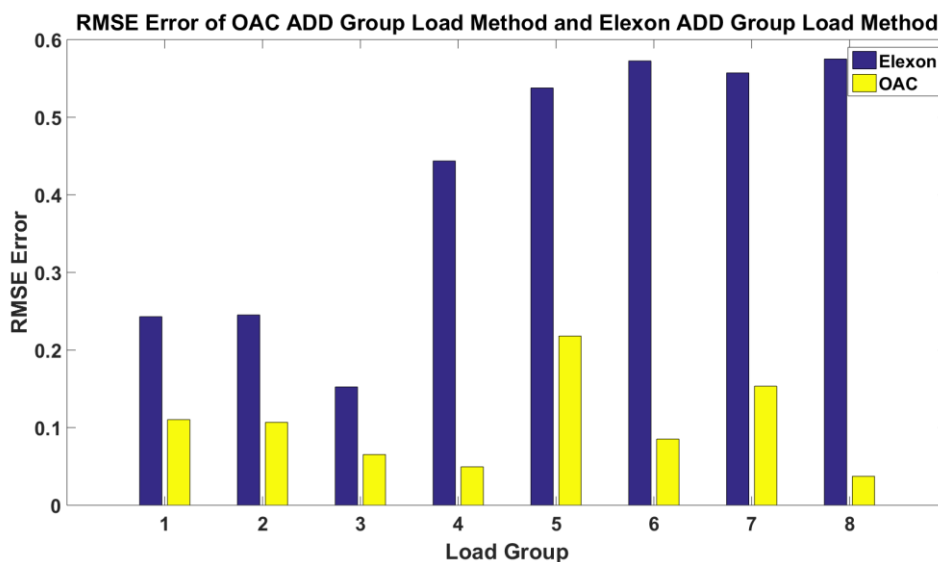


Figure 5-14 – RMSE Error using the OAC ADD and Elexon only methods

Table 5-8 shows the final consumer breakdowns according to their Elexon classification.

Elexon Class	1	2	3	4	5	6	7	8
Group 1	145	17	3	0	0	0	0	0
Group 2	385	14	1	0	0	0	0	0
Group 3	201	10	2	2	0	0	0	0
Group 4	1032	75	8	3	1	0	1	0
Group 5	893	45	36	3	3	3	0	1
Group 6	2424	284	53	5	1	6	2	3
Group 7	705	60	36	3	3	1	3	0
Group 8	2333	207	76	9	2	3	3	2

Table 5-8 – Final Elexon consumer class breakdown for load groups

## 5.8 Conclusions

The rationale for deviations away from the presently used Elexon ADD values has been made in this chapter. In order to accurately modify the expected demand for load groups of varying sizes, clearly those values which are quoted for static customer numbers will not apply. Whilst similar analysis has been carried out in the case of ADMD calculations, to date no such estimations have taken place for ADD values. As commented upon previously, increasing requirements will be made on load modelling at the distribution level to ensure efficient and economic operation of the power system. In this chapter it has been shown that by not taking into account the variations in maximum ADD according to customer numbers can result in significant under or over estimations of total group load.

In addition to variations according to customer number, key differences have been outlined according to the annual consumption of consumers according to their socio-demographic classification. The impact of these variations will be commented upon in the discussion section of this thesis.

## **6 HV Feeder Load Synthesis: Load-Temperature Relationship**

### **6.1 Introduction**

This Chapter will examine the relationship between load and temperature for the grouped loads outlined previously. This topic is of importance to the power system since ambient temperature alongside time of day, represents the most commonly used influential variable on electrical demand [42]. Understanding the nature of this relationship at the distribution level has been hitherto relatively less investigated than at higher and indeed the lowest levels of aggregation.

One of the key aspects of the research presented in this thesis is the determination of available network headroom. Such headroom can be considered as a function of asset capacity minus the load supplied. Whilst RTTRs and DTRs have been discussed as a method to increase an asset's capacity, accurate knowledge of the supplied load is required to allow true estimation of the overall headroom.

Since ambient temperature represents a key influence, understanding how this relationship varies based on time of day, day of week, season, and also on the composition of consumers within the group will give increased accuracy when modelling load at the distribution level.

### **6.2 Chapter Goals / Objectives and Contributions**

#### **6.2.1 Goals / Objectives**

Develop a method capable of determining the sensitivity of consumer groups to ambient temperature to allow for modification of expected demands based on measured temperature values

#### **6.2.2 Transition from existing literature and research / Contribution**

Much of the existing literature discussing the causal links between electrical demand and ambient temperature have done so either in highly detailed models of end-consumer consumptions, sometimes involving building thermal efficiency models; or have considered the relationship at the national demand level. This chapter provides a contribution in its assessment of the relationship at smaller

levels of demand group aggregation, those found at the distribution system level, up to and including the primary MV feeder level (33kV and below). The research presented here represents a novel contribution given the context of the work, although the use of linear correlation values to describe a relationship between demand and ambient temperature has been presented previously. The method to derive a causal link between consumer types, temperature sensitivities and the overall demand groups' relationship with temperature also represents a contribution of this chapter.

### **6.2.3 Attainment of Goals**

A series of temperature sensitivity coefficients have been presented for consumer types to allow for derivation of total demand group's correlation with temperature. This method has been shown to deliver good accuracy when tested against real-world data, and presents a development over the use of ADD profiles such as those from Elexon.

### **6.2.4 Chapter Outline Block Diagram**

Figure 6-1 a block diagram of the inputs, methods and outputs for this chapter. Real-world monitored ambient temperature and electrical data is clustered using the pre-existing DBSCAN clustering algorithm to expose the existing seasonal relationships and to allow for determination of the correlation between load and temperature. These correlation values serve as testing outputs for the proposed generalised correlation model, which uses the socio-demographic ADD profiles derived in Chapter 5 as additional inputs. The outputs from this chapter are both the assessment of clustered load-temperature values, the generalised correlation model and the derived correlation sensitivity coefficients for domestic class consumers.

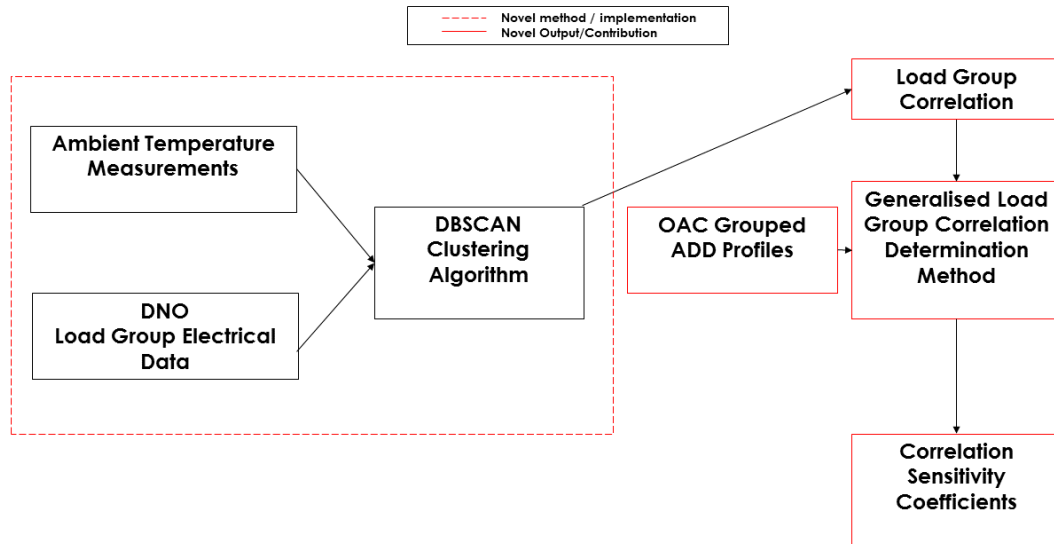


Figure 6-1 – Chapter 6 Block Diagram

### 6.3 Background

The relationship between electrical demand and ambient weather parameters is one which has been studied at length [43-45, 121, 122]. The significant factor in this research however is that analysis has typically been carried out using national, large area or individual consumer level data. The motivation for such research has been to forecast [123] or model the response of load to temperature, in order to ensure economic and reliable operation of the power system [124] or to accurately model individual consumer loads [122]. There is however, a space within this area of research which has not been well documented. This is when examining the effect of weather variables on grouped electrical loads at distribution substations and feeders.

Chapter 7 of this thesis will outline a temperature sensitive method for group load synthesis, with this Chapter acting as a prior study to examine how the relationship varies according to the day, time and seasonal factors discussed previously.

A number of potential methods for assessing this relationship exist, however these typically fall into two main categories, linear and non-linear models. In the case of linear models, a linear regression function is often fitted to the resultant

load and temperature parameters, often in the case of a multiple linear regression (MLR) model [45, 46, 125-129] .

In [126] as in [45, 130-132] the concept of cooling degree and heating degree days are used as part of an MLR modelling structure. Cooling and heating degree days (CDDs and HDDs) refer to the amount of heating required relative to a series a series of threshold temperatures. In the UK the threshold for heating is defined as 15.5°C [131] above which it is theorised that there is no requirement for heating demand.

In [131] HDDs and CDDs have been used to linearize a load temperature relationship in order to provide inputs to a proposed MLR model however this research examined data at the monthly as opposed to half hourly level. The relationship between CDDs and load for UK data at this level has also been shown to have a very limited relationship, due to the minimal demand for air conditioning. HDDs and CDDs have not been used in this research since these add an additional source of variability over the use of ambient temperatures. In [131] one threshold value is used to compute the HDD values of data at the national level. Whilst this assumption is potentially valid for large groups of consumers, there is the potential for such a threshold to inaccurately estimate the behaviour of consumers based on either tariffs or socio-demographics [133]. An investigation of such thresholds based on these variables was beyond the scope of this research, however this is a potential topic for further work to extend the approach taken in in this thesis. An additional factor which has not been taken into account within this research is the nature of temporal lag. Ambient temperature has been discussed as displaying something of a lagged relationship with electrical demand, in effect the causality of the relationship between ambient temperature and demand is not immediate. This represents a limitation of the findings within this research since models have considered the observed ambient temperatures and electrical demands as time-coincident. The rationale behind this approach was to determine if such relationships could be modelled accurately, and also reduce the overall complexity when considering the coincidence between the observed loads and asset capacities delivered by dynamic thermal ratings.

Non-linear models are proposed for the load temperature relationship in [43, 121, 134]. Such non-linear models take the form of multiple order polynomial

relationships as in [121] which also comments on the use of non-parametric methods. A non-linear model is often used in scenarios where demand increases as temperature tends towards the extremes, however as noted previously, the demand for cooling electrical loads in the form of air conditioning in the UK is reduced from that of countries such as Spain [44] and the USA [46]. The decision was therefore taken in this research to model load as a linear function of temperature. The time period over which each relationship will be examined was also a significant factor in the selection of a linear approximation, since it will be shown that for a singular half hour period a linear approximation is valid.

Having selected a linear approximation method to examine the half hourly load temperature relationships, two sets of parameters can be investigated. Firstly, the gradient and y-intercept of the resultant linear approximation and also the normalised parameter of the correlation coefficient. In [135-138] a series of correlation coefficients and linear regression coefficients are derived for a series of wide area load groups, however due to the aggregation level at which the loads are monitored no causal model of the type proposed in this Chapter is presented.

Use of the correlation coefficient to describe the overall relationship at a particular point in time is beneficial for a number of reasons. Firstly, the parameter by definition is normalised and therefore inferences as to the variability of load due to temperature can be made independent of a particular load group. A significant area in which knowledge of the correlation of a particular load group can be beneficial is in load forecasting and modelling. Or more particularly in the case of understanding the impact of input errors to the overall forecast or synthesis model. As noted in [42] whilst many models take into account the influence of weather variables such as ambient temperature [123, 139-141] few take into account the forecasting accuracy of the input variables used. The influence of these errors is discussed in [142] and the conclusion is made that forecasting error of ambient variables affects the resultant load forecast differently at different times of year. [143] uses a perturbation of input forecast variables to show that their method is robust to forecast methods although this data was for a large metropolitan area.

Secondly, from an overall system operation perspective, knowledge of a group's correlation between load and temperature can be used in economic

dispatch scenarios. In [144] a scenario is considered whereby through available interconnection between areas, power can be shifted from locations according to their correlation with weather systems and their resultant probabilities of reaching peak demand. At the distribution level, the problem could be formulated as one of identifying the requirement for ancillary network services due to the probability of peak network demands. As the requirement for flexible resources increases, the economic considerations of such resources will become more central in day to day operation of the power system [8]. Knowledge of a groups' correlation will also prove to be useful when considering the potential variability in the requirement of such network services to mitigate against a shortfall. In a scenario where such services have been scheduled, likely as the result of a forecast or load model, the impact of a deviation away from the forecasted conditions can be said to be a function of the correlation between load and temperature at that particular point in time, and the resultant impact on the required service is identified.

#### **6.4 Outline of the work in this chapter**

Firstly as a method of exposing the complex and time varying relationships between load and temperature when examined at this level, a density based clustering algorithm (DBSCAN) has been used to examine the raw data. Secondly a series of model structures to derive the correlation between load and temperature for a given load group are proposed and tested.

Finally in this Chapter the same modelling structures as proposed previously are used to derive a series of coefficients in order to suitably modify the ADD profiles generated in the previous Chapter. Again these coefficients are performance tested against synthesis methods which do not correct the typical ADD profiles for both diversity and temperature sensitivity dependent upon the time of day.

The purpose of this work is to examine the variability in the relationship between grouped electrical loads and ambient temperature due to composition of those groups. As discussed previously the nature of the model required to deliver the appropriate level of accuracy varies considerably depending upon the aggregation level at which it is required. At high levels of aggregated the functions of load and temperature are simplified from those at the lower levels. At this level

of aggregation the composition of the group, the day of the week and the time of day have been shown to significant impacts on the resultant relationship. In order to demonstrate this, the DBSCAN clustering algorithm outlined previously has been used to determine the number of load-temperature relationships in a half hourly period, dependent upon the day of the week.

As can be seen in Figure 6-2 at some time periods, multiple relationships can exist whereby at the same external air temperature, significantly differing values of resultant load are observed. The cluster shaded in orange represents the section of data which has been identified as a separate cluster within the overall dataset.

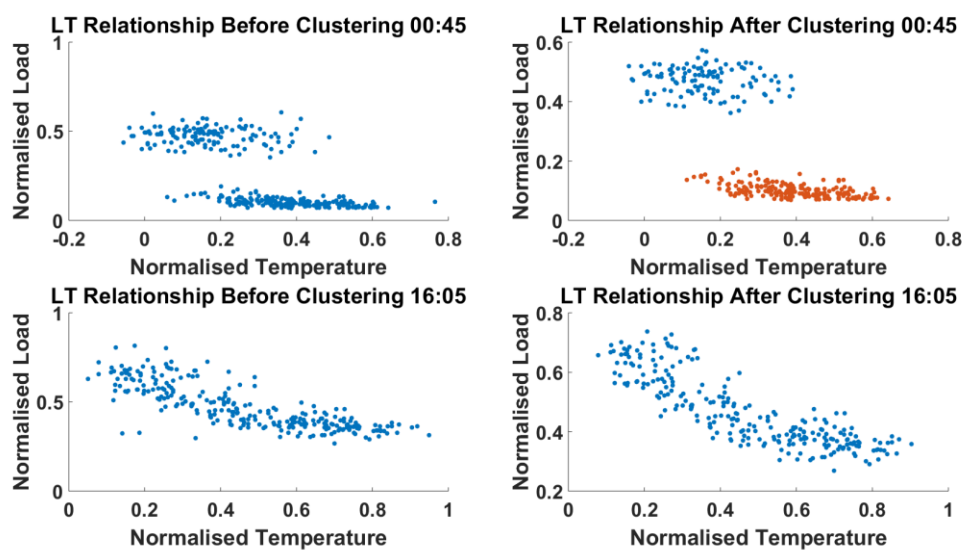


**Figure 6-2 - Examples of half hourly load and temperature values and the resultant DBSCAN derived clusters**

This is inherently due to the composition of the group itself. For example, Class 2 consumers (Economy 7) are those with electric storage heating in their homes. The results in Figure 6-2 show that at points where the storage heating load is not present, the resultant load is significantly diminished, therefore this must be taken into account when simulating the overall group load at this level.

## 6.5 DBSCAN Clustering Algorithm

The DBSCAN clustering algorithm [145] represents a different class of clustering algorithm as opposed to those such as hierarchical or K-means as the

number of clusters is derived as a function of the algorithm as opposed to a manually specified limit. The DBSCAN algorithm has been used for this reason, since the relationships are unknown, but also since the DBSCAN algorithm takes into account the natural noise within the load-temperature relationships.

This algorithm will be used to determine the number of potential load-temperature relationships as a function of time of day, seasonality and group composition. The DBSCAN algorithm begins by randomly selecting a starting point within the dataset. All data points within a particular neighbourhood of the original start point, defined as the 'Eps' are added to the cluster, however a minimum number of data points must be within the original Eps distance otherwise the point is rejected. Clearly if no points are 'reachable' from the initial starting point, the process is iterated until a suitable starting point is located.

There is of course the possibility that this point could be added into the cluster once more points have been located, but for the initial iteration the minimum number of points must be achieved. The search is continued however now, any points which are within the Eps neighbourhood of any of the points already added to the cluster can be added. These points are said to be 'density reachable' from the cluster.

This process is carried out until no further points are with the density reachable domain of the cluster. If all data has been assigned to a cluster, the process ends, however if data still remains, the process is simply repeated with a newly chosen starting point.

A number of parameters must be defined for usage of the algorithm. One, the number of minimum points per cluster has already been discussed and in this research this number has been set to 4. The additional required parameter is that of the Eps.

### **6.5.1 Automated determination of the Eps**

The first stage of the DBSCAN method requires a k-nearest neighbour (KNN) search of the entire dataset. The KNN searches the dataset to locate the 'k' closest points within the dataset to some predefined test point. Neighbours are located due to their distance from the selected test points. A number of distance metrics

are available to generate the KNN search, here the standard Euclidean distance metric has been used.

The choice of 'k' in the context of DBSCAN has been debated [145] where significant improvements in performance of the algorithm were not achieved by increasing the value of 'k' beyond 4. This is value which has been chosen for all clustering using the DBSCAN algorithm.

The knn search results in a series of distances between points which is then sorted. An example of these sorted distances is shown in Figure 6-3.

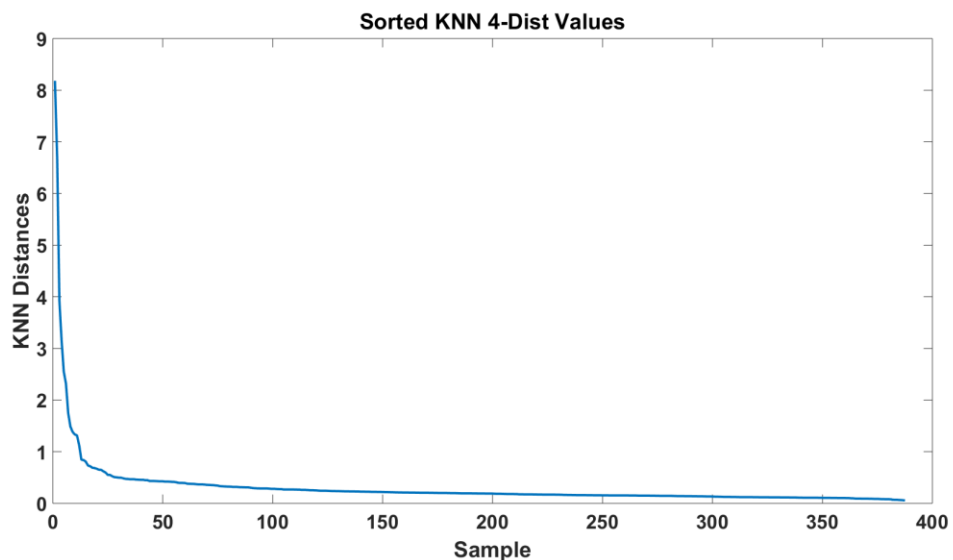


**Figure 6-3 – Example of the Sorted KNN distances from the DBSCAN clustering algorithm inputs**

Figure 6-3 shows the sorted '4-dist' values calculated from the input data. A 'knee point' can clearly be observed in the data samples at around 20 samples. It is this knee point which is used within the DBSCAN algorithm to define the typical neighbourhood or Eps in which the algorithm should search for similar data. The data to the left of the knee point represents noise in the dataset which could distort the end clustering results and reduce performance in determining the correct partitions in the data. In [145] determination of the knee point is done manually, however in this research the 'Kneedle' method [146] has been used to automate this process. Whilst the use of the DBSCAN algorithm itself does not represent a contribution to knowledge, automation of this knee-point determination using the 'Kneedle' method does represent a contribution to use of the DBSCAN method.

### 6.5.1.1 Kneedle' method

The parameter of Eps is required as an input to the DBSCAN algorithm but varies based on the dataset which is being clustered. The knee point of the sorted distance plot can be used a proxy measure for the 'true' value of Eps. An automated method of determining this parameter is therefore of importance, particularly when clustering large quantities of datasets, where visual inspection would be considerably time consuming. The choice of the 'Kneedle' method allows for such automation. This method first calculates the differences between all points in the dataset. Each data point is then analysed to determine if a local maximum exists. These maximums are then referenced to a data derived threshold. If at a particular data point, is found to be below the threshold, before the next local maximum value a knee point is estimated. Since for the difference data considered in here there is typically a single knee point, the index of the first determined knee point has been used to estimate the Eps.

## 6.6 DBSCAN Results

Figure 6-4 shows an example of the input data to the DBSCAN clustering algorithm. In this case, non-normalised load and normalised ambient temperature values are provided as inputs. In this section as in each of the following Chapters, ambient temperature values have been normalised to the maximum observed UK air temperature to date (38.5°C) [147]. The use of normalised air temperature data has an impact on the final clustering selections and the representation of the load-temperature relationship in general. Since the data range of ambient temperature values within each half-hourly period is not constant throughout the course of a day (i.e. there are very few high ambient temperature values in the early morning), a correlation represented as a function of raw as opposed to normalised data results in differing values of correlation. The use of normalised data allows for comparison between different half hourly time periods directly since the normalisation value is independent of time. Since the correlation between load and temperature is derived for each demand group separately, normalising the electrical demand from each load group would have no effect on the half hourly correlation values.

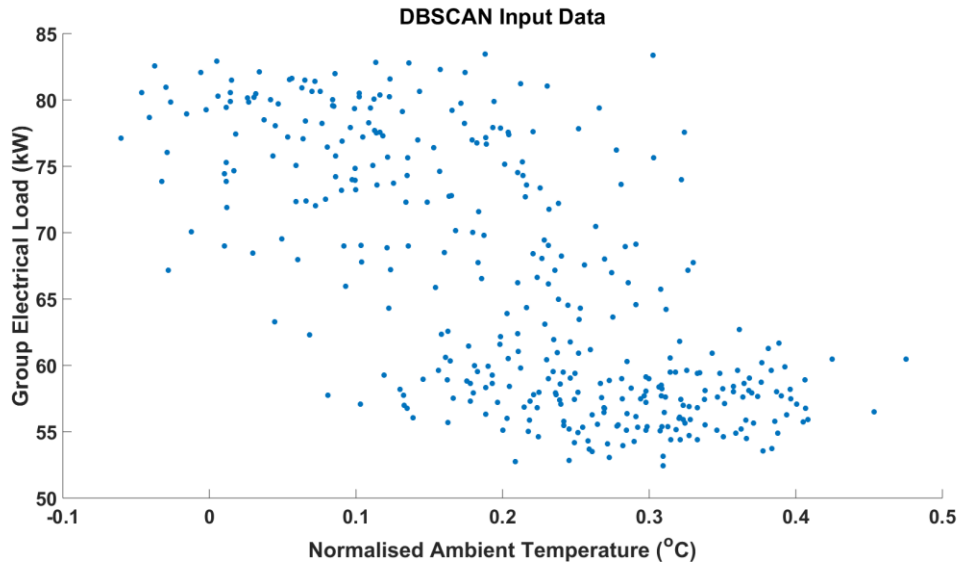


Figure 6-4 – Original half hourly input data

Figure 6-4 shows the presence of two distinct clusters, one at around 55kW and the other at around 80kW. Figure 6-5 shows the results of the DBSCAN clustering algorithm when used upon the data presented in Figure 6-3. In addition to the more prominent clusters noted previously the algorithm also identifies the data in between the two clusters as an independent set.

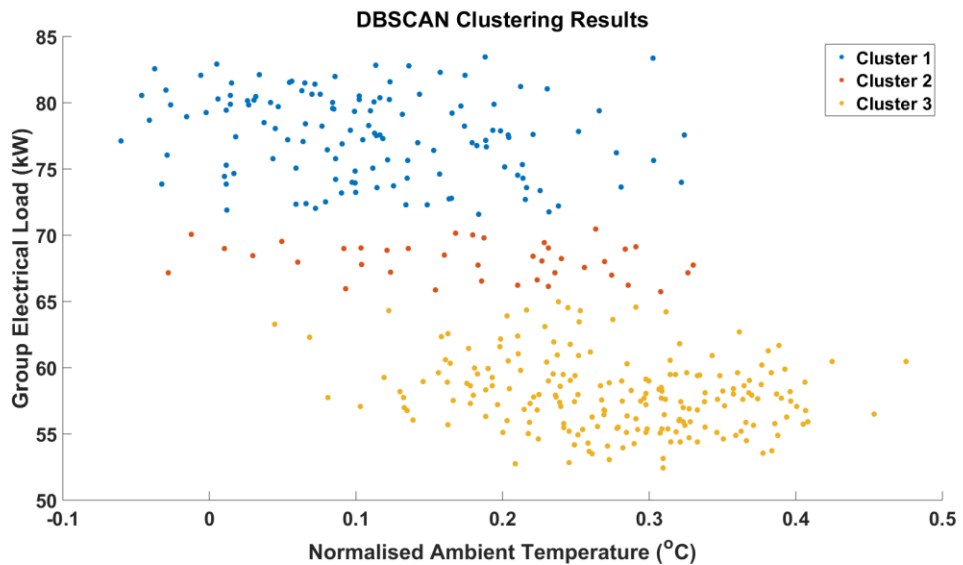


Figure 6-5 – DBSCAN derived clusters within the input dataset

## 6.7 Load-Temperature correlation

When determining the group's correlation between load and temperature, the procedure is as follows. In this research, the commonly implemented Pearson Correlation Coefficient has been used (41).

$$C(Load, T_a) = \frac{cov(Load, T_a)}{\sigma_{Load}\sigma_{T_a}} = \frac{E[(Load - \mu_{load})(T_a - \mu_{T_a})]}{\sigma_{Load}\sigma_{T_a}} \quad (43)$$

Where *cov* is the covariance,  $\sigma$  is the standard deviation, *E* is the expectation and  $\mu$  is the mean.

Firstly the data is organised according to daily period as per the Elexon time periods and then by half hourly time step. The DBSCAN algorithm is then applied to this data to determine the possible number of load and temperature relationships within the period. Each load temperature data point, whilst being assigned to a particular day also belongs to each Elexon seasonal period.

An additional factor to this study is to determine if load temperature correlation varies significantly as a function of seasonality. This represents a research contribution due to its implementation of clustering to determine these relationships, as opposed to manually separating the data based on seasonality or monthly period.

It is important to note that this is subtly different to the wider relationship of demand varying based on temperature values. The correlation refers to the strength of the relationship, i.e. whether the same external stimuli have the same effect on demand for the entire annual period. Within each Elexon seasonal and half hourly period, the modal DBSCAN cluster is identified, along with each clusters' load temperature correlation value. The maximum number of relationships exposed by the algorithm was 5, i.e. one relationship per seasonal period. The breakdown of relationship numbers is shown in Table 6-1.

Number of Load-Temperature relationships	1	2	3	4	5
Percentage of Half Hourly periods with N relationships (%)	28.2	30.5	28.5	11.9	0.9

Table 6-1 - Number of Load-Temperature relationships per half hourly period

If this correlation value has a p-value below the accepted threshold then the correlation value is assigned to that particular season and half hourly period. Here the typical p-value of 0.05 has been used. If the correlation value does not meet the p-value criteria then this correlation value is rejected.

### 6.7.1 Group Correlation Profiles

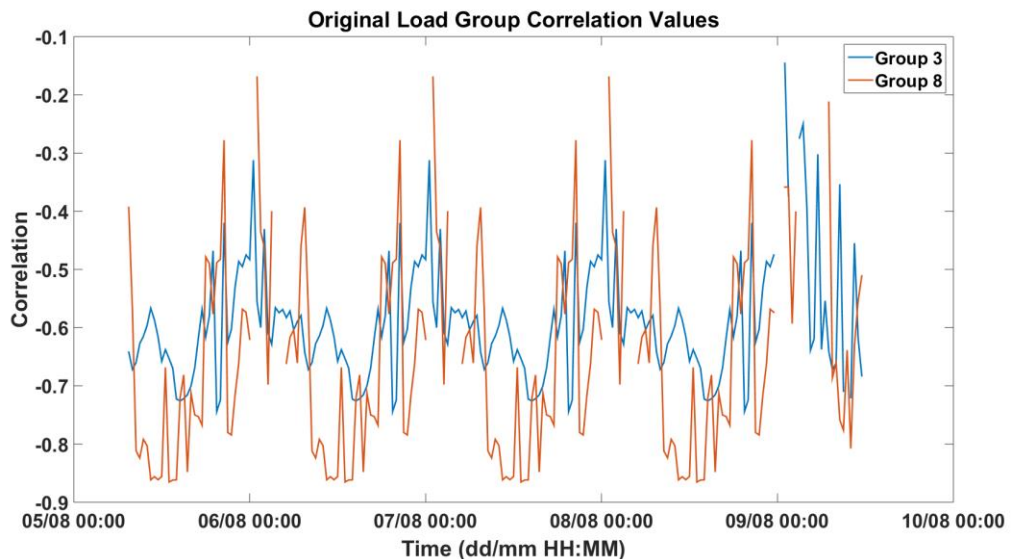


Figure 6-6 - Examples of Group Correlation Profiles

Figure 6-6 shows examples of correlation profiles for two selected load groups. In order to deal with potentially missing correlation values as a result of their p-value rejection, the resultant correlation profile is firstly linearly interpolated. Since most correlation values (99.95%) meet the p-value criteria the number of correlation values which have to be linearly interpolated are minimal.

An additional process to reduce some of the apparent variability in the final correlation values as shown in Figure 6-6 was to pass a smoothing filter over the values. This was of the moving average type with a sliding window of 6 values (equivalent to 3 hours). A number of sliding window lengths were considered for the implementation of this smoothing process. Clearly as the sliding window length is increased, some features of the correlation can be removed, resulting in an over-smoothed profile. 3 hours was found to present the best trade-off between having the shortest window possible and being able to deliver accurate results when developing the final generalised correlation model. The implementation of this smoothing window represents an assumption that this is the best approach

possible, and that the original half hourly correlation values have not been adversely modified such that they no longer represent the original data sufficiently.

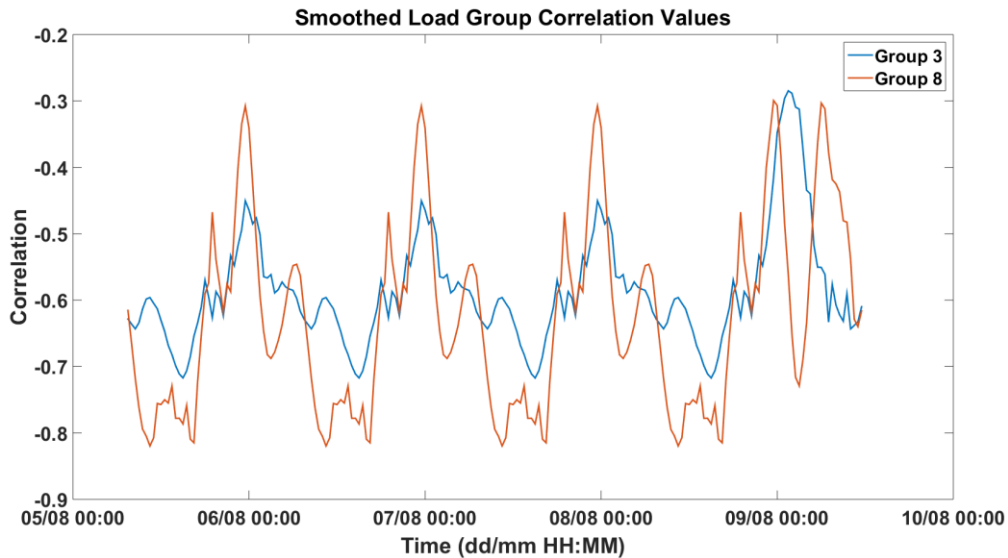


Figure 6-7 – Load Temperature correlation profile after smoothing

As can be seen in Figure 6-7, each group displays differing relationships with temperature over time. For reference, 05/08 refers to the 05/08/2014 which was a Tuesday with 9/08/14 therefore being a Saturday.

Group 8 shows much stronger correlation in the early morning period as opposed to Group 3. This is likely as a result of the relative percentage of Economy 7 customers in this load group as opposed to Group 3.

### 6.7.2 Analysis of Correlation Error

Examples of the finally chosen data clusters for a randomly selected group at two half hourly time periods are shown in Figure 6-8. The correlation of the group at 17:00 is clearly shown to be stronger than that of the group at 03:00. This is as to be expected for this particular group since no Economy 7 consumers are present within this load group, therefore during the early hours of the morning consumption is typically at a minimum. For consumers in the Economy 7 class, this relationship is more likely to demonstrate a stronger correlation. As an additional piece of analysis, the impact of a potential forecasting or modelling error was examined. In this analysis it has been assumed that based on an appropriate

forecasting model using exact information as to the ambient temperature, true estimation of the resultant group demand can be made.

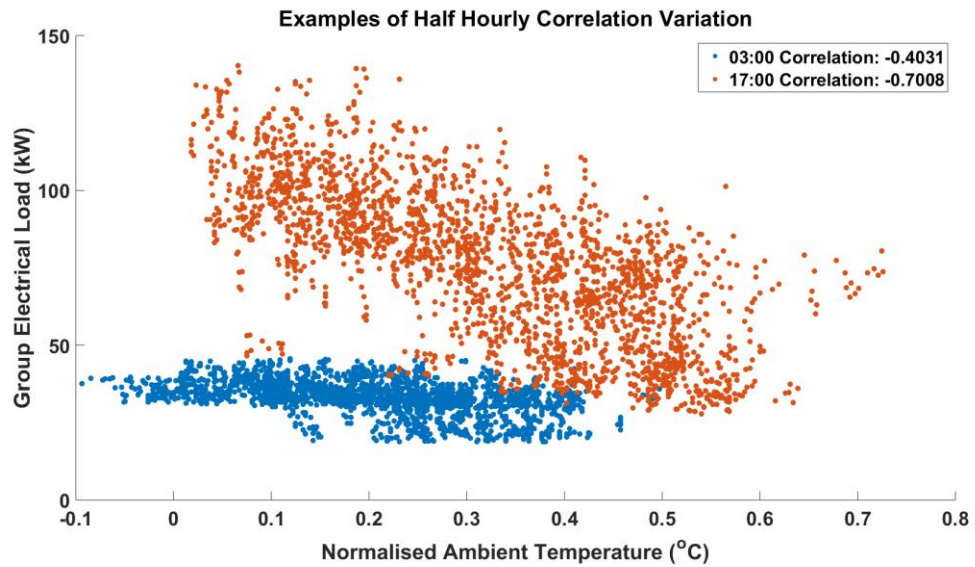


**Figure 6-8 – Examples of half hourly correlation values**

As can be seen in Figure 6-8 if for example the temperature value was forecast at a value of 7.7°C (0.2 when normalised against the maximum value of 38.5), and the time of day was 03:00 then the resultant impact of a forecasting error would be relatively minimal since the set of demand values is relatively similar across the range of normalised ambient temperature values. However it can also be seen that at 17:00 the same forecasting error would not result in the same error in the resultant load. In [148] a Mean Absolute Error (MAE) value for forecasting of ambient temperature was calculated as between 1.15 and 1.75°C based on the time over which the forecast is made. These would relate to a deviation of 0.03 and 0.045 when normalised to 38.5°C respectively. For completeness in this analysis a potential deviation of 0.05 or 1.925°C from a hypothetical forecasted ambient temperature value has been considered. The resultant analysis gives an estimation of the impact of such an error as a function of a groups' correlation.

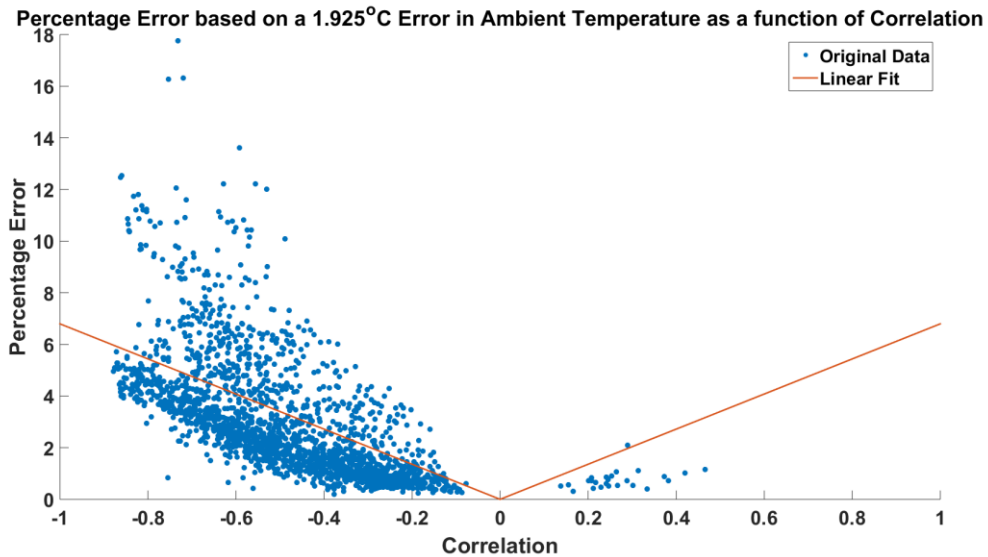


**Figure 6-9 – Percentage Load Error due to ambient temperature error as a function of correlation**

Figure 6-9 shows the variation in percentage error as a function of correlation. Positive correlation data on the right hand side of the graph is relatively limited, since there are limited time periods where demand groups observe a positive correlation with ambient temperature. As can be seen, the percentage error in demand estimation increases as the correlation tends towards its minima as is to be expected. This is as shown in Figure 6-9 whereby an error in temperature estimation, essentially a shifting to the left or right along the x-axis, would result in a more significant deviation in the expected demand for the group at 17:00 as opposed to 03:00. The original data from the analysis is shown alongside a fitted piecewise linear function:

$$Gradient = \begin{cases} -6.797 & \text{if } r < 0 \\ 6.797 & \text{if } r > 0 \end{cases} \quad (44)$$

This function can therefore be used to determine the potential envelope of group demand values at a particular point in time.

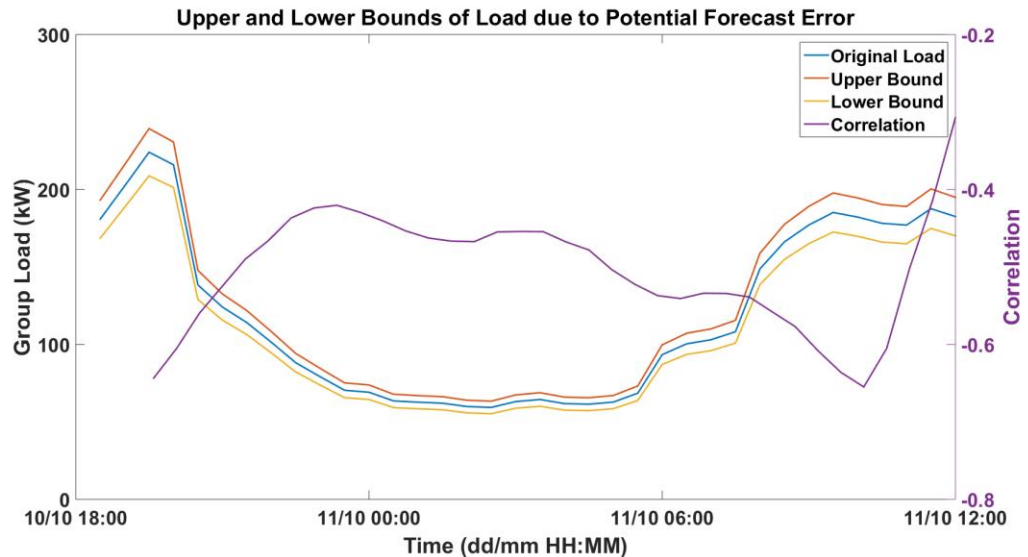


Figure 6-10 – Upper and Lower bounds of demand group load based on ‘forecast error’

Figure 6-10 shows the resultant upper and lower bounds of group load based on the assumed forecast error modelled previously. Between 00:00 and 06:00 the error is at a minima due to the reduced correlation at this time as represented by the narrowing of the upper and lower bounds. The envelope increases as the correlation increases in strength towards 12:00.

## 6.8 Generalised Correlation Model

The final output of this section is to deliver a series of correlation sensitivity coefficients (CSCs) for each of the domestic Elexon classes related to the overall correlation of the load group with temperature. The coefficients given will allow for derivation of a group’s correlation with temperature regardless of load group size or composition.

The correlation model presented in this chapter has two main components. Each  $k^{th}$  class of consumer (i.e. residential or industrial), can be thought of as contributing to the overall demand of group  $i$  ( $L_i$ ), as a function of both their expected real power demands ( $P_k$ ) and the number of consumers in each class. This contribution can be expressed either as raw value, or can be normalised against the group demand and therefore expressed as a percentage. It is this normalisation which allows for the model to generalise across multiple customer combinations not found within the training dataset. In addition to these demand contributions, each class also has associated with it a particular sensitivity to ambient

temperature. The correlation model presented here attempts to determine this sensitivity to allow for derivation of the overall load groups' sensitivity.

The socio-demographic makeup of the local area where the load group data was observed is used in generating the domestic components of the overall load group. This is carried out by calculating the relative maximum ADD values for the OAC supergroups and then calculating a weighted mean based on the actual OAC composition in the area under examination. In order to test this approach, two test cases were used. The first uses accurate knowledge of the relative OAC percentages of the given test area, in this case an LV substation located on the Denwick Primary substation was used. In the second case, the average percentages in each OAC Supergroup category were calculated at the Local Authority (LA) aggregation level. The Denwick Primary substation lies in the Northumberland LA area and the Rise Carr Primary lies in the Darlington LA. When synthesising load profiles using this method, the percentage OAC breakdown statistics as shown in Table 6-2 were used.

OAC Supergroup	Northumberland (%)	Darlington (%)
1	7	27
2	1	0
3	0	0
4	1	0
5	22	14
6	32	20
7	15	9
8	22	30

**Table 6-2 – Percentage of OAC groups per network area**

In order for the finally selected correlation model to be able to generalise across a wide range of potential load groups, the ADD profiles acting as model inputs need to be normalised. As a precursor to the normalisation step however, a selection must be made as to whether the overall group demand represents the most accurate form of normalisation available. This normalisation could be carried out against either the overall group maximum demand regardless of time, as a

function of the overall group demand at that particular point in time, or as a function of some subgroup demand, such as the total domestic ( $L_{Dom}$ ) or Industrial and Commercial ( $L_{I\&C}$ ) load. These represent some of the potential methods by which this normalisation can be carried out. As part of the model testing, one of these candidates will be selected as the most appropriate. The normalised demand profiles  $P_k$  will then be referred to as  $P_{k_{norm}}$  post-normalisation.

Table 6-3 shows the proposed candidate methods for normalisation:

Normalisation Candidate	Method
A	$\frac{P_k(t)}{L_{i_{max}}}$
B	$\frac{P_k(t)}{L_{i_{Dom_{max}}}}$
C	$\frac{P_k(t)}{L_i(t)}$
D	$\frac{P_k(t)}{L_{i_{Dom}}(t)}$

**Table 6-3 – Load group normalisation candidate methods**

Where  $k$  is the class of consumer,  $P_k$  is the total real power demand for the number of consumers of class  $k$  within the overall load group ( $N_k$ ),  $t$  is the half hourly period (1-48) and  $L_{Dom}$  is the total demand profile from domestic consumers within the group, derived as shown in (42) where  $K_{Dom}$  is the total number of domestic consumer classes and  $n$  is the total number of half-hourly data sample points:

$$L_{i_{Dom}} = \sum_{k=1}^{K_{Dom}} P_{k_{1..n}} \quad (45)$$

In methods B and D the component of group demand  $L_{Dom}$  has been isolated from the overall group demand. There is no corresponding isolation of the demand from industrial and commercial customers  $L_{I\&C}$  for two reasons. Firstly due to the relative percentage of industrial consumers in each of the test load groups there was insufficient data in order to accurately determine the required model outputs.

Secondly, the temperature sensitivity of industrial and commercial loads has been discussed as being lower than that of domestic loads [149]. Therefore, though this scoping decision makes an assumption of the relative temperature independence of industrial and commercial loads, the choice not to model these consumers directly as being significantly temperature and therefore correlation sensitive was deemed appropriate. This represents an additional area for further work to develop, or investigate the need for additional sensitivity coefficients for these consumers based upon the monitoring of suitable network demand groups.

The proposed model will provide a series of correlation sensitivity coefficients (CSCs) which can be used in conjunction with the selected normalisation format in order to derive the overall group load-temperature correlation ( $C$ ). These CSC values will be provided for domestic consumers only for the reasons discussed previously. In addition to the normalised consumer class profiles a number of additional model inputs were considered. A value was proposed which takes into account the ratio between the domestic and non-domestic loads ( $R$ ) at a point in time. This is calculated as follows (43):

$$R_k(t) = \frac{P_k(t)}{L_{I\&C}(t)} \quad (46)$$

Where  $L_{I\&C}$  is the total demand profile from Industrial and Commercial consumers within the group derived as shown in (44) and  $K_{I\&C}$  is the total number of Industrial and Commercial consumer classes:

$$L_{I\&C} = \sum_{k=1}^{K_{I\&C}} P_{k_1 \dots n} \quad (47)$$

The final proposed model inputs proposed are the number of domestic consumers within each class ( $N_k$ ), and the total number of domestic consumers ( $\sum N_k$ ). Both ordinary and weighted least squares type models were considered in order to derive the CSC values. Weights ( $w$ ) were considered as functions of the derived correlation  $p\_values$ . These values refer to the ability to reject a null hypothesis of correlation. If the  $p\_value$  falls below a particular threshold, the null

hypothesis can be rejected and a correlation is said to be present between the two variables. In order to provide weights to the least-squares algorithm, the value of  $1 - p\_value$  was used. The least-squares algorithm is solved in the usual manner, with firstly the formation of the correlation vector  $C$  and the weight vector  $W$ :

$$C = [c(1), c(2) \cdots c(n)]^T \quad (48)$$

$$W = [w(1), w(2) \cdots w(n)]^T \quad (49)$$

The format of the input rows of the matrix  $H$ ,  $h_j$  will be determined by testing the proposed model structures against the real-world monitored data. The proposed structures for the rows of  $H$  are shown in Table 6-4:

$$H = [h_1, h_2 \cdots h_n]^T \quad (50)$$

Correlation Model	Method
1	$h_j^T = [P_{k_{norm}}, \cdots, P_{K_{Dom_{norm}}}]$
2	$h_j^T = [P_{k_{norm}}, \cdots, P_{K_{Dom_{norm}}}, N_k, \cdots, N_{K_{Dom}}]$
3	$h_j^T = [P_{k_{norm}}, \cdots, P_{K_{Dom_{norm}}}, \sum_{k=1}^{K_{Dom}} N_k]$
4	$h_j^T = [P_{k_{norm}}, \cdots, P_{K_{Dom_{norm}}}, R_k, R_{K_{Dom}}]$

**Table 6-4 – Proposed Correlation Model Structures**

$$C = H \cdot CSC \quad (51)$$

$$CSC = (H^T H)^{-1} H^T C \quad (52)$$

$$CSC_{weighted} = (H^T W H)^{-1} H^T W C \quad (53)$$

Values of  $C$  were calculated for each of the load groups available from the monitored data. These were then combined to provide the maximum possible training dataset for the model.

Tests were carried out using the principle of Leave one out Cross Validation (LOOCV) in which the entire set of load groups are used to train the model, except that which is used for testing. This is a specific form of *k-fold* validation [150]. This process was carried out for all groups and the model which minimised the error across the total set is chosen as the final model.

Table 6-5 shows the sum of the Root Mean Square error values for each of the models against the testing data.

ADD Inputs	Normalisation Candidate	Model 1		Model 2		Model 3		Model 4	
		NW	W	NW	W	NW	W	NW	W
OAC ADD	1	2.12031	2.12108	2.42222	2.42250	2.23650	2.23719	4.07277	4.07484
	2	1.78190	1.78294	1.90954	1.90957	1.78166	1.78250	2.83679	2.83741
	3	2.12715	2.12729	2.35592	2.35583	2.16704	2.16736	6.31042	6.31142
	4	1.32490	<b>1.32480</b>	1.48627	1.48574	1.35223	1.35233	2.30172	2.30129
Elexon ADD	1	2.09023	2.09108	2.38695	2.38725	2.21203	2.21278	3.90770	3.90975
	2	1.78209	1.78313	1.90757	1.90758	1.77881	1.77963	2.92749	2.92793
	3	2.03207	2.03224	2.30695	2.30684	2.12620	2.12652	5.84697	5.84770
	4	1.32529	<b>1.32519</b>	1.48564	1.48513	1.34947	1.34959	2.40292	2.40214

**Table 6-5 – Total correlation estimation error for all input models**

The results show that the weighted version of Model 1 gives the smallest error when estimating the load group temperature correlation. After the LOOCV stage was used to determine the model which gives the best overall accuracy, all available training data was used for derivation of the final set of CSC values.

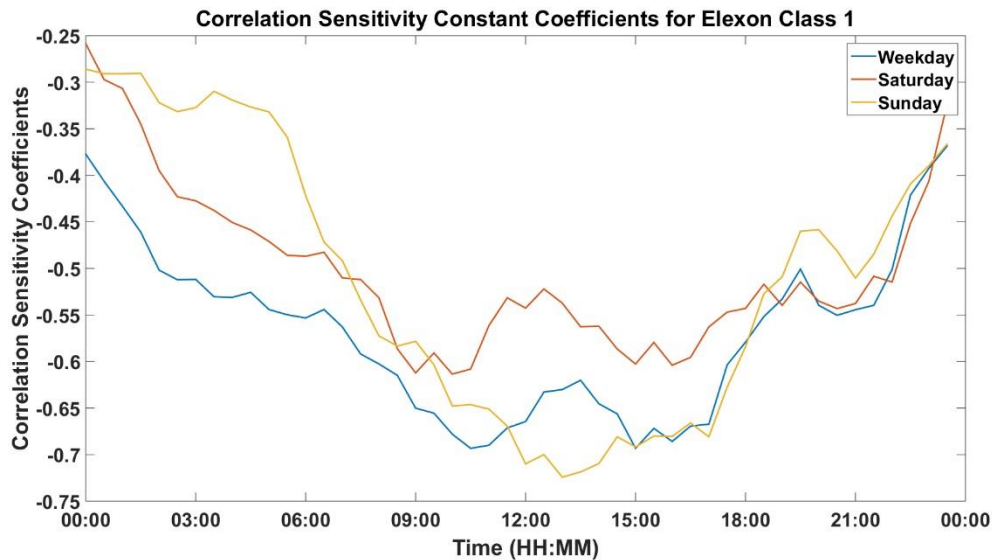


Figure 6-11 - Correlation sensitivity Coefficients for Elexon Class 1 consumers

Coefficients for Elexon Class 1 consumers in the Weekday, Saturday and Sunday periods are shown in Figure 6-11, and the full table of coefficients are located in Appendix 2. The resultant sensitivities are shown to be strongest around midday on Sundays. All sensitivities are shown as similar in the 9pm-Midnight time period, most likely due to the typical occupancy rates of domestic properties at this time. Sensitivities are shown at a minimum on Saturday afternoons, again a likely result of the reduced occupancies at these times.

Figure 6-12 shows a plot of the true correlation for a randomly selected load group and the estimated correlation. These results are taken from the LOOCV phase of testing.

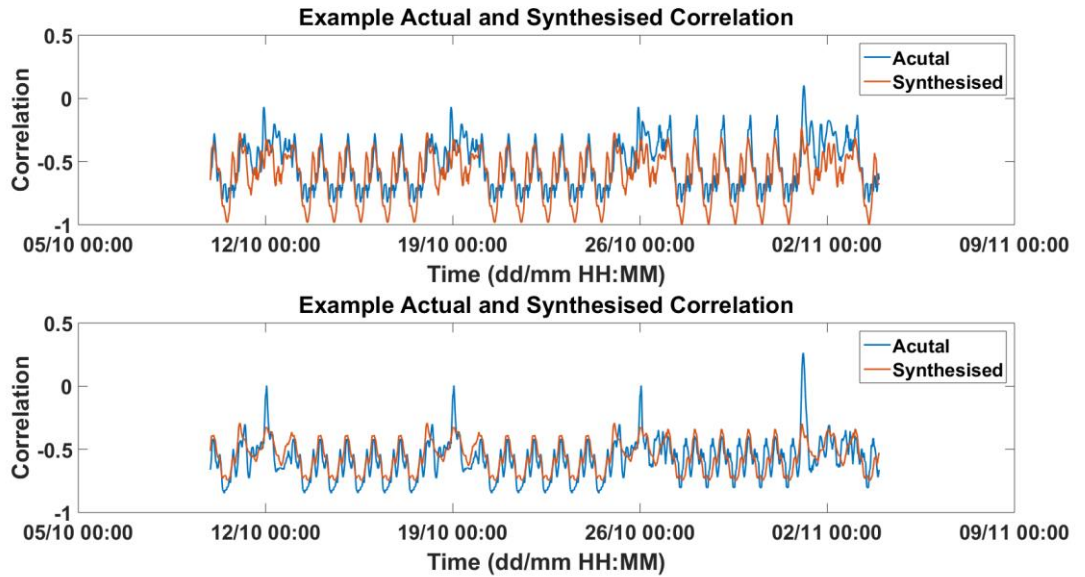
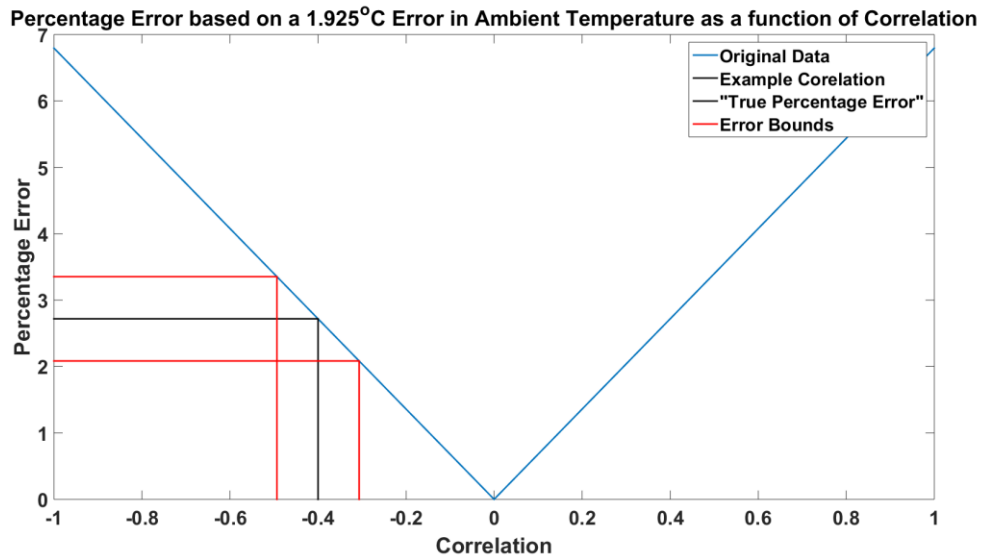


Figure 6-12 – Actual and Synthesised Correlation using the finally selected method

As shown in Figure 6-12 agreement between the synthesised and actual group correlation values is good. As a final stage of the analysis the impact of the correlation modelling error was examined. The Mean absolute error (MAE) values from the LOOCV testing phase ranged from 0.1251 to 0.1906, with mean value of 0.1535. As was previously shown in Figure 6-9 the effect of a theoretical temperature error has a varying effect dependent upon the correlation, however these figures assume exact knowledge of the group correlation. A study was carried out to determine the impact of correlation errors in comparison to the temperature errors as shown in Figure 6-10. Since the estimated correlation values have a typical error value, the resultant upper and lower potential correlation values each have associated with them a particular percentage error value.

Figure 6-13 shows an example of this. In this example a theoretical correlation value of -0.4 is assumed. Using the mean MAE value of 0.1535 the resultant correlation and percentage error values are shown. The red lines are the upper and lower bounds of both the correlation estimation and the percentage error estimation.



**Figure 6-13 – Upper and Lower correlation estimation bounds and the resultant effect on overall percentage error**

Analysis was carried out to determine the typical deviation away from the ‘true’ percentage error as a function of error in the correlation estimation. The results of this analysis are shown in Table 6-6.

Group	% Difference between original percentage error Upper Bound	% Difference between original percentage error Lower Bound
1	0.512	0.553
2	0.471	0.507
3	0.402	0.434
4	0.536	0.571
5	0.563	0.611
6	0.666	0.714
7	0.633	0.686
8	0.560	0.601
Average	0.543	0.585

**Table 6-6 – Percentage differences between ‘temperature forecast’ error bounds and those added as a result of the chosen correlation model**

As can be seen in Table 6-6 the correlation estimation method outlined in this section adds around 0.6% to the overall percentage error as a function of the theoretical temperature estimation error. Whilst estimation of the correlation adds

an additional error to any potential modelling scheme, estimation of the correlation increases knowledge of the overall impact of a forecast.

## **6.9 Conclusions**

This chapter has provided an investigation into the relationships between load and temperature for grouped distribution system loads. The correlation between these two factors has shown to vary based upon time of day, seasonality and on the composition of the group. A generalised model to determine these correlations has been proposed along with a study which outlines the influence of errors when forecasting load as a function of the correlations and also the impact of the resultant modelling errors in the correlation values themselves.

## 7 HV Feeder Load Synthesis – Temperature Sensitive Load

### modelling

#### 7.1 Introduction

Since power system assets in the UK such as OHLs are currently utilised based on their requirement to support the requirement for  $N-d$  security [11], the level of asset utilisation is relatively low in comparison to both the present line rating standard and in particular, the increased capacities delivered by RTTRs and DTRs.

When attempting to critically evaluate the capability of such techniques to contribute to additional network headroom for load, the low network utilisation factors require us to either synthesise data of increased loads, or utilise existing available data, such that detailed assessment can be carried out. Once such data is available, the question of how to demonstrate the potential benefits of RTTRs and DTRs remains.

In [35-37] methods such as Loss of Load Expectation (LOLE) and Expected Energy Not Supplied (EENS) have been used to determine the potential probabilistic increases which RTTRs can offer for load accommodation, however in all of these studies the electrical demand and RTTRs have been assumed to be independent, and loads have been randomly synthesised using random number generation and an appropriate probability density function. This assumption of independence is commented upon as an area for improvement in [37], with particular reference to the requirement to examine the correlation between demand and RTTRs in more detail. In each of these studies a load duration curve (LDC) has been used in conjunction with a derived cumulative distribution function of RTTR values in order to determine the probability of an inability to supply consumers. After derivation of new group load profiles or through the use of existing data, such LDCs could be derived and a similar method applied to the data presented in this thesis. This work however extends this method by taking into account the temporal profile nature of the resultant demand.

Whilst the methods discussed in [35-37] provide useful information as to the potential benefits of RTTR, the work outlined in this thesis provides an

enhancement in three key areas. Firstly, through the use of temporal profiles, the times of day, seasons and days of the week at which OHL conductor temperature excursions occur are exposed. This is useful when considering the network in both the planning and operational timescales, particularly in the case of the scheduling of services. Secondly, the use of temporal load profiles in conjunction with ratings ensures that the existent correlation between the two parameters is fully exploited as opposed to the assumption of independence. Finally, through the use of temporal profiles and the use of Dynamic thermal ratings as opposed to real-time thermal ratings means that the potential requirement of services to mitigate against OHL thermal overloads can be identified.

In order to generalise the findings of this research, and to provide a more significant contribution to knowledge a temperature sensitive load synthesis method capable of deriving accurate profiles for demand groups of any composition has been developed. These load profiles will be used as inputs to the validated dynamic conductor model outlined previously.

## **7.2 Chapter Goals / Objectives and Contributions**

### **7.2.1 Goals and Objectives**

To develop a suitable method for taking into account the temperature sensitivity of distribution network load groups to increase accuracy against seasonal ADD profiles.

### **7.2.2 Transition away from existing literature / Contributions**

As discussed in Chapter 6 typical models which describe the load-temperature relationship for electrical loads are typically at either the individual or large area levels. A causal model has not been presented which relates temperature sensitivity to components of a wider load group using this method which has been developed in this research.

### **7.2.3 Attainment of Goals**

A set of temperature sensitivity coefficients have been developed which quantify the relative sensitivity of load group consumers to temperature. A

generalised synthesis model, building upon the correlation model presented in Chapter 6 has been developed and tested against real-world measured data.

### 7.2.4 Chapter Outline Block Diagram

Figure 7-1 a block diagram of the inputs, methods and outputs for this chapter. This chapter has a very similar block diagram to that of the previous chapter. Here, the generalised correlation model is replaced with that of the generalised temperature synthesis model. Outputs from this chapter are the linear fitting parameters derived from each of the load-temperature clusters, the generalised load temperature synthesis model in order to derive representative time-series profiles of aggregated demand groups, and the temperature sensitivity coefficients for each of the domestic consumer classes.

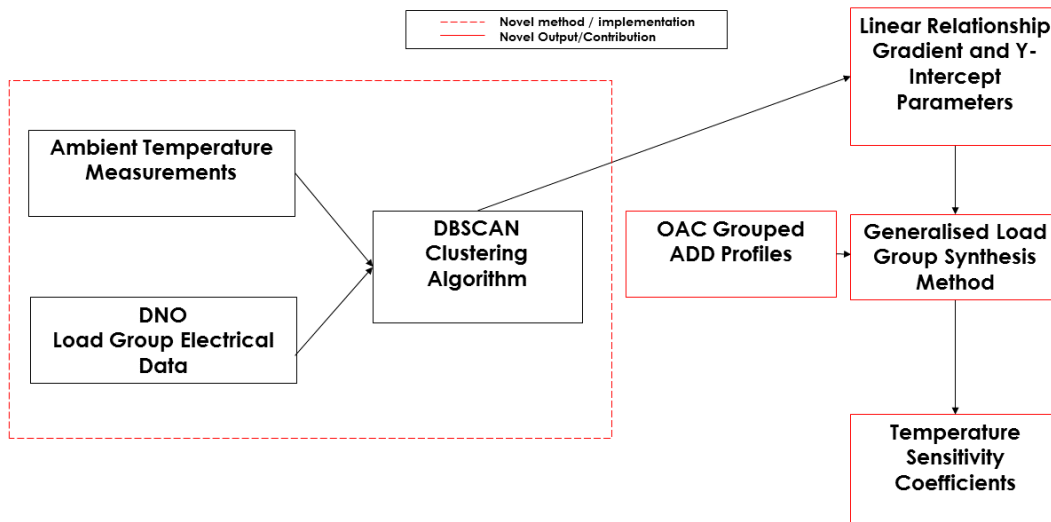


Figure 7-1 – Chapter 7 Block Diagram

### 7.3 Background

Previously in this work a method for derivation of more accurate load group ADD profiles has been proposed, however an additional enhancement of this work is to modify such loads according to their real-time reaction to ambient temperature values.

To date there have been few pure modelling studies carried out to derive temperature sensitive temporal profiles of grouped electrical loads, as most

research has been concerned with the forecasting of demand. Pillai [151] notes the recent shifts towards the modelling of group loads as profiles, as opposed to more traditional forecasting as methods. In [151], Pillai outlines a series of generic representative load group profiles for both group loads and residential consumers using publically available datasets. Whilst profiles for wide area loads in Norway and Finland are produced, only residential models for the UK are provided. In [152] load profiles for a wide area of Taiwan are produced through aggregation of individual load class data which are determined through data analysis of multiple load class types.

Whilst clearly modelling plays a key part in such forecasting studies, the analysis of data at the national, or individual levels means that the nature of such models need refinement in order to develop inputs to the DTR OHL model as required in this research. Where models have been derived for more similar wide area loads such as those in [152] models are typically fitted to individual datasets with no statements as to their transferability to other systems. The work of Charytoniuk in [153] has close resemblance to the temperature sensitive load synthesis method outlined in this section of the thesis.

In this work, a series of conditional probability density functions (PDFs) are estimated for the conditional relationship between demand and temperature. These PDFs are estimated using non-parametric kernel density techniques. The PDFs are then used to deliver estimates of demand for particular day and seasonal periods, in a similar way to as presented in this thesis. These demand estimates combined with a suitable forecast of monthly energy demand are then used as part of an overall Autoregressive Integrated Moving Average (ARIMA) forecasting model.

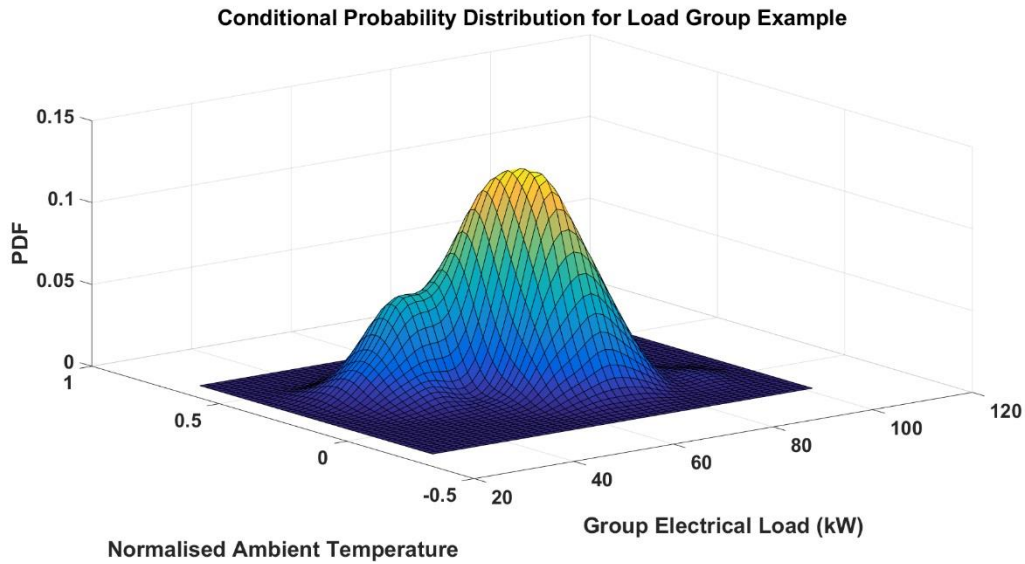


**Figure 7-2 – Example of Conditional PDF for example load group at 00:00**

Figure 7-2 shows an example of such conditional probability distributions for one of the sample monitored load groups at 00:00.

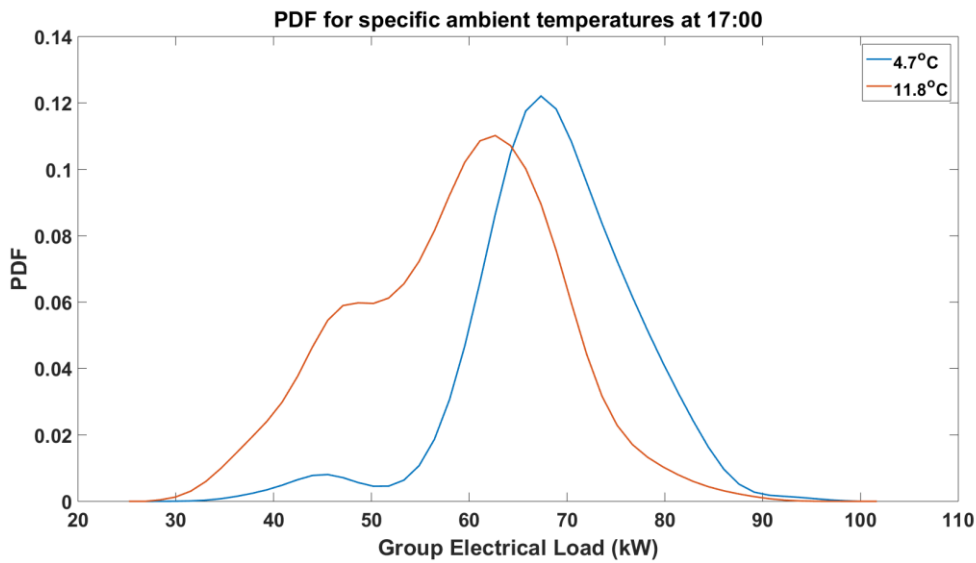


**Figure 7-3 – PDFs evaluated at specific ambient temperatures for example load group at 17:00**

Figure 7-3 shows the conditional PDFs for the sample load group at specific ambient temperature values at 17:00. Both Figure 7-2 and 7-3 show the resultant relationship for the Weekday, Autumn Elexon period. Each of these plots represents an example of those found in [153].

In this work, there is one significant reason as to why this approach has not been investigated further. In [153] suitably homogenous datasets of consumer class load profiles were available. For each of these load groups the procedure as discussed previously can be carried out and a suitable conditional PDF derived. The resultant  $E(\text{Load} | T)$  values can then be determined and aggregated for a particular load group composition. Since in this research such homogenous data was not available it would not be possible to implement this method for the sample data in this research. Since a suitably accurate causal model for deriving temperature synthesised time-series profiles has been proposed in this research it is presented as an alternate method to the one proposed in [153]. Investigation of this approach if such data was to be made available represents an area for potentially extending the research in this thesis, in addition to the investigation of multivariate kernel density estimation models as opposed to the bivariate approach of [153]. The performance results of [153] will be used as a comparison to the results of the model proposed in this thesis. In addition to these results, those from [154] will also be used for comparison. In this work a multi order polynomial is used to ‘de-trend’ a feeder load profile and the overall procedure combines the polynomial coefficients with the significant signal amplitudes identified by a Fourier analysis of the raw data. This approach was not considered due to its non-real-time consideration of temperature variations, however it is noted that a typical modelling error of around 5% is allowable at the network feeder level. It is also unknown as to the number and type of consumers which were modelled in this work.

Following the work of Asbury [130], Meldorf [41] and Corpening [155] the total observed demand can be said to be a function of the expected (base) load and the temperature sensitive load.

$$\begin{aligned}
 & \textit{Total Group Load} \\
 & = \textit{Expected Base Load (Non} \\
 & \quad - \textit{Temperature Sensitive)} \\
 & + \textit{Temperature Sensitive Load}
 \end{aligned} \tag{54}$$

Asbury [130] additionally breaks down the expected base load elements into subgroups according to residential and industrial demands, each with their own specific temperature sensitive element.

Meldorf makes an additional comment as to the presence of stochasticity in the load, however in this research this element has not been included as in [130] and [155]. Estimation of the truly non-temperature sensitive base load for the groups analysed in this thesis was not possible, therefore an approximation of the relationship shown in ((54) has been proposed. The original Elexon ADD profiles [156] have been derived for a set of 10 year average temperature values, however in real time conditions will deviate from these and will therefore have a resultant impact on the loads. As such ((54) has been modified to the form shown in (55).

*Total Group Load*

$$\begin{aligned} &= \textit{After Diversity Demand Profile} && (55) \\ &+ \textit{Additional Temperature Sensitive Element} \end{aligned}$$

The additionally temperature sensitive element accounts for real-time differences from the expected 10 year average temperature conditions. The newly proposed OAC ADD group load method proposed in Chapter 5 will be used to deliver the appropriate After Diversity demand element of (55) whilst this Chapter will outline a new method for determination of the additionally temperature sensitive element of the group's total electrical demand.

The authors of [157] consider the variation of load and temperature with a UK focus. In this work the influence of variations in ambient temperatures on grouped loads is investigated and as per the cases shown in Chapter 6 a linear relationship between the two has been shown to be appropriate.

## **7.4 Load Synthesis Method**

In order to increase their accuracy when tested against actual measured data, a series of coefficients have been derived to modify the original ADD profiles relative to their sensitivity to actual air temperature in addition to their seasonal compensation, calculated from the 10 year average data. These coefficients have been derived for domestic customers only as in the case for derivation of the correlation values in Chapter 6 [149].

When the method is used to synthesise profiles to test performance, the ADD profiles will be the OAC and Elexon group ADD profiles as discussed in Chapter 5. For the purpose of deriving the test inputs themselves the original group ADD profiles will be represented in the form of the half hourly average seasonal group profiles also derived in Chapter 5.

The additionally temperature sensitive load is calculated by subtracting the ADD profile from the original group load values. In order to generalise the results, these temperature sensitive elements are normalised to the peak load of the group ADD profile. The rationale for this choice of normalisation is due to the final use of the model. When the model is used for testing and for deriving new profiles for unseen groups, it is likely that only an estimate of the maximum group ADD value is known, through use of the method shown in Chapter 5. Therefore when using the model in this format, the normalised temperature sensitive elements can therefore be transformed using the maximum of the estimated group ADD values.

After normalisation the relationship between the derived elements and temperature for each seasonal, day and time of day period is examined. The same Elexon periods as per the correlation model outlined in Chapter 6 are used.

$$Seasonal = s = \begin{cases} 1 = Autumn \\ 2 = High Summer \\ 3 = Summer \\ 4 = Spring \\ 5 = Winter \end{cases} \quad Day = d = \begin{cases} 1 = Weekday \\ 2 = Saturday \\ 3 = Sunday \end{cases}$$

Figure 7-4 shows an example of the additionally temperature sensitive elements for a randomly selected seasonal, daily and half hourly period. The linear approximation to the relationship is also shown. This data represents that which will be used to modify the after diversity demand group load profile. The gradient and y-intercept parameters derived for each half hourly, seasonal and day of week period will be estimated by the finally chosen model structure. As per the correlation method, these parameters will be generated through the use of a set of temperature sensitivity coefficients TSCs.

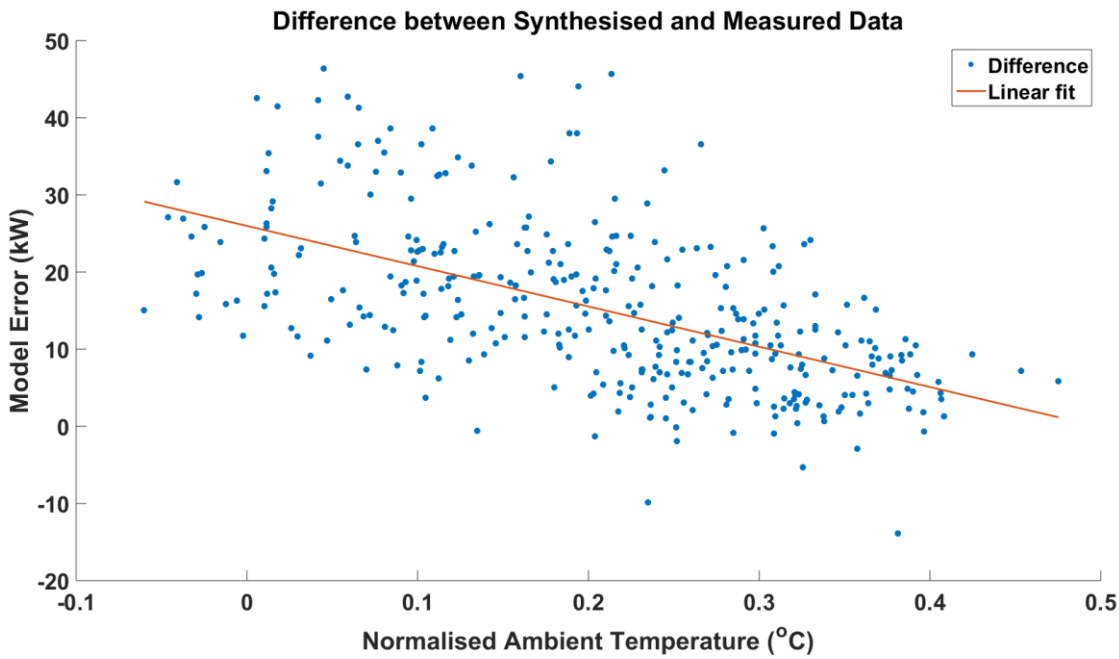


Figure 7-4 – Additionally Temperature Sensitive element and linear fit

After use of the respective gradient and y-intercept TSCs, the resultant estimates of the gradient and y-intercept parameters can be used with the normalised ambient temperature values to generate estimates of the additionally temperature sensitive elements. Once combined with an estimate of the group ADD profile, an overall estimate of the final group load can be made.

In order to derive the TSCs and test the overall accuracy, as previously, two least squares approaches have been taken, weighted and non-weighted. The potential inputs to the model are the candidates outlined in Chapter 6 and are detailed for completeness below.

Normalisation Candidate	Method
A	$\frac{P_k(t)}{L_{i_{max}}}$
B	$\frac{P_k(t)}{L_{i_{Dom_{max}}}}$
C	$\frac{P_k(t)}{L_i(t)}$
D	$\frac{P_k(t)}{L_{i_{Dom}}(t)}$

**Table 7-1 – Load group normalisation candidate methods**

$$C = [c(1), c(2) \dots c(n)]^T \quad (56)$$

$$W = [w(1), w(2) \dots w(n)]^T \quad (57)$$

As per the derivation of the generalised correlation model, the format of the input rows of the matrix H,  $h_j$  will be determined during the testing phase. The proposed structures for the rows of H are shown in Table 7-2:

$$H = [h_1, h_2 \dots h_n]^T \quad (58)$$

Correlation Model	Method
1	$h_j^T = [P_{k_{norm}}, \dots, P_{K_{Dom_{norm}}}]$
2	$h_j^T = [P_{k_{norm}}, \dots, P_{K_{Dom_{norm}}}, N_k, \dots, N_{K_{Dom}}]$
3	$h_j^T = \left[ P_{k_{norm}}, \dots, P_{K_{Dom_{norm}}}, \sum_{k=1}^{K_{Dom}} N_k \right]$
4	$h_j^T = [P_{k_{norm}}, \dots, P_{K_{Dom_{norm}}}, R_k, R_{K_{Dom}}]$

**Table 7-2 – Proposed Correlation Model Structures**

$$C = H \cdot TSC \quad (59)$$

$$TSC = (H^T H)^{-1} H^T C \quad (60)$$

$$TSC_{weighted} = (H^T W H)^{-1} H^T W C \quad (61)$$

$$\textit{Synthesied Group Load} \quad (62)$$

$$\begin{aligned} &= \textit{Group ADD Profile} \\ &+ [(\textit{Gradient TSC} \cdot \textit{Normalised Temp}) \\ &+ (Y - \textit{Intercept TSC} \cdot \textit{Normalised Temp}) ] \end{aligned}$$

The same LOOCV approach has been taken as to testing the model outputs to ensure the selected model is not biased due to a particular set of input values. The results of this analysis are shown in Table 7-3. The best performing models are highlighted in bold.

ADD Inputs	Normalisation Candidate	Model 1		Model 2		Model 3		Model 4	
		NW	W	NW	W	NW	W	NW	W
OAC ADD	1	935.419	934.482	932.579	931.693	928.437	928.061	963.615	971.377
	2	932.414	931.152	928.256	927.953	924.447	<b>923.675</b>	971.510	977.658
	3	930.423	929.854	931.254	931.731	924.102	923.825	973.081	976.947
	4	941.945	941.362	941.236	940.858	935.448	935.355	969.818	975.793
Elexon ADD	1	1075.148	1075.780	1075.546	1076.413	1074.830	1075.311	1095.842	1105.187
	2	1072.491	1073.693	1079.042	1081.034	1070.448	1071.187	1099.338	1106.889
	3	1074.438	1075.041	1068.885	1070.425	<b>1065.016</b>	1065.405	1105.998	1110.104
	4	1075.427	1075.920	1071.542	1072.683	1059.143	1059.311	1098.370	1105.030

Table 7-3 – Total correlation estimation error for all input models

As can be seen in Table 7-3 the OAC models of overall temperature-corrected show improved performance over those for the Elexon ADD models. Model structure 3 with normalisation method 2 as inputs in the weighted form performs the best for the OAC models and the non-weighted version of Model 3 with normalisation method 3 as inputs performs best for the Elexon model.

Figure 7-5 shows the resultant Gradient TSC values for Class 1 and 2 consumers for the Weekday period. As can be seen, Class 1 displays a reduced influence with regards to temperature when considered against Class 2. This is potentially as a result of the relatively high ratio between peak and off peak tariffs regarding electricity usage for these customers.

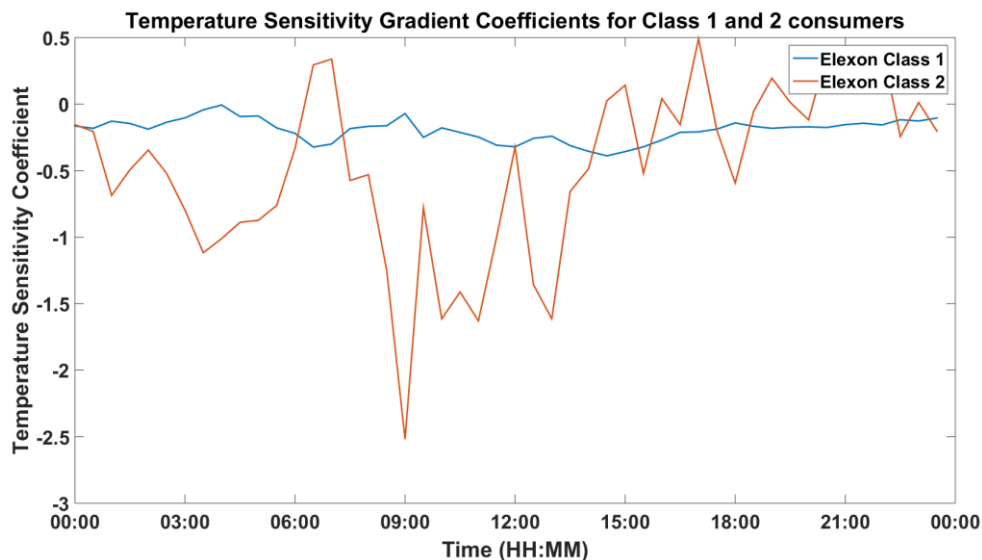


Figure 7-5 – Temperature Sensitivity Coefficients for the Weekday period

Table 7-4 shows the temperature sensitive modelling error in comparison to the synthesised OAC ADD group profiles which have not been modified for temperature. At all sites, excluding in the case of Group 2, the temperature corrected model out performs the non-temperature corrected model. This Group also has the highest RMSE value expressing that there is a potentially poor fit from the original non-temperature corrected model. This is perhaps as a result of deviations in customer numbers beyond those taken into consideration, represents an outlier in terms of overall model accuracy, or is as a result of the assumptions made within this thesis.

Here the term RRMSE has been used as in [153] and RMSE has been expressed as a percentage as in [154] to allow for direct comparison. The RRMSE is defined as:

$$RRMSE = \sqrt{\frac{\sum_{t=1}^N (Load(t) - \widehat{Load}(t))^2}{\sum_{t=1}^N (Load^2(t))}} \quad (63)$$

Performance Metric	RMSE %		RRMSE	
	Temperature Corrected	Non Temperature Corrected	Temperature Corrected	Non Temperature Corrected
Group 1	10.508	10.870	0.1976	0.2016
Group 2	19.329	19.123	0.3438	0.3481
Group 3	8.962	9.245	0.3533	0.3620
Group 4	7.239	7.260	0.1817	0.1775
Group 5	17.230	17.520	0.2842	0.2854
Group 6	10.287	10.488	0.1781	0.1805
Group 7	11.100	11.421	0.2171	0.2174
Group 8	5.894	6.014	0.1136	0.1119

**Table 7-4 – Temperature sensitive load synthesis results shown in comparison to the group ADD profiles developed in Chapter 5**

In [154] the maximum RMSE% error is shown as 6.99% for the finally presented model. As noted previously, the number and type of consumers supplied is not known and the results are also per-unitised, the load profiles show a somewhat smooth profile in comparison to those of the sample load profiles in this research however, and can therefore be assumed to tend towards increased numbers of customers. Groups 6 and 8 represent the largest numbers of customers and are therefore more typical of the results shown in [154]. The overall errors of these load groups have shown to have good performance when compared to those in [154]. In [153] RRMSE values are shown to vary from 0.099 to 0.538 dependent upon the number of customers. The results shown here are within this range

however the groups of customers in this research are significantly greater than those, with results also being presented for a single month as opposed to the 10000 randomly selected half hourly data points as used in this research.

As can be seen, there is improvement over the non-temperature sensitive group ADD profiles. Whilst the improvement does not represent a particularly significant improvement over the non-temperature corrected profiles, even marginal improvements in forecasting and modelling errors have been shown to reduce costs in the overall operation of the power system [158]. Since the OAC ADD group profiles already represent a significant improvement over the Elexon ADD group profiles, this can be viewed of as an additional enhancement. If temperature data is not available for a particular test case, then use of the OAC ADD profiles would not be an inappropriate estimation of group demand.

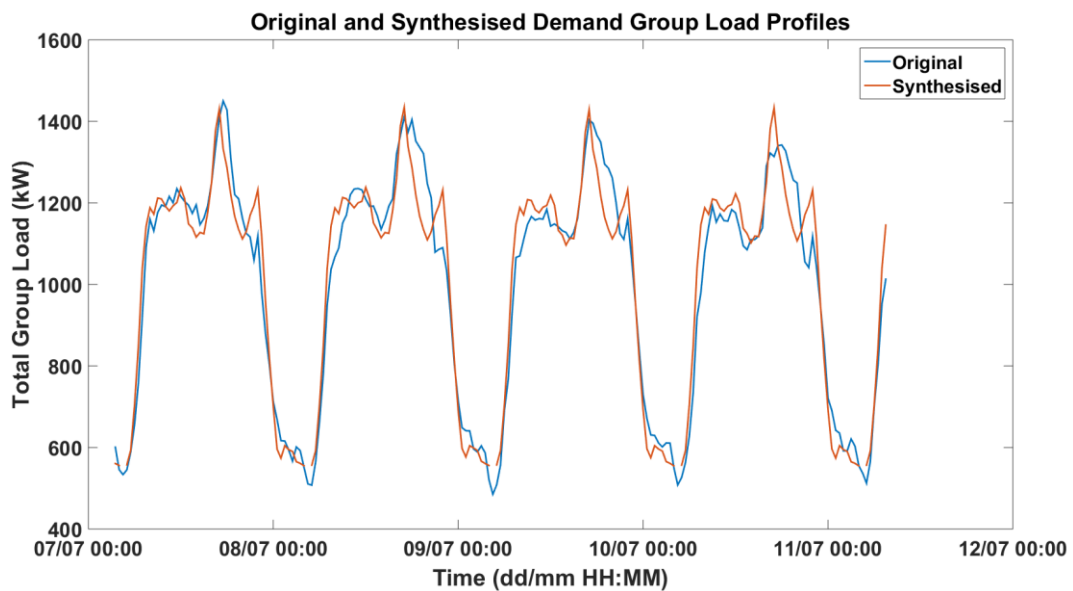


Figure 7-6 – Original and final synthesised group load profile

Figure 7-6 shows an example of the finally synthesised group load profiles and the original group load. For reference, the group shown in Figure 7-6 is Group 8 in Table 7-4.

## 7.5 Conclusions

In this Chapter a temperature sensitive load modelling method has been outlined. This method has shown increases accuracy over the use of non-temperature corrected models such as the OAC ADD and Elexon ADD methods discussed in Chapter 6.

The results show good accuracy when compared to those of comparable research studies although direct comparisons cannot be made since research on UK data at these aggregation levels has not been carried out previously.

A linear approximation has been shown to be suitable in order to describe the additional relationship between load and temperature on a half hourly basis beyond that which is already approximated by the present UK ADD profiles.

The use of the normalisation method in order to estimate the temperature sensitive components of group load has shown to also be a suitable approach and allows for derivation of a causal model which can relate variations in response to external temperature to the contributions of individual domestic consumer classes. This information has the potential to inform network operators of the impact of future customer tariffs for both new and existing customers and can assist in determining the required flexibility in contracted network services.

## **8 Load Group Classification and combination with Dynamic**

### **Thermal Ratings**

#### **8.1 Introduction**

Classification of consumers is carried out for a variety of reasons within the power system, though the core activities are for network modelling purposes and also for consumer billing [159]. Classifications can be used to segment customers based on factors such as overall load shape, tariffs, electrical parameters such as load factor or a combination of each of these. In the transition to the smart grid, new methods are being investigated as to how to classify customers. Chicco [160] outlines a number of potential benefits which can be delivered by improving the accuracy of consumer classifications. These range from improving generation management strategies for network operators, through to enhancing the offers which can be made available to end consumers by supply companies.

Whilst classification techniques have typically been investigated in order to classify individual end users [159-163], recently a number of studies have investigated the classifying of groups of consumers. In [164, 165] a series of generic LV network classifications are proposed in order to assist in the development of smart grid technologies at the lower voltage levels of the distribution system. It is to this field of classifying overall load groups to which the study presented in this thesis contributes. A number of methods for clustering consumers have been presented in the literature ranging from artificial neural networks and self-organising maps, in addition to more traditional clustering techniques such as the K-Means and Hierarchical methods. Since the output of this section is intended to be a set of generic load groups in order to test the capabilities of DTRs, no contribution to the field of clustering algorithms is intended and the commonplace K-Means++ and Hierarchical clustering approaches have been used.

The main contribution from this section is a set of generic distribution network load groups intended as being separate from voltage level, and as such can be used to inform similar DTR analyses with alternate components such as PTRs and UGCs or can be used to as example load groups in distribution network studies.

## **8.2 Chapter Goals / Objectives and Contributions**

### **8.2.1 Goals / Objectives**

After development of a suitable load synthesis method to act as inputs to the dynamic thermal ratings model of the overhead conductor, a series of representative load groups are required for testing purposes. The goal of this chapter is to deliver a series of representative groups based on composition alone. This is to allow for generalisation of the results for overhead lines presented in this thesis, to other power system components such as power transformers and underground cables.

### **8.2.2 Transition from existing literature and research / Contribution**

The development of these representative load groups represents the key contribution from this chapter. The literature to date has presented somewhat similar demand groups using clustering methods, however these have been presented for LV networks only and take into account network parameters in their classification.

### **8.2.3 Attainment of Goals**

A set of representative load groups have been determined which differ from those presently found in the literature.

### **8.2.4 Chapter Outline Block Diagram**

Figure 8-1 a block diagram of the inputs, methods and outputs for this chapter. Information regarding the composition of DNO demand groups serves as the input to this chapter. A series of clustering algorithms are used to determine the potential generic demand groups which represent the output from this chapter.

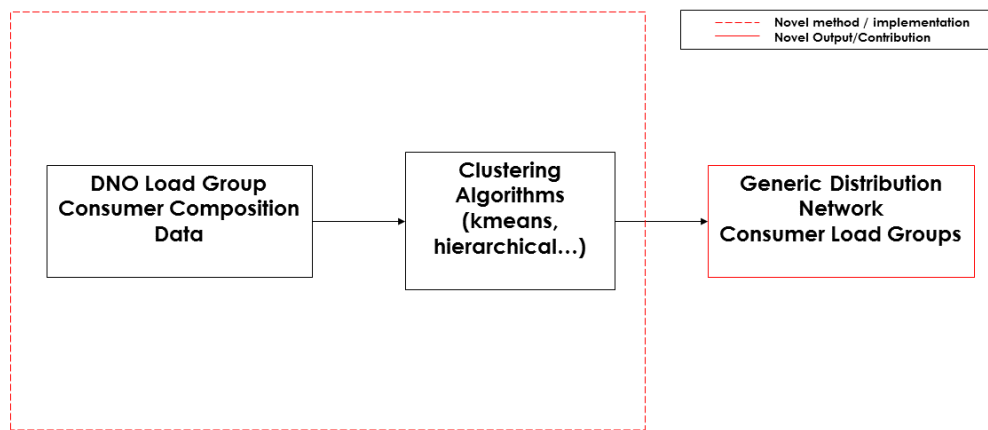


Figure 8-1 – Chapter 8 Block Diagram

### 8.3 Chosen Clustering Approach

After formulation of the temperature sensitive load synthesis method, a series of generic load groups are required in order to test the potential benefits of a DTR system for load accommodation across a range of scenarios. In order to provide such load groups, clustering analysis has been performed on a set of group Elexon composition data. The results of this clustering process are a set of generic load groups based on their composition of consumers. Load profiles will then be derived for each of these load groups across a range of total customer numbers.

In [164] and [165] representative LV feeders are derived using clustering algorithms which focussed on various network parameters such as overall feeder length, maximum demand etc. This work aims to develop a series of representative load groups based only on composition, since the aim of the final clusters is to determine the capability of RTTR to provide additional headroom for increased loads. These representative groups can be used at any aggregation level and thus the performance of a power system component at any level can be assessed.

In order to carry out this synthesis all load groups ranging from LV feeders to HV feeders from the case study networks were tabulated. In total this led to 1415 individual load groups for clustering.

Distribution Network Voltage Level	Total Sample Size
LV Feeders	856
LV Substations	543
HV Feeders	16
<b>Total</b>	<b>1415</b>

Table 8-1 - Clustering Algorithm Sample Sizes

Two approaches were taken to derive representative composition groups.

- A top-down approach whereby clusters were firstly generated from all the available data.
- A bottom up approach where data is clustered at each individual aggregation level and then tested against the overall dataset.

In order to cluster the composition data methods from three different clustering categories were used, and a ‘scorecard’ type method used to determine the clustering method with the greatest accuracy. The two methods used and their respective categories are:

- Hierarchical Agglomerative (Connectivity)
- K-Means++ (Centroid)

For each of the chosen clustering methods other than the DBSCAN approach the number of clusters ( $k$ ) to be derived acts as an input. This is due to their performance in partitioning the data to a given number of sections as opposed to truly determining the actual number of clusters in the dataset. For this, there is no real ‘correct’ answer as to the number of clusters, but the following approach has been taken to minimise the number of clusters accordingly, whilst maintaining a true estimation of existing partitions in the datasets.

Therefore, in order to test each method appropriately, each clustering method was used to populate a set of clusters with  $k \in K \quad K = 1 \dots 25$ .

The widely used K-means++ and Hierarchical clustering algorithms [165] were used to cluster the group composition data and two approaches were tested when considering the levels at which to cluster the data. The DBSCAN algorithm

showed poor performance on this clustering task in initial tests and was therefore not considered as a potential clustering solution in this case.

The first approach involves clustering data from all voltage levels together, hereby referred to as the ‘top-down’ approach; the second relates to clustering of the composition data at each voltage level individually. The accuracy of these top down and bottom up clusters was tested using a series of widely known criteria.

### 8.3.1 Hierarchical Clustering

Hierarchical clustering uses a distance metric to continuously combine similar features until only a single unified cluster remains. A number of distance metrics have been used within the literature, with the Euclidean and Ward distance criteria being typically the most commonly deployed. For the Hierarchical clustering method, the Euclidean distance metric was used along with both the Ward and Average linkage methods. For each of the methods, the maximum number of specified clusters was set to 25. Figure 8-2 shows the results of hierarchically clustering all of the available composition data using the average linkage criteria.

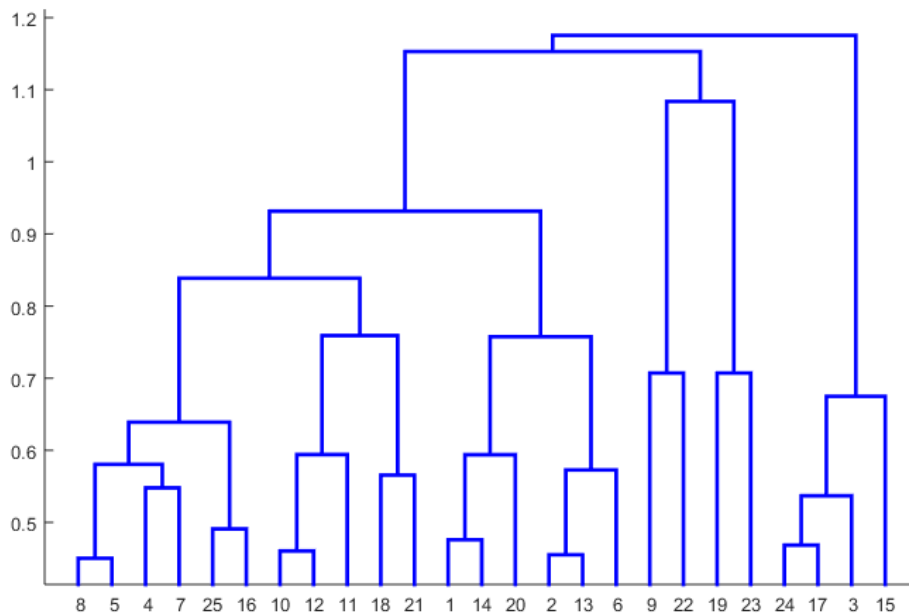


Figure 8-2 - Dendrogram of all data – Average linkage method

### 8.3.2 K-means and K-means++

The K-means algorithm is also a distance based metric. As per hierarchical clustering a number of distance criteria are available. K-means partitions the dataset with a particular number of predetermined cluster numbers. Cluster ‘centroids’ are found which minimise the distance between the centroid and its associated data points.

The K-means++ algorithm makes an initial estimate of the cluster centroids in order to improve accuracy and reduce computational time.

### 8.3.3 Accuracy criteria

Each clustering method is likely to result in slightly differing clustering partitions. In order to assess the results of such algorithms, a number of accuracy criteria metrics exist [160]. Five of these criteria have been calculated for the clusters derived using both the top down and bottom up approaches.

#### 8.3.4 Mean Index Accuracy (MIA)

The Mean index Adequacy (MIA) is the average value of the distances between the members of a cluster and its generated centroid. The MIA is calculated as:

$$MIA = \sqrt{\frac{1}{K} \sum_{k=1}^K d^2(c^{(k)}, C^{(k)})} \quad (64)$$

Where  $d$  represents the Euclidean distance,  $c$  denotes the derived cluster centroids,  $C$  represents the members of the found cluster  $k$  and  $K$  is the total number of clusters.

#### 8.3.5 Similarity Matrix Indicator (SMI)

The SMI as defined in [161] is a function of the distance between centroids of derived clusters. It is calculated as follows, where  $i, j = 1 \cdots K$ .

$$SMI = \max_{i>j} \left\{ \left( 1 - \frac{1}{\ln[d(c^{(i)}, c^{(j)})]} \right)^{-1} \right\} \quad (65)$$

### 8.3.6 Average Silhouette and Global Silhouette Coefficients (AvgSC and GSC)

The silhouette coefficient represents the level of appropriateness with which a cluster member has been categorized. Here, the average and global silhouette coefficients as in [165] have been used, whereby values closer to 1 represent that the cluster members have been appropriately assigned and tend towards -1 where poor clustering has occurred.

### 8.3.7 Within Cluster between Cluster Ratio (WCBCR)

The WCBCR represents the ratio between the within cluster errors, i.e. the distances between the clusters members' and its representative centroid and the distances between the overall cluster centroids. The WCBCR can be calculated as a function of the MIA as follows [160]:

$$WCBCR = K \cdot MIA(K)^2 \left( \sum_{1 \leq i \leq j} d^2(c^{(i)}, c^{(j)}) \right)^{-1} \quad (66)$$

Each of these accuracy criteria functions similarly, with the exception of the SC and GSC in that they tend towards a minima as the adequacy of the derived clusters improves. With an increasing number of clusters however comes greater computational time and an increasingly large set of representative load feeders. In order to minimise the total number of representative feeders whilst maintaining a suitable level of dissimilarity between the feeders a 'knee-method' has been used in line with previous work [166] to determine the point at which the accuracy criteria values no longer decrease at a significant rate. The WCBCR method has been used to determine the overall clustering accuracy across each method as in [166]. A number of methods exist for determination of the knee point but in this

section, as per the DBSCAN knee point determination, the ‘Kneedle’ method [146] has been used.

#### **8.4 Representative Distribution Network Cluster Group Results**

Table 8-2 shows the results of each of the clustering algorithms for both data aggregation approaches. As can be seen, the Hierarchical clustering method with average linkage generates the clusters with the minimum WCBCR. This clustering method was therefore used when determining the final chosen representative load group composition clusters.

	Clustering Method	AvgSC	GSC	SMI	MIA	WCBCR
LV Feeder	Kmeans++	0.5303	0.6184	1.7385	0.5665	0.2120
	Hierarchical Ward	0.5138	0.4876	1.8524	0.3317	0.0690
	Hierarchical Average	0.5707	0.5524	1.2745	0.4143	<b>0.0668</b>
LV Substation	Kmeans++	0.5160	0.6042	1.7256	0.5665	0.2536
	Hierarchical Ward	0.5390	0.4767	1.7730	0.3612	0.0824
	Hierarchical Average	0.6637	0.6007	1.3584	0.3262	<b>0.0524</b>
MV Feeder	Kmeans++	0.9092	0.8981	2.5467	0.3575	0.1568
	Hierarchical Ward	0.9092	0.8981	2.5467	0.1330	<b>0.0217</b>
	Hierarchical Average	0.9092	0.8981	2.5467	0.1330	<b>0.0217</b>
All Data	Kmeans++	0.5376	0.6068	1.7434	0.5891	0.2583
	Hierarchical Ward	0.4551	0.5141	1.9718	0.3410	0.0858
	Hierarchical Average	0.5717	0.5515	1.3925	0.4009	<b>0.0678</b>

**Table 8-2 – Clustering Algorithm Results for all data aggregation levels**

In order to test the overall accuracy of each of the derived cluster sets, each of the derived sets was used to classify data from the alternate aggregation levels, apart from the case of the clusters previously derived for all data. This was in order to remove any bias due to having previously clustered the data at the same level.

A k-nearest neighbour search was used to classify the data using the appropriate centroids.

Table 8-3 shows the accuracy criteria calculated for each of the possible combinations. The centroids formed at the LV substation level have the highest adequacy for both the GSC and WCBCR criteria. The AvgSC value is the second highest and the SMI value is the second lowest. As discussed previously the WCBCR has been detailed as more accurate than the MIA and since overall the LV substation centroids perform well across all the possible data combination these centroids have been used.

<i>Assessment Metric</i>	<i>LV Feeder</i>	<i>LV Substation</i>	<i>MV Feeder</i>	<i>All Data</i>
AvgSC	0.4354	0.5708	0.5353	0.5717
GSC	0.5097	0.7026	0.5066	0.5514
SMI	1.2745	1.3584	2.5467	1.3925
MIA	0.3657	0.3117	0.2534	0.4009
WCBCR	0.0521	0.0479	0.0788	0.0678

Table 8-3 – Adequacy criteria for chosen clustering algorithm in each of the test cases

## 8.5 Derived Generic Customer Load Groups

The resultant load groups which will be used to determine the capacity of RTTR for load accommodation are shown in Table 8-4.

Elexon Class	1 (%)	2 (%)	3 (%)	4 (%)	5 (%)	6 (%)	7 (%)	8 (%)
1	0.0	0.0	33.3	0.0	0.0	66.7	0.0	0.0
2	16.4	0.0	6.9	0.0	43.7	23.0	0.0	10.0
3	18.5	64.1	13.0	3.7	0.2	0.4	0.0	0.1
4	73.4	14.5	8.6	2.5	0.5	0.2	0.2	0.1
5	20.2	0.1	68.3	7.2	1.7	1.7	0.5	0.3
6	0.0	7.6	0.0	80.4	3.7	0.0	0.0	8.3

Table 8-4 – Clustering Results – Percentage Elexon Class per representative load group

## 8.6 Conclusions

This chapter has presented a set of generic distribution network demand groups based on consumer compositions. These demand groups will be used in combination with the temperature sensitive load synthesis method presented in the preceding chapter to provide inputs to the analysis presented in the following chapter. These generic demand groups represent a contribution to the community since they are based on composition alone. Such groups are useful since they are independent of voltage level within the distribution system and can therefore be deployed when considering any study which involves a requirement to model a set of potential demands for a given network scenario.

## **9 Analysis of the requirements for the use of Dynamic Thermal Ratings in Electrical Distribution Networks**

### **9.1 Introduction**

In this Chapter the synthesised temperature sensitive load profiles for each of the generic compositions discussed in the previous Chapter will be used as inputs to a conductor model which uses meteorological data from the selected ‘critical span’. Both the Dynamic and Real-Time implementations of the CIGRÉ OHL model will be used to examine the differences between each approach.

The resultant conductor temperatures from use of the DTR method are evaluated using a similar method to that in [22] in as such that excursions are referred to as 5 minute periods for which the conductor temperature exceeds that of the circuit rated temperature. In this case the circuit rated temperature is held at the present value of 50°C. National Grid has outlined the potential for increasing such temperatures for certain OHL sections, where ground clearances permit [167]. A similar technique would also be the re-tensioning of existing OHLs to increase the present level of ground clearance. Such practices have been considered beyond the scope of this thesis and therefore the original circuit rated temperature values have been maintained.

In [47], the impact of allowing conductor temperatures greater than the circuit rated temperature is examined. The additional ageing of the asset due to these temperatures is quantified and taken into account when considering the overall capacity increases available through the use of Dynamic ratings. In this research, this phenomena has not been considered, and the circuit rated temperature has been used as an absolute figure. This is in order to provide a direct comparison with the present line rating method which quantifies the exceeding of the stipulated circuit rating temperature as opposed to allowing significantly increased operating temperatures.

As discussed in previous Sections, there are periods at which the RTTR or DTR of a particular line section may not be able to support the required load at a period in time. In [35-37] a Monte Carlo type random simulation of conductor

loadings has been carried out to determine the likelihood of these events and their associated levels of network risk. In [37] such simulations are noted as not adequately taking into account the time variable correlation between the loads supplied by the line, and the line rating itself. This in an area in which the research presented in this thesis can directly contribute. In the case of events where the RTTR or DTR cannot support the required load, two metrics of assessment have been commonly used to probabilistically analyse such periods. These are the Loss of Load Expectation (LOLE) [35] and the Expected Energy Not Supplied (EENS) [36, 47]. In the case of RTTRs, the inability to support demand is represented as a function of the line loading exceeding the RTTR at a particular point in time. For DTRs, such periods will be represented as those where the estimated conductor temperature due to the level of line loading exceeds that of the circuit rated temperature.

Whilst calculation of such metrics gives an indication as to the annual probability of being unable to provide headroom for load accommodation there are additional factors to take into account. The most significant of these are the times of day and seasons in which these events occur, which have not been explored previously. Through the use of the time-series load profiles developed in this thesis, in conjunction with dynamic conductor models, these factors can be determined.

In addition to identifying these points, as discussed previously there is the option to contract additional network services to offset potential conductor thermal overloads. Such services however represent an economic cost to the operation of the network, either in the form of service payments, or in energy not supplied to consumers. A Cost Benefit Analysis of such services was considered beyond the scope of this research, however to inform future analysis by the wider community the required magnitude of such services, their distribution throughout the day and the probability and cumulative distribution functions of these services have been developed.

As a reference case, the LOLE and EENS values for both the RTTR and DTR methods at the sheltered OHL site will be calculated. In this research following the work in [35], two definitions of the LOLE have been made. The first follows the same approach for determining the LOLE for RTTRs ( $LOLE_{RTTR}$ ), and an alternate method has been proposed for assessment of the LOLE for DTRs ( $LOLE_{DSR}$ ):

$$LOLE_{RTTR} = \frac{\sum_{t=1}^n P(RTTR_t < I_t)}{n} \quad (67)$$

$$LOLE_{DTR} = \frac{\sum_{t=1}^n P(DSR_t > 0)}{n} \quad (68)$$

Where:

$I$	is the Line Current (A)
$RTTR$	is the Maximum Line Rating (A)
$t$	is the time step
$n$	is the total number of timesteps
$DSR$	is the required service in order to mitigate a conductor thermal excursion at time step $t$ (A).

Since in this research, the monitoring period was greater than one year, the results have been normalised such that the values are in line with those shown in [35]. The EENS has been defined as the total sum of the energy not supplied over the period  $n$ . As per the LOLE, the EENS has been modified somewhat for the DTR analysis.

$$G_t = RTTR_t - L_{i_t} \quad (69)$$

$$EENS_{RTTR} = \sum_{t=1}^n (RTTR_t - L_{i_t}) \Delta t \quad \forall \{G_t | G_t < 0\} \quad (70)$$

$$EENS_{DTR} = \sum_{t=1}^n (DSR_t) \Delta t \quad \forall \{DSR_t | DSR_t > 0\} \quad (71)$$

Where  $G_t$  is the difference between the RTTR at time  $t$  and the circuit loading from demand group  $L_i$ .

## 9.2 Outline of the work in this chapter

In this chapter the capabilities of DTRs will be evaluated against the present UK line rating standard and the potential for increasing the number of consumer

connections will be outlined where possible. In addition to determining the number of possible consumer connections at the same level of thermal overload risk as is currently implemented, an additional increase of connections is examined, coupled with an estimation of the required network ancillary services in order to mitigate against a thermal overload. A novel zonal method based on the duration of the required services is proposed to categorise these requirements.

As noted in [36] additional network constraints such as voltage limits will have an effect on the total number of possible connected customers. In this research it has been assumed that either the customer numbers capable of being supplied in each of the service duration zones is possible without additional control techniques, or that in the future development of the smart grid, such techniques will be available.

### **9.3 Chapter Goals / Objectives and Contributions**

#### **9.3.1 Goals / Objectives**

To critically evaluate the benefits of dynamic thermal ratings for load accommodation. This evaluation includes determining the number of consumer connections capable of being supported through the use of dynamic thermal ratings in scenarios where ancillary network services are both available and unavailable. Where such services are considered to be available, the energy requirement, magnitude, duration and time period between service requirements should be determined.

#### **9.3.2 Transition from existing literature and research / Contribution**

A contribution has been made through the use of DTRs and synthesised load profiles to demonstrate the potential benefits of this network technique. Much of the literature in this domain considers the use of RTTRs as opposed to DTRs and as an enabler of network headroom for generation connections as opposed to demand. RTTRs have been used in combination with LOLE and EENS, however such analysis has utilised load duration curves (LDCs) as opposed to the use of time-series demand profiles.

A key contribution from this chapter is therefore its combination of dynamic thermal ratings with time series load profiles, taking into account the correlation

between the observed ambient parameters, electrical demand and OHL ratings. This approach allows for critical evaluation of the required network ancillary services required to mitigate against conductor thermal overloads.

### **9.3.3 Attainment of Goals**

Results have been presented which comment upon the ability of dynamic thermal ratings to provide additional network headroom for load accommodation. These results show the potential number of customers for the previously derived demand groups capable of being supported, with and without access to ancillary network services. Where such services are necessary in order to maintain thermal network limits, the duration, magnitude and energy requirements of these services have been derived. The ability to derive such values is as a direct function of the approach taken in this thesis.

### **9.3.4 Chapter Outline Block Diagram**

Figure 9-1 shows a block diagram of the inputs, methods and outputs for this chapter. This chapter utilises the outputs from each of the preceding chapters. The temperature sensitive load model is used to synthesis profiles for each the generic demand groups derived in the previous chapter. These then serve as inputs to the dynamic line rating thermal model, using meteorological inputs from the site selected in Chapter 3. These deliver a conductor temperature profile which may, or may not violate the circuit rated temperature, depending upon the number of consumers within the group. Where this limit is exceeded, the network ancillary services required to reduce the OHL temperature to below the circuit limit is estimated.

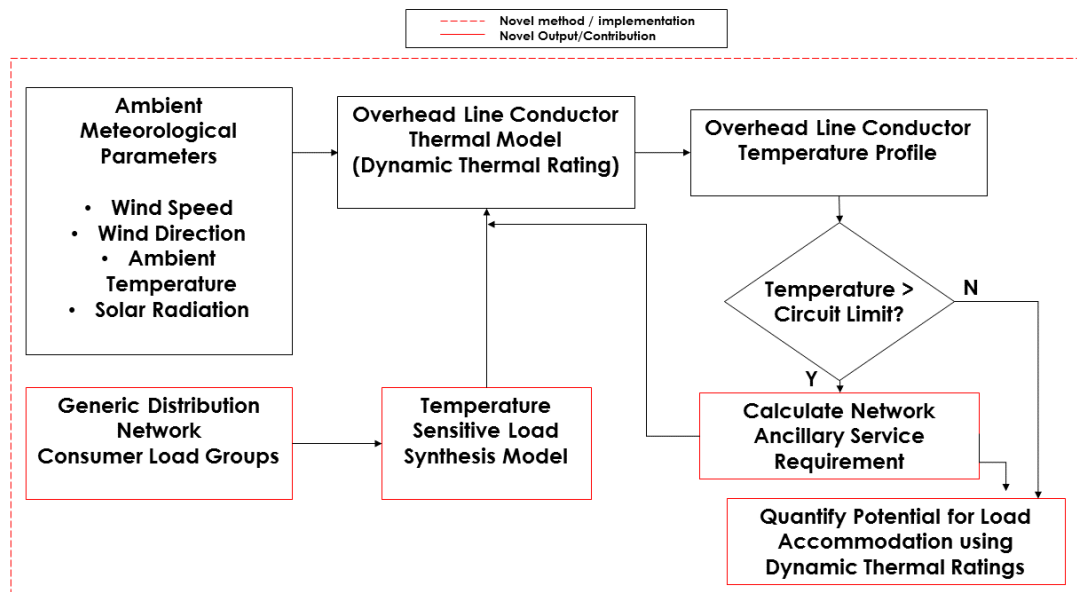


Figure 9-1 – Chapter 9 Block Diagram

#### 9.4 Verification of Derived Conductor Temperatures using the DTR Method

Prior to synthesising load profiles for the groups outlined in the previous chapter, a study was carried out to determine the accuracy of the synthesis method when presented as an input to the DTR OHL model in comparison to the original group feeder loads. In order to do this the original monitored load profile for a test load group was used as an input to the DTR model coupled with meteorological data from the selected sheltered site.

In addition to the use of the measured ambient values directly a series of upper and lower bounds were placed on the resultant conductor temperature values by taking into account the relative upper and lower bounds of measurement error on each of the individual ambient parameters. As noted in Chapter 3, the quoted measurement errors of the ambient sensors are as follows.

- Ambient Temperature  $\pm 0.1^{\circ}\text{C}$
- Wind Speed  $\pm 1\text{m/s}$
- Wind Direction  $\pm 4^{\circ}$
- Solar Radiation  $\pm 5\%$

The sensitivity analysis shown in Chapter 2 was used in conjunction with these measurement errors in order to determine the correct upper and lower bound ambient values at each time period. The meaning of this selection process is as follows.

For parameters such as ambient temperature wind speed and solar radiation selection of the upper and lower bound values is simple since each of the parameters has a monotonically increasing or decreasing function as shown in Figure 2-2. In the case of wind direction an alternative procedure must be used. As the conductor incident wind speed angle approaches 90°, increasing or decreasing the wind direction by the stipulated 4° value will have opposite effects depending upon whether in the range 0-90° or 91-180°. The same procedure is replicated for the ranges 181-270 and 271-360°.

The final stage of selecting the upper and lower bounds is to determine the best and worst case scenarios regarding the ambient measurements. For this the thermal balance equations (2-20) must be considered. The best and worst case scenarios for ambient measurement errors are:

- Worst case
  - Upper bound Ambient Temperature
  - Upper bound Solar Radiation
  - Maximum wind direction using the method as discussed previously
  - Lower bound wind speed
- Best case
  - Lower bound Ambient Temperature
  - Lower bound Solar Radiation
  - Minimum wind direction using the method as discussed previously
  - Upper bound wind speed

After selection of the appropriate total upper and lower bound ambient measurements the measured loads for the sample test group as shown in Figure 7-6 were use as inputs to the DTR OHL model for the following test cases of worst case, best case and actual measured parameters. The results of this test gave the

upper and lower ‘real’ bounds of conductor temperature based on ambient measurement errors alone. After use of the synthesised load profile with the actual measured parameters, a comparison of the resultant conductor temperatures was made.

Percentage of values within upper and lower bounds	Mean error outside of bounds (°C)	99 <sup>th</sup> percentile error outside bounds (°C)	Maximum error outside bounds (°C)
81.8%	0.343	0.980	1.180

**Table 9-1 – Conductor Temperature estimation accuracy of synthesised load group**

Whilst Table 9-1 shows that  $\approx 82\%$  of values are within bounds, the significant factors for reference are the mean, 99<sup>th</sup> percentile and maximum errors. In actual operation of a DTR solution, conductor temperature values will likely be verified through use of a conductor temperature sensor, as in this case of the monitoring sites used in this research. As noted previously in Chapter 3 the accuracy of the conductor temperature measurement system used is quoted at  $\pm 2^\circ$  [106]. The results of this analysis have shown that the maximum error as a function of ambient temperature values only is  $1.18^\circ\text{C}$  and is therefore within the additional bounds which will be added when verifying against the measured conductor temperature error values.

## **9.5 Customer Numbers supported by the present UK OHL rating standard.**

As noted in Chapter 4 the presently used OHL circuit ratings do not deliver the same level of risk as is currently thought to exist, particularly at the sheltered sites discussed in Section 4.4.2. Therefore as an assessment method the newly derived P27 seasonal ratings as shown in Table 4-8 will be used as the baseline comparison of the benefits a DTR solution can make to load accommodation.

Assessing the potential number of consumers supported by P27 is a non-trivial task. Whilst P27 makes reference to a seasonal continuous load condition, clearly continuous load conditions do not actually occur in day to day network operation. This is taken into account by two methods outlined in [109].

For multi-circuit primary supply systems, a procedure involving the expected load duration curve of a particular demand group is used in conjunction with the  $C_T$  factors shown in Table 4-1. For single circuit supply systems, as in the case of the OHL monitoring points within the test network an alternate procedure is described. For such systems, the three hours of peak loading conditions are said to be equivalent of the continuous load conditions. Therefore when determining the number of consumers capable of being supported by P27, the following method has been used:

1. Synthesise the group load profile using the method outline in Chapter 7.
2. Using a sliding window of length three hours, determine the peak loading condition in each window, and for each seasonal rating period.
3. If the maximum demand in the peak three hour window exceeds the newly derived P27 seasonal rating value, this customer increase is rejected, and the number supported by P27 defaults to the previous total number of customers in the load group. If the number does not exceed the rating, increase the total number of customers until this number cannot be supported.

In each iteration of the sliding window approach, the total number of consumers was increased by 50 and distributed proportionally according to their composition within the load group. Also there is no requirement to violate the P27 seasonal ratings in all periods, since thermal violations could occur within any seasonal period. If the maximum observed loads are greater than the seasonal rating for just one of the periods, again, this customer number increase is rejected.

Load group	Number of Customers Supported by P27
1	150
2	150
3	2350
4	3650
5	900
6	450

**Table 9-2 – Number of customers per generic load group supported by revised P276 seasonal ratings**

Table 9-2 shows the number of customers which can be supported through use of the modified P27 seasonal ratings. As can be seen, there are significant variations in the total number of customers which can be supported according to the particular load group composition. Load groups 3 and 4 contain the highest percentages of domestic consumers as shown in Table 8-4 and therefore as expected are those for which the highest numbers of consumers can be connected. The increased number of Economy 7 consumers in Group 3 as opposed to 4 results in fewer total customers being able to be supported by this rating method.

### **9.5.1 Comparison against N-d scenarios**

The numbers of total customers shown in Table 9-2 represent the maximum possible numbers able to be supported by P27. In actual network operation however the network will not be operated at this level in order to provide circuit security of supply for additional feeders. In this case, as the system is of single circuit design it must be capable of supporting the required N-1 feeder switching scenario and must therefore not be utilised fully. In this thesis the consideration of DTRs for such scenarios are not considered. The rationale for this approach is that as the present distribution planning standards are under review [19] the requirement to provide constant N-1 capabilities may no longer be required. The results presented in this section are intended to demonstrate the overall capabilities of DTRs and outline the potential services required to operate at such levels.

## **9.6 Zonal Analysis**

In addition to determining the number of customers supported by the present risk of thermal overload, load profiles for increased numbers of customers have been synthesised in order to determine the potential requirements for such increases. For the purposes of this analysis a zonal method relating to the time of required service has been proposed. In order to provide an upper limit to the service analysis, the decision has been taken to limit the maximum duration of a required response to a period of 4 hours. This duration limit is designed to be cognisant of

the four hour tariff period in the wider CLNR project, and represents the typical duration of network peak demand (4pm to 8pm) in the UK. An assumption has been made regarding the 4 hour limit which will clearly impact upon the magnitudes and durations of the required services. There is the potential to utilise the method presented in this thesis with any given upper service duration limit, however the purpose of the results presented in this thesis is to demonstrate the abilities of DTRs to provide additional headroom as opposed to providing a finite assessment of DTRs in all potential network scenarios.

Any form of DSR which is required to last for longer than 4 hours is deemed to be represent an unfeasible number of additional customer connections.

### **9.6.1 Zone A**

Zone A acts as an extension to the current thermal overload risk as outlined by P27. In P27 the thermal excursion risk is set to a 0.001% probability of exceeding the circuit rated temperature and is equivalent to roughly one five minute period per seasonal rating period. In a Zone A scenario this is simply extended in order to cover any excursions which occur for one 5 minute period. These can have any number of occurrences over a particular seasonal period, however the requirement is such that any thermal overload must be followed by a period below the circuit rated temperature.

### **9.6.2 Zone B**

Zone B relates to the first zone for which some form of ancillary network service such as DSR or EES is required in order to mitigate a thermal overload and return the conductor to a temperature value below that of the circuit rated value. In this research, the assumption has been made that where a service is required, it has been introduced into the network and the conductor temperature returned to below the circuit limiting temperature. If at the next analysis time step an additional service is required this is acting from a starting point of the temperature achieved by the previous service. This represents an assumption regarding the magnitudes of the required services, since each can act as a function of a previous service, however the aim of the method implemented in this research is to develop a profile of required services; and therefore as a network operator, the magnitude

and duration of the services outlined in this chapter are those required in order to maintain the network within its present operating characteristics. Consecutive excursions from 10 minutes up to the maximum DSR duration limit (in this case 4 hours) are defined as being within Zone B. Figure 9-2 shows an example of a service requirement categorised as type Zone B.

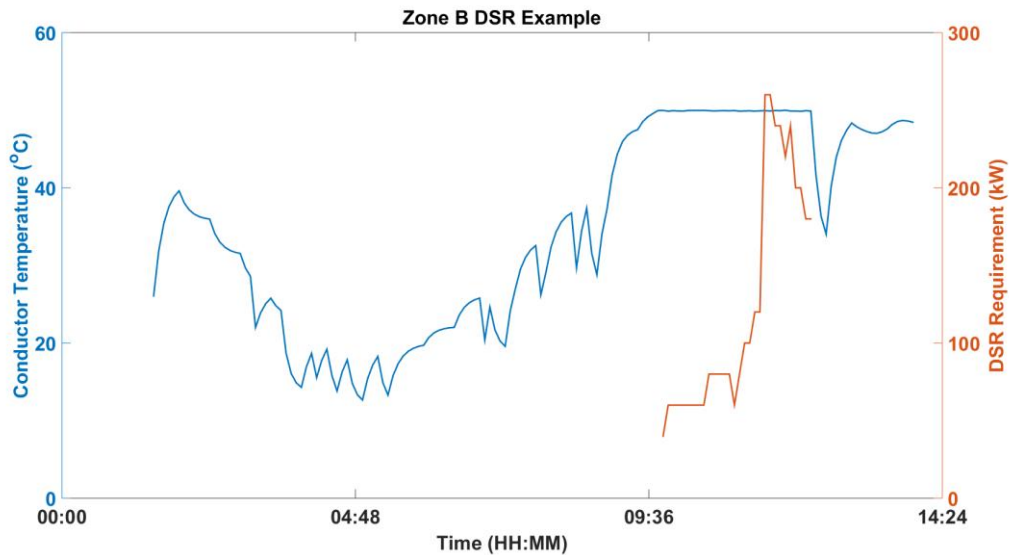
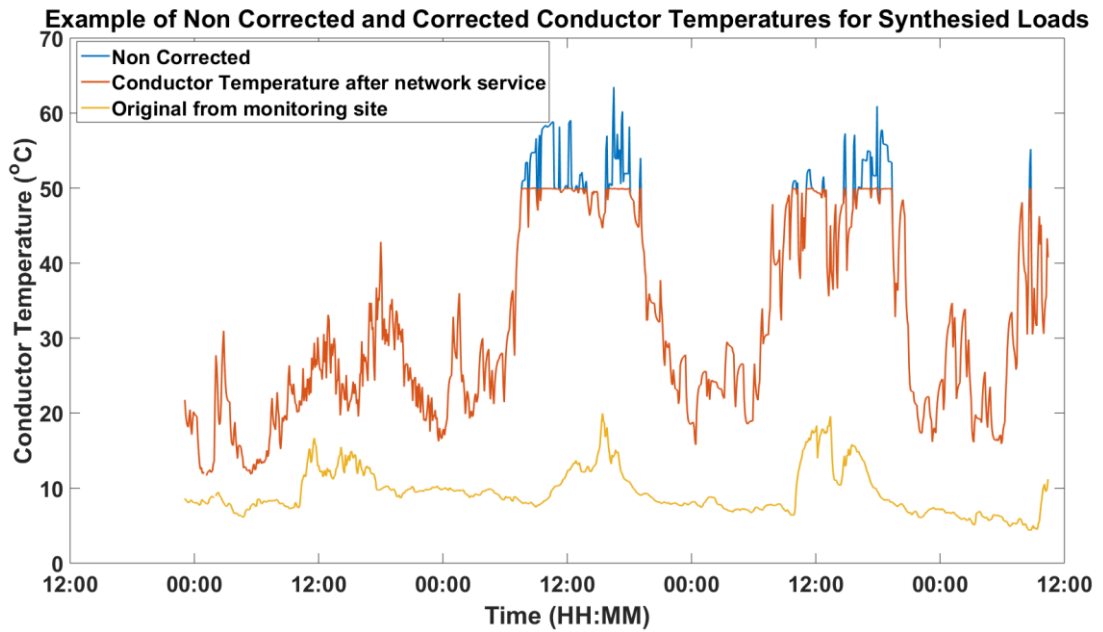


Figure 9-2 – Example of a Zone B service requirement

In this zone, whilst a consecutive excursion exceeding the DSR duration threshold is forbidden, there is the potential scenario with this approach that 2 or more multiple 4 hour service periods could be separated by a single 5 minute window. Clearly in practice this scenario would result essentially in services which exceed the threshold and is a limitation of this method. In order to investigate this aspect in more detail a study was carried out to determine the cumulative distribution functions of both the observed DSR service durations and the time in between required services. This analysis is shown in Section 9.9.3.

Figure 9-3 shows an example of load group temperatures both before and after the required service has been supplied. As can be seen the conductor temperatures are limited to 50°C in the case where network ancillary services have been introduced to compensate for the increased temperatures.



**Figure 9-3 – Example of conductor temperatures before and after provision of network services. Original conductor temperature for actual network loads shown for comparison**

### 9.6.3 Zone C

Zone C services are required where consecutive conductor temperature excursions exist for a period greater than 4 hours. In effect, Zone C does not actually represent a zone since by definition such service durations have been deemed as non-possible. Within this research these have been identified as being greater than the required duration threshold and therefore analysis for this Zone has not been carried out. Clearly this duration threshold has been defined here, however could be extended if such resources were available. This period has been selected simply as an example in this research. The potential to extend this aspect and the requirements for doing so are commented upon in the Discussion section of this thesis.

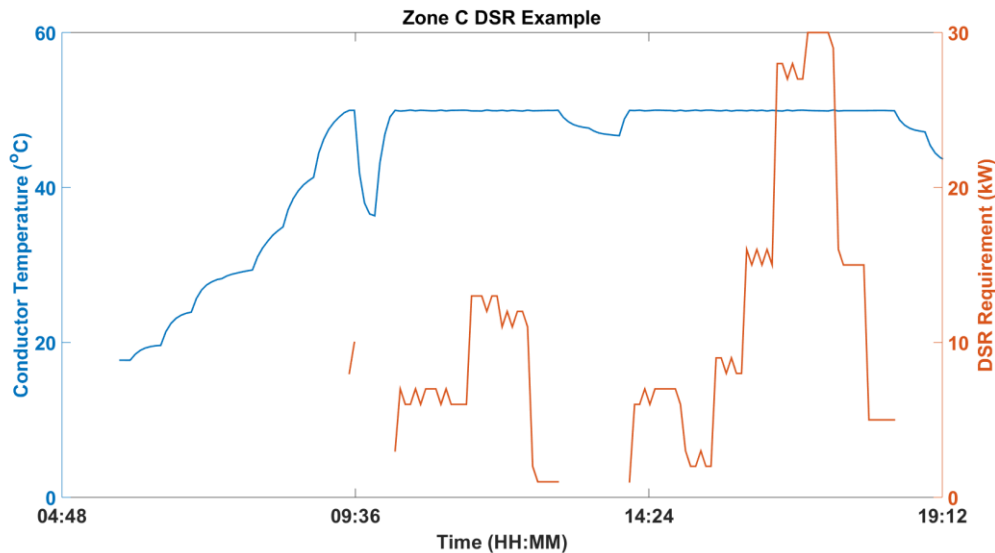


Figure 9-4 – Example of a Zone C service requirement which exceeds the duration threshold

## 9.7 Examining the capabilities of a Dynamic Thermal Rating Solution for Load Accommodation

After synthesis of each group’s load profile it is used alongside the meteorological inputs from the ‘critical span’ and the resultant set of conductor temperature values are obtained. As per the analysis to determine the number of customers able to be supported by the present P27 rating standard, for each load synthesis iteration the total number of customers is increased by 50 each time and then proportionally weighted according to the composition of the overall group.

As a means of presenting an AC current to the DTR model the real power values have been combined with a power factor estimate of 0.95 in order to deliver average feeder current values. This value of 0.95 is in line with the estimations of Elexon in [168] as reactive power synthesis for the overall load groups was considered out of scope for this research. This is considered as a potential method for extending the research and is discussed as such in the further work section of this thesis.

### 9.7.1 Loss of Load Expectation (LOLE)

As discussed in the Introduction to this chapter, LOLE values have been previously derived for a set of RTTR values and comparisons drawn against similar values derived for the present static ratings. In [35] results are presented for varying values of load factor. In this research, the same analysis will be presented

for both RTTRs and DTRs as a function of the total number of consumers in each of the derived generic consumer groups.

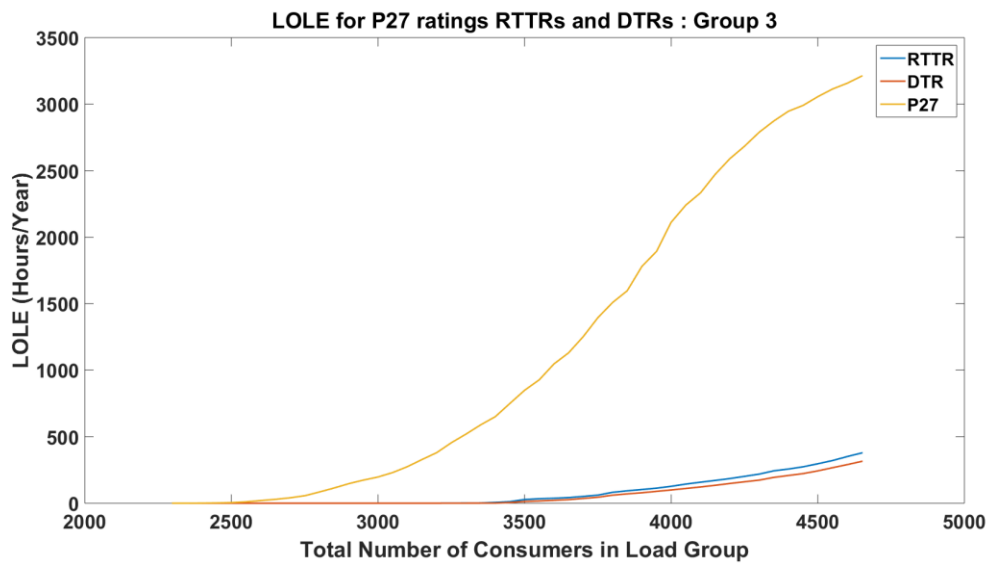


Figure 9-5 – LOLE Values for the RTTR, DTR and P27 rating cases

Figure 9-5 shows the LOLE values for generic load group 3 when evaluated against the RTTR, DTR and P27 seasonal rating values. As was shown in [35] the P27 rating values result in significantly increased probabilities of periods of lost load. Use of the DTR method shows improved performance, in terms of decreased LOLE values, in comparison to the use of the RTTR. This is due to the fact that in cases where the RTTR cannot support demand these are considered as periods of lost load. In the DTR case, the impact of these lost loads is also a function of the inherent correlation between the DTR and the load itself and the thermal history of the conductor over time, therefore not all events where the RTTR offers less network capacity than the demand have the same impact on conductor temperatures. This will be discussed further in Section 9.7.2.1.

### 9.7.2 Expected Energy Not Supplied (EENS)

Figure 9-6 shows the EENS for the same load group as in Figure 9-5, for the RTTR, DTR and P27 cases. As in the case of the LOLE the EENS for the RTTR and DTR cases is significantly lower than that for the P27 case for all total consumer numbers. The EENS in the RTTR case, as with the LOLE values, has

been shown to be greater than that of the DTR, though this relationship has been shown to be non-linear. This is as a result of fundamental differences between the RTTR and DTR approaches.

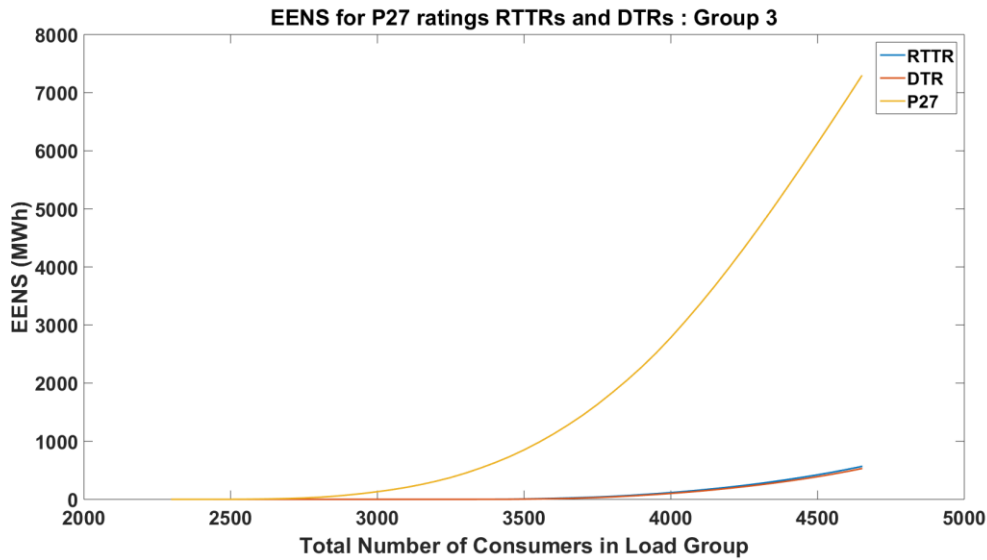
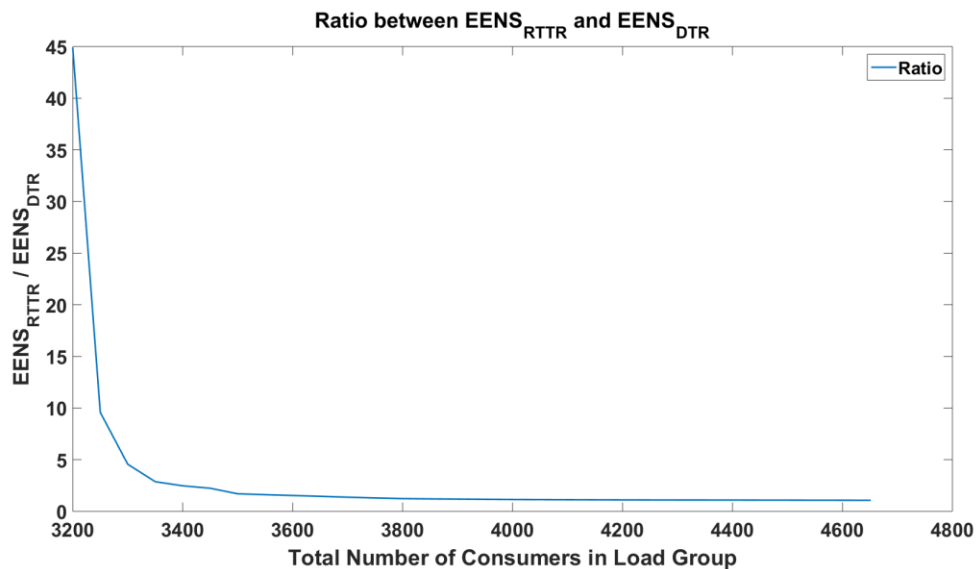


Figure 9-6 – EENS Values for the RTTR, DTR and P27 cases

### 9.7.2.1 Ratio between EENS for RTTR and DTR cases

Figure 9-7 shows the ratio between the EENS values in the RTTR and DTR cases for the same load group as shown in Figure 9-6. The ratios are expressed as a percentage of the DTR EENS values. As can be seen the values exponentially decay towards a value of 1. The reason behind this is as follows. The RTTR represents the maximum conductor loading value such that in after thermal equilibrium has been achieved, the conductor will operate at its maximum allowable temperature. In this case, the circuit rated temperature of 50°C. Therefore if the conductor was to be loaded with the RTTR at the correct intervals as a function of the conductor’s time constant, the theoretical conductor temperature would be constant at 50°C. If the conductor was then to be additionally loaded, this would be classified as being EENS due to the thermal overload.



**Figure 9-7 – Ratio between resultant EENS values for the RTTR and DTR cases, for Load group 3**

In the DTR case, since the decision has been taken to model the required reductions in load (i.e. EENS) the resultant conductor temperatures are also 50°C after the correct network service has been applied. When the conductor is lightly loaded, the available thermal headroom is greater than that considered by the RTTR minus load case, since the EENS essentially acts as a linear function. The inadequacy of this method for such a purpose is discussed in [36] where a risk methodology is presented to take into account the likely severity of an EENS event. Analysis of the differences between the DTR and RTTR did not form a part of this study.

As the conductor becomes more heavily loaded and the requirement for services become more frequent, the conductor will tend towards constant operation at the circuit rated temperature. At this equilibrium point, the requirements for both DSR services to mitigate thermal overload, and the EENS as a function of the RTTR minus the load become the same. Up to this point however, the DTR has been shown to have improvements in the EENS over the use of RTTR.

Beyond this point, by default, the same EENS will be required for both the DTR and RTTR cases. The thermal time constant of OHLs has been discussed as being typically in the range of  $\approx 10 - 20$  minutes. In this research however, due to the relative construction of the OHL, the thermal time constants are closer to five minutes. In the five minute data used in this research represents a good

approximation of the time constant of the conductor [36]. The graph as shown in Figure 9-7 is unlikely to tend exactly to one, since the thermal time constant is not exactly equal to five minutes in all cases and therefore a small modelling error is present in the resultant conductor temperatures.

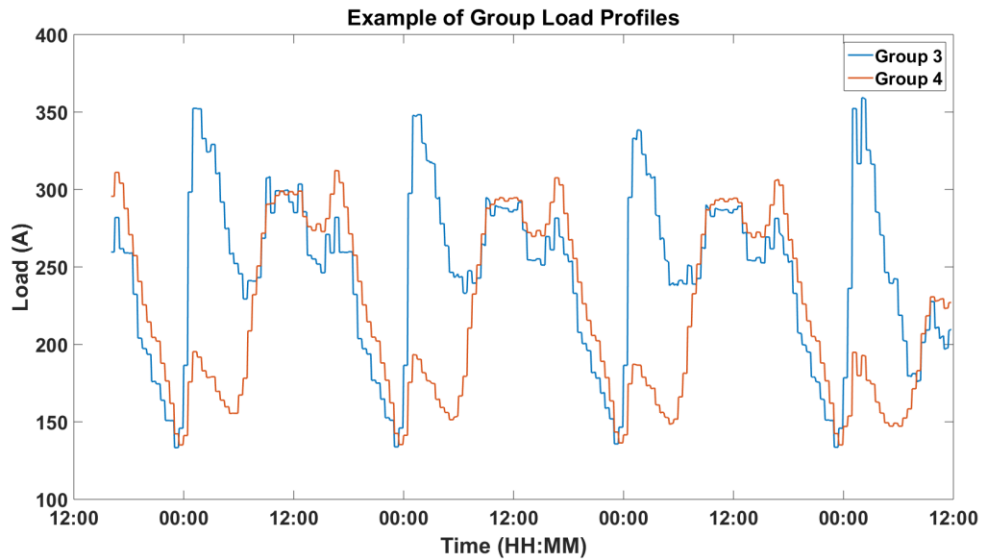
## 9.8 Zonal Analysis of Dynamic Thermal Ratings

Table 9-3 shows the total number of consumers per load group which are capable of being accommodated through the use of DTRs. Numbers have been shown for both the Elexon and OAC temperature sensitive load synthesis methods. In addition to the previously provided total numbers based on the revised P27 support calculations, the numbers for each of the DSR zones has also been derived. As can be seen, for all load groups other than groups 3 and 4, the number of customers supported in the Zone A case is equal to that of the P27 support case. For all load groups in the Zone B case, additional numbers of customers can be supported, where in some cases such as groups 3 and 4, significant customer increases can be made, albeit with the requirement for additional DSR services.

Group	Number Supported by revised P27 ratings	Elexon		OAC	
		Zone A	Zone B	Zone A	Zone B
1	150	150	250	150	250
2	150	150	250	150	250
3	2350	2500	3500	3200	4400
4	3650	3550	4750	3800	5400
5	900	900	1250	900	1250
6	450	450	650	450	650

**Table 9-3 – Total customer numbers per load group in each of the support cases**

Group 3 shows the potential for significant increases in Zone A connections over P27 in comparison to Group 4. Figure 9-8 shows an example of the two load profiles for these groups to outline the potential reasons behind this.



**Figure 9-8 – Examples of Group Load Profiles**

Although for large periods of time the observed load of group 3 is greater than Group 4, 600 additional customers can be connected with Zone A excursions over Group 4. This is a direct function of the correlation between the load profile and the thermal behaviour of the conductor. Since the majority of the load increases over Group 4 occur in the early morning (due to the high Economy 7 percentages in this group) these are at periods where the air temperature is likely to be lower and therefore the potential for thermal headroom increased. Whilst it is not within the scope of this thesis to examine the additional network requirements for LCTs such as Electric Vehicles (EVs), this period of correlation could provide useful information into the design of tariffs considering the charging of vehicles overnight.

### **9.8.1 Comparison of Loss of Load Expectation values**

Table 9-4 shows the LOLE values for both the Zone A and Zone B customer numbers for each group. In the Zone A cases the LOLE values are small by default for the RTTR and DTR cases. Since Zone A allows for any number of five minute conductor excursions, significant gains against the P27 ratings are shown for Groups 3 and 4. For Zone B numbers, again significant increases are shown against the present line ratings. The percentage improvement in terms of reduced LOLE hours/year when comparing the RTTR and DTR methods is also shown. Peak improvement represents a 38% reduction in the expected loss of load when using

the DTR as opposed to the RTTR as a method of assessment. The minimum demonstrated improvement is 18.9%.

Zone	Rating Method	1	2	3	4	5	6
Zone A	P27	0.00	0.00	379.86	47.04	0.00	0.00
	RTTR	0.15	0.00	0.44	0.48	0.26	0.18
	DTR	0.00	0.00	0.04	0.07	0.00	0.00
Zone B	P27	2074.47	1105.26	2946.96	2342.70	1444.44	1511.77
	RTTR	97.34	25.00	257.04	167.30	64.44	74.09
	DTR	70.51	15.50	208.46	131.37	45.87	48.84
	DTR/RTTR (%)	27.56	38.01	18.90	21.48	28.81	34.09

**Table 9-4 – LOLE in hours/year at the Zone A and B total number of customers supported per group**

### 9.8.2 Comparison of EENS values

Table 9-5 shows the EENS values in MWh per year for both the Zone A and Zone B customer numbers for each group. As in the case of the LOLE improvements are shown against the static rating and also against the use of RTTRs as opposed to DTRs. Minimum improvement in terms of EENS is 8.30%, with a maximum of 26.94%.

Zone	Rating Method	1	2	3	4	5	6
Zone A	P27	0.00	0.00	311.37	8.66	0.00	0.00
	RTTR	0.05	0.00	0.30	0.29	0.12	0.15
	DTR	0.00	0.00	0.01	0.02	0.00	0.00
Zone B	P27	3274.20	1226.60	5391.67	4119.81	1994.43	2107.66
	RTTR	63.94	11.47	341.95	146.10	41.98	39.80
	DTR	52.26	8.38	313.56	128.71	34.74	31.11
	DTR/RTTR (%)	18.28	26.94	8.30	11.90	17.25	21.85

**Table 9-5 - EENS in MWh/year at the Zone A and B total number of customers supported per group**

## 9.9 Cumulative Distribution Functions of the Required DSR Services

The following section provides information as to the nature of the required services through the use of cumulative distribution functions. The magnitude, duration and time between required services are shown here. The following section contains information as to the typical times of day at which the services are required, and gives examples for certain load groups. In each of the following analyses, the load profile for the maximum number of customers in the Zone B case for each group has been used. This is in order to determine the distributions of the maximum requirements in the scenario where the greatest number of customers can be accommodated, whilst maintaining the upper duration limit of the service requirement.

### 9.9.1 Cumulative Distribution Function of Required DSR Service Magnitudes

Figure 9-9 and Table 9-6 show the empirical CDFs of the required DSR service magnitudes. Whilst the maximum required service is 4.88 MW, at the 99<sup>th</sup> percentile level the peak value is significantly reduced to 1.6 MW.

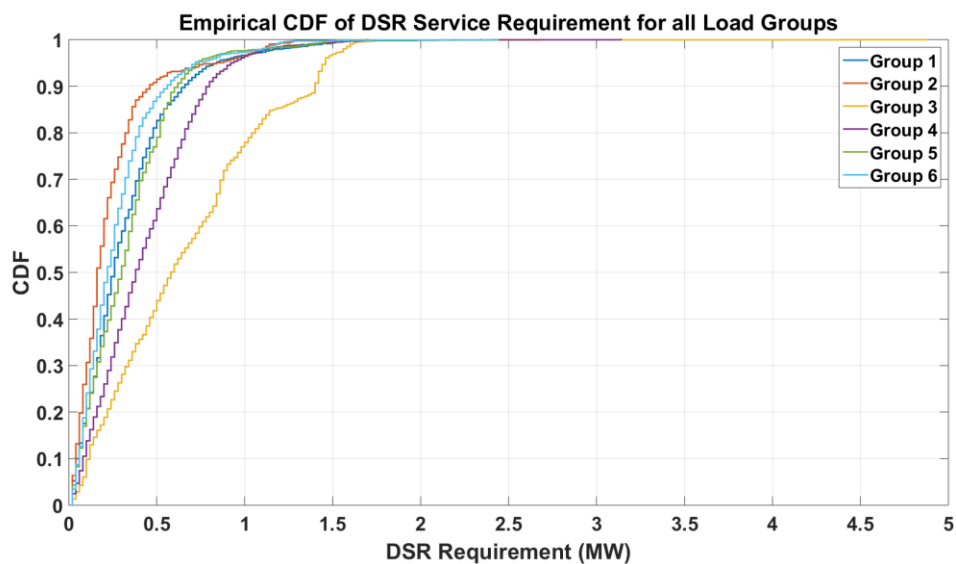


Figure 9-9 – Empirical CDF of the required DSR service magnitudes

Load Group	1	2	3	4	5	6
Maximum Required DSR Service (MW)	2.34	1.70	4.88	3.14	2.20	2.44
99 <sup>th</sup> Percentile (MW)	1.44	1.16	1.60	1.36	1.38	1.18
95 <sup>th</sup> Percentile (MW)	0.84	0.85	1.46	0.92	0.74	0.72
90 <sup>th</sup> Percentile (MW)	0.66	0.46	1.40	0.80	0.62	0.56
80 <sup>th</sup> Percentile (MW)	0.48	0.33	1.06	0.66	0.52	0.40

**Table 9-6 – Maximum and percentiles of required DSR services**

The OHL ratings presented in Table 3-3 have been converted to MVA ratings to allow for comparison with this maximum service requirement. These MVA ratings are shown in Table 9-7.

	Winter	Spring / Autumn	Summer
HV Overhead Line P27 Static Rating (MVA)	10.3	9.5	8.2

**Table 9-7 – HV overhead line P27 static ratings (MVA)**

As can be seen in Table 9-7 the maximum required service is smaller than the presently implemented circuit ratings, though does have the potential to exceed the Summer rating if N-1 circuit security was to be maintained. The magnitude of the service requirement is also closely related to the particular load group. As noted previously, each of the load groups analysed here represents that which is the maximum possible without violating the 4 hour service duration limit, however the maximum required service for Group 2 is  $\approx$  35% of that required for Group 3. Accurate knowledge and modelling of the loads under analysis is therefore of importance in order to adequately estimate the required services and thus contract them accordingly in each scenario.

### **9.9.2 Cumulative Distribution Function of Required DSR Energy Values**

Figure 9-10 and Table 9-8 detail the CDF and percentiles of the required DSR service energy values respectively. As can be seen, the maximum required service is 3.69 MWh for load group 3. At the 99<sup>th</sup> percentile level, thus requirement is reduced to 3.31 MWh and there is a significant decrease towards the 95<sup>th</sup> percentile and below. To mitigate against 80 percent of all required DSR services a maximum

energy capacity of 0.51 MWh is required, representing a significant decrease against the capacity required to provide services in each case. Clearly given the temporal distribution of required services, there is the potential that consecutive services could require an energy capacity greater than the maximum, however this represents a topic considered out of scope within this research, with a potential method of mitigating against this scenario coming from the ability to contract DSR from multiple potential sources.

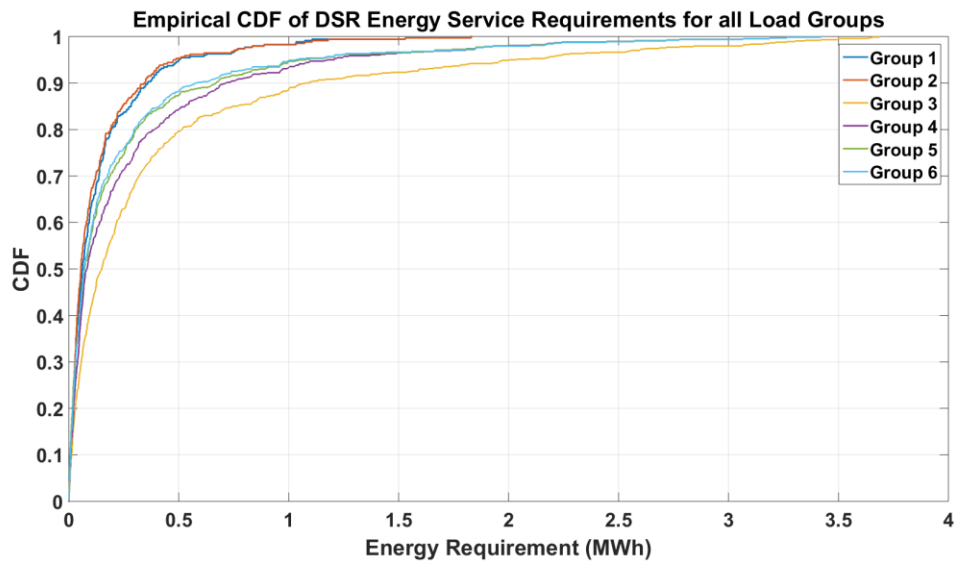


Figure 9-10 - Empirical CDF of the required DSR Energy service values

Load Group	1	2	3	4	5	6
Maximum Required DSR Service (MWh)	1.83	1.83	3.69	3.42	3.42	3.42
99 <sup>th</sup> Percentile (MWh)	1.07	1.11	3.31	2.53	2.56	2.60
95 <sup>th</sup> Percentile (MWh)	0.50	0.48	2.02	1.19	1.07	1.03
90 <sup>th</sup> Percentile (MWh)	0.36	0.34	1.08	0.71	0.67	0.58
80 <sup>th</sup> Percentile (MWh)	0.19	0.19	0.51	0.39	0.31	0.30

Table 9-8 – Maximum and percentiles of required DSR Energy services

### 9.9.3 Cumulative Distribution Functions of DSR Service Durations and Times between Services

The CDFs shown in Figure 9-11 and Figure 9-12 are intended to be considered together. As discussed in Section 9.6.2 due to the nature of the zonal system presented in this thesis, there is the potential for multiple services to be spaced by

a single five minute window, thus effectively ‘chaining’ them together to make one larger service. One benefit of this strategy however is that it allows for analysis of the temporal spacing between these services. As the CDF in Figure 9-11 shows, whilst the maximum DSR duration threshold has been set to 4 hours, the slope of the CDF is such that a very limited number of services are of this duration. At the 80<sup>th</sup> percentile level, all required services are less than one hour in duration.

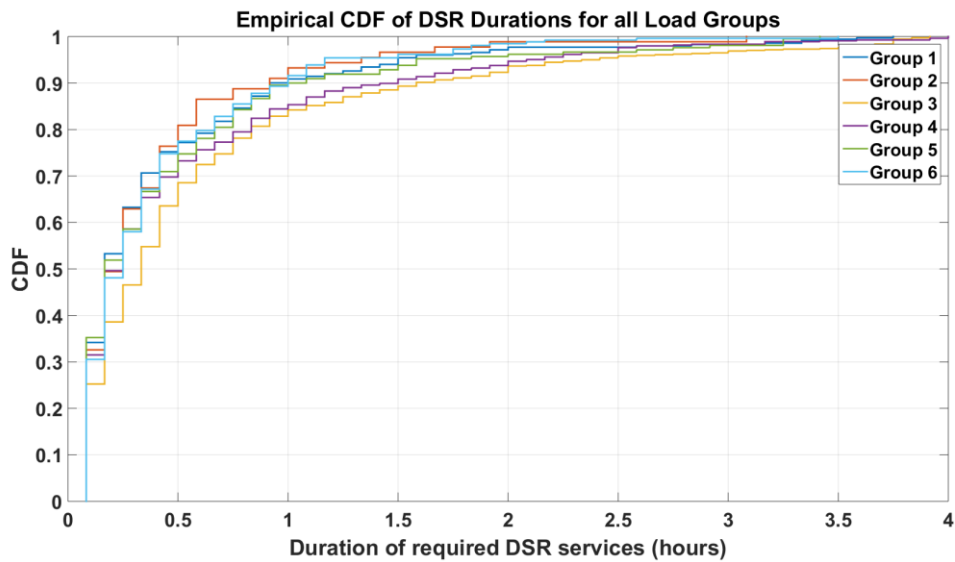


Figure 9-11- Empirical CDF of the required DSR service durations

Load Group	1	2	3	4	5	6
99 <sup>th</sup> percentile	3.33	2.63	3.75	3.42	3.25	2.16
95 <sup>th</sup> percentile	1.50	1.34	2.37	2.10	1.58	1.17
90 <sup>th</sup> percentile	0.95	0.92	1.58	1.49	1.04	1.00
80 <sup>th</sup> percentile	0.67	0.50	0.83	0.83	0.67	0.67

Table 9-9 – Percentiles of DSR service durations

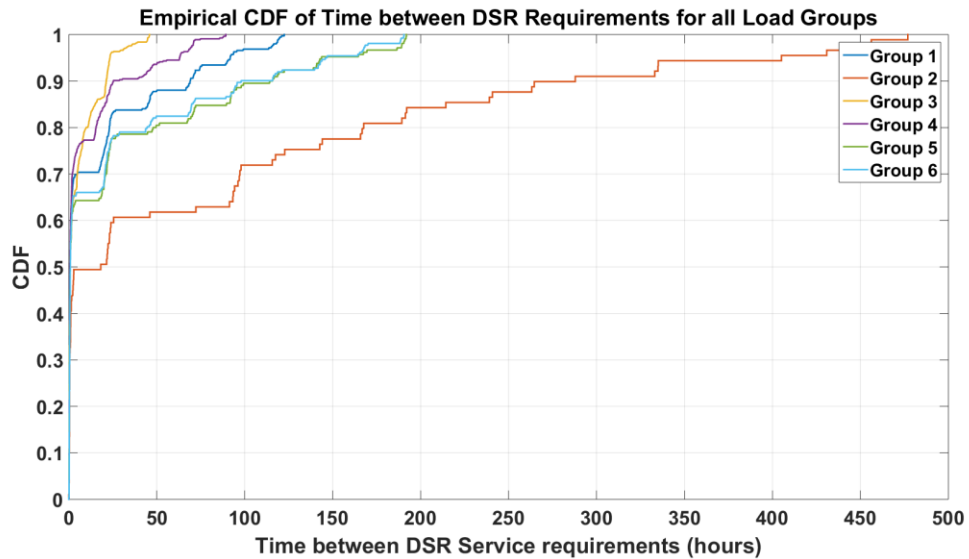


Figure 9-12– Empirical CDF of the time between required DSR services

Table 9-10 shows the percentiles in minutes of the times between the required services. In this case, the 1<sup>st</sup>, 5<sup>th</sup>, 10<sup>th</sup> and 20<sup>th</sup> percentiles have been show since these represent the distribution of the minimum times between required services, which is likely to be of more interest with regards to scheduling. As discussed previously it is important to consider these CDFs together. If the typical times between required services is low, however at the same time the typical service durations are also low, this will be of less impact than long duration services which occur closer together.

Group	1	2	3	4	5	6
1 <sup>st</sup> percentile (mins)	10	3.9	10	10	10	10
5 <sup>th</sup> percentile (mins)	10	15	10	10	10	15
10 <sup>th</sup> percentile (mins)	15	17	10	15	15	15
20 <sup>th</sup> percentile (mins)	20	25	15	15	20	20

Table 9-10 – Percentiles of time between DSR services

There is however clearly a trade-off requirement. As the number of customers grows, the available thermal headroom offered by the DTRs is reduced. Services of greater durations are therefore required to mitigate an increased number of thermal excursions, and by default these will occur at smaller and smaller time intervals between services.

This point is shown by two estimates of the multivariate CDF between the univariate service duration and time between service CDFs. The same kernel density estimation method as in Figure 7-2 has been used to develop these multivariate CDFs. Figure 9-13 shows these example joint CDFs for load group 3 and for a total of 3750 and 4400 customers in the group. As can be seen, in the 4400 customer case the time interval between services has reduced significantly from that of the 3750 customer case. The probability of larger services occurring at these smaller time intervals is also shown, as expected.

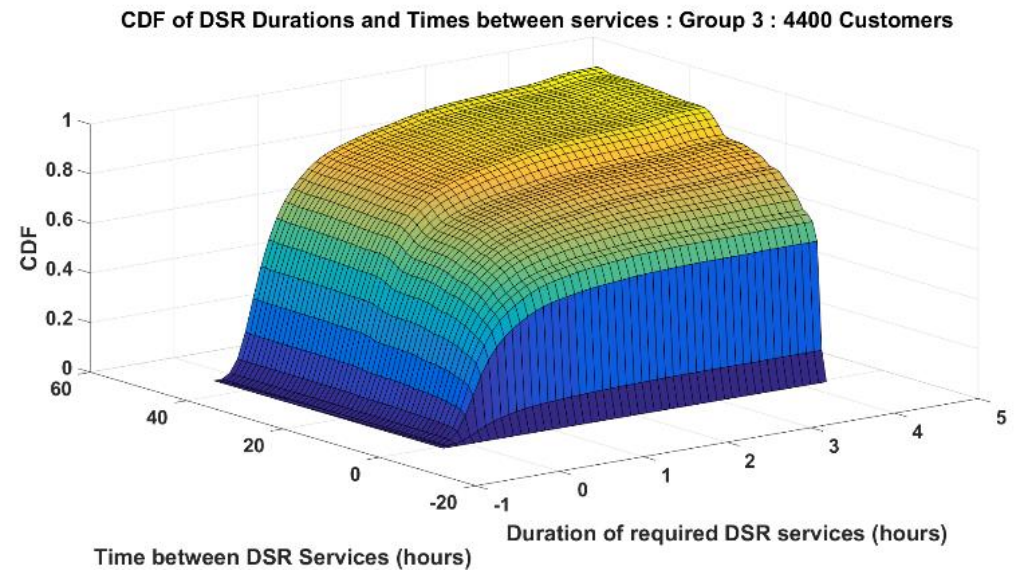
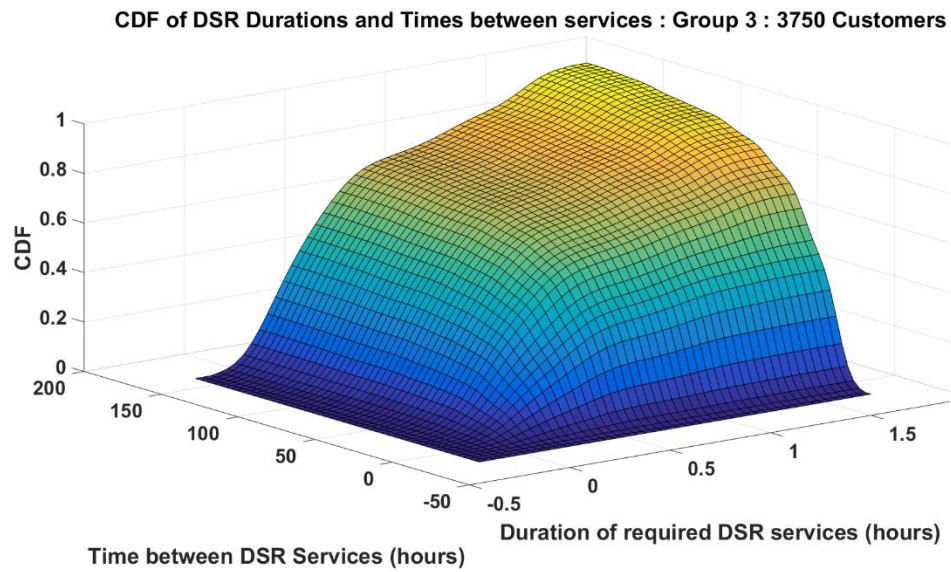


Figure 9-13 – Examples of joint CDFs between service duration and time between services

### 9.9.4 Percentage of Conductor Thermal Excursions per Zone

Figure 9-14 shows the percentage of required DSR services in each duration zone. Results are shown for load group 3 across a range of total customer numbers. For reference, the number of customers supported by the current line rating procedure for this group is 2350. The relationships between the zonal percentages have been shown to be non-linear, i.e. the percentage of customers supported does not transfer linearly between the zones.

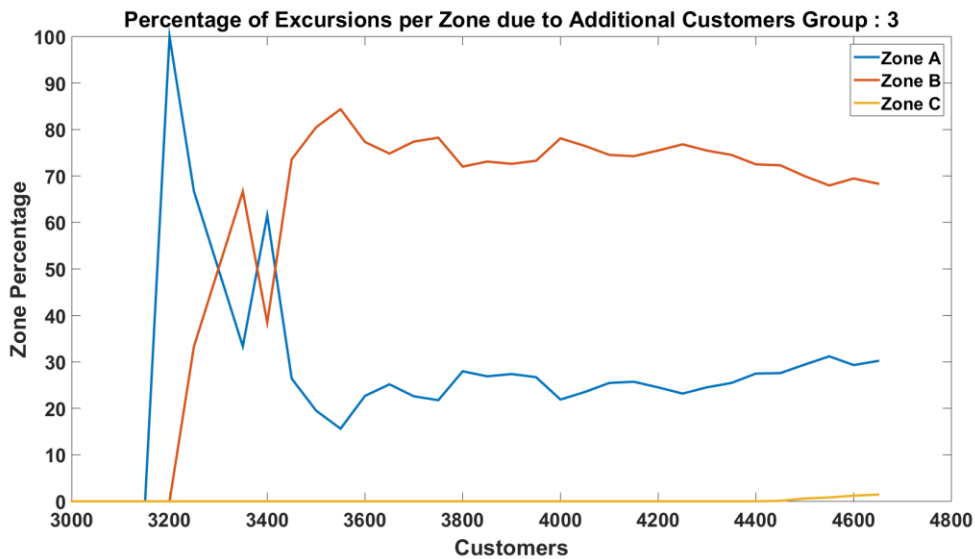


Figure 9-14 – Zonal Results for Load Group 3

This is partly due to a function of the load profiles’ relationship with the resultant DTRs, but also due to the inclusion of DSR services within zone B. As DSR services in this research have been modelled as being constantly available and used where necessary, the resultant conductor temperature profile becomes a function of both the services and the actual conductor loading.

Therefore in certain scenarios the use of a service could result in a single five minute excursion occurring where previously there was no such excursion or vice versa.

### 9.9.5 Example Profiles of Required DSR

In addition to exposing the CDFs of duration, magnitude and time between services, the profile of required services throughout the day can also be derived. This has not been analysed in previous studies. The aim of this approach is to

provide useful information for both network planners and operators, in addition to further research considering the optimal scheduling of such services in the future smart grid.

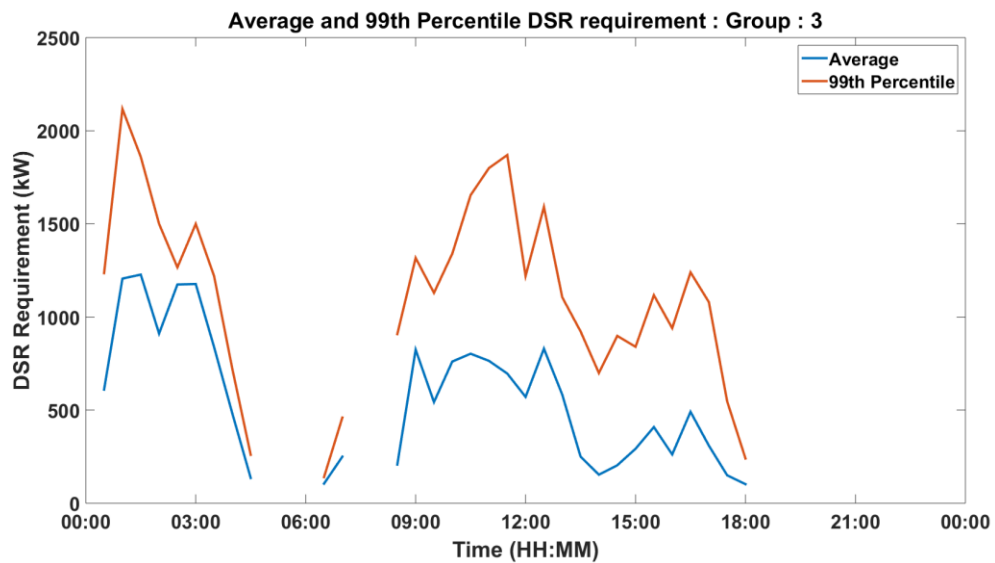


Figure 9-15 – Average and 99<sup>th</sup> percentile profiles of required services for Group 3 – Winter Weekday

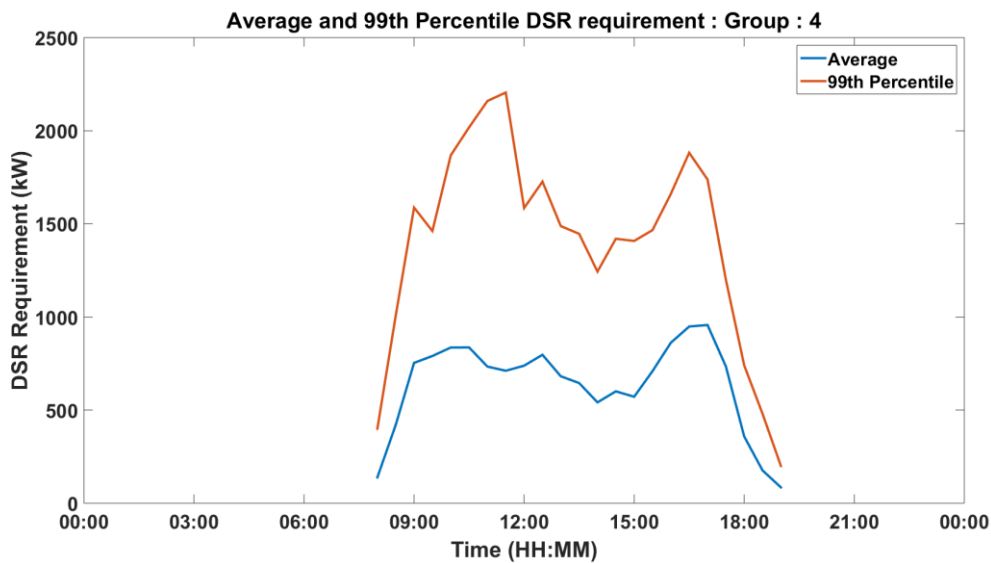


Figure 9-16 - Average and 99<sup>th</sup> percentile profiles of required services for Group 4 – Winter Weekday

Figure 9-15 and Figure 9-16 show two examples of the required DSR services shown as a function of time. In both these cases service profiles are provided for the Winter Weekday scenario. For group 3 loads, as a result of the increased percentages of Economy 7 customers, there is a greater requirement for DSR services in the morning period.

## 9.10 Conclusions

This chapter has investigated the use of DTRs as a method to provide additional network headroom for the accommodation for increased consumer numbers. Two methods of analysis, the LOLE and the EENS have been used to investigate the potential benefits that DTRs can deliver, compared to the presently used line rating method and the use of the RTTR as opposed to the DTR. Improvements of up to 38 and 27% in the resultant LOLE and EENS values respectively have been shown when comparing the use of DTRs against RTTRs for the test cases explored in this chapter. Significant increases in network headroom have also been shown against the present line UK line rating standard, as previously discussed in [36]. The use of the Dynamic as opposed to Real-Time thermal ratings not only exposes the correlation between the load profile and the resultant conductor temperatures, but also exploits the thermal history of the conductor.

Whilst a new series of reduced seasonal line ratings have been developed in this thesis as discussed in Chapter 4, for 4 of the 6 general load groups, no improvement was possible through the use of the DTR over the present line ratings when considering the newly proposed Zone A period. Such excursions did not occur for these load groups since by default the shape of their load profile is such that it leads to excursions greater than five minutes.

This has been shown to typically occur for those load groups which have high percentages of industrial loads and therefore a ‘flatter’ load profile throughout the day. The shape of the load profile is therefore of importance when considering the nature of such thermal excursions and therefore their required services.

The CDFs of the required service magnitudes have shown that whilst the maximum required service has a peak of 4.88 MW (in the worst case presented here), at the 99<sup>th</sup> percentile level of required response, the requirement has a maximum value of 1.60 MW. Whilst this percentile value does not provide the same operational risk as those of the thermal conductor excursions i.e. a 99.999% reliability it provides an indication as to the potential trade-offs in providing 100% or 99% of the required service magnitude.

This is particularly important when considering that the service requirement is not evaluated against the entire yearly period. Whilst 99% of a yearly period

represents a potential 87.6 hours per year where some shortfall is present, 99% of the LOLE per year represents 1% of 208.46 hours or  $\approx 2$  hours.

## **10 Discussion**

### **10.1 Introduction**

In this section of the thesis, the findings from each of the Chapters presented in this research will be discussed. Chapter 3 presents analysis of the meteorological and conductor parameters for the OHL monitoring sites. The most sheltered OHL site is determined in addition to derivations of the RTTRs for the available sites. Chapter 4 details a review of the presently implemented OHL rating standard in the UK. Chapter 5 presents derivation of a new series of ADD profiles, informed by the OAC socio-demographic classification scheme. Chapter 6 investigates the relationship between load and temperature for grouped electrical loads. Chapter 7 provides a novel temperature-sensitive load modelling procedure in order to develop suitable feeder load models to act as inputs to a DTR model of an OHL. Chapter 8 details a clustering study carried out in order to determining a series of generic load groups based on their composition of Elexon class consumers. Chapter 9 presents an evaluation of the use of the DTR model with time-series load profiles and exposes the differences between this method and those which have been previously carried out.

In addition to outlining the limitations of this work, potential areas or methods which could be used to extend the work are also discussed in this Chapter. The areas of further work detailed in this section are both in addition to and complimentary to, the areas of further work discussed in the main body of the thesis.

### **10.2 Current UK network rating practice**

The currently implemented UK standard for the rating of overhead lines has been examined as a base case in demonstrating the potential headroom increase through the use of DTRs. Limitations in the current standard have been exposed through the use of real world monitoring data installed at a series of test sites in the North of England. The results of this analysis have been shown largely to be dependent upon the selection of suitable 'best fit' procedures from the presented experimental results. Whilst admittedly, such research was carried out in a period

of reduced computational ability and allowances can be made for estimation errors, the fundamental factor from this analysis is not the derivation of new seasonal rating factors but is moreover the impact of using a worst case methodology as shown in P27.

For conductors to be rated as a potential worst case scenario it has been shown in Chapter 4 that wind speeds need to be categorised as null. At this value, free as opposed to forced convection occurs and line ratings are therefore reduced. Ambient temperature values have also been demonstrated as differing from those quoted in the current standard. As shown in climate change predictions such as those in the UKCP09 scenarios, ambient temperatures and wind speeds are likely to deviate even further from the stipulated conditions. It has been noted that as part of the review of the current distribution network planning standard the technique of RTTRs and DTRs will play a role. This thesis has shown that their inclusion is important not only for increasing network capacity at lower costs than reinforcement but also since the present line rating standard may not adequately provide the level of risk which is currently assumed.

### **10.3 Socio Demographics and Residential demand side response**

In Chapter 5 results have shown that the present energy assumptions of the Elexon ADD profiles whilst being useful for overall power system planning, vary from those derived as a function of socio-demographics. The findings of this analysis have impact when considering the growth of techniques such as residential DSR [169] [170] [171, 172] or when examining differential charging methods for consumer connections to the distribution network [173].

When considering a form of DSR from consumers, factors such as the number of requests and subsequent rewards for such services are those in which the socio-demographics discussed here could provide input. Requests for services could be made based on electrical or non-electrical factors. In the context of Power Flow Sensitivity Factors (PFSFs) [174], some customers could provide greater impact on the network by their response than others, however continual calls for service from particular consumers could lead to DSR ‘fatigue’.

Energy based socio-demographics could also be used as a method to proportionally reward consumers for their services. Considering two domestic

electrical consumers each of whom provide a response of 1kW to the low voltage network with the same (PFSF). Each consumer provides the same response however one consumer would be classified as socially constrained in their usage, whilst the other has a much higher overall consumption. Whilst electrically these consumers are the same, the relative proportion of their response to their total consumptions are dissimilar. This could be said to be an adaptation of the proportional generation control schemes as presented in [174]. Here the two most appropriate methods for comparison are the ‘Egalitarian’ broadcast and the ‘Technically most appropriate’. In the Egalitarian case, generators are controlled proportional to their relative PFSF as opposed to calling upon those which can simply offer the greatest impact. This approach could be modified in order to take into account the relative PFSFs of consumers and their expected power and energy consumptions based on socio-demographics.

Whilst in this research the OAC socio-demographic classification method has been used, additional classification schemes such as MOSAIC [175] could also be used to develop alternative annual energy values and compared against those using the OAC.

#### **10.4 Investigating the relationship between load and temperature for grouped electrical loads**

Chapter 6 presented novel analysis of the relationship between ambient temperature and load for groups of consumers at the distribution network level. This analysis was carried out in order to examine the requirements for the accurate modelling of consumers at the MV network level of the distribution network. As such, the nature of these relationships may be different for consumers at higher or lower voltage levels. Whilst a linear approximation has been made in this research, at lower voltage levels in particular an alternative modelling approach may be necessary.

The correlations examined in this research are thought to be useful since they give information as to the relative impact of not only temperature on demand, but also on temperature estimation errors. As the move towards the smart grid is made, the economics of the power system will become more complex and the minimising of wasted costs is a key topic.

The potential impact of an example forecasting error has been demonstrated although as a potential piece of further work, examining how this relationship varies according to differing values of forecasting error would be useful to generalise these findings further.

A new modelling technique has been proposed which can be used to derive estimates of these correlation values.

## **10.5 Temperature Sensitive Load Synthesis**

Previous work has considered the temperature sensitive elements of electrical load in order to derive more accurate forecasts or models of such loads, typically in wide area of national studies. This research has presented a causal model which can be used to develop accurate load profile time-series for end-user specified groups. As per the correlation model, a new technique has been developed in order to modify existing or newly derived ADD values of group demand as a function of temperature. As in the case of the correlation models, coefficients for the modification of domestic consumers only was considered. A potential aspect for further work would be to investigate the causal link between ambient temperature and non-domestic loads in greater detail.

As climate change affects electrical demand in the future shifts away from the linear approximation as taken in this research are likely to occur. As shown in additional work from countries where the prevalence for air conditioning is higher, there is likely to be a shift towards a more non-linear relationship. As noted in the introduction to this thesis, RTTRs and DTRs are an available solution to network operators at present and there are network scenarios in which such solutions could deliver benefits to the network.

This factor has significantly influenced the nature of load synthesis in this research and has therefore an effect on the choices with regards to the loads modelled, and their relationship with temperature. Whilst LCTs are likely to influence network loading significantly in future they have not been considered in this research. This is perhaps the key area to consider as a method for expanding on the research presented in this thesis. Following a similar approach as presented here, the influence of temperature on consumers with EVs, Air or Ground Source Heat Pumps and photovoltaic generation could be estimated.

## **10.6 Consumer Load Group Classifications**

In order to generalize the findings from this research, a group composition clustering study has been carried out to determine a set of ‘typical’ consumer load groups across the LV and MV levels of distribution networks.

Whilst these classes have been derived based on composition alone, this was to serve a specific purpose within this research. As in other clustering studies, there is the potential to classify load groups according to their profile. This could be carried out using two differing sets of profiles:

1. Classifications could be made according to the load profile time-series of the groups
2. Classification could be performed on the resultant network service requirement profiles.

The intention of a combined load and DTR solution is such that consumers are connected for the maximum possible period of time and as the research in this thesis has shown, for certain load groups significant customer number increases are possible beyond the current rating standard in a ‘fit and forget’ type scenario. The use of time-series load profiles in conjunction with DTRs has estimated the requirement for potential services where necessary in order to provide the same level of network risk regarding thermal overloads. There is the potential that after such service determination that classification can be made according to the magnitude and duration of the required services as opposed to the load groups which are actually served.

## **10.7 Identification of the potential network service requirements**

In Chapter 9 the synthesised temperature sensitive load profiles for each of the identified consumer load groups is used in conjunction with a DTR model using meteorological information from a highly sheltered site. A novel service-duration based zonal method is proposed which ranks the number of potential consumer connections based upon the duration of the network services which are required to mitigate conductor temperature excursions.

In this research a stipulated four hour limit has been placed on the duration of available responses to mitigate thermal overload conditions for an OHL. An extension of this work would be to consider a network model such as the UK GDS or IEEE test networks and to consider the potential connections of EES and DSR resources available to the network operator and optimise the available responses according to network costs and aspects such as power flow sensitivity factors. In this research the requirements from some form of network ancillary services has been discussed.

### **10.7.1 Network Risk**

Where a requirement has been made on such services they have been assumed to be available at all times in order to develop a suitable overall profile of required response. Clearly in the real-time operational power system, taking into account reliability and economic variables, a 100% secure source of network services is unlikely to be available. As in [36] a similar risk method could be examined which combines the probability of being unable to deliver a service at a particular point in time, with its resultant effect on conductor thermal behaviour.

There is also the potential to follow the procedure discussed in [47] whereby the conductor would be allowed to exceed the circuit rated temperature, and the effects of these increases calculated. This would potentially allow for increased connection capacities, although the level of risk of operation in this mode must be clearly quantified accurately so as not to accelerate the ageing of conductors too rapidly.

Since studies in [47] were carried out on an IEEE test network, the current state of real network assets is not discussed. As shown in Chapter 4 of this thesis, there is the potential that for certain OHL sites, the conductor may, in network fault scenarios be operating at higher temperatures than previously thought. The lack of knowledge of these events at present being as a result of the lack of monitoring at this level. It is therefore vital if exploitation of the ageing of the conductor is to be carried out, that a line study is carried out prior to implementation to determine the correct state of the asset's existing health.

## 10.8 Issues with Demand Side Response as a Control Technique

As noted throughout this thesis the concept of demand side response has not been made specific as to a single source. In the case of EES the resource is clearly independent of any social or personal function, although is not completely dependable in its service provision due to state of charge and its potential additional requirements to provide network services such as frequency response. If DSR is examined as being supplied by residential consumers there are a number of factors which should be considered. It has been commented that DSR can reduce the natural diversity of demand, therefore impacting upon the load modelling methods outlined in this thesis. Strbac in [52] outlines a potential scenario whereby cold appliances such as fridges and freezers are automatically switched off as the result of a DSR call. At the start of the call each of the appliances will have differing thermal states. Depending upon the duration of the DSR period, all of the appliances could approach their maximum threshold temperature and require power for cooling at the end of the period. This issue of payback is one which will require careful management when considering a combined DTR and load accommodation strategy to prevent thermal overloads upon load reintroduction. Techniques such as phasing in loads to prevent surges in demand could play a key role in such systems. Also payback is clearly a function of the demands used to provide the DSR. Kirschen in [176] notes that lighting is an example of one load reduction which has little if any payback.

The potential for unwanted peak shifting is also of importance for investigation and is subtly different to the nature of payback. The pure reduction of loads as a result of a network requirement is clearly beneficial. The management of payback is possible through techniques such as those outlined previously, however the reintroduction of load at unfavourable times as a result of energy practice 'shifts' [177] is one which could have significant impacts on the power system if not understood correctly.

## 10.9 Forecasting

This research has predominantly analysed the capabilities of DTRs in the network planning domain. In the operational domain, clearly meteorological

conditions will vary from those outlined in this research and in real-time, operational decisions will be required as to the scheduling of the services discussed in this thesis. Forecasting of both the meteorological conditions in order to derive conductor ratings, and also the resultant load will ensure that economic operation of the power system is improved. Services can be deferred, contracted or negated based on such forecasts.

Regarding the issue of network services, in this work where a requirement for such services has been made, these have been provided such as to reduce the conductor temperature below the circuit rated temperature however no lower. If a forecasting scheme was to be made used in conjunction with this scheme then more efficient services can be scheduled as a function of, for example availability. Forecasts of network service availability could inform the scheduling of increases services at a particular point in time in order to mitigate against a lack of available resources at a time where a conductor temperature excursion is forecast in the future.

A lack of suitable forecasting techniques has been cited as a key barrier to the implementation of RTTRs and DTRs in BaU system operation. Without such visibility, confidence in these systems is potentially below that in order to deploy these systems on a wider scale. Since the present network standard essentially uses similar methods as to that taken in this research to evaluate the level of allowable network risk, it is felt that this research has contributed towards the inclusion of such systems as more typical BaU schemes. A network operator is likely to have information as to the consumer types connected to a particular area and if typical weather data for the potential DTR site was available, an estimation of the required services for the proposed connection numbers can be made.

## **11 Conclusions**

In this research, the potential benefits of DTRs for load accommodation have been evaluated. Improvements have been shown over the present line rating standard used in the UK, in addition to improvements against the use of RTTRs. A time-series load modelling approach as opposed to those used in other studies has exposed the thermal history of the conductor, and has shown this to be important when considering the capabilities of this technique for load accommodation in particular.

### **11.1 RTTRs for Sheltered OHL sites**

Whilst this work utilises the RTTR approach of some previous work, the study of highly sheltered OHLs at this particular voltage level has not been carried out previously. This work has shown that although for certain seasonal periods at sheltered OHL sites, the observed rating can be below that of the presently used circuit ratings, there are still appreciable increases in network headroom available for around 80% of the period.

### **11.2 Presently Implemented UK Line Rating Standard**

Presently the rating of OHLs in the UK stipulates the use of single seasonal conductor ratings, with a set of a worst case scenario meteorological conditions intended to result in a minimal risk of exceeding a conductor's maximum rated temperature. This work has shown not only that there is the potential for these ratings to overstate the capacity of existing assets but also shows that RTTRs even at sheltered locations are capable of providing significant capacity increases above the existing methods with and without the need for network interventions.

The analysis presented in Chapter 4 of this thesis has examined the current UK OHL rating standard. Since no statement is made as to the method used to describe the relationship between the percentages of conductor thermal excursions and continuous line ratings a review of the line of best fit values was undertaken. Whilst small improvements have been shown over the stated values using a new approach, perhaps the most important conclusion from these findings is that these small improvements can lead to significant differences in the estimated ratings

when the approach used in [21] is used. Two OHL monitoring sites representing a sheltered and non-sheltered location were also used to assess the validity of the assumptions made in the standard. Good agreement was shown between the newly estimated circuit ratings and those derived as a result of the new line of best fit approach, whilst at the sheltered site, significant reductions in the seasonal circuit ratings were required. The effect of these potential de-ratings is unlikely to have significant effects on network operation on a day-to-day basis since both the RTTR and the nature of typical line loading is such that thermal events are unlikely. The main aspect of these findings is in the difference in the perceived level of risk which is presently thought to exist within these networks.

### **11.3 Socio-Demographic ADD Modelling**

Chapter 5 demonstrated the variability in annual energy consumption values as a function of the OAC socio-demographic classifications. The use of this socio-demographics based modelling approach has shown improvements in the modelling of ADDs for grouped loads over the use of Elexon ADD profiles.

### **11.4 Load-Temperature Relationship for Distribution Network Load groups**

The relationships between load and temperature for distribution network load groups have been shown as highly time variable and dependent upon day of week and as a function of the consumers within the load group. The use of the DBSCAN clustering algorithm has exposed the fact that these relationships for the same group are also variable depending upon the seasonal periods used in this research. A linear approximation as to this relationship has been used in this work, although in future, the potential increase in the use of air conditioning loads in the UK will likely require that these relationships be re-evaluated. The speed at which and RTTR or DTR solution can be implemented is the main rationale for investigating the present load-temperature relationships, as opposed to those predicted in various climate change scenarios.

### **11.5 Time-Series Feeder Load Modelling**

A novel temperature-sensitive method has been proposed in order to deliver accurate load group representations over time. The purpose of this modelling

strategy is to deliver load inputs to a DTR model at the MV level of distribution networks, therefore a temperature sensitive adaptation of an ADD method for load estimation was taken. For assessment at lower or higher voltage levels in the distribution network it is likely that alternate methods may result in representative models with increased performance over the generalised models and methods presented in this research.

## **11.6 Evaluation of the benefits of DTRs for Load Accommodation**

Results have been demonstrated for a sheltered test location and as such the results presented in this thesis are thought to be suitably generalised as to alternate network locations in which such a system may be implemented. RTTRs have been analysed in this research in addition to DTRs for load accommodation. As has been shown previously, significant increases in asset capacity in terms of the LOLE and EENS can be made over the presently used rating methods. The use of time-series load profiles in comparison to the real-time ambient conditions also takes into account the correlation between the demand and the asset's thermal capabilities. Where time-series load profiles are compared to the dynamically calculated behaviour of the asset the thermal history of the conductor is taken into account. Since this thermal history is not taken into account through the use of an RTTR method, improved values of EENS and LOLE have been demonstrated in this case.

The typical temporal and seasonal periods at which potential network ancillary services may be necessary to support customer connections are also exposed through the analysis of load profiles in conjunction with the DTR. These have been demonstrated as highly related to the composition of the load groups which are under investigation. The typical distributions of network service durations and magnitudes have also been examined, in addition to the typical distributions of times between the required services. This analysis aims to provide useful inputs as to the scheduling and operation of the required services.

## 12 References

- [1] "The size and performance of the UK low-carbon economy," D. f. B. I. a. Skills, Ed., ed. <https://www.gov.uk/government/publications/low-carbon-economy-size-and-performance>, 2015.
- [2] S. L. Walker, A. Hope, and E. Bentley, "Modelling steady state performance of a local electricity distribution system under UK 2050 carbon pathway scenarios," *Energy*, vol. 78, pp. 604-621, 12/15/ 2014.
- [3] M. Barnacle, E. Robertson, S. Galloway, J. Barton, and G. Ault, "Modelling generation and infrastructure requirements for transition pathways," *Energy Policy*, vol. 52, pp. 60-75, 1// 2013.
- [4] P. S. Georgilakis, "Technical challenges associated with the integration of wind power into power systems," *Renewable and Sustainable Energy Reviews*, vol. 12, pp. 852-863, 2008.
- [5] L. Xie, P. M. S. Carvalho, L. A. F. M. Ferreira, J. Liu, B. H. Krogh, N. Popli, *et al.*, "Wind integration in power systems: Operational challenges and possible solutions," *Proceedings of the IEEE*, vol. 99, pp. 214-232, 2011.
- [6] S. Eftekharnejad, V. Vittal, G. T. Heydt, B. Keel, and J. Loehr, "Impact of increased penetration of photovoltaic generation on power systems," *IEEE transactions on power systems*, vol. 28, pp. 893-901, 2013.
- [7] J. V. Paatero and P. D. Lund, "Effects of large-scale photovoltaic power integration on electricity distribution networks," *Renewable Energy*, vol. 32, pp. 216-234, 2// 2007.
- [8] P. Denholm and M. Hand, "Grid flexibility and storage required to achieve very high penetration of variable renewable electricity," *Energy Policy*, vol. 39, pp. 1817-1830, 3// 2011.
- [9] H. Holttinen, P. Meibom, A. Orths, B. Lange, M. O'Malley, J. O. Tande, *et al.*, "Impacts of large amounts of wind power on design and operation of power systems, results of IEA collaboration," *Wind Energy*, vol. 14, pp. 179-192, 2011.
- [10] N. Grid, "Future Energy Scenarios available from: <http://fes.nationalgrid.com/fes-document/>," 2016.
- [11] E. N. A. (ENA), "Engineering Recommendation P2/6—Security of Supply, ," 2006.
- [12] S. Blake, P. Davison, P. Taylor, D. Miller, and A. Webster, "Use of real time thermal ratings to support customers under faulted network conditions," in *Electricity Distribution (CIRED 2013), 22nd International Conference and Exhibition on*, 2013, pp. 1-4.
- [13] S. Blake, P. Davison, P. Taylor, D. Miller, and A. Webster, "Use of real time thermal ratings to Increase Network Reliability under Faulted Conditions," presented at the CIGRÉ Regional South-East European Conference (RSEEC 2012) Sibiu, Romania, 2012.
- [14] <https://www.ofgem.gov.uk/electricity/distribution-networks/gb-electricity-distribution-network>.
- [15] <https://www.ofgem.gov.uk/network-regulation-riio-model>.
- [16] W. Tobiasson, C. Beesterm, and T. Jamasb, "Public Engagement in Electricity Network Development: A Case Study of the Beauldy Denny Project in Scotland," 1915.
- [17] T. J. Foxon, G. P. Hammond, and P. J. G. Pearson, "Developing transition pathways for a low carbon electricity system in the UK," *Technological Forecasting and Social Change*, vol. 77, pp. 1203-1213, 2010.
- [18] J. Yi, P. Wang, P. C. Taylor, P. J. Davison, P. F. Lyons, D. Liang, *et al.*, "Distribution network voltage control using energy storage and demand side response," in *Innovative Smart Grid Technologies (ISGT Europe), 2012 3rd IEEE PES International Conference and Exhibition on*, 2012, pp. 1-8.

- [19] "Review of Engineering Recommendation P2/6 ", ed. [http://www.smarternetworks.org/NIA\\_PEA\\_PDF/NIA\\_ENWL003\\_1551.pdf](http://www.smarternetworks.org/NIA_PEA_PDF/NIA_ENWL003_1551.pdf).
- [20] M. Cotton and P. Devine-Wright, "Making electricity networks" visible": Industry actor representations of" publics" and public engagement in infrastructure planning," *Public Understanding of Science*, 2010.
- [21] E. N. A. (ENA), "Engineering Recommendation P27 – Current rating guide for high voltage overhead lines operating in the UK distribution system.," 1986.
- [22] C. F. Price, "A Statistical Approach to the Thermal Rating of Zebra Conductor based on Real Eeather Observations CERL Report No. RD/L/N 129/79," ed.
- [23] E. Fernandez, I. Albizu, M. T. Bedialauneta, A. J. Mazon, and P. T. Leite, "Review of dynamic line rating systems for wind power integration," *Renewable and Sustainable Energy Reviews*, vol. 53, pp. 80-92, 1// 2016.
- [24] D. Susa, M. Lehtonen, and H. Nordman, "Dynamic thermal modelling of power transformers," *IEEE transactions on Power Delivery*, vol. 20, pp. 197-204, 2005.
- [25] D. Susa and M. Lehtonen, "Dynamic thermal modeling of power transformers: Further development-Part II," *IEEE Transactions on Power Delivery*, vol. 21, pp. 1971-1980, 2006.
- [26] J. H. Neher and M. H. McGrath, "The calculation or the temperature rise and load capability of cable systems," *RATIO*, vol. 50, p. 5, 1994.
- [27] A. Michiorri, P. C. Taylor, and S. C. E. Jupe, "Overhead line real-time rating estimation algorithm: description and validation," *Proceedings of the Institution of Mechanical Engineers, Part A: Journal of Power and Energy*, vol. 224, pp. 293-304, 2010.
- [28] T. B. Phillips, I. Senocak, J. P. Gentle, K. S. Myers, and P. Anderson, "Investigation of a Dynamic Power Line Rating Concept for Improved Wind Energy Integration Over Complex Terrain," in *ASME 2014 4th Joint US-European Fluids Engineering Division Summer Meeting collocated with the ASME 2014 12th International Conference on Nanochannels, Microchannels, and Minichannels*, 2014, pp. V01DT39A005-V01DT39A005.
- [29] T. Yip, C. An, G. Lloyd, M. Aten, and B. Ferri, "Dynamic line rating protection for wind farm connections," in *Integration of Wide-Scale Renewable Resources Into the Power Delivery System, 2009 CIGRE/IEEE PES Joint Symposium*, 2009, pp. 1-5.
- [30] A. K. Kazerooni, J. Mutale, M. Perry, S. Venkatesan, and D. Morrice, "Dynamic thermal rating application to facilitate wind energy integration," in *PowerTech, 2011 IEEE Trondheim*, 2011, pp. 1-7.
- [31] P. B. Belben and C. D. Ziesler, "Aeolian uprating: how wind farms can solve their own transmission problems," in *Proceedings of 1st World Wind Energy Conference and Exhibition*, 2002.
- [32] H. T. Yip, C. An, G. J. Lloyd, P. Taylor, A. Michiorri, S. Jupe, *et al.*, "Dynamic thermal rating and active control for improved distribution network utilisation," in *Developments in Power System Protection (DPSP 2010). Managing the Change, 10th IET International Conference on*, 2010, pp. 1-5.
- [33] A. Michiorri, R. Currie, P. Taylor, F. Watson, and D. Macleman, "Dynamic line ratings deployment on the Orkney smart grid," in *Proceedings of the 21st International Conference on Electricity Distribution*, 2011.
- [34] R. Currie, D. Macleman, G. McLorn, and R. Sims, "Operating the orkney smart grid: Practical experience," in *Proc. 21st International Conference on Electricity Distribution, Frankfurt, Germany*, 2011.
- [35] D. M. Greenwood and P. C. Taylor, "Investigating the impact of real-time thermal ratings on power network reliability," *IEEE Transactions on Power Systems*, vol. 29, pp. 2460-2468, 2014.
- [36] D. M. Greenwood and P. C. Taylor, "Unlocking the benefits of real-time thermal ratings through probabilistic power network planning," *IET Generation, Transmission & Distribution*, vol. 8, pp. 2055-2064, 2014.

- [37] D. M. Greenwood, "Quantifying the benefits and risks of real-time thermal ratings in electrical networks," PhD, Newcastle University, 2014.
- [38] S. W. Heunis and R. Herman, "A thermal loading guide for residential distribution transformers based on time-variant current load models," *IEEE Transactions on Power Systems*, vol. 19, pp. 1294-1298, 2004.
- [39] S. Ghosh and D. Das, "Method for load-flow solution of radial distribution networks," *IEE Proceedings - Generation, Transmission and Distribution*, vol. 146, pp. 641-648, 1999.
- [40] G. P. Harrison and A. R. Wallace, "Optimal power flow evaluation of distribution network capacity for the connection of distributed generation," *IEE Proceedings - Generation, Transmission and Distribution*, vol. 152, pp. 115-122, 2005.
- [41] M. Meldorf, U. Treufeldt, and J. Kilter, "Temperature dependency of electrical network load," *Oil Shale*, vol. 24, pp. 237-247, 2007.
- [42] H. S. Hippert, C. E. Pedreira, and R. C. Souza, "Neural networks for short-term load forecasting: a review and evaluation," *IEEE Transactions on Power Systems*, vol. 16, pp. 44-55, 2001.
- [43] R. F. Engle, C. W. J. Granger, J. Rice, and A. Weiss, "Semiparametric Estimates of the Relation between Weather and Electricity Sales," *Journal of the American Statistical Association*, vol. 81, pp. 310-320, 1986/06/01 1986.
- [44] E. Valor, V. Meneu, and V. Caselles, "Daily Air Temperature and Electricity Load in Spain," *Journal of Applied Meteorology*, vol. 40, pp. 1413-1421, 2001/08/01 2001.
- [45] A. Pardo, V. Meneu, and E. Valor, "Temperature and seasonality influences on Spanish electricity load," *Energy Economics*, vol. 24, pp. 55-70, 1// 2002.
- [46] D. J. Sailor and J. R. Muñoz, "Sensitivity of electricity and natural gas consumption to climate in the USA—methodology and results for eight states," *Energy*, vol. 22, pp. 987-998, 1997.
- [47] C. Tumelo-Chakonta and K. Kopsidas, "Assessing the value of employing dynamic thermal rating on system-wide performance," in *Innovative Smart Grid Technologies (ISGT Europe), 2011 2nd IEEE PES International Conference and Exhibition on*, 2011, pp. 1-8.
- [48] K. Kopsidas, "Impact of thermal uprating and emergency loading of OHL networks on interconnection flexibility," in *2016 18th Mediterranean Electrotechnical Conference (MELECON)*, 2016, pp. 1-6.
- [49] J. P. Barton and D. G. Infield, "Energy storage and its use with intermittent renewable energy," *IEEE transactions on energy conversion*, vol. 19, pp. 441-448, 2004.
- [50] A. Keane, A. Tuohy, P. Meibom, E. Denny, D. Flynn, A. Mullane, *et al.*, "Demand side resource operation on the Irish power system with high wind power penetration," *Energy Policy*, vol. 39, pp. 2925-2934, 5// 2011.
- [51] A. Ipakchi and F. Albuyeh, "Grid of the future," *IEEE Power and Energy Magazine*, vol. 7, pp. 52-62, 2009.
- [52] G. Strbac, "Demand side management: Benefits and challenges," *Energy Policy*, vol. 36, pp. 4419-4426, 12// 2008.
- [53] A. S. Masoum, S. Deilami, P. S. Moses, M. A. S. Masoum, and A. Abu-Siada, "Smart load management of plug-in electric vehicles in distribution and residential networks with charging stations for peak shaving and loss minimisation considering voltage regulation," *IET Generation, Transmission & Distribution*, vol. 5, pp. 877-888, 2011.
- [54] H. Devine-Wright and P. Devine-Wright, "From demand-side management to demand-side participation: Tracing an environmental psychology of sustainable electricity system evolution," *Journal of Applied Psychology*, vol. 6, pp. 167-177, 2005.
- [55] Ofgem, "Circumstances in which DNOs will use DSR," 2014.
- [56] IEC, "IEC 60287 Electric cables — Calculation of the current rating", ed, 1994.

- [57] C. International Electrotechnical, "IEC 60076-7 Power transformers Part 7: Loading guide for oil-immersed power transformers," ed: December, 2005.
- [58] ENA, "ER P17 Current ratings for distribution cables Part 2: Solid type cables for 33 kV " 1976.
- [59] ENA, "ER P17 Current ratings for distribution cables Part 3: Ratings for 11 kV and 33 kV cables having extruded insulation " 2004.
- [60] ENA, "ER P17 Part 1 Current ratings for distribution cables Part 1: Cables for 11 kV " 1976.
- [61] ENA, "ER P15 Transformers loading guide - a guide to the loading of double-wound transformers having nominal ratings of 120MVA and below. Supplying systems at 66kV and below the supergrid and 132kV system, (See ACE 31, 1973) " 1971.
- [62] C. F. Price and R. R. Gibbon, "Statistical approach to thermal rating of overhead lines for power transmission and distribution," *IEE Proceedings C - Generation, Transmission and Distribution*, vol. 130, pp. 245-256, 1983.
- [63] J. Gentle, K. Myers, T. Baldwin, I. West, K. Hart, B. Savage, *et al.*, "Concurrent wind cooling in power transmission lines," in *Western Energy Policy Research Conf*, 2012.
- [64] D. A. Douglass, D. C. Lawry, A. A. Edris, and E. C. Bascom, "Dynamic thermal ratings realize circuit load limits," *IEEE Computer Applications in Power*, vol. 13, pp. 38-44, 2000.
- [65] IEEE, "IEEE Standard for Calculating the Current-Temperature of Bare Overhead Conductors, IEEE Std. 738-2006, ," 2006.
- [66] IEC, "IEC 61597 - Overhead Electrical Conductors - Calculation methods for stranded bare conductors " 1995.
- [67] C. W. 22.12, "The thermal behaviour of overhead conductors," *Electra*, vol. 144, pp. 107-125, October 1992 1992.
- [68] A. Michiorri, P. C. Taylor, S. C. E. Jupe, and C. J. Berry, "Investigation into the influence of environmental conditions on power system ratings," *Proceedings of the Institution of Mechanical Engineers, Part A: Journal of Power and Energy*, vol. 223, pp. 743-757, 2009.
- [69] N. P. Schmidt, "Comparison between IEEE and CIGRE ampacity standards," *IEEE Transactions on Power Delivery*, vol. 14, pp. 1555-1559, 1999.
- [70] V. T. Morgan, "Effect of elevated temperature operation on the tensile strength of overhead conductors," *IEEE Transactions on Power Delivery*, vol. 11, pp. 345-352, 1996.
- [71] K. Kopsidas, S. M. Rowland, and B. Boumeid, "A Holistic Method for Conductor Ampacity and Sag Computation on an OHL Structure," *IEEE Transactions on Power Delivery*, vol. 27, pp. 1047-1054, 2012.
- [72] M. W. Davis, "A new thermal rating approach: The real time thermal rating system for strategic overhead conductor transmission lines--Part I: General description and justification of the real time thermal rating system," *IEEE Transactions on Power Apparatus and Systems*, vol. 96, pp. 803-809, 1977.
- [73] M. W. Davis, "A new thermal rating approach: The real time thermal rating system for strategic overhead conductor transmission lines--Part II: Steady state thermal rating program," *IEEE Transactions on Power Apparatus and Systems*, vol. 96, pp. 810-825, 1977.
- [74] W. Z. Black and W. R. Byrd, "Real-time ampacity model for overhead lines," *IEEE Transactions on Power Apparatus and Systems*, pp. 2289-2293, 1983.
- [75] V. T. Morgan, "The radial temperature distribution and effective radial thermal conductivity in bare solid and stranded conductors," *IEEE Transactions on Power Delivery*, vol. 5, pp. 1443-1452, 1990.
- [76] V. T. Morgan, "Rating of bare overhead conductors for continuous currents," in *Proceedings of the Institution of Electrical Engineers*, 1967, pp. 1473-1482.

- [77] V. T. Morgan, "The thermal rating of overhead-line conductors Part I. The steady-state thermal model," *Electric Power Systems Research*, vol. 5, pp. 119-139, 1982/06/01 1982.
- [78] S. C. E. Jupe, M. Bartlett, and K. Jackson, "Dynamic thermal ratings: the state of the art," in *21st Int. Conf. on Electricity Distribution (CIRED)*, 2011.
- [79] R. Bernardo, A. Coelho, N. Diogo, and E. D. P. Distribuição–Portugal, "Increasing the operation efficiency of EDP DISTRIBUIÇÃO overhead power lines," in *Proceedings of the 21st international conference and exhibition on electricity distribution (CIRED 2011). Frankfurt*, 2011.
- [80] D. Roberts, P. Taylor, and A. Michiorri, "Dynamic thermal rating for increasing network capacity and delaying network reinforcements," in *SmartGrids for Distribution, 2008. IET-CIRED. CIRED Seminar*, 2008, pp. 1-4.
- [81] P. M. Callahan and D. A. Douglass, "An experimental evaluation of a thermal line uprating by conductor temperature and weather monitoring," *IEEE Transactions on Power Delivery*, vol. 3, pp. 1960-1967, 1988.
- [82] S. D. Foss and R. A. Maraio, "Dynamic line rating in the operating environment," *IEEE Transactions on power Delivery*, vol. 5, pp. 1095-1105, 1990.
- [83] F. R. McElvain and S. S. Mulnix, "Statistically determined static thermal ratings of overhead high voltage transmission lines in the Rocky Mountain region," *IEEE Transactions on Power Systems*, vol. 15, pp. 899-902, 2000.
- [84] S. D. Foss, S. H. Lin, H. R. Stillwell, and R. A. Fernandes, "Dynamic Thermal Line Ratings Part II Conductor Temperature Sensor and Laboratory Field test Evaluation," *IEEE Transactions on Power Apparatus and Systems*, pp. 1865-1876, 1983.
- [85] "[http://www.nexans.us/eservice/US-en\\_US/fileLibrary/Download\\_540172710/US/files/CAT-1\\_Brochure1.pdf](http://www.nexans.us/eservice/US-en_US/fileLibrary/Download_540172710/US/files/CAT-1_Brochure1.pdf)," (Accessed 5 September 2016).
- [86] P. Schell, B. Godard, J.-L. Lilien, H.-M. Nguyen, V. De Wilde, O. Durieux, *et al.*, "Large penetration of distributed productions: Dynamic line rating and flexible generation, a must regarding investment strategy and network reliability," in *Integration of Renewables into the Distribution Grid, CIRED 2012 Workshop*, 2012, pp. 1-5.
- [87] P. Schell, H. M. Nguyen, and J.-L. Lilien, "Quantifying the limits of weather based dynamic line rating methods," in *CIGRE Canada Conference on Power Systems, Halifax (Canada)*, 2011.
- [88] P. Schell, J.-J. Lambin, B. Godard, H.-M. Nguyen, and J.-L. Lilien, "Using Dynamic Line Rating to minimize curtailment of Wind power connected to rural power networks," in *Proceedings of the 10th International Workshop on Large-Scale Integration of Wind Power into Power Systems*, 2011, p. 5.
- [89] C. Mensah-Bonsu, U. Fernandez, G. T. Heydt, Y. Hoverson, J. Schilleci, and B. Agrawal, "Application of the Global Positioning System to the Measurement of Overhead Power Transmission Conductor Sag," *IEEE Power Engineering Review*, vol. 21, pp. 64-64, 2001.
- [90] S. C. E. Jupe, "Active Management of Distributed Generation based on Component Thermal Properties," Durham University, 2010.
- [91] S. Jupe, G. Murphy, and A. K. Kazerooni, "De-risking the implementation of real-time thermal ratings," in *Electricity Distribution (CIRED 2013), 22nd International Conference and Exhibition on*, 2013, pp. 1-4.
- [92] C. J. Wallnerstr, x00F, P. Hilber, S. P, x00F, derstr, *et al.*, "Potential of dynamic rating in Sweden," in *Probabilistic Methods Applied to Power Systems (PMAPS), 2014 International Conference on*, 2014, pp. 1-6.
- [93] M. Z. Degefa, M. Humayun, A. Safdarian, M. Koivisto, R. J. Millar, and M. Lehtonen, "Unlocking distribution network capacity through real-time thermal

- rating for high penetration of DGs," *Electric Power Systems Research*, vol. 117, pp. 36-46, 12// 2014.
- [94] A. Michiorri, H.-M. Nguyen, S. Alessandrini, J. B. Bremnes, S. Dierer, E. Ferrero, *et al.*, "Forecasting for dynamic line rating," *Renewable and Sustainable Energy Reviews*, vol. 52, pp. 1713-1730, 12// 2015.
- [95] A. Michiorri and P. C. Taylor, "Forecasting real-time ratings for electricity distribution networks using weather forecast data," in *Electricity Distribution-Part 1, 2009. CIRED 2009. 20th International Conference and Exhibition on*, 2009, pp. 1-4.
- [96] L. M. Chittock, D. Strickland, and C. Harrap, "Weather forecasting to predict practical dynamic asset rating of overhead lines," in *IET International Conference on Resilience of Transmission and Distribution Networks (RTDN) 2015*, 2015, pp. 1-6.
- [97] P. Schell, L. Jones, P. Mack, B. Godard, and J. L. Lilien, "Dynamic prediction of energy delivery capacity of power networks: Unlocking the value of real-time measurements," in *2012 IEEE PES Innovative Smart Grid Technologies (ISGT)*, 2012, pp. 1-6.
- [98] H.-M. Nguyen, J.-L. Lilien, and P. Schell, "Dynamic line rating and ampacity forecasting as the keys to optimise power line assets with the integration of res. The European project Twenties Demonstration inside Central Western Europe," in *Electricity Distribution (CIRED 2013), 22nd International Conference and Exhibition on*, 2013, pp. 1-4.
- [99] (2011, 5 September 2016). *UKCP09 see: <http://ukclimateprojections.metoffice.gov.uk/>.*
- [100] L. C. Cradden and G. P. Harrison, "Adapting overhead lines to climate change: Are dynamic ratings the answer?," *Energy Policy*, vol. 63, pp. 197-206, 12// 2013.
- [101] B. Simon, D. Peter, G. David, and W. Neal, "Climate change risks in electricity networks," *Infrastructure Asset Management*, vol. 2, pp. 42-51, 2015.
- [102] P. Davison, "CLNR Trial Analysis EHV and HV Real-Time Thermal Rating Trials," 2014.
- [103] C. F. Price and R. R. Gibbon, "Statistical approach to thermal rating of overhead lines for power transmission and distribution," *Generation, Transmission and Distribution, IEE Proceedings C*, vol. 130, pp. 245-256, 1983.
- [104] R. F. M. Aten, T. Yip, C. An, G. Lloyd, "Field Measurements Analysis for Dynamic Line Rating," presented at the 21st International Conference on Electricity Distribution (CIRED 2011), 2011.
- [105] R. A. Bush, W. Z. Black, T. C. Champion, and W. R. Byrd, "Experimental Verification of a Real-Time Program for the Determination of Temperature and SAG of Overhead Lines," *IEEE Transactions on Power Apparatus and Systems*, vol. PAS-102, pp. 2284-2288, 1983.
- [106] <https://www.gegridsolutions.com/multilin/catalog/fmc.htm>.
- [107] M. Matus, D. Sáez, M. Favley, C. Suazo-Martínez, J. Moya, G. Jiménez-Estévez, *et al.*, "Identification of critical spans for monitoring systems in dynamic thermal rating," *IEEE Transactions on Power Delivery*, vol. 27, pp. 1002-1009, 2012.
- [108] "IMP/001/011 – Code of Practice for Guidance on the Selection of Overhead Line Ratings," <http://www.northernpowergrid.com/asset/0/document/1887.pdf2015>.
- [109] E. N. Association, "ACE Report 104 Report on the Derivation of Overhead Line Ratings Applicable to High Voltage Distribution Systems," 1986.
- [110] I. Richardson, M. Thomson, D. Infield, and C. Clifford, "Domestic electricity use: A high-resolution energy demand model," *Energy and Buildings*, vol. 42, pp. 1878-1887, 2010.
- [111] I. Hernando Gil, Li, F., Collin, A. and Djokic, S. Z. , "Development of Sub-Transmission Network Equivalentents and After-Diversity-Demand Values: Case

- Study of the UK Residential Sector," in *18th Mediterranean Electrotechnical Conference (MELECON)*, 2016.
- [112] "[http://ukedc.rl.ac.uk/cgi-bin/edc\\_search.pl?GoButton=Detail&WantComp=42&WantResult=&WantText=EDC0000041](http://ukedc.rl.ac.uk/cgi-bin/edc_search.pl?GoButton=Detail&WantComp=42&WantResult=&WantText=EDC0000041)."
- [113] Available at: <https://www.elexon.co.uk/reference/technical-operations/profiling/>.
- [114] "Postcode level electricity estimates: 2013 (experimental)," DECC, Ed., ed, 2015.
- [115] "Regional and local authority electricity consumption statistics: 2005 to 2014," DECC, Ed., ed.
- [116] D. Vickers and P. Rees, "Creating the UK National Statistics 2001 output area classification," *Journal of the Royal Statistical Society: Series A (Statistics in Society)*, vol. 170, pp. 379-403, 2007.
- [117] A. Druckman, P. Sinclair, and T. Jackson, "A geographically and socio-economically disaggregated local household consumption model for the UK," *Journal of Cleaner Production*, vol. 16, pp. 870-880, 5// 2008.
- [118] A. Druckman and T. Jackson, "Household energy consumption in the UK: A highly geographically and socio-economically disaggregated model," *Energy Policy*, vol. 36, pp. 3177-3192, 2008.
- [119] M. J. Lawson, P. C. Taylor, S. Bell, D. Miller, and N. S. Wade, "An interdisciplinary method to demand side participation for deferring distribution network reinforcement," in *Innovative Smart Grid Technologies (ISGT Europe), 2011 2nd IEEE PES International Conference and Exhibition on*, 2011, pp. 1-8.
- [120] C. Barteczko-Hibbert, "After Diversity Maximum Demand Report available at: <http://www.networkrevolution.co.uk/wp-content/uploads/2015/02/After-Diversity-Maximum-Demand-Insight-Report.pdf>," 2015.
- [121] A. Henley and J. Peirson, "Non-Linearities in Electricity Demand and Temperature: Parametric Versus Non-Parametric Methods," *Oxford Bulletin of Economics and Statistics*, vol. 59, pp. 149-162, 1997.
- [122] A. Henley and J. Peirson, "Residential energy demand and the interaction of price and temperature: British experimental evidence," *Energy Economics*, vol. 20, pp. 157-171, 1998.
- [123] S. Ruzic, A. Vuckovic, and N. Nikolic, "Weather sensitive method for short term load forecasting in electric power utility of Serbia," *IEEE Transactions on Power Systems*, vol. 18, pp. 1581-1586, 2003.
- [124] G. T. Heinemann, D. A. Nordman, and E. C. Plant, "The Relationship Between Summer Weather and Summer Loads - A Regression Analysis," *IEEE Transactions on Power Apparatus and Systems*, vol. PAS-85, pp. 1144-1154, 1966.
- [125] C. J. Wallnerström, J. Setréus, P. Hilber, F. Tong, and L. Bertling, "Model of capacity demand under uncertain weather," in *Probabilistic Methods Applied to Power Systems (PMAPS), 2010 IEEE 11th International Conference on*, 2010, pp. 314-318.
- [126] M. L. C. Douglas and E. W. Henry, "Modeling the Impact of Summer Temperatures on National Electricity Consumption," *Journal of Applied Meteorology*, vol. 20, pp. 1415-1419, 1981.
- [127] M. S. Owayedh, A. A. Al-Bassam, and Z. R. Khan, "Identification of temperature and social events effects on weekly demand behavior," in *Power Engineering Society Summer Meeting, 2000. IEEE*, 2000, pp. 2397-2402.
- [128] V. Dordonnat, S. J. Koopman, M. Ooms, A. Dessertaine, and J. Collet, "An hourly periodic state space model for modelling French national electricity load," *International Journal of Forecasting*, vol. 24, pp. 566-587, 10// 2008.
- [129] V. Bianco, O. Manca, and S. Nardini, "Electricity consumption forecasting in Italy using linear regression models," *Energy*, vol. 34, pp. 1413-1421, 9// 2009.
- [130] C. E. Asbury, "Weather load model for electric demand and energy forecasting," *IEEE Transactions on Power Apparatus and Systems*, vol. 94, pp. 1111-1116, 1975.

- [131] H. Ching-Lai, S. J. Watson, and S. Majithia, "Analyzing the impact of weather variables on monthly electricity demand," *IEEE Transactions on Power Systems*, vol. 20, pp. 2078-2085, 2005.
- [132] A. D. Papalexopoulos and T. C. Hesterberg, "A regression-based approach to short-term system load forecasting," *IEEE Transactions on Power Systems*, vol. 5, pp. 1535-1547, 1990.
- [133] M. Hekkenberg, H. C. Moll, and A. J. M. S. Uiterkamp, "Dynamic temperature dependence patterns in future energy demand models in the context of climate change," *Energy*, vol. 34, pp. 1797-1806, 11// 2009.
- [134] J. Moral-Carcedo and J. Vicens-Otero, "Modelling the non-linear response of Spanish electricity demand to temperature variations," *Energy economics*, vol. 27, pp. 477-494, 2005.
- [135] S. M. Moghaddas-Tafreshi and Mahdi, "A linear regression-based study for temperature sensitivity analysis of Iran electrical load," in *Industrial Technology, 2008. ICIT 2008. IEEE International Conference on*, 2008, pp. 1-7.
- [136] L. Hernández, C. Baladrón, J. M. Aguiar, L. Calavia, B. Carro, A. Sánchez-Esguevillas, *et al.*, "A Study of the Relationship between Weather Variables and Electric Power Demand inside a Smart Grid/Smart World Framework," *Sensors*, vol. 12, p. 11571, 2012.
- [137] F. Tong, "Capacity demand and climate in Ekerö: Development of tool to predict capacity demand under uncertainty of climate effects," 2007.
- [138] S. Avdakovic, A. Ademovic, and A. Nuhanovic, "Correlation between air temperature and electricity demand by linear regression and wavelet coherence approach: UK, Slovakia and Bosnia and Herzegovina case study," in *Archives of Electrical Engineering* vol. 62, ed, 2013, p. 521.
- [139] J. W. Taylor and R. Buizza, "Neural network load forecasting with weather ensemble predictions," *IEEE Transactions on Power Systems*, vol. 17, pp. 626-632, 2002.
- [140] E. G. Contaxi and S. Kavatza, "Application of a weather-sensitive peak load forecasting model to the Hellenic system," in *Electrotechnical Conference, 2004. MELECON 2004. Proceedings of the 12th IEEE Mediterranean*, 2004, pp. 819-822 Vol.3.
- [141] S. T. Chen, D. C. Yu, and A. R. Moghaddamjo, "Weather sensitive short-term load forecasting using nonfully connected artificial neural network," *IEEE Transactions on Power Systems*, vol. 7, pp. 1098-1105, 1992.
- [142] A. P. Douglas, A. M. Breipohl, F. N. Lee, and R. Adapa, "The impacts of temperature forecast uncertainty on Bayesian load forecasting," *IEEE Transactions on Power Systems*, vol. 13, pp. 1507-1513, 1998.
- [143] D. K. Ranaweera, G. G. Karady, and R. G. Farmer, "Effect of probabilistic inputs on neural network-based electric load forecasting," *IEEE Transactions on Neural Networks*, vol. 7, pp. 1528-1532, 1996.
- [144] C. J. Ziser, Z. Y. Dong, and T. K. Saha, "Investigation of weather dependency and load diversity on queensland electricity demand," in *Australasian Universities Power Engineering Conference 2005*, 2005, pp. 457-462.
- [145] M. Ester, H.-P. Kriegel, J. Sander, and X. Xu, "Density-based spatial clustering of applications with noise-DBSCAN," in *Proceedings of 2nd International Conference on Knowledge Discovery and Data Mining (KDD-96)*, 1996, pp. 226-231.
- [146] V. Satopaa, J. Albrecht, D. Irwin, and B. Raghavan, "Finding a "Kneedle" in a Haystack: Detecting Knee Points in System Behavior," in *Distributed Computing Systems Workshops (ICDCSW), 2011 31st International Conference on*, 2011, pp. 166-171.
- [147] (07/09/2016). <http://www.metoffice.gov.uk/public/weather/climate-extremes/#?tab=climateExtremes>.

- [148] J. Eynard, S. Grieu, and M. Polit, "Wavelet-based multi-resolution analysis and artificial neural networks for forecasting temperature and thermal power consumption," *Engineering Applications of Artificial Intelligence*, vol. 24, pp. 501-516, 4// 2011.
- [149] F. Apadula, A. Bassini, A. Elli, and S. Scapin, "Relationships between meteorological variables and monthly electricity demand," *Applied Energy*, vol. 98, pp. 346-356, 10// 2012.
- [150] R. Kohavi, "A study of cross-validation and bootstrap for accuracy estimation and model selection," in *Ijcai*, 1995, pp. 1137-1145.
- [151] G. G. Pillai, G. A. Putrus, and N. M. Pearsall, "Generation of synthetic benchmark electrical load profiles using publicly available load and weather data," *International Journal of Electrical Power & Energy Systems*, vol. 61, pp. 1-10, 10// 2014.
- [152] C. S. Chen, M. S. Kang, J. C. Hwang, and C. W. Huang, "Synthesis of power system load profiles by class load study," *International Journal of Electrical Power & Energy Systems*, vol. 22, pp. 325-330, 6// 2000.
- [153] W. Charytoniuk, M. S. Chen, P. Kotas, and P. V. Olinda, "Demand forecasting in power distribution systems using nonparametric probability density estimation," *IEEE Transactions on Power Systems*, vol. 14, pp. 1200-1206, 1999.
- [154] D. He, T. Habetler, M. J. Mousavi, and N. Kang, "A ZIP model-based feeder load modeling and forecasting method," in *2013 IEEE Power & Energy Society General Meeting*, 2013, pp. 1-5.
- [155] S. L. Corpening, N. D. Reppen, and R. J. Ringlee, "Experience with Weather Sensitive Load Models for Short and Long-Term Forecasting," *IEEE Transactions on Power Apparatus and Systems*, vol. PAS-92, pp. 1966-1972, 1973.
- [156] ELEXON,  
["http://data.ukedc.rl.ac.uk/simplebrowse/edc/efficiency/residential/LoadProfile."](http://data.ukedc.rl.ac.uk/simplebrowse/edc/efficiency/residential/LoadProfile)  
 ed.
- [157] D. Shi, R. Li, R. Shi, and F. Li, "Analysis of the relationship between load profile and weather condition," in *2014 IEEE PES General Meeting | Conference & Exposition*, 2014, pp. 1-5.
- [158] B. F. Hobbs, S. Jitprapaikulsarn, S. Konda, V. Chankong, K. A. Loparo, and D. J. Maratukulam, "Analysis of the value for unit commitment of improved load forecasts," *IEEE Transactions on Power Systems*, vol. 14, pp. 1342-1348, 1999.
- [159] A. Mutanen, M. Ruska, S. Repo, and P. Jarventausta, "Customer classification and load profiling method for distribution systems," *IEEE Transactions on Power Delivery*, vol. 26, pp. 1755-1763, 2011.
- [160] G. Chicco, "Overview and performance assessment of the clustering methods for electrical load pattern grouping," *Energy*, vol. 42, pp. 68-80, 6// 2012.
- [161] G. Chicco, R. Napoli, and F. Piglione, "Application of clustering algorithms and self organising maps to classify electricity customers," in *Power Tech Conference Proceedings, 2003 IEEE Bologna*, 2003, p. 7 pp. Vol.1.
- [162] G. Chicco, R. Napoli, F. Piglione, P. Postolache, M. Scutariu, and C. Toader, "Comparisons among clustering techniques for electricity customer classification," *IEEE TRANSACTIONS ON POWER SYSTEMS PWRS*, vol. 21, p. 933, 2006.
- [163] B. Stephen, A. J. Mutanen, S. Galloway, G. Burt, J. P. x00E, *et al.*, "Enhanced Load Profiling for Residential Network Customers," *IEEE Transactions on Power Delivery*, vol. 29, pp. 88-96, 2014.
- [164] R. Li, C. Gu, F. Li, G. Shaddick, and M. Dale, "Development of Low Voltage Network Templates&#x2014;Part I: Substation Clustering and Classification," *IEEE Transactions on Power Systems*, vol. 30, pp. 3036-3044, 2015.
- [165] V. Rigoni, L. F. Ochoa, G. Chicco, A. Navarro-Espinosa, and T. Gozel, "Representative Residential LV Feeders: A Case Study for the North West of England," *IEEE Transactions on Power Systems*, vol. 31, pp. 348-360, 2016.

- [166] G. J. Tsekouras, N. D. Hatziaargyriou, and E. N. Dialynas, "Two-Stage Pattern Recognition of Load Curves for Classification of Electricity Customers," *IEEE Transactions on Power Systems*, vol. 22, pp. 1120-1128, 2007.
- [167] "National Grid Electricity Ten Year Statement available at: <http://www2.nationalgrid.com/UK/Industry-information/Future-of-Energy/Electricity-Ten-Year-Statement/>," 2015.
- [168] "Available at: [https://www.elexon.co.uk/wp-content/uploads/2016/02/BSCP516\\_v10.0.pdf](https://www.elexon.co.uk/wp-content/uploads/2016/02/BSCP516_v10.0.pdf)."
- [169] K. Buchanan, N. Banks, I. Preston, and R. Russo, "The British public's perception of the UK smart metering initiative: Threats and opportunities," *Energy Policy*, vol. 91, pp. 87-97, 4// 2016.
- [170] M. J. Fell, D. Shipworth, G. M. Huebner, and C. A. Elwell, "Exploring perceived control in domestic electricity demand-side response," *Technology Analysis & Strategic Management*, vol. 26, pp. 1118-1130, 2014/11/26 2014.
- [171] V. Hamidi, F. Li, and F. Robinson, "Demand response in the UK's domestic sector," *Electric Power Systems Research*, vol. 79, pp. 1722-1726, 12// 2009.
- [172] P. Palensky and D. Dietrich, "Demand Side Management: Demand Response, Intelligent Energy Systems, and Smart Loads," *IEEE Transactions on Industrial Informatics*, vol. 7, pp. 381-388, 2011.
- [173] *Common Distribution Charging Methodology available from: <https://www.ofgem.gov.uk/electricity/distribution-networks/charging-arrangements>.*
- [174] S. C. E. Jupe, P. C. Taylor, and A. Michiorri, "Coordinated output control of multiple distributed generation schemes," *IET Renewable Power Generation*, vol. 4, pp. 283-297, 2010.
- [175] S. Haben, M. Rowe, D. V. Greetham, P. Grindrod, W. Holderbaum, B. Potter, *et al.*, "Mathematical solutions for electricity networks in a low carbon future," in *Electricity Distribution (CIRED 2013), 22nd International Conference and Exhibition on*, 2013, pp. 1-4.
- [176] D. S. Kirschen, "Demand-side view of electricity markets," *IEEE Transactions on Power Systems*, vol. 18, pp. 520-527, 2003.
- [177] G. Powells, H. Bulkeley, S. Bell, and E. Judson, "Peak electricity demand and the flexibility of everyday life," *Geoforum*, vol. 55, pp. 43-52, 8// 2014.

## Appendix 1 – OAC Annual Consumption Values

### OAC Group Energy Consumption Statistics

OAC Group Classification	Class 1 Energy Consumption (kWh)	Class 2 Energy Consumption (kWh)
Elexon Profile	3915	6929
1a	4980.712	8814.987
1b	4472.885	7916.222
1c	4666.919	8259.629
2a	3349.828	5928.609
2b	3692.962	6535.896
2c	3061.061	5417.541
2d	3859.308	6830.299
3a	3074.9	5442.034
3b	2860.637	5062.826
3c	2798.154	4952.243
3d	3228.361	5713.632
4a	3197.924	5659.765
4b	3242.586	5738.809
4c	3666.15	6488.444
5a	3374.314	5971.944
5b	3726.25	6594.81
6a	4200.52	7434.184
6b	3567.611	6314.047
7a	3000.593	5310.524
7b	2612.166	4623.076
7c	2962.035	5242.284
7d	2804.238	4963.01
8a	3380.13	5982.238
8b	3228.115	5713.199
8c	3283.555	5811.317
8d	3290.473	5823.56

## Subgroup OAC Energy Consumption Statistics

OAC Subgroup Classification	Class 1 Energy Consumption (kWh)	Class 2 Energy Consumption (kWh)
Elexon Profile	3915	6929
1a1	4912.028	8693.43
1a2	5182.946	9172.907
1a3	5191.55	9188.133
1a4	4114.837	7282.541
1b1	4096.718	7250.473
1b2	5007.776	8862.885
1b3	4153.226	7350.481
1c1	5249.413	9290.541
1c2	4172.318	7384.271
1c3	4676.524	8276.628
2a1	3826.195	6771.694
2a2	3419.06	6051.138
2a3	3216.806	5693.182
2b1	2953.745	5227.611
2b2	4173.001	7385.48
2c1	3232.529	5721.009
2c2	2628.151	4651.366
2c3	2971.742	5259.462
2d1	3716.056	6576.768
2d2	3912.423	6924.303
2d3	3925.721	6947.839
3a1	2994.218	5299.241
3a2	3173.497	5616.534
3b1	2722.817	4818.91
3b2	2739.99	4849.303
3b3	3141.038	5559.087
3c1	2865.18	5070.866
3c2	2455.169	4345.219
3d1	3268.399	5784.493

3d2	3258.57	5767.098
3d3	3159.888	5592.449
4a1	3198.319	5660.464
4a2	3088.931	5466.867
4a3	3334.208	5900.964
4b1	3296.98	5835.077
4b2	3171.592	5613.161
4c1	3626.4	6418.092
4c2	3603.833	6378.152
4c3	3751.219	6639
5a1	3348.638	5926.503
5a2	3572.449	6322.608
5a3	3207.505	5676.721
5b1	4097.633	7252.092
5b2	3721.613	6586.602
5b3	3520.17	6230.083
6a1	4643.811	8218.732
6a2	4294.911	7601.24
6a3	3835.051	6787.369
6a4	4311.323	7630.286
6b1	3622.361	6410.944
6b2	3644.301	6449.775
6b3	3433.381	6076.483
6b4	3578.83	6333.902
7a1	3034.552	5370.625
7a2	2992.166	5295.61
7a3	2991.492	5294.416
7b1	2682.381	4747.344
7b2	2578.633	4563.729
7b3	2584.334	4573.819
7c1	2930.328	5186.167
7c2	2978.968	5272.25
7c3	2974.196	5263.805
7d1	2877.216	5092.169
7d2	2495.34	4416.314

7d3	2990.351	5292.396
7d4	2412.542	4269.776
8a1	3409.594	6034.383
8a2	3335.479	5903.214
8b1	3173.606	5616.727
8b2	3308.648	5855.728
8c1	3294.072	5829.93
8c2	3391.614	6002.562
8c3	3175.496	5620.071
8d1	3317.482	5871.362
8d2	3302.454	5844.766
8d3	3228.756	5714.331

## Appendix 2 - Correlation Sensitivity Coefficients

	Class 1 CSC			Class 2 CSC		
	W	Sa	Su	W	Sa	Su
00:30	-0.3773	-0.2586	-0.2859	-0.5567	-0.9740	-0.5462
01:00	-0.4064	-0.2972	-0.2908	-0.3519	-0.4045	-0.4159
01:30	-0.4332	-0.3067	-0.2910	-0.2488	-0.2637	-0.3766
02:00	-0.4610	-0.3449	-0.2903	-0.2424	-0.2214	-0.3558
02:30	-0.5018	-0.3949	-0.3220	-0.2471	-0.2285	-0.3690
03:00	-0.5122	-0.4230	-0.3316	-0.2678	-0.2553	-0.4142
03:30	-0.5118	-0.4274	-0.3273	-0.3059	-0.2914	-0.4783
04:00	-0.5304	-0.4378	-0.3097	-0.3815	-0.3226	-0.5026
04:30	-0.5311	-0.4507	-0.3193	-0.4695	-0.3249	-0.4918
05:00	-0.5257	-0.4587	-0.3266	-0.5727	-0.2781	-0.4822
05:30	-0.5442	-0.4711	-0.3319	-0.6251	-0.2371	-0.4665
06:00	-0.5498	-0.4859	-0.3593	-0.6243	-0.2080	-0.3931
06:30	-0.5532	-0.4870	-0.4220	-0.5644	-0.2281	-0.3033
07:00	-0.5441	-0.4826	-0.4718	-0.5767	-0.3098	-0.2081
07:30	-0.5628	-0.5102	-0.4916	-0.6196	-0.3514	-0.1594
08:00	-0.5919	-0.5120	-0.5340	-0.6516	-0.4192	-0.0548
08:30	-0.6026	-0.5316	-0.5724	-0.9053	-0.4459	0.0149
09:00	-0.6148	-0.5862	-0.5834	-1.3193	-0.0818	0.0591
09:30	-0.6501	-0.6122	-0.5783	-1.3906	0.1004	-0.0768
10:00	-0.6555	-0.5908	-0.6035	-1.5247	-0.0106	-0.0325
10:30	-0.6780	-0.6135	-0.6477	-1.2691	0.1131	0.2959
11:00	-0.6932	-0.6081	-0.6462	-0.9748	-0.0842	0.2821
11:30	-0.6899	-0.5614	-0.6511	-1.0433	-0.4663	0.3252
12:00	-0.6713	-0.5315	-0.6694	-1.1494	-0.6811	0.4897
12:30	-0.6644	-0.5426	-0.7099	-1.2326	-0.6353	0.6120
13:00	-0.6328	-0.5220	-0.6999	-1.6237	-0.8826	0.3200
13:30	-0.6301	-0.5372	-0.7242	-1.9418	-0.5957	0.4939
14:00	-0.6201	-0.5626	-0.7186	-2.0530	-0.6063	0.4040
14:30	-0.6454	-0.5621	-0.7096	-1.7371	-0.6568	0.0924
15:00	-0.6562	-0.5865	-0.6808	-1.6500	-0.5592	-0.0454
15:30	-0.6931	-0.6027	-0.6917	-1.1538	-0.3945	0.0865
16:00	-0.6718	-0.5795	-0.6800	-1.1895	-0.7354	0.1602
16:30	-0.6858	-0.6039	-0.6804	-0.9990	-0.3117	0.3739
17:00	-0.6693	-0.5955	-0.6660	-1.0539	-0.1766	0.4634
17:30	-0.6673	-0.5628	-0.6808	-0.5939	-0.2282	0.7264
18:00	-0.6036	-0.5469	-0.6274	-0.9099	-0.2202	0.6177
18:3	-0.5792	-0.5429	-0.5842	-0.6638	-0.1546	0.4646

19:0	-0.5518	-0.5170	-0.5272	-0.6572	-0.3593	-0.0650
19:30	-0.5329	-0.5396	-0.5090	-0.7930	-0.1590	-0.1147
2:00	-0.5007	-0.5147	-0.4599	-1.2029	-0.4059	-0.3750
0:30	-0.5397	-0.5351	-0.4585	-0.9082	-0.2235	-0.3917
21:00	-0.5504	-0.5431	-0.4813	-1.2035	-0.0851	-0.2924
21:30	-0.5444	-0.5377	-0.5104	-1.2709	0.0055	0.0939
22:00	-0.5396	-0.5084	-0.4847	-1.0156	-0.1140	-0.0280
22:30	-0.5012	-0.5146	-0.4437	-1.1050	0.2916	-0.3974
23:00	-0.4213	-0.4518	-0.4093	-1.5158	-0.0383	-0.4722
23:30	-0.3926	-0.4065	-0.3898	-1.1971	-0.2149	-0.5823
00:00	-0.3685	-0.3236	-0.3666	-0.7952	-0.5419	-0.5036

### Appendix 3 - Temperature Sensitivity Coefficients

	Class 1 Gradient Coefficient			Class 2 Gradient Coefficient			$\sum_{j=1}^2 N_j$ Gradient Coefficient		
	W	Sa	Su	W	Sa	Su	W	Sa	Su
00:30	-0.164210	-0.143856	-0.159481	-0.155100	0.049780	-0.531468	0.000019	0.000009	0.000040
01:00	-0.181614	-0.308666	-0.136963	-0.205077	0.654590	-0.283277	0.000017	0.000020	0.000023
01:30	-0.127541	-0.251793	-0.300362	-0.686285	-0.181790	0.032978	0.000013	0.000019	0.000027
02:00	-0.145597	-0.384410	-0.306997	-0.493404	-0.014549	0.054987	0.000019	0.000014	0.000004
02:30	-0.188039	-0.166259	-0.386501	-0.345045	-0.536069	-0.251311	0.000015	0.000012	0.000033
03:00	-0.135673	-0.355294	-0.498172	-0.520049	-0.197839	-0.088248	0.000020	0.000018	0.000024
03:30	-0.103444	-0.296823	-0.448651	-0.795760	-0.249641	-0.531810	0.000025	0.000006	0.000047
04:00	-0.042844	-0.257750	-0.264251	-1.116896	-0.470474	-1.677593	0.000034	0.000005	0.000068
04:30	-0.006382	-0.240946	-0.241438	-1.010824	-0.627623	-1.483290	0.000023	0.000019	0.000053
05:00	-0.092994	-0.424423	-0.382020	-0.888216	-0.198356	-0.854346	0.000025	0.000006	0.000038
05:30	-0.088750	-0.326215	-0.583157	-0.873381	-0.530562	-0.006460	0.000022	0.000017	0.000030
06:00	-0.178330	-0.277620	-0.368431	-0.761750	-0.499452	-0.874783	0.000031	0.000013	0.000038
06:30	-0.219531	-0.352135	-0.456423	-0.331507	-0.103656	-0.241674	0.000025	0.000023	0.000024
07:00	-0.322652	-0.415720	-0.579318	0.295033	0.339242	0.348884	0.000024	0.000013	0.000033
07:30	-0.299252	-0.397736	-0.417732	0.338803	0.528382	0.703350	0.000027	0.000021	0.000024
08:00	-0.183704	-0.154225	-0.283942	-0.573926	-0.076684	0.545204	0.000047	0.000009	0.000010
08:30	-0.166601	-0.250798	-0.195471	-0.529828	0.074528	0.257297	0.000041	0.000031	0.000015
09:00	-0.162536	-0.206115	-0.237716	-1.249807	-0.340634	-0.100465	0.000042	0.000028	0.000049
09:30	-0.070835	-0.282972	-0.321404	-2.519157	-0.497805	0.993017	0.000044	0.000066	0.000026
10:00	-0.249800	-0.280197	-0.280404	-0.779225	-0.919492	0.512643	0.000035	0.000056	0.000037

10:30	-0.178173	-0.329689	-0.350648	-1.614090	-0.100436	0.993454	0.000036	0.000058	0.000026
11:00	-0.212784	-0.380784	-0.409295	-1.411941	1.272337	1.012580	0.000029	0.000032	0.000032
11:30	-0.247364	-0.438895	-0.274291	-1.629651	0.755212	-0.303411	0.000037	0.000053	0.000028
12:00	-0.308651	-0.379285	-0.420099	-0.994501	0.589469	-0.138997	0.000032	0.000039	0.000063
12:30	-0.320540	-0.377587	-0.387089	-0.321043	1.191082	0.817593	0.000029	0.000026	0.000026
13:00	-0.257414	-0.385343	-0.348854	-1.356866	1.615443	0.007545	0.000030	0.000018	0.000043
13:30	-0.240591	-0.344920	-0.377236	-1.614269	1.325655	0.565065	0.000039	0.000012	0.000035
14:00	-0.311853	-0.342799	-0.518319	-0.656554	0.363757	1.776533	0.000026	0.000021	0.000045
14:30	-0.354505	-0.370386	-0.638887	-0.486420	0.552967	2.252632	0.000025	0.000030	0.000018
15:00	-0.388552	-0.407687	-0.540649	0.024767	0.183389	0.639077	0.000018	0.000041	0.000056
15:30	-0.356825	-0.319778	-0.486430	0.142151	-0.167849	0.944402	0.000019	0.000027	0.000017
16:00	-0.320571	-0.356391	-0.491596	-0.520973	0.281101	1.771838	0.000030	0.000039	0.000018
16:30	-0.269789	-0.448636	-0.463615	0.041890	1.137569	2.368313	0.000012	0.000035	-0.000003
17:00	-0.211663	-0.280507	-0.254165	-0.154133	0.835027	0.603573	0.000017	0.000009	0.000005
17:30	-0.208111	-0.184938	-0.343685	0.491557	-0.425511	0.919853	0.000010	0.000015	0.000030
18:00	-0.187744	-0.158753	-0.236540	-0.196271	0.130600	0.195537	0.000018	-0.000004	0.000023
18:30	-0.140947	-0.231916	-0.217054	-0.592963	0.552702	0.568713	0.000026	0.000014	0.000018
19:00	-0.166710	-0.296346	-0.269402	-0.054906	1.293191	0.904858	0.000016	0.000009	0.000025
19:30	-0.181548	-0.201818	-0.156450	0.195622	0.636695	0.133159	0.000019	0.000016	0.000016
20:00	-0.173324	-0.204525	-0.192761	0.012705	0.725749	-0.251692	0.000032	0.000022	0.000046
20:30	-0.170757	-0.181198	-0.237682	-0.117670	-0.061886	0.567534	0.000037	0.000039	0.000021
21:00	-0.175376	-0.220372	-0.237845	0.385569	0.849145	-0.019401	0.000021	0.000022	0.000045
21:30	-0.154008	-0.191558	-0.261163	0.177113	0.259893	0.783404	0.000017	0.000011	0.000021
22:00	-0.143524	-0.136713	-0.198944	0.179427	-0.495185	0.162950	0.000021	0.000048	0.000022
22:30	-0.156004	-0.199961	-0.224435	0.428436	0.430096	1.000817	0.000017	0.000040	0.000007
23:00	-0.117233	-0.230193	-0.256751	-0.243792	0.611449	1.013495	0.000028	0.000041	0.000012
23:30	-0.126518	-0.173943	-0.346622	0.011839	0.459740	2.148800	0.000018	0.000030	0.000009
00:00	-0.104351	-0.190694	-0.228475	-0.202683	0.178451	0.518302	0.000023	0.000034	0.000011

	Class 1 Y-Intercept Coefficient			Class 2 Y-Intercept Coefficient			$\sum_{j=1}^2 N_j$ Y-Intercept Coefficient		
	W	Sa	Su	W	Sa	Su	W	Sa	Su
00:30	0.035478438	0.034402074	0.038563146	0.095422406	-0.026954618	0.215979464	-4.28E-06	-5.28E-07	-9.81E-06
01:00	0.044478378	0.090622358	0.034300027	0.054838599	-0.224017518	0.114836499	-3.74E-06	-4.44E-06	-5.37E-06
01:30	0.035667325	0.056928162	0.084139058	0.114449849	0.099998298	-0.106671127	-2.33E-06	-5.45E-06	-3.93E-06
02:00	0.032353702	0.113353675	0.087670155	0.098643584	-0.03825087	-0.050633496	-2.58E-06	-2.33E-06	1.05E-06
02:30	0.048966975	0.022517978	0.102984394	0.055919625	0.147200089	0.016892827	-2.67E-06	-8.08E-07	-6.24E-06
03:00	0.043450451	0.08092459	0.144926519	0.063122982	0.066491637	-0.095883569	-2.00E-06	-4.28E-06	-2.12E-06
03:30	0.017620466	0.059504232	0.105932306	0.175678575	0.094590855	0.094782091	-4.54E-06	-6.52E-07	-8.46E-06
04:00	0.010514643	0.072044561	0.051289674	0.244517451	0.113016025	0.411564971	-6.52E-06	-1.99E-06	-1.46E-05
04:30	-0.003808852	0.053757436	0.0349891	0.230251985	0.161629137	0.370937095	-4.37E-06	-5.15E-06	-9.60E-06
05:00	0.017251447	0.096238531	0.087605277	0.2107723	0.061566051	0.130835974	-4.83E-06	-1.97E-06	-6.16E-06
05:30	0.017464308	0.067021035	0.11786054	0.194938541	0.136565955	0.03957558	-4.24E-06	-3.39E-06	-6.18E-06
06:00	0.029892875	0.045521838	0.070098701	0.200242377	0.181104412	0.261611949	-6.83E-06	-3.27E-06	-8.31E-06
06:30	0.038761692	0.080851627	0.09331417	0.099619135	0.034726626	0.074342102	-5.03E-06	-5.19E-06	-4.92E-06
07:00	0.064019815	0.102438895	0.114359422	-0.043832264	-0.090126685	-0.006634525	-5.15E-06	-2.26E-06	-7.57E-06
07:30	0.054170104	0.107932564	0.110775027	-0.015990818	-0.196152717	-0.223477011	-5.93E-06	-3.62E-06	-5.25E-06
08:00	0.03936242	0.033406687	0.066820131	0.185218323	0.072022079	-0.096343068	-1.18E-05	-3.08E-06	-2.99E-06
08:30	0.034015966	0.061991654	0.052945748	0.216317127	0.042805944	-0.033383871	-1.12E-05	-8.74E-06	-5.00E-06
09:00	0.035760822	0.04331401	0.051012492	0.448182799	0.232456427	0.2028133	-1.16E-05	-8.32E-06	-1.51E-05
09:30	0.012731531	0.078554204	0.091177291	0.865416048	0.208800113	-0.237920628	-1.41E-05	-1.98E-05	-7.58E-06
10:00	0.064983202	0.086218578	0.080388576	0.376537521	0.369402193	-0.097369041	-1.16E-05	-1.96E-05	-1.15E-05
10:30	0.043698477	0.105500112	0.106348532	0.628909415	0.033797292	-0.250489422	-1.12E-05	-1.82E-05	-9.25E-06
11:00	0.059313777	0.126245243	0.121589295	0.584568088	-0.316149359	-0.173122455	-9.84E-06	-1.24E-05	-1.19E-05
11:30	0.071707166	0.156596735	0.073327435	0.700184529	-0.280430051	0.292299898	-1.37E-05	-1.95E-05	-8.31E-06
12:00	0.098182968	0.131330455	0.135674306	0.442133833	-0.172829287	0.110211536	-1.12E-05	-1.43E-05	-2.15E-05

12:30	0.099011692	0.125050994	0.120032329	0.2941852	-0.401541373	-0.117522145	-1.12E-05	-7.27E-06	-1.03E-05
13:00	0.069587366	0.137843345	0.114709649	0.696835816	-0.592142394	0.014715804	-1.01E-05	-5.48E-06	-1.21E-05
13:30	0.073368596	0.107801334	0.112071943	0.665175313	-0.229387052	-0.0014944	-1.40E-05	-5.38E-06	-1.35E-05
14:00	0.110908443	0.141928599	0.174205401	0.134497225	-0.335584157	-0.545636657	-7.26E-06	-6.87E-06	-1.65E-05
14:30	0.126001555	0.118796071	0.211542292	0.132546013	-0.120407538	-0.59672485	-8.15E-06	-8.48E-06	-8.24E-06
15:00	0.134683245	0.14389041	0.178546282	-0.021860858	-0.140775474	0.039487147	-4.57E-06	-1.18E-05	-2.31E-05
15:30	0.122082142	0.11145598	0.162309819	-0.09947279	0.056560901	-0.110250696	-4.57E-06	-6.56E-06	-9.11E-06
16:00	0.093429736	0.138876663	0.155636618	0.353286949	-0.227351346	-0.425130344	-1.12E-05	-1.43E-05	-8.19E-06
16:30	0.084074439	0.168268081	0.147481949	-0.143071364	-0.565573167	-0.836416008	8.67E-07	-1.11E-05	3.73E-06
17:00	0.055017177	0.078508399	0.072050628	0.034924536	-0.126922913	-0.11556294	-1.05E-06	-2.34E-06	-3.42E-06
17:30	0.053934096	0.053911207	0.08913183	-0.131739646	0.088849225	0.00706941	-1.39E-06	-7.59E-07	-1.50E-05
18:00	0.052663105	0.031611553	0.070406094	0.124445587	0.056172247	0.010787884	-6.58E-06	4.46E-06	-1.02E-05
18:30	0.027968952	0.056544885	0.058053079	0.309081921	-0.044408945	-0.081904712	-8.64E-06	-3.23E-06	-4.79E-06
19:00	0.038457212	0.086217071	0.077732242	0.131448442	-0.326416126	-0.196498779	-5.00E-06	-3.20E-06	-7.68E-06
19:30	0.04683368	0.053708011	0.042110179	-0.019423641	-0.160909347	0.015684694	-4.80E-06	-3.49E-06	-4.27E-06
2:00	0.04193874	0.053444096	0.057018806	0.073083067	-0.178647596	0.014472254	-9.15E-06	-4.91E-06	-1.08E-05
0:30	0.040283647	0.051760051	0.057935301	0.126933703	0.055198727	-0.063076258	-1.06E-05	-1.23E-05	-4.90E-06
21:00	0.039583501	0.056535848	0.065666723	-0.010748728	-0.203083658	-0.028256322	-7.11E-06	-5.56E-06	-1.06E-05
21:30	0.037372561	0.052587545	0.07441063	0.010312475	-0.072354681	-0.259715097	-4.70E-06	-3.14E-06	-4.81E-06
22:00	0.032804066	0.032981353	0.035144618	0.009482348	0.190724011	0.178515368	-5.88E-06	-1.29E-05	-7.19E-06
22:30	0.037800154	0.055339264	0.054644226	-0.074511139	-0.151449843	-0.20244661	-4.09E-06	-9.66E-06	-2.38E-06
23:00	0.027735265	0.058364586	0.053992393	0.077534524	-0.143885081	-0.151992864	-6.53E-06	-1.02E-05	-2.09E-06
23:30	0.031812983	0.035676999	0.084054177	0.003658019	-0.029940305	-0.504316505	-4.54E-06	-7.05E-06	-1.80E-06
00:00	0.026350046	0.0451217	0.044264481	0.061580863	-0.010695048	-0.023281798	-5.68E-06	-8.31E-06	-2.52E-06